The official bi-monthly publication of Bhabha Atomic Research Centre

BARC newsletter

November-December 2024 ISSN: 0976-2108

- Cancer Biology
- Nuclear Agriculture
- Food Science
- Microbiology

Tribute to Dr. R. Chidambaram

THE POWER and *Potential of Life*

BARC Newsletter
November-December 2024
ISSN: 0976-2108

About front cover picture

A tiny living cell remains an enduring enigma, holding countless secrets awaiting to be unravelled by researchers. The intricate dynamics of life's power and potential reside within its delicate structure. As depicted on the front cover, a vibrant live cell reveals its vital components: Mitochondria (the powerhouses fuelling cellular energy) in green colour, lysosomes (the waste management factories maintaining cellular homeostasis) in red colour, and the nucleus (the command centre governing the fate of the cell) in blue colour.

डॉ. राजगोपाल चिदंबरम को भावपूर्ण श्रद्धांजलि

एक दूरदर्शी वैज्ञानिक, प्रणेता एवं देशभक्त

डॉ. आर. चिदंबरम पऊवि सम्मेलन केंद्र, मुंबई में एशियाई विकिरण अनुसंधान कांग्रेस के उद्घाटन समारोह के दौरान बीज व्याख्यान देते हुए

भारतीय विज्ञान एवं प्रौद्योगिकी में एक प्रख्यात व्यक्ति डॉ. राजगोपाल चिदंबरम का जन्म 12 नवंबर, 1936 को चेन्नई में हुआ था। उनके पिता सशस्त्र बलों के केंद्रीय कमान कार्यालय, मेरठ में रक्षा लेखा नियंत्रक के रूप में कार्यरत थे, जहाँ डॉ. चिदंबरम ने अपनी प्रारंभिक विद्यालयी शिक्षा ग्रहण की और उच्च शिक्षा विशिष्ट उपलब्धि सहित प्राप्त की, उन्होंने प्रेसीडेंसी कॉलेज, चेन्नई से बी. एससी की डिग्री तथा भारतीय विज्ञान संस्थान (आईआईएससी), बैंगलुरू से भौतिकी (विशेष) में एम.एससी की डिग्री हासिल की। वर्ष 1962 में, वे न्यूट्रॉन क्रिस्टलोग्राफी वर्ग, भापअ केंद्र से जुड़े तथा एक शानदार कैरियर की शुरूआत की और भारत के परमाणु ऊर्जा कार्यक्रम में अपना महत्वपूर्ण योगदान दिया। इन वर्षों को दौरान, उन्होंने परमाणु ऊर्जा के विभिन्न क्षेत्रों पर एक अमिट छाप छोड़ते हुए भापअ केंद्र के निदेशक (1990-1993) और परमाणु ऊर्जा आयोग (1993-2000) के अध्यक्ष के रूप में कार्य किया।

इसके अतिरिक्त, डॉ. चिदंबरम ने वर्ष 2001 से 2018 तक भारत सरकार के प्रधान वैज्ञानिक सलाहकार (पीएसए) के रूप में कार्य करते हुए, देश में वैज्ञानिक प्रगति को आगे बढ़ाया। प्रधान वैज्ञानिक सलाहकार के रूप में, उन्होंने भारतीय विज्ञान एवं प्रौद्योगिकी के भविष्य को आकार देने वाली विभिन्न पहलों का समर्थन किया। इनमें ग्रामीण प्रौद्योगिकी कार्य वर्ग जिसने ग्रामीण समुदायों को नवाचार समाधानों से सशक्त बनाया और इलेक्ट्रॉनिक ट्रांजैक्शन एवं सुरक्षा हेतु सोसायटी शामिल है जिसने भारत की साइबर सुरक्षा क्षमताओं को बढ़ाया है। उनके नेतृत्व में, सहयोग एवं नवाचार को बढ़ावा देने के लिए पूरे भारत में अनुसंधान एवं शैक्षणिक संस्थानों को जोड़ने के लिए राष्ट्रीय ज्ञान नेटवर्क शुरू किया गया था। डॉ. आर. चिदंबरम ने वर्ष 2005 के सफल भारत-अमेरिका असैन्य नाभिकीय साझेदारी समझौते की ओर ले जाने वाली चर्चाओं में सक्रिय भूमिका निभाई, जिसने वैश्विक नाभिकीय समुदाय में भारत के एकीकरण को प्रगति प्रदान की।

डॉ. चिदंबरम ने राष्ट्रीय सुरक्षा एवं नाभिकीय ऊर्जा के अलावा, अनुसंधान एवं विकास में नवाचार को बढ़ावा देने के लिए मौलिक अनुसंधान को मजबूती के साथ आगे बढ़ाया, विशेष रूप से खाद्य एवं जल सुरक्षा, सार्वजनिक स्वास्थ्य और सतत विकास जैसे क्षेत्रों में नाभिकीय प्रौद्योगिकियों के अनुप्रयोग पर जोर दिया। भापअ केंद्र के जैव-विज्ञान वर्ग तक विस्तारित उनके दूरदर्शी नेतृत्व का प्रभाव प्रोटीन क्रिस्टलोग्राफी में अनुसंधान और जैविक मैक्रोमोलिक्यूल्स का अध्ययन करने के लिए न्यूट्रॉन किरणपुंज और सिंक्रोट्रॉन स्रोतों के उपयोग को बढ़ावा दिया। उनके इन प्रयासों ने लक्षित दवा अभिकल्पन में प्रगति का मार्ग प्रशस्त किया। डॉ. चिदंबरम ने नवंबर 2022 में, मुंबई में भापअ केंद्र द्वारा पऊवि सम्मेलन केंद्र में आयोजित 5वीं एशियाई विकिरण अनुसंधान कांग्रेस में सोसायटी फॉर रेडिएशन रिसर्च-इंडिया और एशियन एसोसिएशन फॉर रेडिएशन रिसर्च सहयोग में मुख्य अतिथि के रूप में उपस्थित होकर जैव विज्ञान समुदाय को गौरवान्वित किया। इस विकिरण अनुसंधान कांग्रेस में 17 देशों के वैज्ञानिकों ने भाग लिया। डॉ. चिदंबरम ने अपने वाक्पटु अंदाज़ में अभिभाषण प्रस्तुत करते हुए, सूक्ष्म जीवों, पौधों और मानव कोशिकाओं में विकिरण अनुक्रिया की प्रक्रिया को समझने के महत्वपूर्ण पहलुओं को रेखांकित किया। उन्होंने, मानव स्वास्थ्य, कृषि और खाद्य सुरक्षा में आयनीकरण विकिरण के उभरते अनुप्रयोगों पर प्रकाश डाला तथा भविष्य में कैंसर उपचार के लिए प्रोटॉन किरणपुंज, बोरॉन-न्यूट्रॉन कैप्चर थेरेपी पर प्रगत विकिरण जैविकी और आवेशित कणों के साथ-साथ विकिरण सुरक्षा हेतु निम्न-डोज़ वाले विकिरण जैविकी अनुसंधान को प्रोत्साहित किया।

जुलाई २०२४ में, डॉ. चिदंबरम ने भापअ केंद्र के वैज्ञानिकों और टीएमसी के डॉक्टरों के बीच एक महत्वपूर्ण बैठक की अध्यक्षता करके ट्रांसलेशनल अनुसंधान पर चर्चा शुरू की। इस बैठक के दौरान गठित कार्य बल का प्रयोजन कैंसर के उपचार के लिए भापअ केंद्र-अनुसंधान/प्रौद्योगिकियों और नए विकिरण भेषजिक के क्लिनिकल ट्रांसलेशन को त्वरित करना है, साथ ही चिकित्सा प्रतिबिंबन, कैंसर निदान और विकिरण चिकित्सा की गुणवत्ता को बढ़ाने में कृत्रिम मेधा की क्षमता का पता लगाना है।

डॉ. चिदंबरम एक कुशल वैज्ञानिक, दूरदर्शी नेतृत्वकर्ता, एक सच्चे देशभक्त एवं अत्यंत दयालु प्रवृत्ति के व्यक्ति थे। 4 जनवरी, 2025 को उनका निधन भारत की वैज्ञानिक और तकनीकी प्रगति में एक उल्लेखनीय युग का अंत है। भापअ केंद्र के जैव-विज्ञान वर्ग का वैज्ञानिक समुदाय आत्माभिमान के साथ डॉ. राजगोपाल चिदंबरम की स्मृति में संजोए रखने हेतु भापअ केंद्र न्यूज़लेटर के इस विशेष अंक को समर्पित करता है। उनके अद्वितीय मार्गदर्शन और प्रेरणा हमें वैश्विक जैव विज्ञान परिदृश्य को प्रभावित करते हुए अनुसंधान एवं प्रौद्योगिकी को उन्नत करने हेतु सदैव प्रोत्साहित करेगी।

डॉ पी. ए. हसन
सह निदेशक, जैव-विज्ञान वर्ग
भाभा परमाणु अनुसंधान केंद्र

Tribute to Dr. Rajagopala Chidambaram

A Visionary Scientist, Leader, and Patriot

Dr. Rajagopala Chidambaram, an illustrious figure in Indian science and technology, was born on November 12, 1936, in Chennai. His father served as the Controller of Defense Accounts in the Central Command Office of the Armed Forces in Meerut, where Dr. Chidambaram completed his early schooling and pursued higher education with distinction, earning a B.Sc. degree from Presidency College, Chennai and M.Sc. in Physics (Hons) from the Indian Institute of Science (IISc), Bengaluru. In 1962, he joined the Neutron Crystallography Group at BARC, embarking on an illustrious career and contributed significantly for India's atomic energy program. Over the years, he served as Director of BARC (1990–1993) and Chairman of the Atomic Energy Commission (1993–2000), leaving an indelible mark on various domains of Atomic Energy. Dr. Chidambaram further propelled scientific advancements in the country as the Principal Scientific Adviser (PSA) to the Govt. of India, from 2001 to 2018. Later, he involved himself actively as the Chairman (Honorary) of the DAE Institute of Advanced Studies and on the Boards of several IITs.

Dr. R. Chidambaram delivering the key note address during inauguration ceremony of 5th Asian Congress of Radiation Research at DAE Convention Centre in Anushakti Nagar.

As PSA, he championed various initiatives that shaped the future of Indian science and technology. These included the Rural Technology Action Group, which empowered rural communities with innovative solutions, and the Society for Electronic Transactions and Security, which enhanced India's cybersecurity capabilities. Under his leadership, the National Knowledge Network was launched, connecting research and educational institutions across India to foster collaboration and innovation. Dr. R. Chidambaram played an active role in the discussions leading to the successful Indo-US Civil Nuclear partnership pact of 2005, which significantly advanced India's integration into the global nuclear community.

Beyond national security and nuclear power, Dr. Chidambaram strongly supported fundamental research to foster innovation in R&D, particularly emphasizing the application of nuclear technologies in areas such as food and water security, public health, and sustainable development. His visionary leadership extended to the Bio-Science Group, BARC, promoted research in protein crystallography and the use of neutron beams and synchrotron sources to study biological macromolecules. These efforts paved the way for advancements in targeted drug design. In November 2022, Dr. Chidambaram honoured the bioscience community as the Chief Guest at the 5th Asian Congress of Radiation Research, organized by BARC in association with the Society for Radiation Research–India and the Asian Association for Radiation Research at DAE Convention Centre, Mumbai. The Congress of Radiation Research witnessed participation from scientists across 17 countries. In his eloquent keynote address, Dr. Chidambaram underscored the pivotal role of understanding the mechanisms of radiation response in microbes, plants, and human cells. He highlighted emerging applications of ionizing radiation in human health, agriculture and food security and encouraged advanced radiobiology research on proton beam, boron-neutron capture therapy, and charged particles for future cancer treatments as well as low-dose radiobiology for radiation protection.

In July 2024, Dr. Chidambaram further initiated a discussion on translational research by chairing a crucial meeting between BARC scientists and TMC doctors. The task force formed during this meeting aimed to accelerate the clinical translation of BARC-research/technologies and new radiopharmaceuticals for cancer treatment, as well as to explore the potential of artificial intelligence in medical imaging, cancer diagnosis, and enhancing the quality of radiation therapy in India.

Dr. Chidambaram was an accomplished scientist, visionary leader, a true patriot and a deeply compassionate human being. His passing away on January 4, 2025 marks the end of a remarkable era in India's scientific and technological advancement. The scientific community of the Bio-Science Group, BARC, proudly dedicates this special issue of the *BARC Newsletter* to the cherished memory of Dr. Rajagopala Chidambaram. His unparalleled guidance and inspiration will forever encourage us for advancing research and technology, impacting global Bioscience landscape.

Dr. P. A. Hassan
Associate Director, Bio-Science Group
Bhabha Atomic Research Centre

ASSOCIATE EDITORS' *message*

Emerging Frontier Areas of Research in Biology at BARC

As a premier multidisciplinary research institute, Bhabha Atomic Research Centre is well-known for carrying out research in the frontier areas of Science and Technology. Along with R&D being carried out in the areas pertaining to nuclear power, BARC has made considerable progress in research that has immediate societal implications. We are extremely pleased to launch this issue of BARC Newsletter that describes the cutting-edge research carried out in biological sciences, particularly in the field of nuclear medicine, precision cancer therapeutics, radiation-guided diagnosis as well as therapy. Furthermore, other research topics such as agriculture, biotechnology and high-quality basic research are covered in terms of feature articles or short thesis reports. In this regard, sixteen articles highlight the contemporary biological research and technologies evolved in the area of health, while four articles emphasize the new approaches in the field of food and agriculture, whereas one article deals with a biotechnological application for clean environment.

This special issue also showcases the snapshots of the research performed by young minds, who are currently pursuing, or have just finished, their PhDs in the Life Science discipline. Thus, we do hope that we have been able to provide a glimpse of the wide expanse of work being carried out in fundamental areas as well as application-oriented research in Biosciences at BARC. We are optimistic that these articles will enlighten and stimulate the minds of researchers as well as students, energizing them to take up societal problems that need to be urgently resolved today.

We take this opportunity to sincerely thank all the authors for their active role and enthusiastic support in finalizing the articles promptly. Our whole-hearted thanks to Dr. S. Adhikari, former Director, Knowledge Management Group (KMG), for extending this opportunity and steering us throughout this publication process. We also take this opportunity to thank Dr. A.K. Dureja, Associate Director, KMG, Shri Manoj Singh, Head, SIRD, Shri. Madhav N., and the entire SIRD Newsletter Editorial team for their painstaking effort in curating the content, designing/formatting the articles in their final form and for providing proofs. We are very thankful to Dr. P. A. Hassan, Associate Director, Bio-science Group, for his generous support in bringing out this special issue.

Dr. Birija Sankar Patro
Head, Bio-Organic Division

Dr. Anand Ballal
Head, Nuclear Agriculture & Biotechnology Division

RESEARCH AND DEVELOPMENT IN BIOSCIENCE

CONTENTS

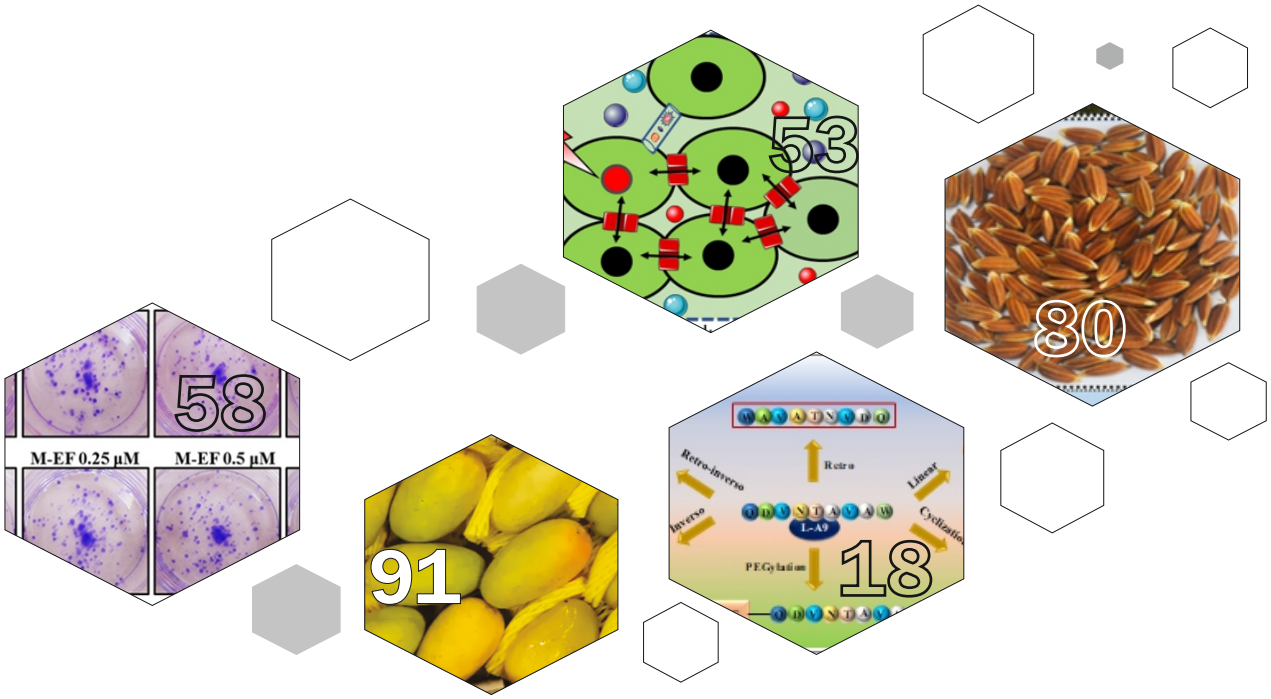

ARTICLES OF FORTHCOMING ISSUE

- Research and Development of Advanced Fuels for High Temperature Reactors
- Harnessing Boron Molecular Emission Spectra in Laser-Induced Plasma
- Antimicrobial Efficacy of a Novel Cold Atmospheric Plasma Device for Infection Control on Dental Surfaces
- National Science Day 2025 in BARC
  Transition to Clean, Green Viksit Bharat: Advanced Materials & Nuclear Technology

This page intentionally left blank

कैंसर चिकित्सा हेतु प्रकाश-सुग्राहीकारक

1

एक नोवेल-बोडिपी -संयुग्मित डाई द्वारा एंडोप्लाज़्मिक रेटिकुलम और लिपिड बूंदों की सटीक प्रकाश-गतिकी चिकित्सा हेतु दोहरा प्रतिबिंबन

नितीश चौहान[1,2], **मृणेश कोली**[1,2], **आनंद गुहा मजूमदार**[1,2], **सौम्यादित्य मुला**[1,2] **और बिरिजा शंकर पात्रो**[1,2]*
[1]जैव-कार्बनिक प्रभाग , भाभा परमाणु अनुसंधान केंद्र , ट्रांबे-400085, भारत
[2]होमी भाभा राष्ट्रीय संस्थान , अणुशक्ति नगर ,मुंबई-400094, भारत

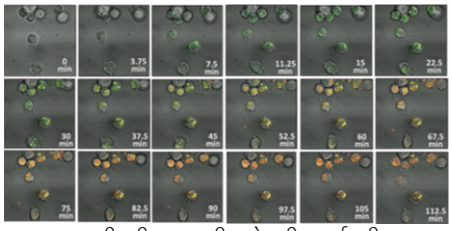

एन. बी. बी., एक बी. ओ. डी. आई. पी. वाई.-नैफ्थोलिमिन-बी. एफ. 2 डायड के कोशिकीय ग्रहण की गतिविज्ञान

सारांश

प्रकाश गतिकी चिकित्सा का अगला उत्पादन प्रकाश-सुग्राहीकता का विकसित करने पर केंद्रित है, जो संवेदनशील अंगों में कैंसर को प्रभावी ढंग से लक्षित कर सकता है। चूंकि, अग्नाशय के कैंसर हार्मोन संश्लेषण के लिए एंडोप्लाज्मिक रेटिकुलम पर बहुत अधिक निर्भर होते हैं, इसलिए अग्नाशय के कैंसर में एंडोप्लाज़्मिक रेटिकुलम (ईआर) का प्रतिबिंबन और सटीक लक्ष्यीकरण विकसित करना अग्नाशय के कैंसर के उपचार की असाध्य चुनौती को साध कर सकता है। इस संबंध में, हमने एक नए PS, एक BODIPY-नेफ्थोलिमाइन-BF2 डायड (NbB) के संश्लेषण को इंजीनियर किया है, जो एकल उत्तेजना के साथ एक साथ ER और लिपिड बूंदों (LDs) की बिंब बना सकता है और अग्नाशय के कई कैंसर कोशिकाओं के मज़बूत प्रकाश-सुग्राहीकता को प्रेरित कर सकता है। यांत्रिक रूप से, NbB कोशिकाओं में सिंगलेट ऑक्सीजन के उत्पादन और ग्लूटाथियोन के खंडन के माध्यम से गंभीर ER तनाव का कारण बनता है।

Photosensitizers for Cancer Therapy

1

Precision Photodynamic Therapy Dual Imaging of Endoplasmic Reticulum and Lipid Droplets by a Novel BODIPY-conjugate Dye

Nitish Chauhan[1,2], **Mrunesh Koli**[1,2], **Ananda Guha Majumdar**[1,2], **Soumyaditya Mula**[1,2] **and Birija Sankar Patro**[1,2]*
[1]Bio-Organic Division, Bhabha Atomic Research Centre, Trombay-400085, INDIA
[2]Homi Bhabha National Institute, Anushakti Nagar, Mumbai-400094, INDIA

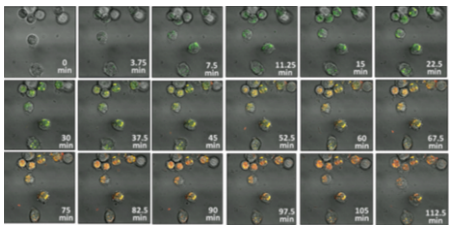

Kinetics of cellular uptake of NbB, a BODIPY-naphtholimine-BF2 dyad

ABSTRACT

Next generation photodynamic therapy is focused on developing photosensitizers (PS), which can effectively target sensitive organelles in cancer. Since, pancreatic cancers are heavily dependent on Endoplasmic Reticulum (ER) for hormone synthesis, developing imaging and precision targeting agents for ER in pancreatic cancers may address the unmet challenge of pancreatic cancer treatment. In this regard, we have engineered synthesis of a novel PS, a BODIPY-naphtholamine-BF2 dyad (NbB), which can image ER and lipid droplets (LDs) simultaneously with single excitation wavelength and induces robust photosensitization of multiple pancreatic cancer cells. Mechanistically, NbB causes severe ER stress through generation of singlet oxygen and depletion of glutathione in the cells.

KEYWORDS: *Dual imaging, Endoplasmic reticulum, Lipid droplets, Pancreatic cancer, Precision photodynamic therapy*

**Author for Correspondence: Birija Sankar Patro*
E-mail: bisank@barc.gov.in

Introduction

Pancreatic cancer, especially pancreatic ductal carcinoma (PDAC) is one of the most difficult to treat cancers. It remains an incurable malignancy for half a century due to no or limited therapeutic options[1]. Recently, photodynamic therapy (PDT) has emerged as a promising approach for the treatment of pancreatic cancers[2]. PDT agents like meso-Tetra (hydroxyphenyl)chlorin (mTHPC) and verteporfin showed some positive therapeutic outcomes for the treatment of PDAC patients in the clinic[3]. In order to enhance the therapeutic efficacy, next-generation PDT agents are designed to target cancer cells. Since pancreatic cancer cells heavily rely on endoplasmic reticulum (ER) for the synthesis of inherent requirements of hormones, ER is considered as an attractive target for the development of precision medicine for the treatment of PDAC[4,5]. ER is closely associated with lipid droplets, the latter is known to be positively correlated with advanced clinical staging, metastasis, and poor survival[6]. Considering the importance of ER and LDs in PDAC, there is an urgent need for the development of a precision photomedicine or photosensitizer (PS), which can (1) specifically accumulate to ER and LD, (2) image ER and LDs and (3) photosensitize PDAC cells through ER and LD stress. To the best of our knowledge, only one report shows dual imaging of ER and LDs by single probe at single excited wavelength[7]. In order to have all three properties (ER targeting, dual fluorescence imaging of ER and LD and photosensitization) in one molecule, we have chosen BODIPY based skeleton to fuse with an ER-targeting scaffold, like naphthalene moiety, for appropriate functional tuning. In this regard, we have rationally designed and synthesized a new class of bis-chromophoric fluorescent probes by fusing naphtholamine-BF2 derivative at *meso*-linked BODIPY (N*m*B) and *β*-linked BODIPY (N*b*B) (Fig.1A). Rational designing is based on the fact that position of the naphthalene moiety in N*m*B and N*b*B may influence (1) the efficient generation of triplet excited state and singlet oxygen for PDT, (2) dual fluorescence in ER and LD in polar and non-polar milieu, respectively and (3) photodamage to ER and LDs in PDAC cells.

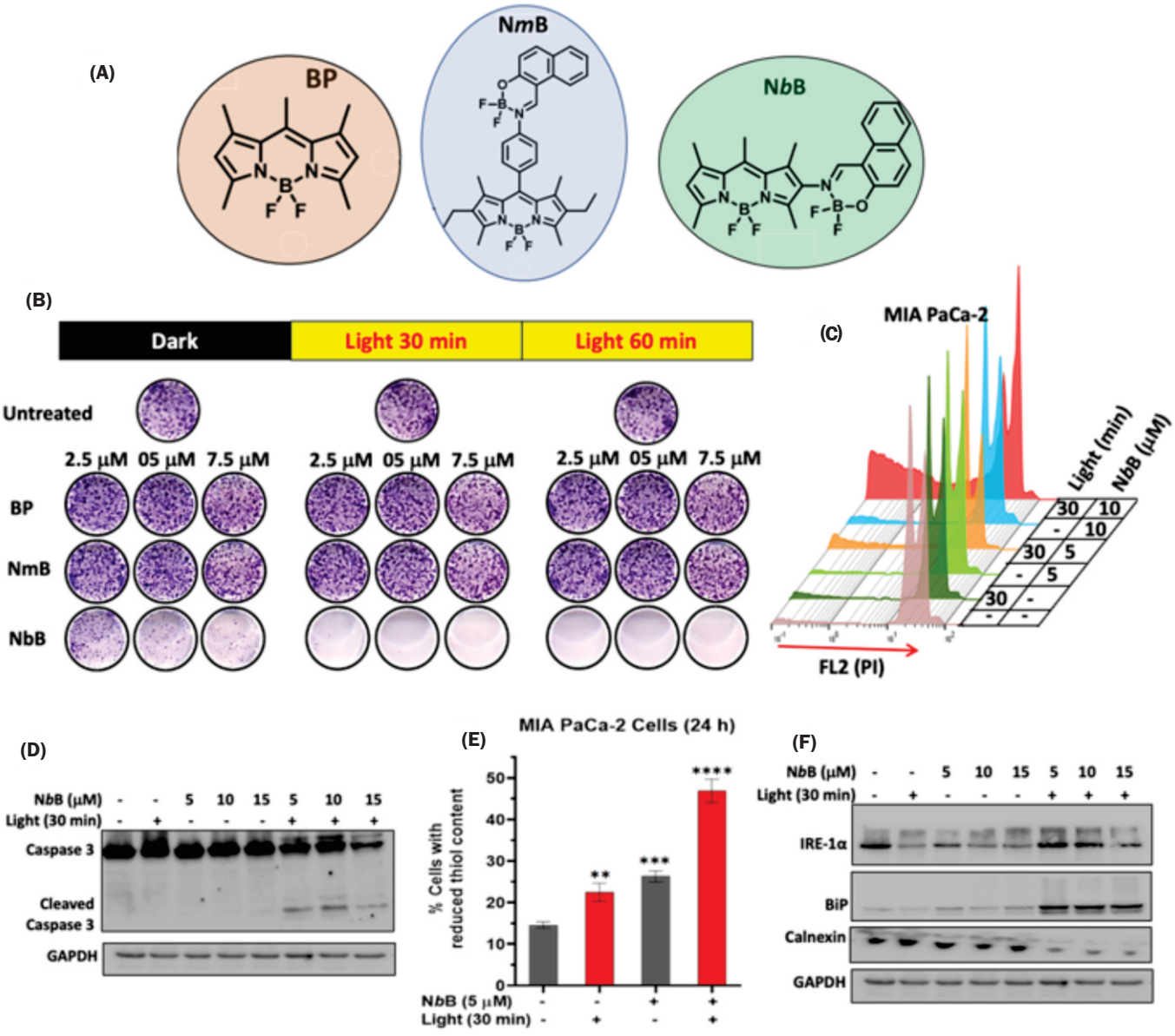

Fig.1: (A) Structure of BP, NmB and NbB. (B) Photosensitization effects of BP, NmB and NbB in MIA-PaCa-2 PDAC cells. (C, D) Sub-G1 and Caspase 3 activation analysis in response to photosensitizing effects of NbB in MIA-PaCa-2 PDAC cells. (E) Flowcytometry analysis of GSH (monobromobimane) content in cells in response to photosensitizing effects of NbB, (F) NbB mediated induction of ER stress in MIA-PaCa-2 PDAC cells in the presence/absence of light. (Adopted from our previous report[8]).

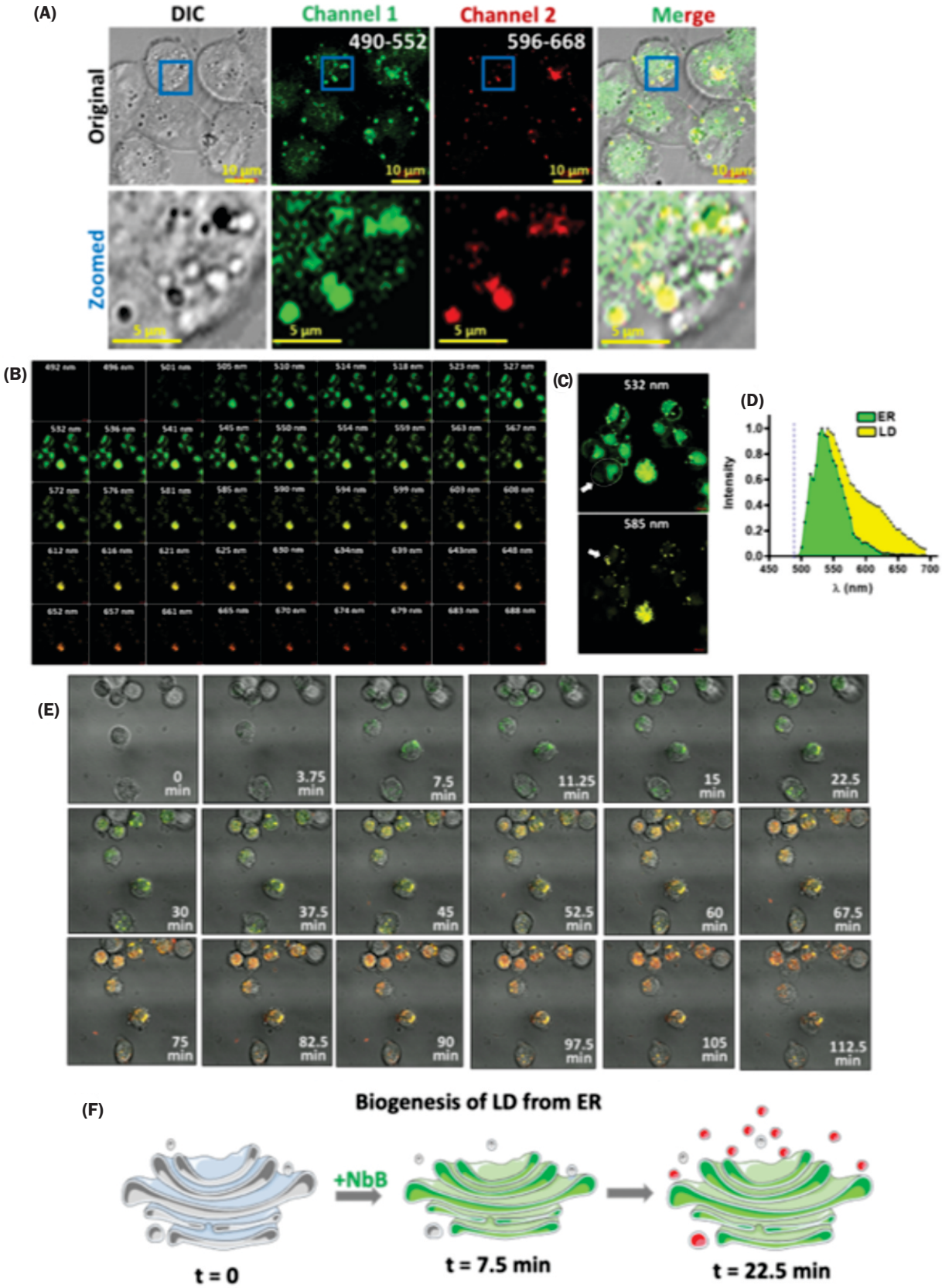

Fig.2: (A) Confocal microscopic analysis of the distribution of NbB in MIA-PaCa-2 cells, acquired in DIC, green and red channel. (B) Lambda mode spectral scanning of NbB emission in MIA-PaCa-2 cells in the range of 492-688 nm, upon excitation with 488 nm laser. (C, D) Representative images of above experiment at 532 nm and 585 nm were shown in C. ER and LD specific ROIs were marked and indicated with an arrow. Emission spectra of NbB in ER and LD specific ROIs, respectively, were shown. (E, F) Kinetics of cellular uptake of NbB and its distribution in ER and LDs in MIA-PaCa-2 cells. (Adopted from our previous report[8]).

Results and Discussion

In order to assess the photosensitization effects, PDAC (MIA-PaCa-2) cells were incubated with BP, N*m*B and N*b*B for 30 min and exposed to visible light for different time periods (Fig.1B). Our results revealed that BP and N*m*B were not effective in killing MIA-PaCa-2 cells in the dark or upon light exposure. Interestingly, N*b*B induced robust photokilling of the PDAC cells in a concentration and light dose dependent manner (Fig.1B). Dark toxicity was apparent only at higher concentrations of N*b*B. Further, Combenefit software-based

analysis showed a strong synergistic interaction of N*b*B and light for the photokilling of PDAC cells. Together, our result confirms the photosensitizing ability of N*b*B while BP and N*m*B do not have any PDT properties. Further, N*b*B found to induce robust apoptosis in MIA-PaCa-2 in the presence of light, as assessed for induction of sub-G1 by flow cytometry (Fig.1C). Similar photosensitization effects were also observed with other PDAC (PANC-1) cells. In corroboration with sub-G1 data, NbB treatment induced photoactivation of caspase-3 through its cleavage (Fig.1D). Mechanistically, NbB induced oxidative stress through lowering of cellular glutathione level and damaged ER, leading to ER stress (Fig.1E). Upon light exposure, NbB elicited the level of IRE-1α and BiP and reduced calnexin level significantly, indicating the induction of ER stress in PDAC cells by N*b*B (Fig. 1F).

Considering the impressive photosensitization properties of N*b*B, we ventured to explore its cellular distribution and photoimaging properties of N*b*B. Confocal microscopy analysis revealed a rapid cellular uptake of N*b*B, where N*b*B is localized to ER and LDs. Interestingly, upon excitation at single wavelength (488 nm), N*b*B fluoresces green in ER while it appeared both green and red in LD particles, due to polar and non-polar milieu in these two organelles, respectively (Fig. 2A).

To further confirm the dual emission fluorescence of N*b*B in ER and LDs, the fluorescence emission of the spectrum of the dye in ER and LDs was assessed by Lambda Scanning Mode (LSM) in confocal microscopy. Our data showed fluorescence emission of N*b*B in the region of 505-565 nm while fluorescence emission drops sharply at >570 nm in ER-specific ROI (region of interest), when 488 nm excitation wavelength was used (Fig.2B-D). In contrast, fluorescence emission of N*b*B was significantly retained in both green (505-565 nm) and red channels (570-638 nm) in LD specific ROI, upon excitation with 488 nm laser (Fig.2B-D). These results showed that, both ER and LD can be simultaneously visualized with one probe i.e., N*b*B at single excitation wavelength. Next, colocalization studies with commercially available dyes, ER (ER Tracker Red/Blue), mitochondria (Mito Tracker Red) and lysosomes (Lyso Tracker Red), showed that N*b*B is specifically localized to ER and LD with no apparent accumulation in lysosomes and mitochondria. In order to assess the kinetics of cellular distribution of N*b*B, time-lapse confocal imaging was employed. Our results showed a rapid uptake of N*b*B into ER (green fluorescence only; t = <10 min) initially, while during lipid droplet biogenesis, N*b*B was distributed to LDs and appeared as yellow punctate (due to emission of green and red fluorescence; t = >12 min) (Fig.2E-F). Of note, the above properties were observed with multiple cell lines with excellent photoimaging properties at concentrations as low as 0.5 μM.

Conclusion

Current investigation showed a first case of design of a novel single bis-chromophoric molecule with three biological functions: specific targeting of the dye/photomedicine to ER and LDs, simultaneous dual imaging of ER and LDs, robust photosensitization of pancreatic cancers, especially PDAC cells. A detailed investigation on the synthesis, photophysical/photochemical and biological properties and its effect on PDAC cells are reported elsewhere[8].

References

[1] P. Rawla, T. Sunkara, V. Gaduputi, Epidemiology of Pancreatic Cancer: Global Trends, Etiology and Risk Factors, World J Oncol., 2019, 10, 10–27. https://doi.org/10.14740/wjon1166.

[2] V. Karimnia, F.J. Slack, J.P. Celli, Photodynamic Therapy for Pancreatic Ductal Adenocarcinoma, Cancers (Basel), 2021, 13, 4354. https://doi.org/10.3390/cancers13174354.

[3] M.T. Huggett, M. Jermyn, A. Gillams, R. Illing, S. Mosse, M. Novelli, E. Kent, S.G. Bown, T. Hasan, B.W. Pogue, S.P. Pereira, Phase I/II study of verteporfin photodynamic therapy in locally advanced pancreatic cancer, Br J Cancer 2014, 110, 1698–1704. https://doi.org/10.1038/bjc.2014.95.

[4] S. Oyadomari, E. Araki, M. Mori, Endoplasmic reticulum stress-mediated apoptosis in pancreatic beta-cells, Apoptosis, 2002, 7, 335–345. https://doi.org/10.1023/a:1016175429877.

[5] S. Li, Y. Chen, Y. Wu, S. Yao, H. Yuan, Y. Tan, F. Qi, W. He, Z. Guo, An Endoplasmic Reticulum Targeting Type I Photosensitizer for Effective Photodynamic Therapy against Hypoxic Tumor Cells, Chemistry – A European Journal, 2022, 28, e202202680. https://doi.org/10.1002/chem.202202680.

[6] J. Li, D. Gu, S.S.-Y. Lee, B. Song, S. Bandyopadhyay, S. Chen, S.F. Konieczny, T.L. Ratliff, X. Liu, J. Xie, J.-X. Cheng, Abrogating cholesterol esterification suppresses growth and metastasis of pancreatic cancer, Oncogene, 2016, 35, 6378–6388. https://doi.org/10.1038/onc.2016.168.

[7] L. Guo, M. Tian, Z. Zhang, Q. Lu, Z. Liu, G. Niu, X. Yu, Simultaneous Two-Color Visualization of Lipid Droplets and Endoplasmic Reticulum and Their Interplay by Single Fluorescent Probes in Lambda Mode, J. Am. Chem. Soc., 2021, 143, 3169–3179. https://doi.org/10.1021/jacs.0c12323.

[8] N. Chauhan, M. Koli, R. Ghosh, A.G. Majumdar, A. Ghosh, T.K. Ghanty, S. Mula, B.S. Patro, A BODIPY-Naphtholimine-BF2 Dyad for Precision Photodynamic Therapy, Targeting, and Dual Imaging of Endoplasmic Reticulum and Lipid Droplets in Cancer, JACS Au, 2024, 4, 2838–2852. https://doi.org/10.1021/jacsau.3c00539.

न्यूरोएंडोक्राइन ट्यूमर का पीईटी-प्रतिबिंबन

2

^{68}Ga-NODAGA-JR11 के सरल और सुविधाजनक संरूपण हेतु एकल-वॉयल किट का विकास : न्यूरोएंडोक्राइन ट्यूमर के निदान हेतु पीईटी कर्मक

कुसुम वत्स* और दृष्टी सतपति
रेडियोफार्मास्यूटिकल्स प्रभाग ,भाभा परमाणु अनुसंधान केंद्र ,ट्रांबे ,400085-भारत

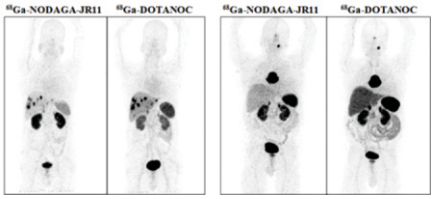

नेट रोगियों में ^{68}Ga-NODAGA-JR11 और ^{68}Ga-DOTANOC का पी. ई. टी./सीटी स्कैन

सारांश

^{68}Ga-NODAGA-JR11 न्यूरोएंडोक्राइन ट्यूमर की PET-प्रतिबिंबन के लिए एक आशाजनक सोमैटोस्टैटिन एंटागोनिस्ट के रूप में उभरा है। मानव कैंसर रोगियों में कारक की आरंभिक के सफलता पूर्ण मूल्यांकन हेतु आगे के बहु-केंद्रित नैदानिक परीक्षणों की आवश्यकता है। अस्पताल रेडियोफार्मेसी में ^{68}Ga-NODAGA-JR11 का एकल-चरण निर्माण बहु-केंद्र परीक्षणों को सुविधाजनक बनाने वाले अस्पतालों की बढ़ती भागीदारी को प्रोत्साहित करेगा। इस प्रकार, ^{68}Ga-NODAGA-JR11 के सुविधाजनक निर्माण के लिए फ्रीज-ड्राय किट विकसित किए गए और न्यूरोएंडोक्राइन कैंसर रोगियों में प्रारंभिक नैदानिक अध्ययन किए गए। सरूपित किट ^{68}Ga-NODAGA-JR11 ने प्राथमिक और साथ ही मेटास्टेटिक घावों में उच्च अवशोषण प्रदर्शित किया।

PET-imaging of Neuroendocrine Tumors

2

Development of Single-vial Kit for Simple and Convenient Formulation of ^{68}Ga-NODAGA-JR11: PET Agent for Diagnosis of Neuroendocrine Tumor

Kusum Vats* and Drishty Satpati
Radiopharmaceuticals Division, Bhabha Atomic Research Centre, Trombay-400085, INDIA

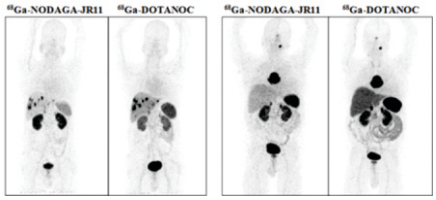

PET/CT scan of ^{68}Ga-NODAGA-JR11 and ^{68}Ga-DOTANOC in NET patients

ABSTRACT

^{68}Ga-NODAGA-JR11 has emerged as a promising somatostatin antagonist for PET-imaging of neuroendocrine tumors. Preliminary success of the agent necessitates further multi-centric clinical trials for complete evaluation in human cancer patients. Single-step formulation of ^{68}Ga-NODAGA-JR11 at hospital radiopharmacy shall encourage increased participation of hospitals facilitating multi-centre trials. Thus, freeze-dried kits were developed for convenient formulation of ^{68}Ga-NODAGA-JR11 and preliminary clinical studies were performed in neuroendocrine cancer patients. Kit formulated ^{68}Ga-NODAGA-JR11 exhibited high uptake in primary as well as metastatic lesions.

KEYWORDS: *NODAGA-JR11, Neuroendocrine tumor, Somatostatin antagonist, Freeze-dried kit, PET/CT imaging*

*Author for Correspondence: Kusum Vats
E-mail: vkusum@barc.gov.in

Introduction

^{68}Ga-NODAGA-JR11 (^{68}Ga-OPS202), a novel radiolabeled somatostatin receptor (sstr) antagonist exhibiting high affinity towards sst_2 receptors, has emerged as a promising radiotracer for PET imaging of neuroendocrine tumors (NETs) [1,2]. Radiolabeled somatostatin agonists have shown great clinical value in diagnosis and management of patients with NETs [3,4]. However, recent literature reports have shown that radiolabeled somatostatin antagonists may perform better than radiolabeled somatostatin agonists in terms pharmacokinetics and tumor visualization [5,6]. Amongst the several somatostatin antagonists investigated, ^{68}Ga-NODAGA-JR11 has demonstrated encouraging results. Consequently, ^{68}Ga-NODAGA-JR11 has now reached phase-II clinical trials for detection of NETs [1,5]. ^{68}Ga-NODAGA-JR11 is reported to exhibit higher sensitivity and better image contrast than ^{68}Ga-labeled sstr agonists (^{68}Ga-DOTA-TATE/TOC/NOC) in detection of NETs [5,6]. The higher sensitivity is attributed to lower uptake of ^{68}Ga-NODAGA-JR11 in liver, intestine and pancreas in contrast to ^{68}Ga-labeled sstr agonists.

The simple kit-type radiolabeling would encourage hospitals to participate and facilitate the evaluation of ^{68}Ga-NODAGA-JR11 in broader patient population. Freeze-dried kits containing pre-assembled sterile ingredients in dry powder form allow for simple and hassle-free preparation of the radiopharmaceutical at hospital radiopharmacy [7]. The single-vial kit is particularly attractive for formulation of ^{68}Ga-radiopharmaceuticals as the short half-life of Ga-68 ($t_{½}$ = 68 min) necessitates for rapid and robust radiolabeling protocol.

Present study reports optimization of different parameters for successful development of a single-vial NODAGA-JR11 freeze-dried kit. The kits were formulated with $^{68}GaCl_3$ eluted from ITG ^{68}Ge/^{68}Ga generator (Isotope Technologies, GmbH, Germany) and evaluated in patients with NET.

Materials and Methods

Optimization of radiolabeling parameters for NODAGA-JR11 (piCHEM, Austria) was carried out by addition of $^{68}GaCl_3$ (0.05 N HCl) from ^{68}Ge/^{68}Ga generator (ITG, Germany). Radiolabeling was performed varying different parameters such as amount of peptide, amount of buffer, incubation time and temperature to optimize conditions prior to kit formulation. Freeze-dried NODAGA-JR11 kits were prepared based on the optimized wet chemistry protocol. A 10 vial batch of JR11 kits was prepared with each kit vial containing 50 µg NODAGA-JR11 and 11.5 mg sodium acetate.

For the kit-based preparation of ^{68}Ga-NODAGA-JR11,$^{68}GaCl_3$ (2 mL, 3-15 mCi) eluted in 0.05 N HCl was added and the reconstituted kit vial was incubated at 90^{0}C for 10 min. Radiochemical yield of ^{68}Ga-NODAGA-JR11 was determined by performing paper chromatography (PC) and reversed phase high performance liquid chromatography (RP-HPLC).

In vitro stability of the kit-formulated ^{68}Ga-NODAGA-JR11 was evaluated at 1 h and 2 h post preparation. Long term shelf-life of kits was assessed by reconstitution at periodic intervals (1 month and 3 months) and subsequent analysis of the radiolabeling yield. The pharmacokinetics of kit formulated ^{68}Ga-NODAGA-JR11 was studied by performing biodistribution studies in normal Swiss mice. Preliminary clinical evaluation of kit-formulated ^{68}Ga-NODAGA-JR11 was carried out in AIIMS, Bhubaneswar after obtaining approval from institutional ethical committee clearance.

Results and Discussion

^{68}Ga-NODAGA-JR11 could be formulated using freeze-dried kits in >95% radiochemical yield (Fig. 1). Kit-formulated ^{68}Ga-NODAGA-JR11 stored at room temperature was observed to be stable till 2 h post-reconstitution as there was no significant change in the HPLC profile. Freeze-dried kits have

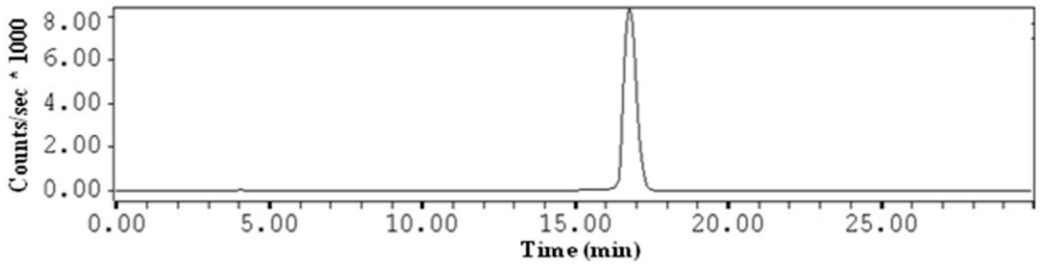

Fig.1: Radio-HPLC chromatogram of ^{68}Ga-NODAGA-JR11 formulated using freeze-dried kit.

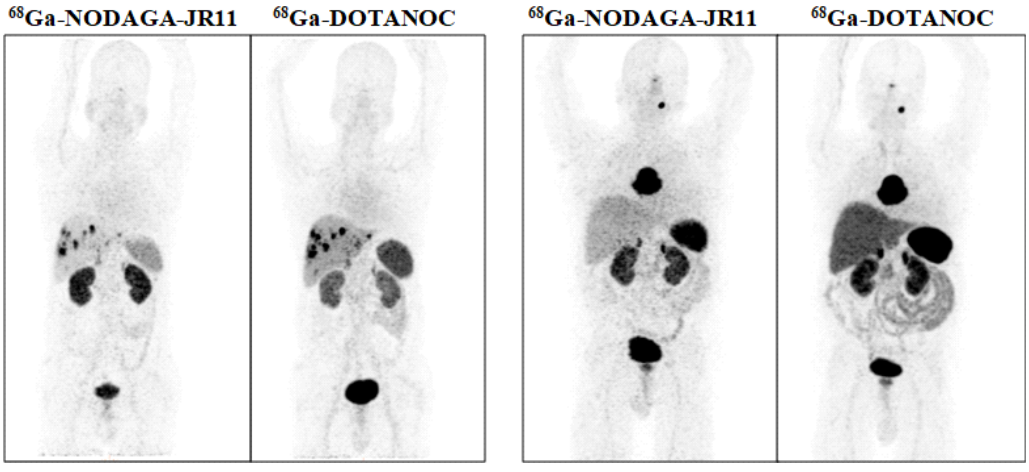

Fig.2: PET/CT scan of ^{68}Ga-NODAGA-JR11 and ^{68}Ga-DOTANOC in NET patients.

been tested to be stable till 3 months post-preparation when stored at 0°C.

Preliminary clinical evaluation in NET patients indicated high uptake in primary as well as metastatic lesions. Comparative PET/CT images with ^{68}Ga-DOTA-NOC (in the same patient) suggested comparable tumor uptake but better liver and background clearance for ^{68}Ga-NODAGA-JR11. Present studies indicate promising potential of ^{68}Ga-NODAGA-JR11 towards detection of liver metastatic lesions (Fig. 2).

Conclusion

Single-vial NODAGA-JR11 freeze-dried kits amenable for formulation with $^{68}GaCl_3$ eluted in 0.05 N HCl from ITG ^{68}Ge/^{68}Ga generator was developed. These kits resulted in simple and quick preparation of ^{68}Ga-NODAGA-JR11 in high yields. Kit-formulated ^{68}Ga-NODAGA-JR11 could clearly identify the primary as well as metastatic lesions with good accuracy and specificity in patients with NETs. The facile formulation of ^{68}Ga-NODAGA-JR11 using the freeze-dried kit provides a valuable advantage, facilitating its use in clinical settings.

Acknowledgement

Authors are thankful to Dr. P. K. Mohapatra, Associate Director, Radiochemistry & Isotope Group and Dr. Tapas Das, Head, Radiopharmaceuticals Division for their support and encouragement. Authors acknowledge the help rendered by the staff of the animal house facility of Bhabha Atomic Research Centre. The authors are also thankful to Dr. Kanhaiya Agrawal of AIIMs, Bhubaneswar for performing the clinical evaluation studies.

References

[1] G. P. Nicolas, S. Beykan, H. Bouterfa, J. Kaufmann , A. Bauman, M. Lassmann, J. C. Reubi, J. E. F. Rivier, H. R. Maecke, M. Fani and D. Wild, Safety, Biodistribution, and Radiation Dosimetry of 68Ga-OPS202 in Patients with Gastroenteropancreatic Neuroendocrine Tumors: A Prospective Phase I Imaging Study, Journal of Nuclear Medicine, 2018, 59, 909-914.

[2] M. Fani, F. Braun, B. Waser, K. Beetschen, R. Cescato, J. Erchegyi, J. E. Rivier, W. A. Weber, H. R. Maecke and J. C. Reubi, Unexpected Sensitivity of sst2 Antagonists to N-Terminal Radiometal Modifications, Journal of Nuclear Medicine, 2012, 53, 1481-1489.

[3] M. M. Graham, X. Gu, T. Ginader, P. Breheny and J. J. Sunderland, 68Ga-DOTATOC Imaging of Neuroendocrine Tumors: A Systematic Review and Meta-analysis. Journal of Nuclear Medicine, 2017, 58, 1452–1458.

[4] FDA Letter of Approval for NETSPOTTM. [(accessed on 05 April 2024)]; Available online:https://www.accessdata.fda.gov/drugsatfda_docs/appletter/2016/208547Orig1s000ltr.pdf

[5] G. P. Nicolas, N. Schreiter, F. Kaul, J. Uiters, H. Bouterfa, J. Kaufmann, T. E. Erlanger, R. Cathomas, E. Christ, M. Fani and D. Wild, Sensitivity Comparison of 68Ga-OPS202 and 68Ga-DOTATOC PET/CT in Patients with Gastroenteropancreatic Neuroendocrine Tumors: A Prospective Phase II Imaging Study, Journal of Nuclear Medicine, 2018, 59, 915-921.

[6] Z. Lin, R. Lin, J. Zhang, S. Yao and W. Miao, 68Ga-DOTATATE and 68Ga-NODAGA-JR11 PET/CT Images in a Patient With Gastric Neuroendocrine Tumor, Clinical Nuclear Medicine, 2021, 46, 853-855.

[7] K. Vats, R. Sharma, M. Kameswaran, D. Satpati and A. Dash, Single vial cold kits optimized for preparation of gastrin releasing peptide receptor (GRPR)-radioantagonist 68Ga-RM2 using three different 68Ge/68Ga generators. Journal of Pharmaceutical and Biomedical Analysis, 2019, 163, 39-44.

कैंसर का चयनात्मक लक्ष्यीकरण

3

कैंसर प्रभावी अंगों (स्थानों) की बेहतर स्थिरता और प्रभावी लक्ष्यीकरण के लिए पेप्टाइड रूपांतरण कार्यनीतियाँ

दृष्टी सतपति [1,2]*, **अमित कुमार शर्मा** [2] **और रोहित शर्मा** [1,2]

[1]रेडियोफार्मास्युटिकल्स प्रभाग, भाभा परमाणु अनुसंधान केंद्र, ट्रांबे-४०००८५, भारत

[2]होमी भाभा राष्ट्रीय संस्थान ,अणुशक्ति नगर, मुंबई-400094, भारत

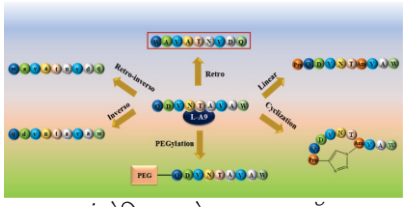

संशोधित A9 पेप्टाइड एनालॉग
(सबसे अच्छा एनालॉग, रेट्रो A9 बॉक्स में इंगित)

सारांश

पेप्टाइड्स, ट्यूमर कोशिकाओं पर उच्च घनत्व में निष्पीडित रिसेप्टर्स (अभिग्राही) के प्रति उत्कृष्ट रूप से उच्च चयनात्मकता वाले आकर्षक अणु हैं। हालांकि, पेप्टाइड्स की एंजाइमेटिक संवेदनशीलता चरणबद्ध निम्नीकरण की ओर ले जाती है जिसके परिणामस्वरूप कम लक्ष्य संचय का तीव्र निष्कासन होता है। यहाँ स्तन कैंसर में बढ़े हुए HER 2-रिसेप्टर स्तरों को लक्षित करने वाले मूल A9 पेप्टाइड को बेहतर चयापचय स्थिरता, कुशल लक्ष्यीकरण और अंततः कैंसर प्रभावित अंगों के आण्विक प्रतिबिंबन और चिकित्सा के लिए नैदानिक उपयोगिता हेतु विभिन्न कार्यनीतियों को अपनाकर रूपांतरित किया गया।

Selective Targeting of Cancers

3

Peptide Modification Strategies for Enhanced Stability and Effective Targeting of Cancer Sites

Drishty Satpati[1,2]*, Amit Kumar Sharma[2] and Rohit Sharma[1,2]

[1]Radiopharmaceuticals Division, Bhabha Atomic Research Centre, Trombay-400085, INDIA

[2]Homi Bhabha National Institute, Anushakti Nagar, Mumbai-400094, INDIA

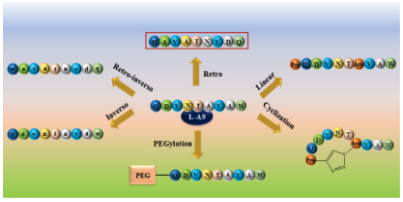

Modified A9 peptide analogs
(best analog, Retro A9 indicated in the box)

ABSTRACT

Peptides are excellently attractive molecules with high selectivity towards receptors expressed in high density on tumor cells. However enzymatic sensitivity of peptides leads to systemic degradation resulting in rapid clearance with low target accumulation. Here the original A9 peptide targeting elevated HER2-receptor levels in breast cancer was modified by adopting different strategies for improved metabolic stability, efficient targeting and ultimately clinical utility for molecular imaging and therapy of cancer sites.

KEYWORDS: *HER2, Lu-177, D-peptide, Retro peptide, Click chemistry*

**Author for Correspondence: Drishty Satpati*
E-mail: drishtys@barc.gov.in

Introduction

Rapid rise in cancer cases worldwide is an alarming situation demanding essential development of cancer specific molecules for precise molecular imaging and treatment of the disease. Breast cancer is the most prevalent cancer in human population accounting for highest mortality (15.5%) amongst women [1]. However, detection at an early stage through radiolabeled peptides targeting elevated receptor (HER2) levels shall expedite treatment thereby improving the chances of survival [2].

Peptides serve as wonder probes by virtue of their high selectivity towards the target (receptors) and favorable biological profile (high tumor penetration, quick blood clearance, low toxicity) [3]. Besides, simple synthetic methodologies with options allowing suitable modification, is an added advantage of peptides. However, peptides are highly sensitive towards enzymatic degradation leading to rapid kidney clearance thereby reducing bioavailability and target accumulation limiting their clinical applicability. To overcome these limitations several modification strategies can be adopted to confer enzymatic resistance to peptides: (i) introduction of polyethylene glycol (PEG); (ii) cyclization; (iii) incorporation of D-amino acids (inverso peptide); (iv) arrangement of D-amino acids in reverse order (retro-inverso peptide); (v) arrangement of L-amino acids in reverse order (retro peptide). In this regard, A9 peptide (QDVNTAVAW) targeting HER2-receptors overexpressed in breast cancer was synthesized and above-mentioned modifications were conferred to the original peptide.

Materials and Methods

Peptides, DOTA-A9, DOTA-PEG_4-A9 (pegylated), DOTA-c[Tz]A9 (cyclic), DOTA-D-A9 (inverso), DOTA-rD-A9 (retro-inverso) and DOTA-rL-A9 (retro) were synthesized manually by Fmoc solid-phase peptide synthesis (Fig. 1).

Cyclic peptide was prepared by introduction of azide functional group bearing azidoalanine (Aza) and alkyne bearing propargyl glycine (Pra): *Pra*-Gln-Asp-Val-Asn-Thr-*Aza*-Val-Ala-Trp-NH_2. Cyclization of the linear peptide [Pra, Aza]A9 was performed on solid phase by Cu(I)-catalyzed 'click chemistry' reaction. The inverso peptide was synthesized by substituting L-amino acids with D-amino acids. The retro- and retro-inverso A9 peptide variants were prepared by coupling of L-amino acids and D-amino acids respectively in reverse order (swapping of C- and N-terminal). Purified and characterized peptides were radiolabeled with Lu-177. CD spectra were recorded to obtain information about the secondary structure stabilization of modified peptides. Molecular docking studies were performed to analyse the change in interaction of the peptide sequence with the receptor. Biological efficacy was tested in HER2-positive SKBR3 cells and SKBR3 tumor-bearing SCID female mice xenografts.

Results and Discussion

The original A9 peptide, [^{177}Lu]Lu-DOTA-A9 exhibited quite low tumor uptake, rapid urinary clearance and poor metabolic stability. Introduction of PEG_4 moiety could not improve the tumor uptake or metabolic stability to significant levels [4]. Hence with an aim to impart conformational rigidity and improve the pharmacokinetic pattern the A9 peptide was cyclized and triazole as peptide bond isostere was introduced. Enhanced conformational stability was confirmed by CD spectral studies (Fig. 2a) and molecular modelling studies established retention of binding efficiency towards the receptor. Improved metabolic stability and higher retention in the tumor was observed for [^{177}Lu]Lu-DOTA-c[Tz]A9. To further improvise the pharmacokinetic features all L-amino acids were replaced by D-amino acids. D-amino acids having chirality

Fig.1: Solid Phase Peptide Synthesis Facility Set-Up.

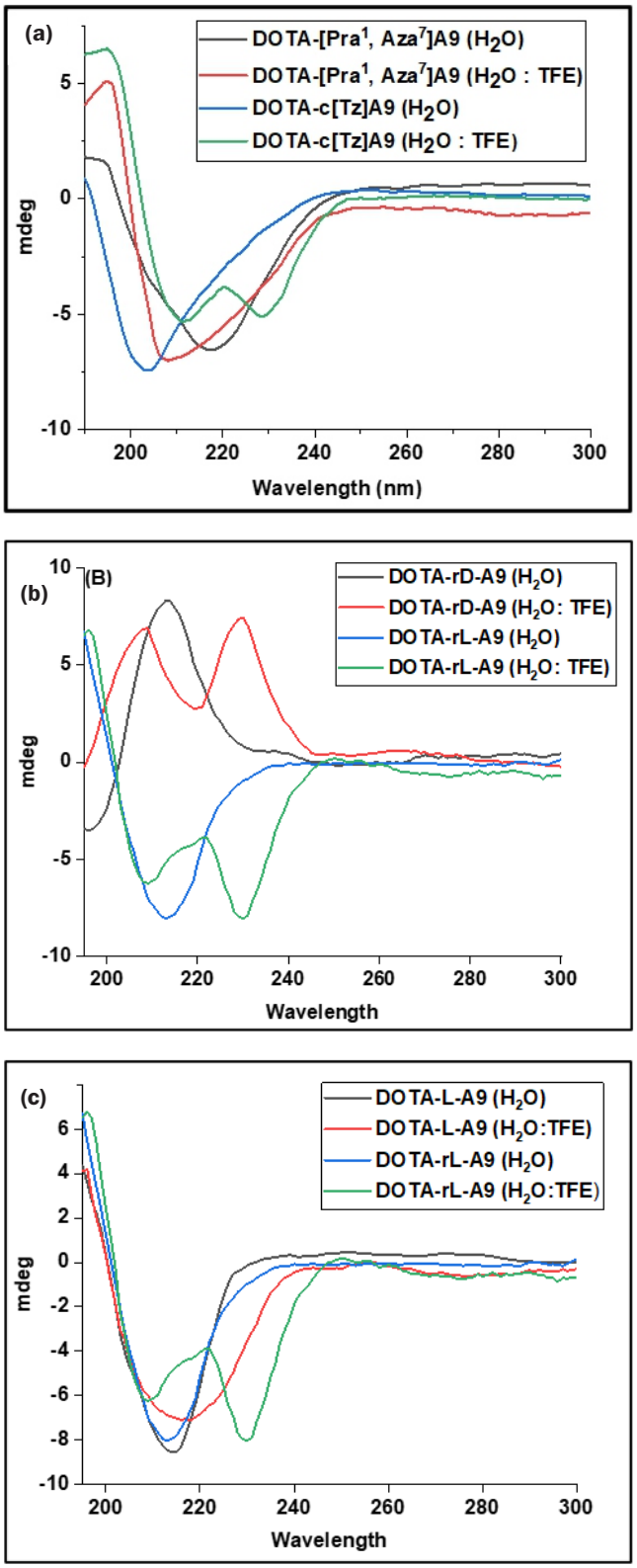

Fig.2: CD spectra of (a) DOTA-c[Tz]A9, (b) DOTA-rD-A9, (c) DOTA-rL-A9.

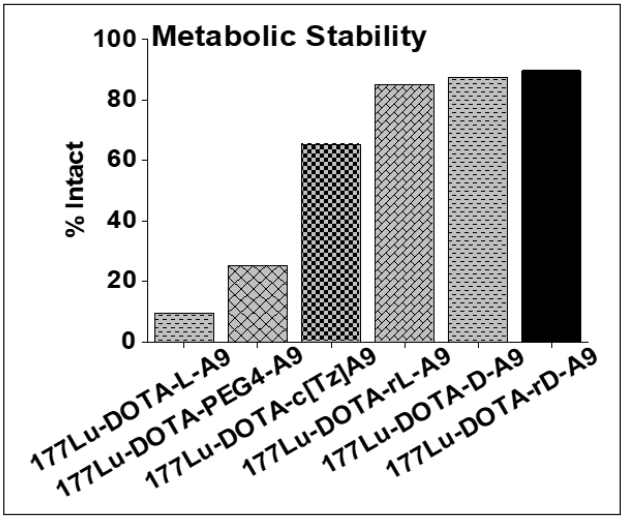

Fig.3: Metabolic stability of modified A9 peptide analogs.

opposite to that of L-amino acids are not recognized by enzymes and hence confer resistance towards enzymatic degradation leading to enhanced metabolic stability. The CD spectra of D-amino acids incorporated peptides, DOTA-D-A9 and DOTA-rD-A9 was observed to be mirror image of their respective L-peptides, DOTA-L-A9 and DOTA-rL-A9 highlighting the opposite chirality of D- and L-amino acids (Fig. 2b). The inverso analogue, [^{177}Lu]Lu-DOTA-D-A9 despite being metabolically stable, did not exhibit any improvement in tumor accumulation over the original L-peptide. The retro-inverso analog, [^{177}Lu]Lu-DOTA-rD-A9 however exhibited high metabolic stability along with enhanced tumor accumulation.

The retro A9 analogue, DOTA-rL-A9 demonstrated enhanced conformational stability (CD spectra, Fig. 2c) and significantly enhanced receptor interaction (molecular modeling) [5]. Arrangement of L-amino acids in reverse direction results in topochemical similarity to the D-peptide hence leading to higher metabolic stability than the original L-peptide. The retro A9 analogue, [^{177}Lu]Lu-DOTA-rL-A9 demonstrated excellent pharmacokinetic features (high tumor uptake and retention, rapid clearance) amongst all the analogues studied resulting in a promising and an efficient radiopharmaceutical.

Conclusion

Amongst the several strategies adopted for modification of HER2-targeting A9 peptide for boosting the metabolic stability (Fig. 3) and bioavailability, best attributes were

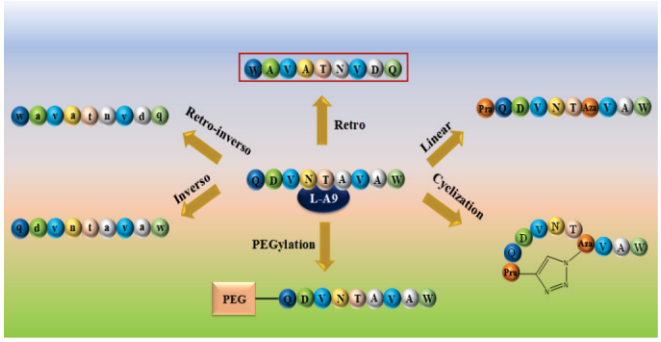

Fig.4: Modified A9 peptide analogs (best analog, Retro A9 indicated in the box).

demonstrated by the retro peptide, rL-A9 (Fig. 4). Arrangement of L-amino acids in reverse manner alters the backbone of peptides resulting in change in bond angles and bond lengths affecting the overall conformation. Thus, better pharmacokinetic features of retro peptide indicate plausible involvement and interaction of the peptide backbone amide groups with the receptor whereby enhanced conformational stability might have induced better receptor fitting.

Acknowledgement

Authors are grateful to Dr. Tapas Das, Head, Radiopharmaceuticals Division, and Dr. P. K. Mohapatra, Associate Director, Radiochemistry & Isotope Group for their constant support.

References

[1] B.S. Chhikara and K. Parang, Global Cancer Statistics 2022: The trends projection analysis, Chem. Biol. Lett., 2023, 10(1), 451.

[2] C.F. Ramogida and C. Orvig, Tumor targeting with radiometals for diagnosis and therapy, Chem. Commun., 2013, 49(42), 4720.

[3] M. Langer and A. Beck-Sickinger, Peptides as carrier for tumor diagnosis and treatment, Anticancer Agents Med Chem., 2001, 1(1), 71.

[4] A.K. Sharma, R. Sharma, K. Vats, H.D. Sarma, A. Mukherjee, T. Das and D. Satpati, Synthesis and Comparative Evaluation of 177Lu-labeled PEG and non-PEG variant peptides as HER2-targeting probes, Sci. Rep., 2022, 12, 15720.

[5] A.K. Sharma, R. Sharma, H.D. Sarma, A. Mukherjee, T. Das and D. Satpati, Synthesis and 177Lu-labeling of First Retro Analog of HER2-Targeting A9 Peptide. Bioconjugate Chem., 2023, 34, 1576.

स्तन कैंसर चिकित्सा हेतु महौषध

4

टैलाज़ोपैरिब और रेस्वेराट्रोल के संयोजन से ऑटोफ़ैगी का विनियमन व्यापक डीएनए क्षति और सहक्रियात्मक कोशिका प्रेरण

गणेश पाई बेलारे [1,2] **और बिरिजा शंकर पात्रो** [1,2]*
[1]जैव-कार्बनिक प्रभाग ,भाभा परमाणु अनुसंधान केंद्र ,ट्रांबे-400085, भारत
[2]होमी भाभा राष्ट्रीय संस्थान ,अणुशक्ति नगर ,मुंबई -400094,भारत

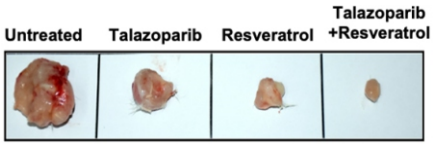

अकेले टैलाज़ोपेरिब, अकेले रेसवेराट्रोल या उनके संयोजन के साथ उपचार के बाद MCF-7 जेनोग्राफ्ट वाले एससीआईडी चूहों से निकाले गए ट्यूमर की प्रतिनिधि छवियाँ

सारांश

समरूप पुनर्संयोजन (एच. आर.) कुशल कैंसरों में पॉली (ADP-Ribose) पोलीमरेज़ अवरोधकों (PARPi) की सीमित प्रभावशीलता के कारण उनकी उपयोगिता का विस्तार करने के लिए PARPis के साथ नये औषधि संयोजनों की आवश्यकता होती है। BRCA1/2 की स्थिति की परवाह किए बिना स्तन कैंसर में PARP1 का अत्यधिक निष्पीडन कीमो-सुग्राहीकारक के साथ PARPi के प्रभावी लक्ष्यीकरण के लिए एक चिकित्सीय अवसर प्रस्तुत करती है। ऑटोफैगी स्तन कैंसर में नवीन PARPi प्रतिरोध प्रदान करता है। हमने इस अध्ययन में, स्तन कैंसर में टैलाज़ोपेरिब (BMN373, PARPi) के प्रभावों को बढ़ाने में एक प्राकृतिक अणु कीमो-सुग्राहीकारक, रेस्वेराट्रोल के व्यवहार की जांच की। रेस्वेराट्रोल ने इन-विट्रो में एचआर-कुशल स्तन कैंसर कोशिकाओं में टैलाज़ोपेरिब-प्रेरित कोशिका मृत्यु (क्षय) को प्रभावी ढंग से संवेदनशील बनाया। रेस्वेराट्रोल विषम टैलाज़ोपेरिब प्रेरित प्रो-सर्वाइवल ऑटोफैजिक फ्लक्स, लाइसोसोमल-मेम्ब्रेन-पारगम्यता (एल. एम. पी.) के माध्यम से ऑटोफैगोसोम-लाइसोसोम संलयन को कम करके, टैलाज़ोपेरिब-प्रेरित डी. एन. ए. क्षति को बढ़ाता है। विशेष रूप से, टैलाज़ोपेरिब प्लस रेस्वेराट्रोल संयोजन ने पूर्व-नैदानिक एससीआईडी-माइस मॉडल जीवे में ट्यूमर की मात्रा को प्रभावी ढंग से कम किया। यह काम रेस्वेराट्रोल को नैदानिक सेटिंग्स में एचआर-कुशल स्तन कैंसर के लिए टैलाज़ोपेरिब के साथ एक संभावित कीमो-सुग्राहीकारक के रूप में प्रस्तुत करता है।

Adjuvants for Breast Cancer Therapy

4

Dysregulation of Autophagy by the Combination of Talazoparib Plus Resveratrol Induces Extensive DNA Damage & Synergistic Cancer Cell Death

Ganesh Pai Bellare[1,2] **and Birija Sankar Patro**[1,2]*
[1]Bio-Organic Division, Bhabha Atomic Research Centre, Trombay-400085, INDIA
[2]Homi Bhabha National Institute, Anushakti Nagar, Mumbai-400094, INDIA

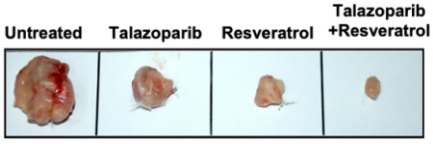

Representative images of tumours excised from SCID mice bearing MCF-7 xenografts post treatment with talazoparib alone, resveratrol alone or their combination

ABSTRACT

The limited efficacy of Poly (ADP-Ribose) polymerase inhibitors (PARP*i*) in homologous recombination (HR) proficient cancers necessitates novel drug combinations with PARP*i*s to expand their utility. Over-expression of *PARP1* in breast cancers irrespective of BRCA1/2 status presents a therapeutic opportunity for effective targetting of PARP*i* with chemo-sensitizers. Autophagy confers *de novo* PARP*i* resistance in breast cancers. In this study, we investigated the role of resveratrol, a natural molecule chemosensitizer in enhancing the effects of talazoparib (BMN673, PARPi) in breast cancers. Resveratrol effectively sensitized talazoparib-induced cell death in HR-proficient breast cancer cells *in vitro*. Resveratrol impaired talazoparib-induced pro-survival autophagic flux, by attenuating autophagosome-lysosome fusion *via* lysosomal-membrane-permeabilization (LMP), enhancing talazoparib-induced DNA damage. Notably, talazoparib *plus* resveratrol combination effectively reduced tumour volume *in vivo* in pre-clinical SCID-mice model. This work presents resveratrol as a potential chemosensitizer with talazoparib for HR-proficient breast cancers in clinical settings.

KEYWORDS: *Autophagy, Resveratrol, PARP inhibitor, Resistance, Talazoparib*

*Author for Correspondence: Birija Sankar Patro
E-mail: bisank@barc.gov.in

Introduction

Poly(ADP-Ribose) polymerase (PARP) inhibitors, used predominantly in the treatment of breast, ovarian, prostate and pancreatic cancers with homologous recombination deficiency, work on the principle of synthetic lethality [1]. Notably, this precision therapy has been marred by various intrinsic and acquired resistance mechanisms [2]. Moreover, PARP*i* therapy is by and large inefficient in HR-proficient cancers. Therefore, novel combinatorial approaches involving PARP*i* are warranted to target HR-proficient cancers and PARP*i*-resistant HR-deficient cancers which have recrudescent HR. Resveratrol (3,5,4'-trihydroxy-trans-stilbene) is a natural stilbene found in many food items such as grapes and berries. Resveratrol possesses potent anti-cancer activity and its effects, in the cellular context, are manifested through modulation of multiple pathways including autophagy [3]. Additionally, resveratrol sensitizes the effects of different drugs to better their anti-cancer potential [3]. We have previously reported that talazoparib (Tal), a potent, 3rd generation PARPi induces robust autophagic flux in cells which plays a role in *de novo* resistance to talazoparib in HR proficient breast cancer cells [4]. In the current study, we aimed to understand i) if resveratrol treatment could sensitize the effects of talazoparib in the induction of breast cancer cell death, ii) whether autophagy modulation was involved in this sensitization process.

Materials and Methods

PARP1 expression in breast cancer tissue *vis-à-vis* normal tissue was performed on the TCGA (The Cancer genomic Atlas) breast cancer dataset using Gene Expression Profiling Interactive Analysis (GEPIA) tool. For *in vitro* mechanistic analyses, MCF-7 cells breast adenocarcinoma cell line was used as the model system. Cells were routinely cultured in in Dulbecco's Modified Eagle's medium with 10 % fetal bovine serum and 1 % penicillin-streptomycin solution in a CO_2 incubator (95 % relative humidity; 5 % CO_2; 37 ^{0}C). Cell viability was assessed by MTT (3-[4,5-dimethylthiazol-2-yl]-2,5 diphenyl tetrazolium bromide) assay. Synergy analysis of the cell viability data was carried out using Combenefit software. Cumulative cell death was ascertained by clonogenic assay, and apoptosis was assessed using propidium iodide staining-based sub-G1 analysis by flow cytometry. Autophagy reporter cell lines- GFP-LC3 MCF-7 and tf-LC3 (tandem fluorescence, mRFP-EGFP-LC3)- were generated by lipofectamine-based transfection of plasmids in wild-type MCF-7 cells. These cells were further used for autophagy assessment by confocal microscopy. The level of autophagic proteins and DNA damage markers was assessed by immunoblotting. Analysis of lysosomal integrity and functional homologous recombination using flow cytometry was performed by acridine orange staining and DR-GFP reporter assay, respectively. MCF-7 xenograft SCID mice were utilized for the assessment of anti-cancer efficacy of the combination of agents. Statistical analyses (t-test, ANOVA as applicable) were performed using GraphPad Prism 5.0 software. Values indicated in graphs are Mean ± SD or SEM. Significance in *P* values are as **p*<0.05, ***p*<0.01, ****p*<0.001 compared to respective untreated/vehicle group. Inter-group comparisons are indicated wherever applicable in the graphs.

Results and Discussion

PARP1 is overexpressed in breast cancer patients

PARP1 is a vital protein contributing to a highly diverse set of essential processes in cells including DNA repair, DNA replication, transcription etc [5]. Analysis of the breast cancer patient sample dataset available in TCGA using GEPIA tool (http://gepia.cancer-pku.cn/) showed that PARP1 levels were significantly upregulated in breast cancer irrespective of BRCA1/2 status (Fig. 1A). This indicated a therapeutic opportunity in targeting PARP1 in breast cancers irrespective of HR status.

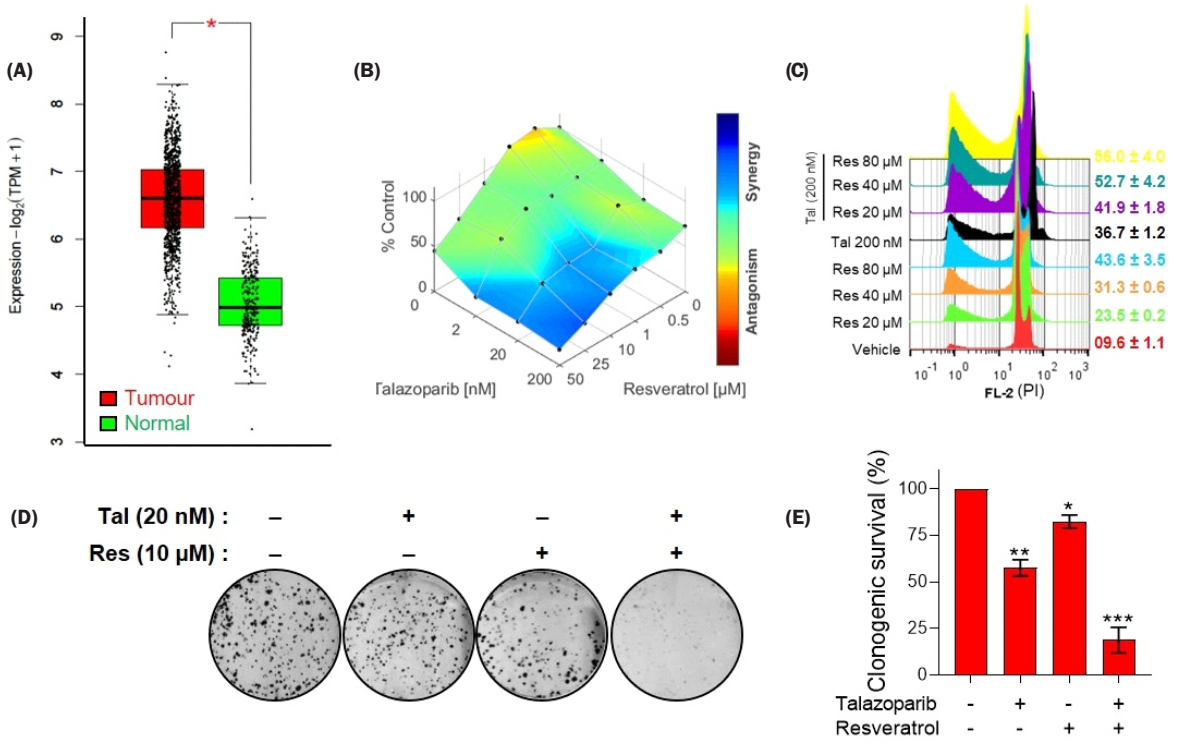

Fig.1: **Resveratrol sensitizes talazoparib induced cell death in MCF-7 cells.** *(A) PARP1 expression in breast cancer and normal patients. (B) Combenefit visualization plot for the MCF-7 cell viability assessment using MTT assay. (C) Assessment of apoptosis in MCF-7 cells by sub-G1 assay by flow cytometry. (D, E) Colony formation assay for the assessment of cumulative breast cancer cell death. (Adapted from Pai Bellare G and Patro BS, 2022[7]).*

Resveratrol sensitizes talazoparib induced cell death in breast cancer cells

Further, we assessed the effect of resveratrol (Res) in sensitizing the effects of talazoparib (Tal) in HR proficient MCF-7 breast cancer cells. MTT-based cell viability assay indicated a concentration dependent effect of individual treatments of talazoparib and resveratrol in MCF-7 cells (Fig. 1B). Interestingly, a synergistic increase was observed in the induction of cell death in MCF-7 cells in the combination of talazoparib *plus* resveratrol at multiple concentrations as indicated in Combenefit analysis. Apoptosis induction at 72 h was found to be greater in the combination of talazoparib and resveratrol compared to individual treatments (Fig. 1C). We also observed that resveratrol effectively sensitized the effects of talazoparib in MCF-7 colony formation assay compared to individual treatments (Fig. 1D, E). Together, the combination of talazoparib and resveratrol synergistically induced breast cancer cell death *in vitro*.

Autophagy is dysregulated in cells treated with the combination of talazoparib and resveratrol

Talazoparib induces pro-survival autophagy leading to *de novo* resistance to talazoparib in HR proficient MCF-7 breast cancer cells [4]. Thus, further, we ventured to assess the status of autophagy under the talazoparib, resveratrol and the combination treatment conditions. Employing EGFP-LC3 reporter transfected MCF-7 cells [6], it was observed that the number of autophagosomes as indicated by the green punctae were increased under talazoparib only, resveratrol and talazoparib *plus* resveratrol treated conditions compared to the control at 48 h, indicating a robust autophagosome formation (Fig. 2A, B).

Further, we employed tf-LC3 reporter MCF-7 cells to understand the status of the autophagic flux in cells [6]. Talazoparib alone treatment showed increased red punctae (RFP^+ and GFP^-, autophagolysosomes) indicative of an effective

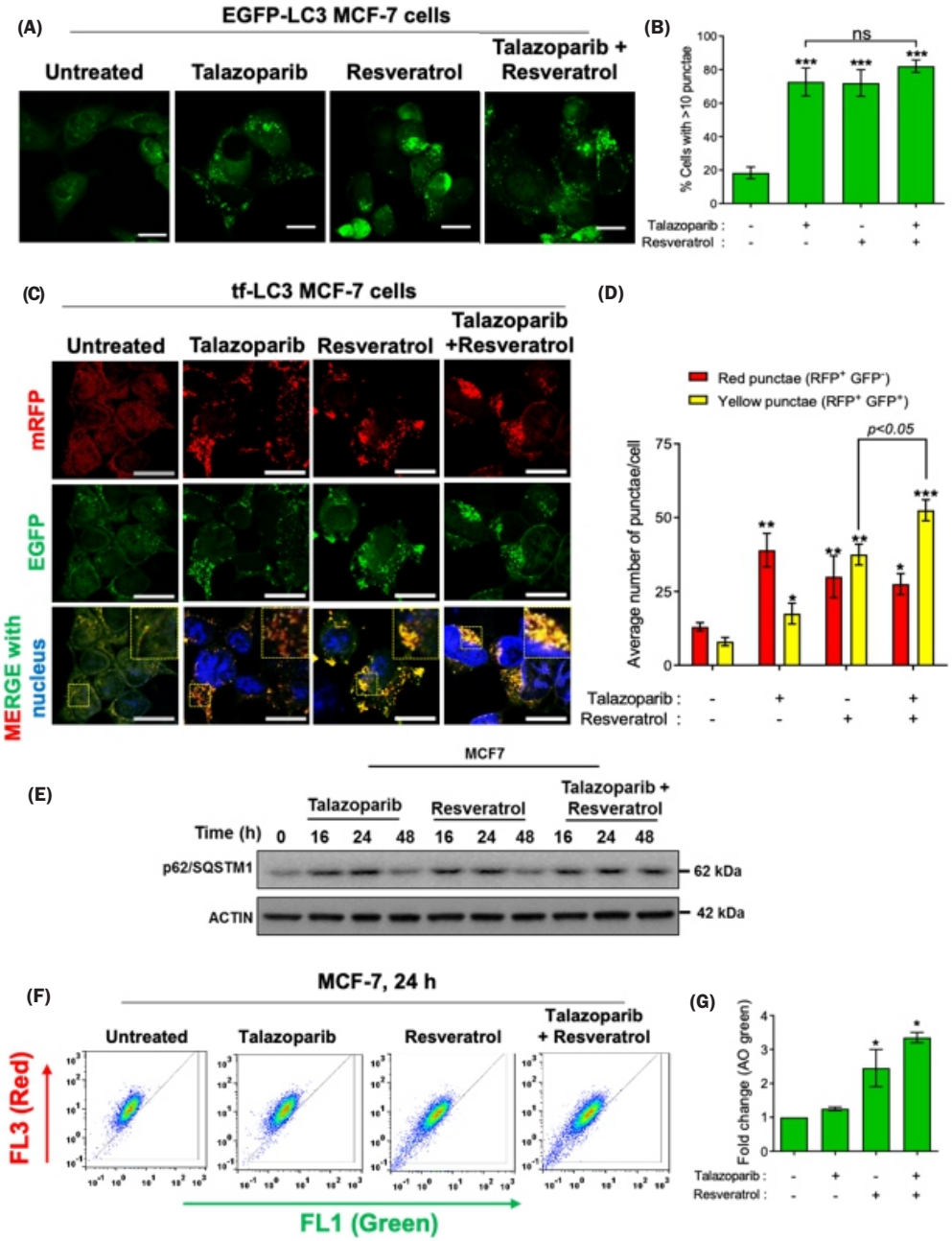

Fig.2: **Resveratrol dysregulates talazoparib induced pro-survival autophagy.** *(A, B) Determination of autophagy induction at 48 h using EGFP-LC3 stably expressing MCF-7 cells by confocal microscopy with quantification. (C, D) Assessment of autophagic flux in MCF-7 cells stably expressing tf-LC3 by confocal microscopy. (E) Immunoblot analysis showing the level of p62 and loading control β-Actin post respective treatment for 24 h. (F, G) Analysis of LMP using acridine orange (10 μM) staining assay by flow cytometry with quantification. Scale bars: 20 μm. (Adapted from Pai Bellare G and Patro BS, 2022 [7]).*

autophagic flux through fusion of autophagosomes with lysosomes at 48 h (Fig. 2C, D). Intriguingly, resveratrol treatment enhanced yellow punctae (RFP^+ and GFP^+; unfused autophagosomes), which was significantly enhanced in response to combination treatment (Fig. 2C, D), indicating the inhibition of fusion of autophagosomes with lysosomes (i.e., defective autophagy flux) in the presence of resveratrol. Similarly, p62 protein (SQSTM1, an autophagic adapter protein), whose levels decrease upon autophagic activation in a time-dependent manner, was found to be stabilized in resveratrol and combination treatment in contrast to talazoparib only treatment (Fig. 2E). Induction of lysosomal membrane permeabilization (LMP) by resveratrol leads to loss of lysosomal integrity. Acridine orange staining based flow cytometry analysis indicated a significant increase in LMP in the combination of talazoparib *plus* resveratrol compared to the talazoparib or resveratrol alone treatments at 24 h (Fig. 2F, G). This may have led to the observed inhibition or delay of the fusion of autophagosome with the lysosomes (i.e. late-stage autophagy inhibition) [8,9]. Taken together, talazoparib induced pro-survival autophagy in MCF-7 cells was significantly hampered by resveratrol treatment which may have led to the increased cell death observed in the combination treatment conditions.

Co-treatment of talazoparib and resveratrol induces extensive DNA damage and suppresses homologous recombination

Autophagy supports effective repair of DNA damage via faithful homologous recombination pathway [10]. Late stage autophagy inhibition by resveratrol under resveratrol alone and combination treatment could potentially lead to extensive DNA damage. In agreement with this, DNA damage induced by talazoparib, assessed by γ-H2AX(S139) level, was greatly enhanced by resveratrol in a concentration dependent manner at 24 h (Fig. 3A). Interestingly, resveratrol induced γ-H2AX(S139) level was further enhanced in the presence of talazoparib. Further, DR-GFP reporter based functional assay for HR showed that HR was marginally increased in talazoparib treated conditions and decreased under resveratrol treatment. Notably, HR was significantly downregulated in the combination of talazoparib and resveratrol in concordance with the inhibition of autophagy in response to resveratrol treatment (Fig. 3B, C).

Talazoparib plus resveratrol reduces tumour burden in pre-clinical models of breast cancer

The efficacy of the resveratrol mediated sensitization of PARP inhibitor effects were further evalauated in MCF-7 xenograft SCID mice model (Fig. 4A). The individual treatments of talazoparib (1 mg/kg body weight) and resveratrol (50 mg/kg body weight) reduced the tumour volume. However, the reduction in tumour volume was significantly greater upon treatment with 15 doses of the combination of talazoparib *plus* resveratrol in comparison to the individual treatments (Fig. 4A-C) with no observable side-effects. Together, the data suggested high efficacy of the combination treatment of talazoparib *plus* resveratrol over individual treatments in pre-clinical model.

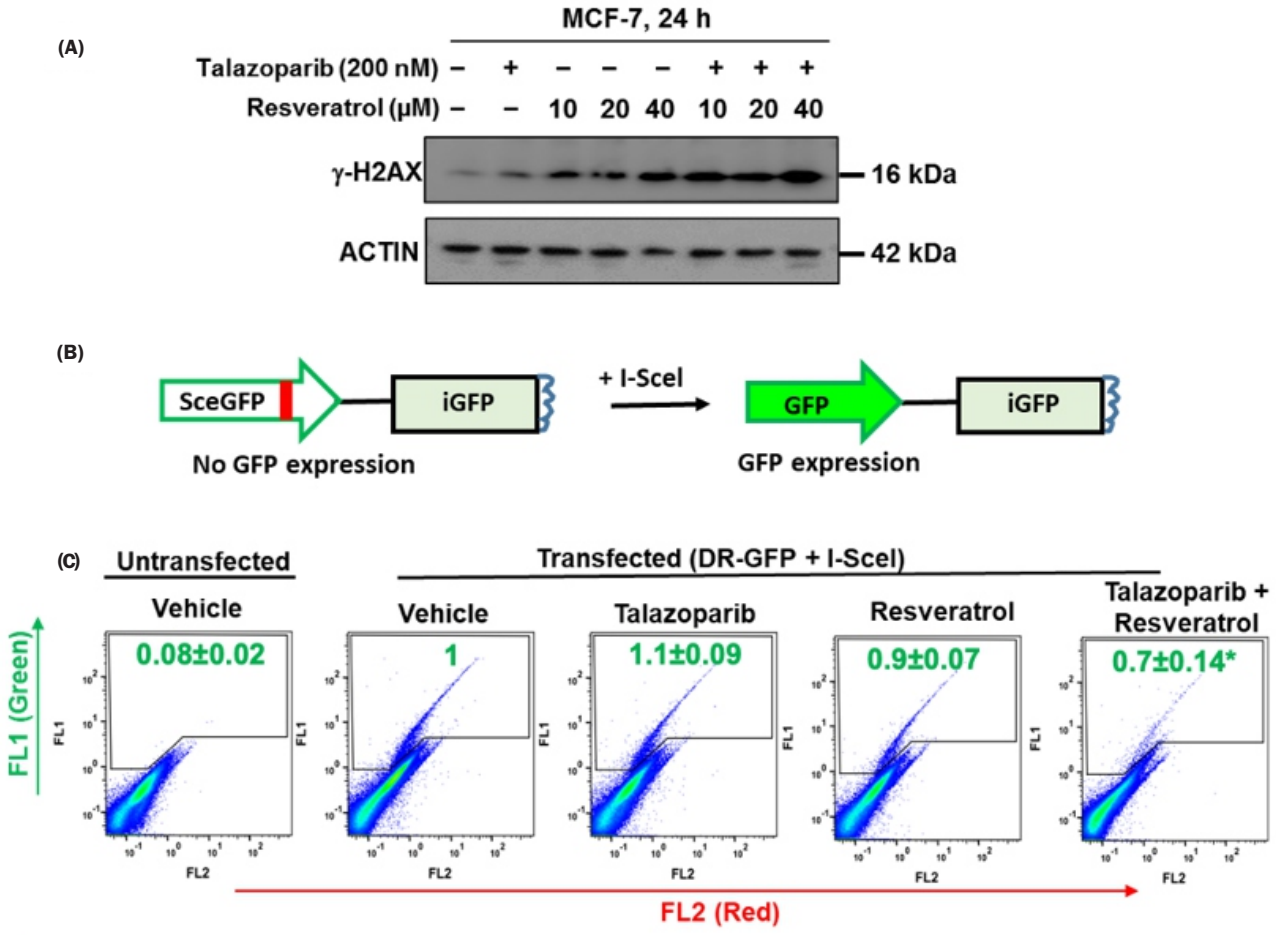

Fig.3: **Combination of talazoparib and resveratrol induces extensive DNA damage and suppresses homologous recombination.** *(A) Immunoblot analysis showing the level of DNA damage marker γ-H2AX with loading control β-Actin post indicated treatments for 24 h. (B) Scheme for the DR-GFP HR reporter assay. (C) Assessment of functional HR in the cells using DR-GFP HR reporter assay by flow cytometry. (Adapted from Pai Bellare G and Patro BS, 2022 [7]).*

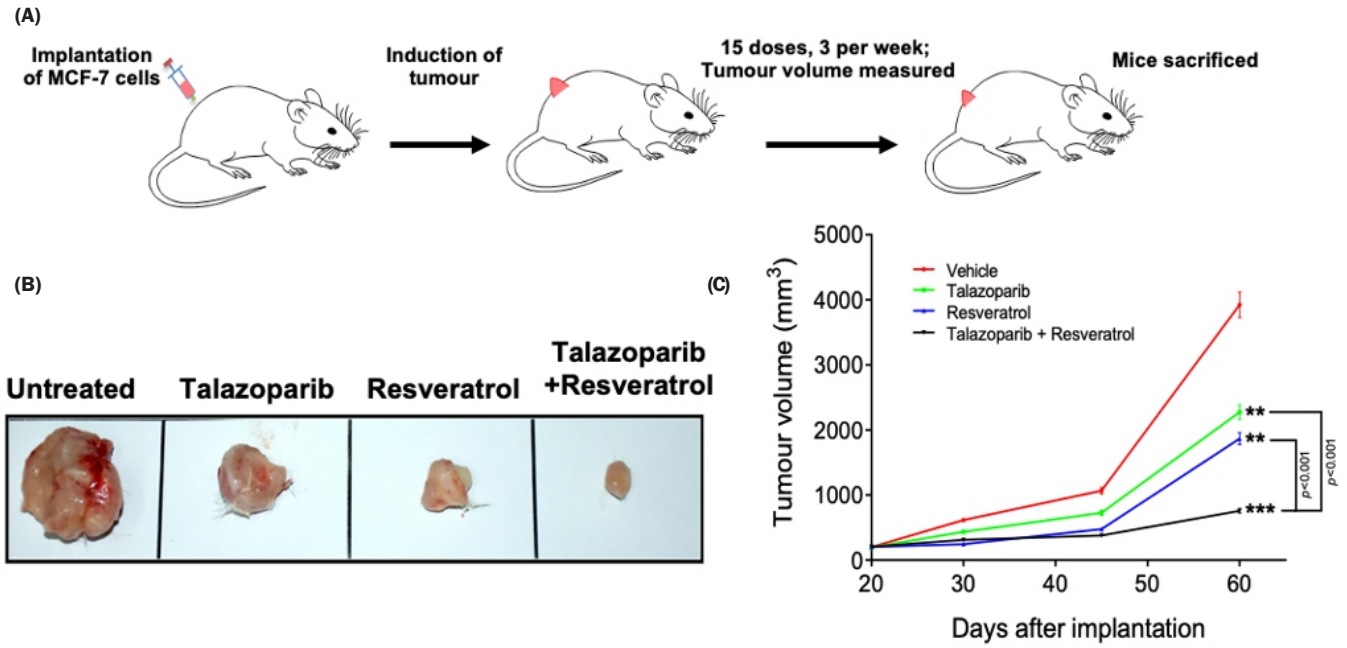

Fig.4: **Resveratrol is effective in sensitizing tumour xenografts in SCID mice to talazoparib treatment.** *(A) Scheme of the SCID mice experiment. (B, C) Representative images of the tumours excised from SCID mice bearing MCF-7 xenografts post treatment with 15 doses of talazoparib alone (1 mg/kg), resveratrol alone (50 mg/kg) or their combination. Quantification of tumour volume is indicated in C. (Adapted from Pai Bellare G and Patro BS, 2022 [7]).*

Conclusion

This work provides compelling evidence that the combination of talazoparib and resveratrol is effective in mitigating breast cancer *in vitro* and *in vivo*. Mechanistically, inhibition of late-stage autophagy i.e. fusion of autophagosomes with the lysosomes due to LMP induction by resveratrol in combination with talazoparib leads to extensive DNA damage induction and eventually, induction of breast cancer cell death. This combination can have potential implications in the treatment of homologous recombination proficient and PARPi resistant homologous recombination deficient breast cancers in the clinical setting.

Acknowledgements

We would like to acknowledge the scientific inputs received from our colleagues at Bio-organic Division, BARC. We would also acknowledge the help of central animal facility at BARC in animal experimentation.

References

[1] Lord CJ, Ashworth A., PARP inhibitors: Synthetic lethality in the clinic, Science, 2017, 355(6330), 1152– 1158.

[2] Gogola E, Rottenberg S, Jonkers J., Resistance to PARP Inhibitors: Lessons from Preclinical Models of BRCA-Associated Cancer, Annual Review of Cancer Biology, 2019, 3(1), 235–54.

[3] Berman AY, Motechin RA, Wiesenfeld MY, Holz MK., The therapeutic potential of resveratrol: a review of clinical trials, npj Precision Oncology, 2017, 1(1), 35.

[4] Pai Bellare G, Saha B, Patro BS., Targeting autophagy reverses de novo resistance in homologous recombination repair proficient breast cancers to PARP inhibition. British Journal of Cancer, 2021.

[5] Ray Chaudhuri A, Nussenzweig A., The multifaceted roles of PARP1 in DNA repair and chromatin remodelling, Nature Reviews Molecular Cell Biology, 2017.

[6] Mizushima N, Yoshimori T, Levine B., Methods in Mammalian Autophagy Research, Cell. 2010,140(3), 313–26.

[7] Pai Bellare G, Sankar Patro B., Resveratrol sensitizes breast cancer to PARP inhibitor, talazoparib through dual inhibition of AKT and autophagy flux, Biochemical Pharmacology, 2022, 199, 115024.

[8] Hwang HY, Cho SY, Kim YJ, Yun NK, Yoo SJ, Lee E, et al., Autophagic Inhibition via Lysosomal Integrity Dysfunction Leads to Antitumor Activity in Glioma Treatment, Cancers, 2020, 12(3).

[9] Wang F, Salvati A, Boya P., Lysosome-dependent cell death and deregulated autophagy induced by amine-modified polystyrene nanoparticles, Open Biology, 2020, 8(4), 170271.

[10] Hewitt G, Korolchuk VI., Repair, Reuse, Recycle: The expanding role of autophagy in genome maintenance, Trends in Cell Biology, 2017, 27(5), 340–51.

कैंसर कीमो-रेडियोथेरेपी

5

कैंसर कीमो-रेडियोथेरेपी की चुंबकीय अतिताप मध्यस्थता में वृद्धि हेतु लक्षित नैनोकण

नीना जी. शेतके [1,2], **अमित कुमार** [1,2] **और बद्री एन. पांडे** [1,2]*
[1]विकिरण जीवविज्ञान एवं स्वास्थ्य विज्ञान प्रभाग, भाभा परमाणु अनुसंधान केंद्र, ट्रांबे-400085, भारत
[2]होमी भाभा राष्ट्रीय संस्थान, अणुशक्ति नगर, मुंबई-400094, भारत

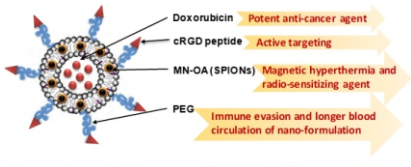

Tumor targeted liposomes (cRGD-LMD)
Indian patent No. 441803

मल्टी-मॉडल नैनो-फॉर्मूलेशन लक्षित ट्यूमर सी. आर. जी. डी.-एल. एम. डी. के डिजाइन के लिए योजना

सारांश

कीमो-रेडियोथेरेपी (CRT) गैर-ट्यूमर विशिष्टता की सीमा में होती है, जो इन विधियों की चिकित्सीय प्रभावकारिता को महत्वपूर्ण रूप से बाधित करती है और अक्सर सामान्य ऊतक की विषाक्तता और रोगी के जीवन की गुणवत्ता से संबद्ध होती है। अतिताप थेरेपी (HT) ट्यूमर के ऑक्सीकरण को बढ़ाकर, ट्यूमर ग्रस्त अंग पर औषधि की सांद्रता बढ़ाने और सेलुलर प्रोटीन के विकृतीकरण को प्रेरित करके DNA की प्रतिकृति, सुधार, कोशिका प्रसार और उत्तरजीविता जैसी महत्वपूर्ण सेलुलर प्रक्रियाओं को विकृत कर CRT की प्रभावकारिता में सुधार करने के लिए जानी जाती है। हालांकि, पारंपरिक HT की चिकित्सीय प्रभावकारिता ट्यूमर कोर के अकुशल तापन और ताप-सह्यता के विकास तक सीमित है। पारंपरिक HT के विपरीत, सुपर-पैरामैग्नेटिक आयरन ऑक्साइड नैनोपार्टिकल्स (SPIONs) मध्यस्थता वाली चुंबकीय अतिताप थेरेपी (MHT) ट्यूमर कोर के ४२-४३ डिग्री सेल्सियस के अतितापन के तापमान तक पर्याप्त और समान तापन को प्रेरित करती है और ताप-सह्यता के विकास को बाधित करती है। वर्तमान शोध में MHT के लिए एक तर्कसंगत रूप से अभिकल्पित ट्यूमर लक्षित चक्रीय RGD (cRGD) पेप्टाइड क्रियाशील लिपोसोमल नैनो-वाहक (cRGD-LMD) के विकास और म्यूरिन फाइब्रोसारकोमा कैंसर कोशिकाओं और इसके ट्यूमर मॉडल में CRT प्रभावकारिता में सुधार का वर्णन किया गया है। लिपोसोम की झिल्ली में SPIONs अनुकूल प्रतिस्थापन ताप के प्रति संवेदनशील कैंसर कोशिका झिल्ली तक इनकी आपूर्ति की सुविधा प्रदान करती है, जिससे MHT की बेहतर प्रभावकारिता सुनिश्चित होती है। इसके अलावा, cRGD लेबलिंग ν ३ इंटीग्रिन रिसेप्टर ओवर-एक्सप्रेसिंग अन्य ऑफ-टारगेट अंगों (जैसे, यकृत, तिल्ली, गुर्दे, हृदय और फेफड़े) की तुलना में माइस के ट्यूमर कोशिकाओं और इसके नव-संवहनी तंत्र में cRGD-LMD के ~ २-९ गुना अधिक संचय को सक्षम बनाता है। उल्लेखनीय रूप से, सीरम CK-MB स्तरों और कार्डियक फाइब्रोसिस के अध्ययन के अनुसार स्वास्थ्य के संदर्भ में हृदय-संवहनी cRGD-LMD को सुरक्षित पाया गया है। cRGD-LMD को भारतीय पेटेंट (सं. ४४१८०३) प्राप्त हुआ है और हमारे परिणाम कैंसर CRT में सुधार के लिए लक्षित नैनो-फॉर्मूलेशन के रूप में इसकी नैदानिक ट्रांसलेशन क्षमता को दर्शाता है।

Cancer Chemo-Radiotherapy

5

Targeted Nanoparticles for Magnetic Hyperthermia Mediated Enhancement of Cancer Chemo-Radiotherapy

Neena G. Shetake[1,2], **Amit Kumar**[1,2] **and Badri N. Pandey**[1,2]*
[1]Radiation Biology & Health Sciences Division, Bhabha Atomic Research Centre, Trombay-400085, INDIA
[2]Homi Bhabha National Institute, Anushakti Nagar, Mumbai-400094, INDIA

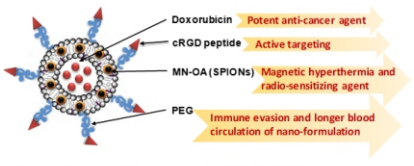

Tumor targeted liposomes (cRGD-LMD)
Indian patent No. 441803

Scheme for design of cRGD-LMD, a tumor targeted multi-modal nano-formulation

ABSTRACT

Chemo-radiotherapy (CRT) suffers the limitation of non-tumor specificity, which significantly hampers the therapeutic efficacy of these modalities and is often associated with normal tissue toxicities and patient's quality of life. Hyperthermia therapy (HT) has been known to improve the efficacy of CRT by increasing tumor oxygenation, increasing drug concentration at tumor site and inhibiting crucial cellular processes such as DNA replication, repair, cell proliferation and survival via inducing denaturation of cellular proteins. However, therapeutic efficacy of conventional HT is limited by the in-efficient heating of tumor core and development of thermo-tolerance. Contrary to conventional HT, super-paramagnetic iron oxide nanoparticles (SPIONs) mediated magnetic hyperthermia therapy (MHT) can induce sufficient and uniform heating of tumor core to hyperthermic temperatures of 42-43°C and prevent development of thermo-tolerance. Present work describes the development of a rationally designed tumor targeted cyclic RGD (cRGD) peptide functionalized liposomal nano-carrier (cRGD-LMD) for MHT and improvement of CRT efficacy in murine fibrosarcoma cancer cells and its tumor model. The strategic placement of SPIONs in the membrane of the liposomes facilitates their delivery to the heat sensitive cancer cell membrane, ensuring improved MHT efficacy. Furthermore, cRGD labelling enables ~ 2-9 fold higher accumulation of cRGD-LMD in αvβ3 integrin receptor over-expressing mice tumor cells and its neo-vasculature compared to other off-target organs (viz., liver, spleen, kidney, heart and lungs). Notably, cRGD-LMD was found to be safe in terms of cardio-vascular health as studied by serum CK-MB levels and cardiac fibrosis. cRGD-LMD has received an Indian patent (No. 441803) and our results demonstrate its clinical translational potential as a targeted nano-formulation for improvement of cancer CRT.

KEYWORDS: *Magnetic hyperthermia therapy, Magneto-liposomes, Radio-sensitization, Cardio-toxicity; Heat Shock Proteins*

*Author for Correspondence: Badri N. Pandey
E-mail: bnp@barc.gov.in

Introduction

Approximately 60 % of solid tumors are treated with Chemo-Radio Therapy (CRT) [1-2]. However, the efficacy of CRT is severely hampered by its non tumor-specificity leading to dose-limiting toxicities and subsequent development of resistance to CRT [2]. Thus, development of alternate and more efficient strategies for cancer treatment has become indispensable.

Nanoparticles mediated Magnetic Hyperthermia Therapy (MHT): Heating Tumors to Death

Hyperthermia therapy (HT) involves heating the tumors in the range of 40 - 43 °C which can either kill the cells directly or sensitize them for subsequent CRT. In clinics, conventional HT is applied using infrared, microwaves, high intensity focused ultrasound, sauna bath or water bath [3]. However, conventional HT suffers the limitations of in-sufficient and non-homogenous heating of tumors often leading to development of thermo-tolerance during subsequent HT sessions [3-4]. Thus, development of alternate and more efficient hyperthermia modalities with ability to induce nano-heating effects at intra-cellular level becomes crucial. In this direction, photothermal therapy (PTT) and magnetic hyperthermia therapy (MHT) are two such modalities with superior hyperthermia efficacies and better therapeutic abilities as compared to conventional HT [5-6]. In the present work we have developed super-paramagnetic iron oxide nanoparticles (SPIONs) for MHT applications. As against conventional HT, SPIONs mediated MHT can induce more efficient and homogenous heating of tumor cells and significantly improve the therapeutic index of CRT. MHT utilizes SPIONs to generate heat under the influence of an alternating current (*AC*) magnetic field (AMH) predominantly by Néel or Brownian relaxation [6]. Unlike conventional HT, in MHT, SPIONs can be functionalized using tumor targeting surface ligands to specifically internalize in the tumor cells and distribute to cellular compartments such as plasma membrane which is known to be a more sensitive target of heat as compared to cytosolic compartment. Thus, in present work we have designed cell membrane targeting SPIONs functionalized with hydrophobic, oleic acid termed as 'MN-OA' and have demonstrated its membrane localization and significant anti-cancer efficacy in combination with MHT in cancer cell cells and its tumor model (Fig. 1A-E) [7-8].

cRGD-LMD : A Targeted and Multi-modal Anti-tumor Nano-formulation

For further improving the tumor cell targeting of MN-OA and to impart multi-modal cancer therapy ability, we have designed a liposomal nano-formulation termed as 'cRGD-LMD'. These liposomes are co-encapsulated with MN-OA and doxorubicin (Dox) in the bilayer and core of the liposomes, respectively and to impart tumor-specificity, they have been functionalized with cyclic RGD (cRGD) peptide. cRGD functionalization enables the targeting of tumor cells and its neo-vasculature over-expressing the αvβ3 integrin receptors [9]. cRGD-LMD has spherical shape and is predominantly unilamellar with MN-OA and Dox encapsulation visible mainly in the bilayer and core of liposomes, respectively as suggested by cryo-TEM (transmission electron microscopy) (Fig. 2A-B). *In vitro* evaluation showed significantly higher cyto-toxicity of cRGD-LMD as compared to commercial nano-formulation of DOX (Lippod™), in cancer cells of skin, breast, lung and brain

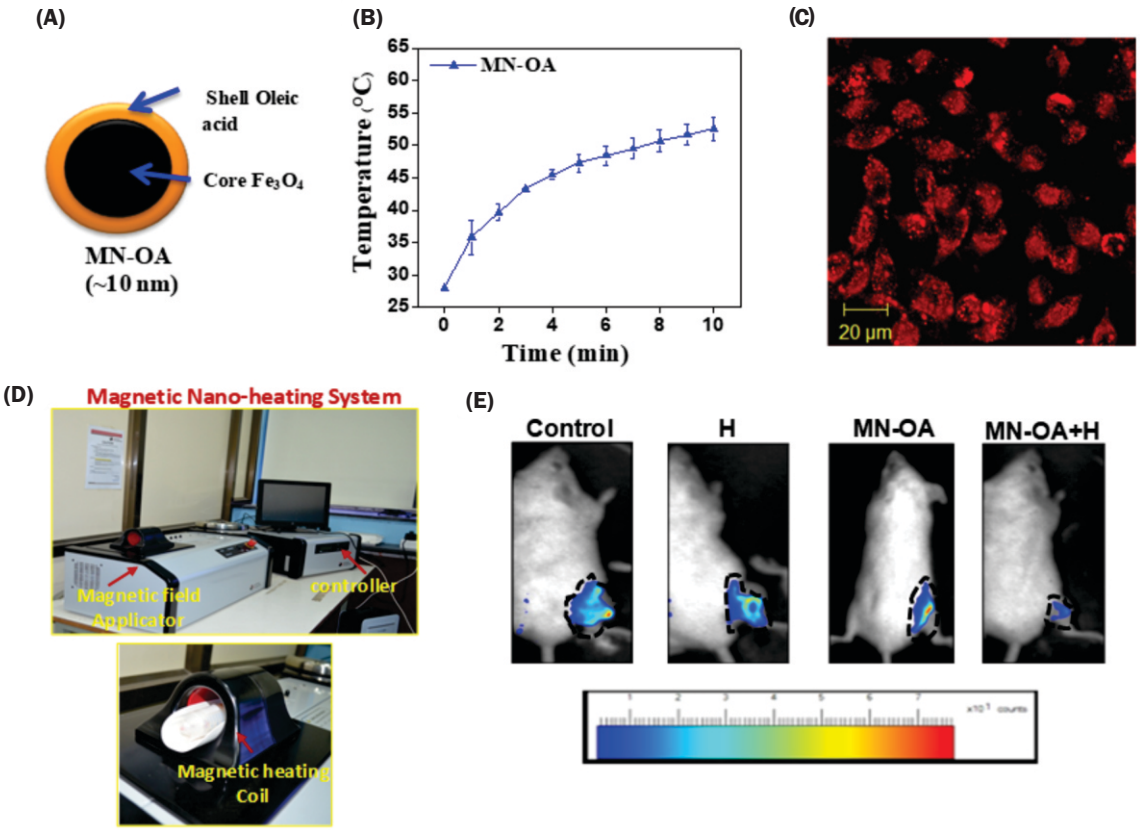

Fig.1: (A) Scheme for SPIONs coated with oleic acid termed as 'MN-OA', (B) graph for temperature achieved by MN-OA (10 mg/mL) under alternating current magnetic field conditions (335Oe, 265 kHz for 10 min) (C) representative confocal microscopy image of WEHI-164 cells treated with MN-OA and stained with nile Blue A. Red foci depict membrane localization of MN-OA, (D) digital photographs of magnetic nano-heating system. Lower image shows the placement of restrained mice inside the copper coils of the instrument during magnetic hyperthermia therapy, (E) representative real time in vivo bio-luminescence imaging of tumor cell growth in fibrosarcoma tumor bearing mice after indicated treatments. (H: magnetic hyperthermia therapy). Reproduced with permission from Elsevier, source: Colloids and Surfaces B: Biointerfaces 108 (2013) 158–168.

origin. Importantly, the cyto-toxicity of cRGD-LMD was significantly lower in normal lung epithelial cells as compared to cancer cells [9]. Moreover, cRGD-LMD showed significant radio-sensitization of murine fibrosarcoma cells predominantly via activation of JNK mediated pro-apoptotic pathway. In addition, cRGD-LMD also showed significant heating of tumors after MHT as determined by thermal imaging using IR camera. (Fig. 2C-E).

Tumor Targeting and Combinatorial Therapy Efficacy of cRGD-LMD: *In vivo* Studies

In vitro studies suggested the superior anti-cancer efficacy of cRGD-LMD in multiple cancer cells. Further, to determine their *in vivo* tumor targeting ability, cRGD-LMD was labelled with a near infrared dye, indocyanine green (ICG). The ICG labelled cRGD-LMD showed ~2-9 folds higher accumulation in fibrosarcoma tumors as compared to other off-target organs (liver, spleen, kidney, heart and lungs) [9]. Anti-tumor efficacy of cRGD-LMD was evaluated in fibrosarcoma tumor model either alone or in combination with radiation (R) or MHT (H) or both. Lippod™ was used as a comparative clinical formulation control. A TGD of ~ 7 days was obtained for cRGD-LMD + H + R as compared to ~ 5 days for cRGD-LMD + R, 4 days for cRGD-LMD + H, 3 days for cRGD-LMD, 0.2 days for Lippod™ and ~ 2 days for Lippod™ + R treatments (Fig. 3A-C).

Toxicological Evaluation of cRGD-LMD in Healthy Animals

To study the toxicological parameters, healthy BALB/c mice were treated with cRGD-LMD or Lippod™ or Dox at 3 mg/Kg dose for 4 days, followed by analysis of whole blood and serum parameters and histopathology of major organs. Dox at 20 mg/Kg of was used as positive control. Serum analysis showed increased expression of early cardiac damage marker, CK-MB in Lippod™ and Dox (20 mg/kg) group but not in cRGD-LMD as compared to control [9]. Furthermore, cRGD-LMD showed in-significant changes in DOX-induced cardiac fibrosis as suggested by trichrome staining and immuno-fluorescence detection of phospho-Smad3, which is one of the mediators of TGFβ induced fibrosis in heart tissue (Fig. 3D-E). These results suggest in-significant toxicity of cRGD-LMD in healthy mice re-emphasizing its plausible clinical potential as a targeted and multi-modal anti-tumor agent.

Conclusion

Present study demonstrates the superior anti-cancer efficacy of cRGD-LMD as compared to Lippod™. The optimized phospholipid composition, size and charge of the liposomes and cRGD functionalization resulted in a significantly (6-18 folds) higher targeting of cRGD-LMD to tumor site as compared to other off-target organs, such as liver, spleen, kidney, lungs, heart and intestine. Thus, these pre-clinical findings support the targeted and combinatorial anti-tumor capabilities of cRGD-LMD involving ferroptosis mediated immunogenic mode of tumor control (10). Currently, toxicological studies in higher rodents and pharmaco-kinetic studies are being carried out to further facilitate the clinical translation of cRGD-LMD.

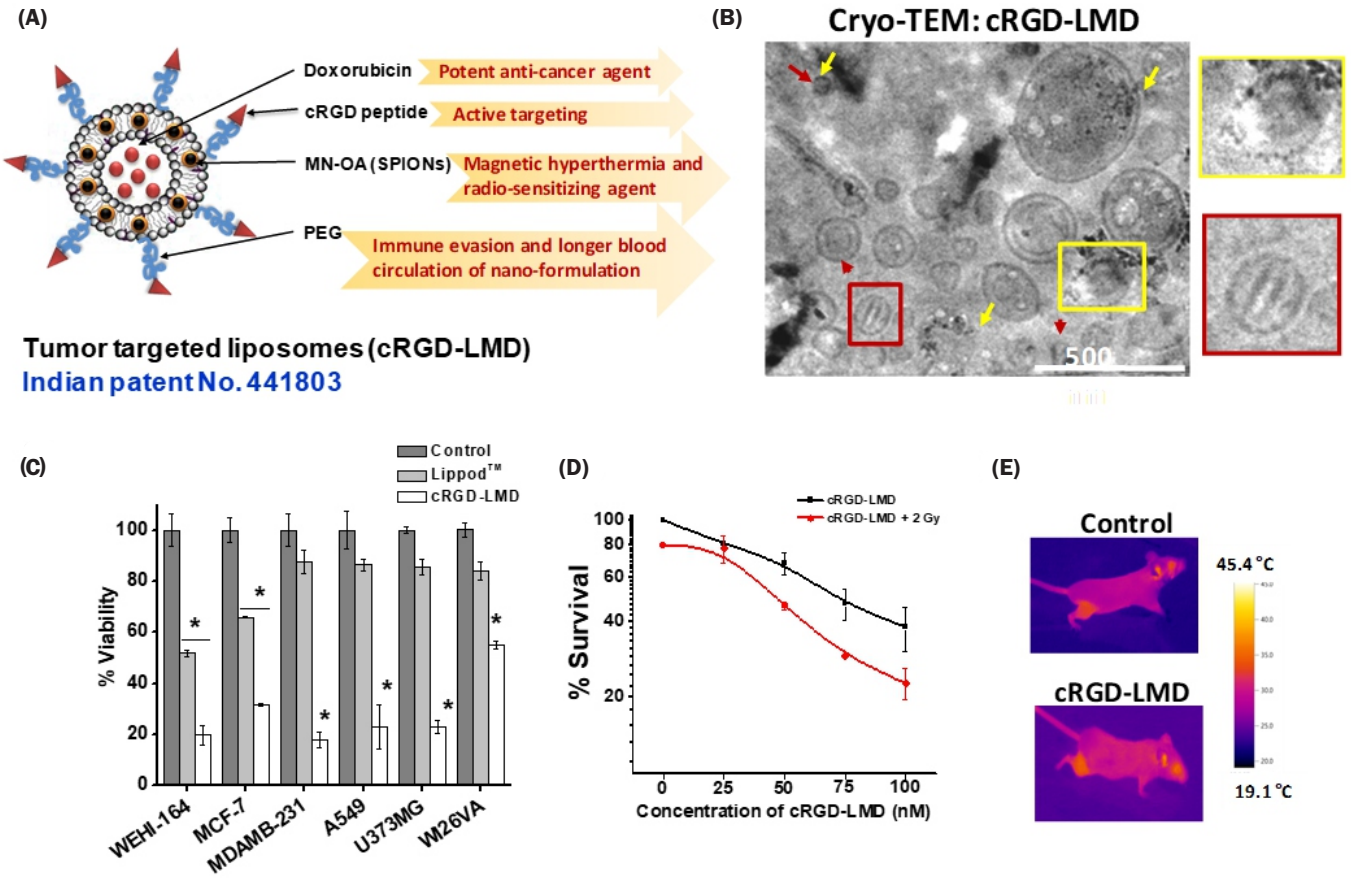

Fig.2: (A) Scheme for design of cRGD-LMD, a tumor targeted multi-modal nano-formulation, (B) representative cryo-TEM image of cRGD-LMD. yellow and red arrows depict MN-OA and doxorubicin (DOX) deposition in predominantly in the bilayer and core of liposomes, respectively. Zoomed inset shows the deposition of MN-OA (yellow box) and DOX (red box). (C) Graph for percentage viability of cancer cells of skin (WEHI-164), breast (MCF-7 and MDAMB-231), lung (A549) and brain (U373MG) and normal lung epithelial cells (WI26VA4) as determined by MTT assay after indicated treatments at 48 h, (D) graph for % survival as determined by clonogenic cell survival assay after indicated treatments. Gamma radiation dose of 2 Gy was used. (E) Representative thermal image captured using IR camera for mice injected with cRGD-LMD intra-venously and subjected to MHT. Reproduced with permission from Elsevier, source: Biomaterials Advances, 142 (2022) 213147.

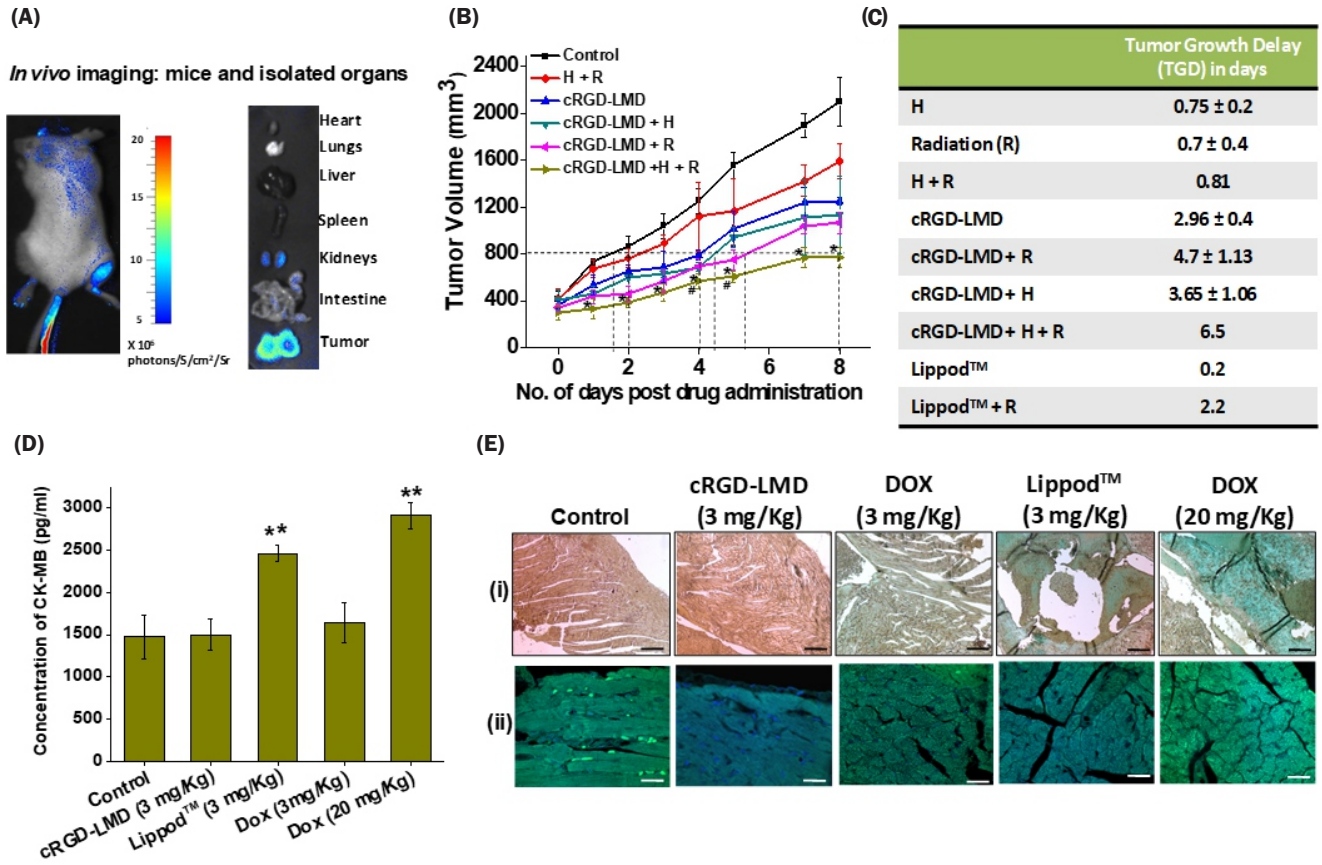

Fig.3: (A) representative real time in vivo fluorescence image of fibrosarcoma tumor bearing in mice on day 7 post intra-venous injection with cRGD-LMD labelled with near infrared dye (indocyanine green:ICG). Right side of the image shows the distribution of ICG fluorescence signal in isolated organs on day 8 after sacrifice of mice,(B) graph for tumor growth kinetics of fibrosarcoma tumors after indicated treatments, (C) table for tumor growth delay obtained after indicated treatments in fibrosarcoma tumor bearing mice, H: MHT and R: Gamma radiation (2 Gy X 3) (D)serum levels of CK-MB, an early cardiac damage marker after indicated treatments in fibrosarcoma tumor bearing mice and (E) representative image of tumor tissue sections after (i) trichrome staining and (ii) immuno-fluorescence staining of p-smad3 expression after indicated treatments. blue color in panel (i) indicates collagen deposition suggesting cardiac fibrosis and green fluorescence in panel (ii) suggests increased expression of p-smad3 suggesting activation of TGF-β mediated cardiac fibrosis pathway. Scale bar : 20 µm. Dox (20 mg/Kg) was used as a positive control. Reproduced with permission from Elsevier, source: Biomaterials Advances 142 (2022) 213147.

Acknowledgment

The authors gratefully acknowledge support and guidance of Head, Radiation Biology & Health Sciences Division and Associate Director, Bioscience Group.

References

[1] Abbas, Z. and S. Rehman, An Overview of Cancer Treatment Modalities, Neoplasm ed., H.N. Shahzad, 2018, London, IntechOpen.

[2] Rajamanickam Baskar, et al., Cancer and Radiation Therapy: Current Advances and Future Directions, Int J Med Sci., 2012, 9(3), 193-199.

[3] Habash RW, Bansal R, Krewski D, Alhafid H T., Thermal therapy, part 2: hyperthermia techniques, Crit Rev Biomed Eng., 2006, 34, 491-542.

[4] Cheung AY, Neyzari A., Deep local hyperthermia for cancer therapy: external electromagnetic and ultrasound techniques, Cancer Res., 1984, 44, 4736-4744.

[5] Jingyi Chen,Charles Glaus, Richard Laforest, Qiang Zhang, Miaoxian Yang, Michael Gidding, Michael J. Welch, and Younan Xia, Gold Nanocages as Photothermal Transducers for Cancer Treatment, Small 2010, 6(7), 811–817.

[6] Kozissnik B, Bohorquez AC, Dobson J, Rinaldi C., Magnetic fluid hyperthermia: Advances, challenges, and opportunity, Int J Hyperthermia, 2013, 29, 706–714.

[7] Jadhav NV, Prasad AI, Kumar A, Mishra R, Dhara S, Babu KR, et al., Synthesis of oleic acid functionalized Fe3O4 magnetic nanoparticles and studying their interaction with tumor cells for potential hyperthermia applications, Colloids Surf B Biointerfaces, 2013, 108, 158-68.

[8] Shetake NG, Kumar A, Gaikwad S, Ray P, Desai S, Ningthoujam RS, Vatsa RK, Pandey BN, Magnetic nanoparticle-mediated hyperthermia therapy induces tumour growth inhibition by apoptosis and Hsp90/AKT modulation, International Journal of Hyperthermia, 2015, 31(8), 909-919.

[9] Shetake NG, Ali M, Kumar A, Bellare J, Pandey BN, Theranostic magnetic nanoparticles enhance DNA damage and mitigate doxorubicin-induced cardio-toxicity for effective multi-modal tumor therapy, Biomaterials Advances, 2022, 142, 213147.

[10] Shetake NG, Das SK, Kumar A, Pandey BN, Nano-inducer of ferroptosis for targeted chemotherapy of human triple negative breast carcinoma, Biomater Adv., 2024, 161, 213868.

कोशिकाओं में जीनोमिक स्थिरता

6

जीनोम अखंडता को बनाए रखने में एपिजेनेटिक कारकों की भूमिका का अध्ययन

एस . जयकुमार*
मुक्त मूलक जैविकी अनुभाग, विकिरण जीवविज्ञान और स्वास्थ्य विज्ञान प्रभाग, भाभा परमाणु अनुसंधान केंद्र, ट्रांबे-400085, भारत

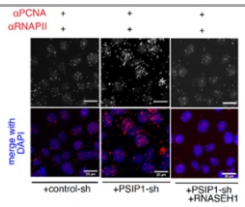

नियंत्रण और PSIP1-KD RWPE-1 कोशिकाओं से प्राप्त α-PCNA और α -RNAPII एंटीबॉडी के बीच प्रतिनिधि पी. एल. ए. छवि

सारांश

रोग के विकास और उसके उपचार का अध्ययन करने के लिए कोशिकाओं में जीनोमिक अखंडता को बनाए रखने में शामिल आण्विक तंत्रों का अध्ययन महत्वपूर्ण है। इस अध्ययन में, ट्रांसक्रिप्शन के दौरान अनिर्धारित आर-लूप को हल करने के लिए एक एपिजेनेटिक कारक, PSIP1 की भूमिका का अध्ययन किया गया है। PSIP1 की कमी से सक्रिय रूप से ट्रांस्क्रिप्ट करने वाले जीन निकायों के आर-लूप में उल्लेखनीय वृद्धि होती है, जिससे ट्रांसक्रिप्शन-रेप्लिकेशन द्वंद्व में वृद्धि के कारण डीएनए की क्षति में वृद्धि होती है। ये परिणाम कोशिकाओं में जीनोमिक स्थिरता बनाए रखने में PSIP1 की भूमिका के बारे में एक नई अंतर्दृष्टि प्रदान करते हैं।

Genomic Stability in Cells

6

Understanding the Role of Epigenetic Factors in Maintenance of Genome Integrity

S. Jayakumar*
Free Radical Biology Section, Radiation Biology & Health Sciences Division, Bhabha Atomic Research Centre, Trombay-400085, INDIA

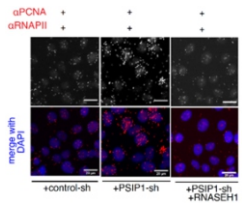

Representative PLA image between α-PCNA and α-RNAPII antibodies obtained from control and PSIP1-KD RWPE-1 cells

ABSTRACT

Studying the molecular mechanisms involved in maintaining genomic integrity in cells is important for understanding disease development and their treatment. In this study, the role of an epigenetic factor, PSIP1 has been understood in resolving unscheduled R-loops during transcription. Depletion of PSIP1 lead to significant increase in R-loops in the actively transcribing gene bodies leading to increase in DNA damage by increased transcription-replication conflicts. These results show a novel insight into the role of PSIP1 in maintaining genomic stability in the cells.

KEYWORDS: *Genome Integrity, R-loops, PSIP1, Epigenetics, DNA damage*

**Author for Correspondence: S. Jayakumar*
E-mail: kumarsj@barc.gov.in

Introduction

Deoxyribonucleic acid (DNA) is the central molecule in the functioning of the eukaryotic cells. They code all the necessary information for the cells to thrive, organise themselves and propagate. Faithfully maintaining the integrity of the genome is vital to this cycle. However, numerous internal cellular processes and external factors, both physical and chemical, pose threats to DNA stability. To counteract potential damage, cells employ antioxidant mechanisms and various repair pathways, ensuring the restoration of DNA integrity. Any deviations or dysregulations in this process can lead to deleterious consequences to the cells. The fundamental reasons for many of the diseases like cancer is traced back to the failure of the cells to maintain the integrity of their genome. Hence, comprehending the pathways and mechanisms responsible for maintaining genomic integrity is imperative for disease understanding and therapeutic development. Compounding the challenge of genomic maintenance is the inherent length of DNA, requiring significant compaction within the confines of the cellular environment. Furthermore, they have to be decompacted during replication and transcription (the process of decoding the information from DNA). This compaction and packaging of the DNA in the form of chromatin is achieved by the cells by deploying special class of basic (alkaline) proteins called histone proteins. These histone proteins undergo multitude of post-translational modifications (PTMs) like acetylation, methylation, phosphorylation, ubiquitination etc., in their amino acid residues present especially in their N-terminal regions. These modifications further acts as signals and anchoring points for recruitment of other regulatory proteins. In this way, the histone proteins not only provide the structural fabric for the genome but also play core role in functional regulation of the genome. The histone PTMs themselves are regulated by complex network of reader, writer and eraser proteins and functional regulation of genome through these histone PTMs and its associated factors is called as epigenetic mechanism of gene regulation. Beyond regulating gene expression, the role of epigenetics in DNA damage and repair is emerging as a important area of research [1]. PC4 and SF2 interacting protein (PSIP), is a multifunctional chromatin protein, that binds to methylated

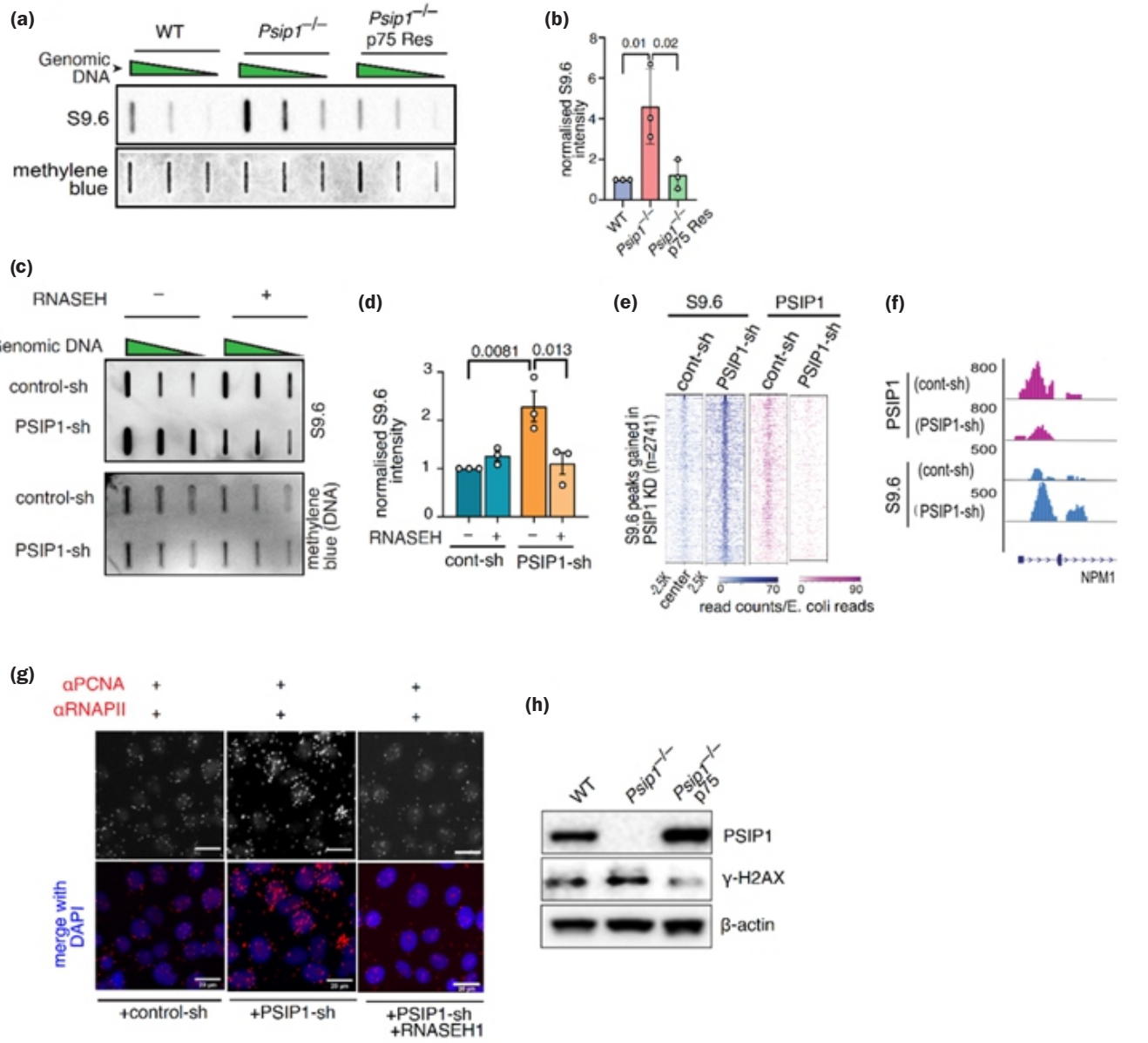

Fig.1: (a). R-loops levels seen by slot blot using S9.6 antibody in wild-type, Psip1$^{-/-}$ and Psip1$^{-/-}$ p75R MEFs. The band intensity was normalized to loading control (methylene blue) and plotted (b). (c). Similar to (a) but in RWPE-1 cells and the normalized band intensity has been plotted (d). (e). Heatmap showing R-loop and PSIP1 levels in PSIP1-KD and control RWPE-1 cells. (f). Genome browser track showing the CUT&Tag signal (read counts) for PSIP1 and R-loop in control and PSIP1-KD RWPE-1 cells. (g). Representative PLA image between α-PCNA and α-RNAPII antibodies obtained from control and PSIP1-KD RWPE-1 cells. (h). Immunoblot images of PSIP1, γ-H2AX and β-actin for lysate from wild-type, Psip1$^{-/-}$ and Psip1$^{-/-}$ p75R MEFs. (adopted from [5]).

histone H3 lysine 36 (H3K36me) via the PWWP domain, and PSIP1 binding is enriched at the sites of RNAPII transcription and helps in transcription initiation and elongation. Previous study has shown that the absence of PSIP1 in the cells leads to increased DNA damage [2]. Additionally, studies employing immunoprecipitation of PSIP1 revealed interactions with various proteins involved in transcription, RNA processing, and DNA repair. Notably, these interacting proteins overlap with those identified in R-loop complexes [2,3].

R-loops are RNA-DNA hybrid structures formed during transcription when newly produced RNA molecules bind back to the DNA template strand. Unscheduled R-loops, if not resolved, can impede transcription and trigger DNA damage due to transcription-replication conflicts. The complete pathway and the proteins involved in R-loops resolution in cells remain unclear. This work proposes a novel role for PSIP1 in resolving R-loops, thereby safeguarding genome integrity during transcription.

Materials and Methods

For the study, human prostate epithelial cells (RWPE-1) and mouse embryonic fibroblast cells (MEFs) were used. For estimating the R-loops, cells were lysed in lysis buffer with proteinase K and incubated at 55^{0}C overnight. Isopropanol was added to the lysate and the DNA was pelleted using centrifugation. The DNA was quantified and different quantities of DNA were blotted onto the N+ nitrocellulose membrane using a slot blot apparatus. Then the membrane was baked at 80^{0}C for 2 hours, incubated in blocking buffer (5% skimmed milk in PBS) for 1 hour, followed by incubation with S9.6 antibody overnight at 4^{0}C in a nutator. Blots were washed and then incubated with secondary antibody for 2 hours at room temperature, washed and developed. The same blots were stained with methylene blue to quantify total DNA. Cleavage under targets & Tagmentation (CUT&Tag) was performed and the sequence reads were processed according to protocol [4]. Proximity Ligation Assay (PLA) was performed using Duolink In Situ Red Starter kit (Mouse/Rabbit) according to the manufacturer protocol (Merck, DUO92101).

Results and Discussion

To understand the role of PSIP1 in R-loop homeostasis, the levels of R-loops were studied in MEF cells with PSIP1 knock out, using S9.6 antibody through blotting experiment. Knockout of PSIP1 lead to stark increase in the R-loops accumulation that could be reversed by restoring the expression of PSIP1 in those cells (Fig. 1a and b), implicating the role of PSIP1 in R-loop resolution. Similarly, in RWPE-1 cells, when PSIP1 was depleted it lead to increase in R-loops and that increase could be reversed by overexpression of RNASEH1-an enzyme that can act specifically on RNA-DNA hybrid and degrades them. (Fig. 1c and d). Further to understand the genome wide accumulation of R-loops and its link with PSIP1 depletion, CUT&Tag-seq, a modified form of chromatin immunoprecipitation was used. In this assay, the cells were permeabilized, the targets were bound with antibody and the antibody bond region was cleaved using transposase. These cleaved DNA fragments are isolated, amplified, sequenced, aligned to the reference genome and the enriched regions are found out. From the CUT&Tag analysis, it was found that upon PSIP1 depletion 2741 peaks were showing accumulation of R-loops and these regions are occupied by the PSIP1 in the control cells, again indicating the role of PSIP1 in R-loop resolution (Fig. 1e and f). These peaks are mostly seen in the gene bodies. The consequence of this R-loop accumulation in terms of transcription-replication conflict (TRC) was then probed by performing PLA between PCNA (part of replication) and RNAPII (part of transcription). Results indicated the increased TRCs linked to PSIP1 depletion and that can be reversed by overexpressing RNASH1 (Fig. 1g). Further this increase in TRC lead to DNA damage as seen by the increased γ-H2AX levels, and that damage could be reversed by re-expression of PSIP1 (Fig. 1h).

Conclusion

These results demonstrated a novel role of PSIP1 in resolving unscheduled R-loops that arise during transcription and thereby preventing TRC and DNA damage in the transcriptionally active part of the genome [5].

Acknowledgements

The author thank the European Research Commission for providing with Marie-Curie Individual Fellowship and Dr. Pradeepa Madapura and other Lab members of Madapura Lab, Queen Mary University of London, London, UK, for help in carrying out the project. Author also thank Dr. Santosh K. Sandur, Head, RB&HSD, BARC for the help and encouragement.

References

[1] Millán-Zambrano, G., Burton, A., Bannister, A.J. et al., Histone post-translational modifications — cause and consequence of genome function, Nat Rev Genet., 2022, 23, 563–580.

[2] Jayakumar, S., Taylor, G. C. A., von Kriegsheim, A. & Pradeepa, M. M., H3K36me3 and PSIP1/LEDGF associate with several DNA repair proteins, suggesting their role in efficient DNA repair at actively transcribing loci., Wellcome Open Res., 2021, 2, 83.

[3] Pradeepa, M. M., Grimes, G. R., Taylor, G. C. a, Sutherland, H. G. & Bickmore, W. a. Psip1/Ledgf p75 restrains Hox gene expression by recruiting both trithorax and polycomb group proteins, Nucleic Acids Res., 2014, 42, 9021–32.

[4] Kaya-Okur, H. S. et al. CUT & Tag for efficient epigenomic profiling of small samples and single cells, Nat. Commun., 2019, 101(10), 1–10.

[5] Jayakumar, S., Patel, M., Boulet, F. et al., PSIP1/LEDGF reduces R-loops at transcription sites to maintain genome integrity, Nat Commun., 2024, 15, 361.

कैंसर प्रतिरोध पर विजय

7

कैंसर कोशिकाओं को कुशलतापूर्वक नष्ट करने के लिए टोपोआइसोमरेज़ 1 और PARP1 के लिए दोहरे अवरोधक का विकास

आनंद गुहा मजूमदार [1,2], **पापिया डे**[1], **शिखा श्री**[1,2], **महेश सुब्रमण्यम**[1,2] **और बिरिजा शंकर पात्रो** [1,2]*
[1]जैव कार्बनिक प्रभाग, भाभा परमाणु अनुसंधान केंद्र, ट्रांबे-40085, भारत
[2]होमी भाभा राष्ट्रीय संस्थान, अणुशक्ति नगर, मुंबई-400094, भारत

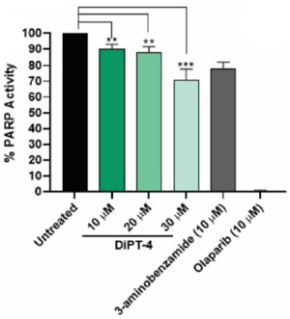

DiPT-4 की उपस्थिति या अनुपस्थिति में शुद्ध मानव PARP1 के साथ इन विट्रो PARP गतिविधि परख।

सारांश

टोपोआइसोमेरस 1 (TOP1) मनुष्यों में क्रमिक रूप से संरक्षित प्रोटीन है जो रेप्लिकेशन और ट्रांसक्रिप्शन के दौरान डीएनए सुपरकॉयल को हटाता है। TOP1, कोशिका उत्तरजीविता के लिए आवश्यक होने के कारण, एक पसंदीदा चिकित्सीय लक्ष्य है। TOP१-लक्षित उपचार TOP1-DNA सहसंयोजक संकुलों (TOP1ccs, जो TOP1 उत्प्रेरक के अनिवार्य मध्यवर्ती हैं) को स्थिर करते हैं, परिणामस्वरूप भारी TOP1-DNA एडक्ट्स और घातक DNA डबल स्ट्रैंड ब्रेक का संचय होता है। पॉली (ADP-राइबोज) पॉलीमरेज़ 1 (PARP1) एक प्रमुख DNA क्षय प्रतिक्रिया नियामक है जो TOP1ccs को दूर करने में महत्वपूर्ण भूमिका निभाता है, और इसलिए TOP1 अवरोधकों के प्रतिरोध के एक प्रमुख तंत्र के रूप में कार्य करता है। परिणामस्वरूप, कई नैदानिक परीक्षणों के दौरान कॉम्बिनेटरियल TOP1 और PARP1 अवरोध का उपयोग किया गया। इस अध्ययन में, हमने एकल अणु दोहरे अवरोधक (DiPT-4) की पहचान की है जो एकल कर्मक TOP1 अवरोधकों के लिए चिकित्सीय प्रतिरोध को दूर करने के लिए TOP1 और PARP दोनों के प्रति महत्वपूर्ण अवरोधक गतिविधि रखता है।

Overcoming Cancer Resistance

7

Development of a Dual Inhibitor for Topoisomerase 1 and PARP1 for Efficient Killing of Cancer Cells

Ananda Guha Majumdar[1,2], **Papiya Dey**[1], **Shikha Shree**[1,2], **Mahesh Subramanian**[1,2] **and Birija Sankar Patro**[1,2]*
[1]Bio-Organic Division, Bhabha Atomic Research Centre, Trombay-400085, INDIA
[2]Homi Bhabha National Institute, Anushakti Nagar, Mumbai-400094, INDIA

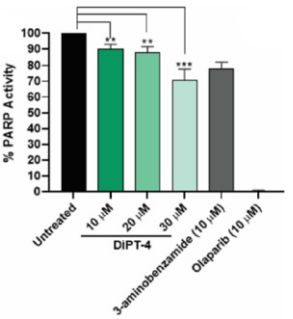

In vitro PARP activity assay with purified human PARP1 in the presence or absence of DiPT-4

ABSTRACT

Topoisomerase 1 (TOP1) is an evolutionarily conserved protein in humans which removes DNA supercoils during replication and transcription. TOP1, being essential for cell survival, is an attractive therapeutic target. TOP1-targeted therapies stabilize TOP1-DNA covalent complexes (TOP1ccs, which are obligate intermediates of TOP1 catalysis), resulting in accumulation of bulky TOP1-DNA adducts and lethal DNA double strand breaks. Poly (ADP-ribose) polymerase 1 (PARP1) is a key DNA damage response regulator which plays instrumental roles in removal of TOP1ccs, and hence acts as a key mechanism of resistance to TOP1 inhibitors. Consequently, combinatorial TOP1 and PARP1 inhibition has been subjected to multiple clinical trials. In this study, we have identified a single molecule dual inhibitor (DiPT-4) having significant inhibitory activity towards both TOP1 and PARP to overcome therapeutic resistance to single agent TOP1 inhibitors.

KEYWORDS: *Topoisomerase 1, PARP1, Dual Inhibitor, Resistance to Topoisomerase 1, TOP1 poison*

**Author for Correspondence: Birija Sankar Patro*
E-mail: bisank@barc.gov.in

Introduction

Cancer cells have high dependence on TOP1 due to its indispensable roles in replication and transcription. Hence, TOP1-targeted therapies are widely used in colorectal, lung, ovarian and pancreatic cancers. However, TOP1 inhibitors often suffer from development of therapy resistance. PARP1, a key DNA damage response protein, is instrumental in recruiting multiple proteins to TOP1 inhibitor-induced DNA damage sites and also in proteasomal degradation of TOP1ccs [1]. Hence, combinatorial inhibition of TOP1 and PARP1 is expected to improve therapy outcomes [2]. However, clinical trials with combinations of TOP1 and PARP1 have met with limited success due to dose limiting toxicities, often arising from pharmacokinetic incompatibilities between these two classes of drugs [3]. Single molecule dual inhibitors have generated significant interest among medicinal chemists due to their capability of eliminating pharmacokinetic incompatibility between drug classes by combining two different inhibitory activities in one molecule. Here, we report the development of a novel dual inhibitor of TOP1 and PARP which shows promising activity against both TOP1 and PARP, thus providing a proof-of-concept for further development of such inhibitors for clinical use.

Materials and Methods

Colorectal cancer (HCT116), pancreatic cancer (MIA PaCa-2 and PANC-1) and immortalized normal breast epithelium (MCF-10A) cell lines were used in this study. Cytotoxicity was evaluated using clonogenic survival and MTT assays. Rapid Approach to DNA Adduct Recovery (RADAR) assay [4] was used to quantify TOP1cc stabilization. TOP1 catalytic activity was measured using *in vitro* plasmid relaxation assay employing purified human TOP1 and supercoiled pUC19 plasmid. *In vitro* activity of purified PARP1 was measured using a PARP activity kit based on colorimetric estimation of biotinylated poly (ADP-ribose) (PAR) chains on histone substrates. Protein levels were quantified using Western blotting. PARP-trapping was evaluated using Western blotting with chromatin extracts. DNA damage was visualized using immunofluorescence and confocal microscopy.

Results and Discussion

In order to develop promising dual TOP1/PARP inhibitors, we utilized 1,8-naphthalimide and benzylphthalazin-1(2H)-one pharmacophores (for TOP1 and PARP inhibition respectively) connected through a 1, 3, 4-oxadiazole linker (Fig. 1A). Our cytotoxicity screen against HCT116, MIA PaCa-2 and PANC-1 cell lines revealed DiPT-4 (Fig. 1B), a candidate with (a) a fluorine side group in the benzylphthalazin-1(2H)-one phenyl ring, (b) a 1-carbon spacer between benzylphthalazin-1(2H)-one phenyl ring and 1, 3, 4-oxadiazole and (c) Sulphur linker between 1, 3, 4-oxadiazole and naphthalimide as the most promising molecule with superior cytotoxic activity (IC_{50} of 4, 4.5 and 4 μM respectively against HCT116, MIA PaCa-2 and PANC-1) compared to its parent molecules i.e., 1,8-naphthalimide (corresponding IC_{50} values of 15, 18 and 20 μM respectively) and Olaparib (corresponding IC_{50} values of 9, 8 and 7 μM respectively). Further, DiPT-4 showed selectively toxicity towards cancer cells and not cells of non-cancerous origin (MCF-10A).

We found that DiPT-4 induces DNA damage, a robust G2/M arrest, and finally, apoptosis in HCT116 cells.

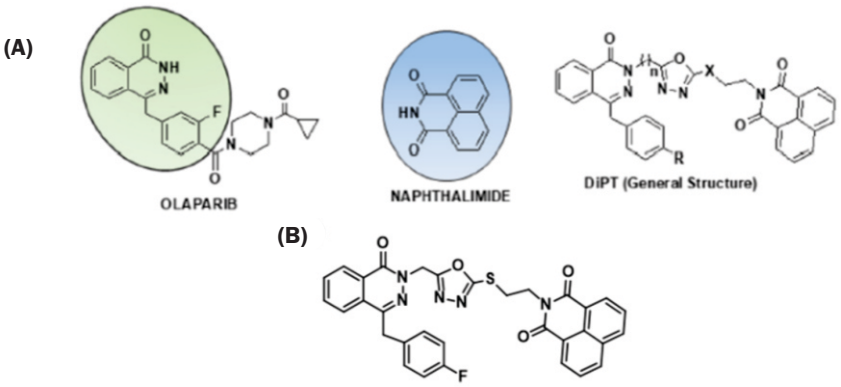

Fig.1: (A) Pharmacophores utilized for development of the DiPT series of molecules. (B) Structure of DiPT-4, the most promising candidate with superior activity compared to both parents. Adapted from [5].

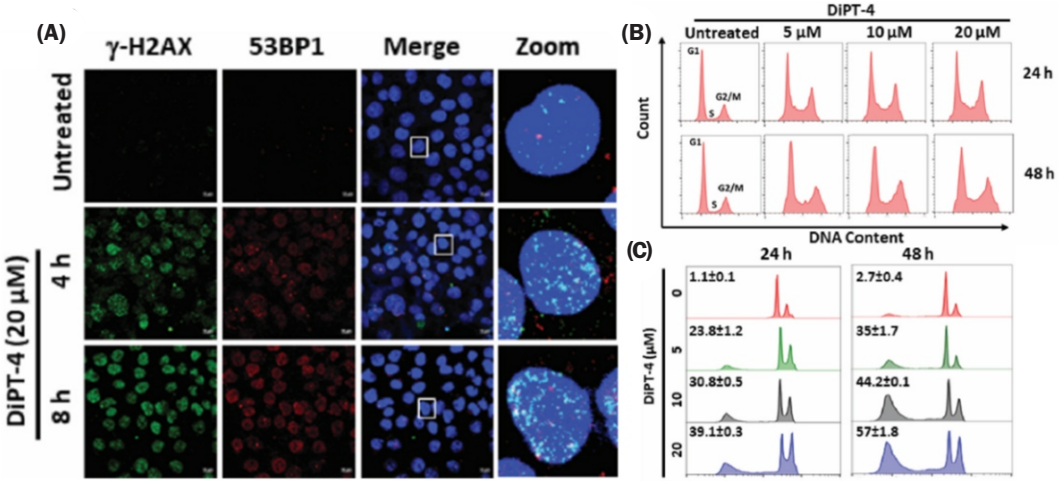

Fig.2: (A) Immunofluorescence-mediated microscopic detection of γ-H2AX and 53BP1 (DNA damage markers) foci in DiPT-4-treated HCT116 cells. (B) Cell cycle and (C) SubG1 (apoptotic population) analysis of HCT116 cells treated with different concentrations of DiPT-4 for 24 or 48 h. Adapted from [5].

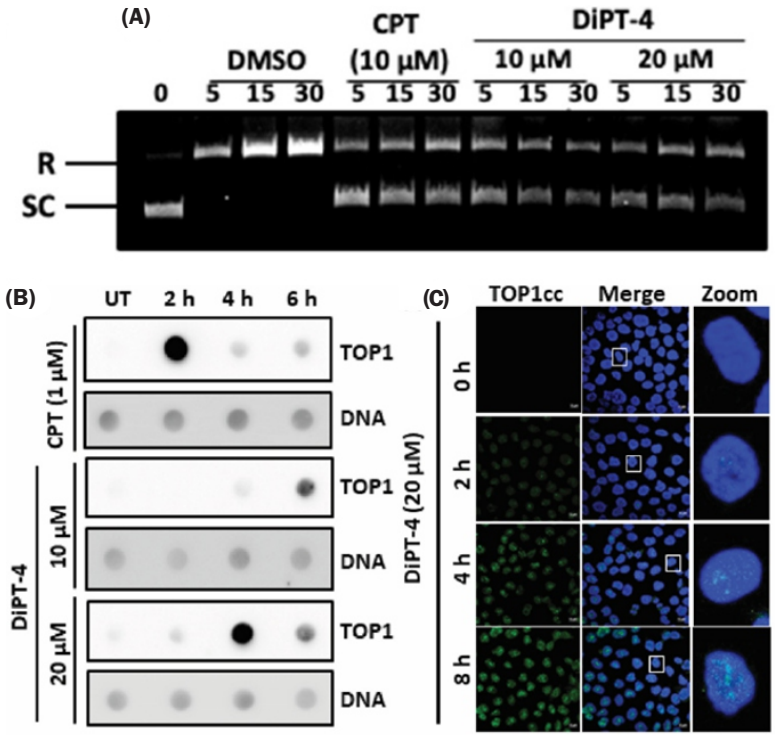

Fig.3: (A) In vitro plasmid relaxation assay with purified human TOP1 in the presence or absence of DiPT-4. R: relaxed DNA; SC: supercoiled DNA. (B) RADAR assay and (C) microscopic detection of time and concentration-dependent TOP1cc stabilization by DiPT-4. Camptothecin (CPT) was used as a positive control. Adapted from [5].

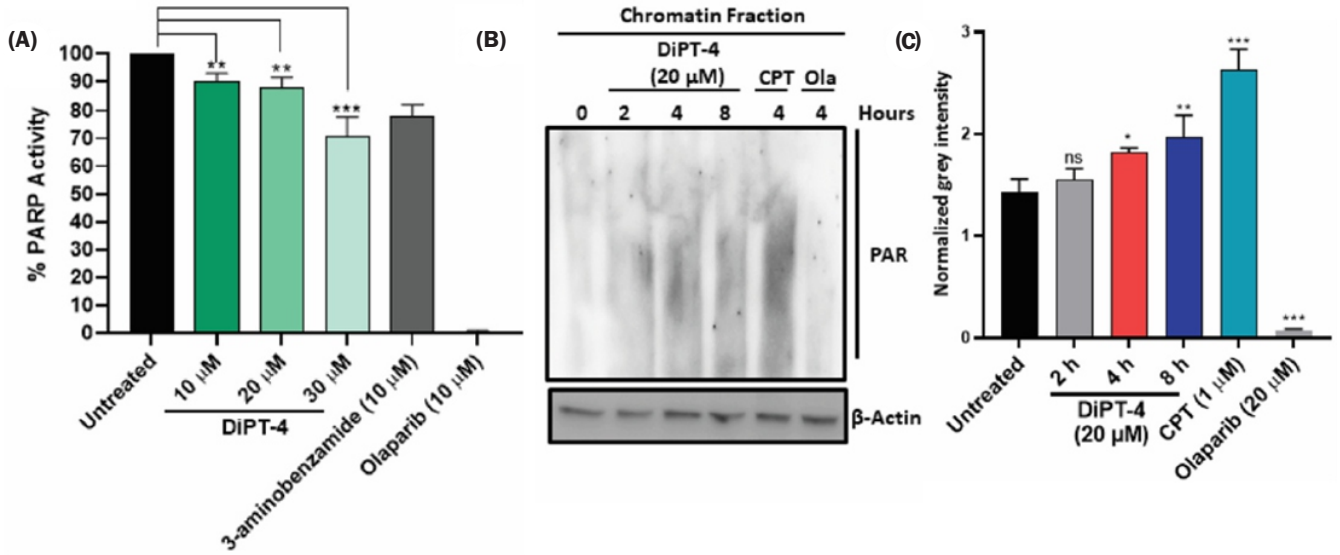

Fig.4: (A) In vitro PARP activity assay with purified human PARP1 in the presence or absence of DiPT-4. (B, C) Total PARylation levels in chromatin fraction of cells treated with DiPT-4, CPT (classical TOP1 inhibitor) and Olaparib (PARP inhibitor). Adapted from [5].

DiPT-4 was found to inhibit TOP1 catalytic activity *in vitro* (Fig. 3A) coupled with TOP1cc stabilization in a time (Fig. 3B, C) and concentration (Fig. 3B) dependent manner.

We also investigated the ability of DiPT-4 to inhibit PARP activity. DiPT-4 was found to inhibit PARP1 catalytic activity *in vitro* (Fig. 4A). Interestingly, DiPT-4 induced significantly lower PARP-mediated poly (ADP-ribosylation) i.e., PARylation in chromatin-bound proteins compared CPT, a classical TOP1 inhibitor (Fig. 4B, C).

Finally, we performed computational calculations to predict pharmacokinetic parameters of DiPT-4. Our calculations revealed that DiPT-4 satisfied both Lipinski and Veber criteria with a single violation (pertaining to molecular weight), suggesting that DiPT-4 possesses favourable drug-like characteristics (Fig. 5).

In addition to the presented findings, other interesting observations were made. As expected of an effective dual inhibitor, DiPT-4 induced copious DNA damage in cells without

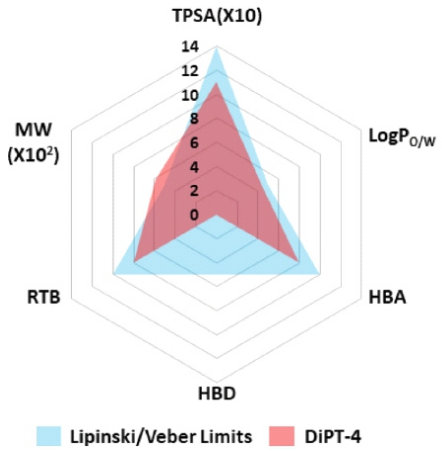

Fig.5: Radar plot of drug-like characteristics of DiPT-4 vs Lipinski and Veber criteria. MW: molecular weight; TPSA: topological polar surface area; LogP$_{O/W}$: lipophilicity; HBA: Hydrogen bond donors; HBD: Hydrogen bond donors; RTB: rotatable bonds. Adapted from [5].

robust induction of PARylation which plays a critical role in removal of TOP1ccs and cellular survival in response to DNA damage. We also observed that TOP1ccs stabilized by DiPT-4 have a longer half-life compared to those stabilized by conventional TOP1-targeted therapies. Also, in contrast to conventional TOP1 inhibitors, treatment with DiPT-4 does not induce global TOP1 downregulation, which is a major protective mechanism which imparts resistance to TOP1 inhibitors. Take together, our results provide a promising proof-of-concept for development of a single molecule dual inhibitor of TOP1 and PARP, which may form the basis for development of more such potent inhibitors with clinical relevance.

References

[1] B.B. Das, S.N. Huang, J. Murai, I. Rehman, J.-C. Amé, S. Sengupta, S.K. Das, P. Majumdar, H. Zhang, D. Biard, H.K. Majumder, V. Schreiber, Y. Pommier, PARP1-TDP1 coupling for the repair of topoisomerase I-induced DNA damage, Nucleic Acids Res., 2014, 42, 4435–4449.https://doi.org/10.1093/nar/gku088.

[2] J. Murai, Y. Zhang, J. Morris, J. Ji, S. Takeda, J.H. Doroshow, Y. Pommier, Rationale for Poly(ADP-ribose) Polymerase (PARP) Inhibitors in Combination Therapy with Camptothecins or Temozolomide Based on PARP Trapping versus Catalytic Inhibition, J Pharmacol Exp Ther., 2014, 349, 408–416. https://doi.org/10.1124/jpet.113.210146.

[3] P.M. LoRusso, J. Li, A. Burger, L.K. Heilbrun, E.A. Sausville, S.A. Boerner, D. Smith, M.J. Pilat, J. Zhang, S.M. Tolaney, J.M. Cleary, A.P. Chen, L. Rubinstein, J.L. Boerner, A. Bowditch, D. Cai, T. Bell, A. Wolanski, A.M. Marrero, Y. Zhang, J. Ji, K. Ferry-Galow, R.J. Kinders, R.E. Parchment, G.I. Shapiro, Phase I Safety, Pharmacokinetic, and Pharmacodynamic Study of the Poly(ADP-ribose) Polymerase (PARP) Inhibitor Veliparib (ABT-888) in Combination with Irinotecan in Patients with Advanced Solid Tumors, Clin Cancer Res., 2016, 22, 3227–3237. https://doi.org/10.1158/1078-0432.CCR-15-0652.

[4] K. Kiianitsa, N. Maizels, A rapid and sensitive assay for DNA–protein covalent complexes in living cells, Nucleic Acids Research, 2013, 41, 104. https://doi.org/10.1093/nar/gkt171.

[5] A. Guha Majumdar, S. Shree, A. Das, B.K. Kumar, P. Dey, M. Subramanian, B.S. Patro, Design, synthesis and development of a dual inhibitor of Topoisomerase 1 and poly (ADP-ribose) polymerase 1 for efficient killing of cancer cells, European Journal of Medicinal Chemistry, 2023, 258, 115598. https://doi.org/10.1016/j.ejmech.2023.115598.

तीव्र विकिरण सिंड्रोम के प्रभावों का न्यूनीकरण

8

तीव्र विकिरण सिंड्रोम में रेडियोसुरक्षा और ऊतक पुनर्जनन के लिए व्हार्टन की जेली से प्राप्त स्टेम कोशिकाओं की क्षमता का उपयोग

धर्मेंद्र कुमार मौर्य[1,2]*, **प्रशस्ति शर्मा** [1,2] **और संतोष कुमार संदुर** [1,2]*
[1]विकिरण जीवविज्ञान और स्वास्थ्य विज्ञान प्रभाग ,भाभा परमाणु अनुसंधान केंद्र ,ट्रांबे- 400085,भारत
[2]होमी भाभा राष्ट्रीय संस्थान ,अणुशक्ति नगर ,मुंबई- 400095, भारत

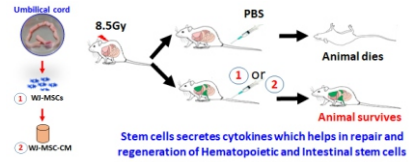

WJ-MSCs (1)और उनके वातानुकूलित माध्यम (2) द्वारा चिकित्सीय रेडियो सुरक्षा

सारांश

अप्रत्याशित परिस्थितियों में यदि कोई व्यक्ति आयनकारी विकिरण के उच्च डोज़ के संपर्क में आता है, तो इससे शरीर के भीतर महत्वपूर्ण रेडियोसंवेदनशील ऊतकों को नुकसान हो सकता है, जिसमें हेमटोपोइएटिक प्रणाली और जठरांत्र संबंधी मार्ग शामिल हैं। अप्रत्याशित विकिरण जोखिम की घटनाओं के बाद इन ऊतकों को पुनर्जीवित करने के लिए तत्काल प्रभावी उपचार की आवश्यकता है। वर्तमान में, मुख्य रूप से रक्त विकारों जैसे न्यूट्रोपेनिया, एनीमिया और थ्रोम्बोसाइटोपीनिया के लिए केवल चार वृद्धि कारक/साइटोकिन्स; न्यूपोजेन, न्यूलास्टा, ल्यूकिन और एनप्लेट को रेडियोमिटिगेटर के रूप में पुन: उपयोग किया जाता है। रेडियोथेरेपी से संबंधित क्षति के लिए एफ. डी. ए.-अनुमोदित औषधियाँ एमिफोस्टिन और पैलिफर्मिन तक सीमित हैं। तीव्र विकिरण सिंड्रोम प्रभावों को कम करने में स्टेम सेल थेरेपी, विशेष रूप से व्हार्टन की जेली मेसेनकाइमल स्टेम सेल्स (डब्ल्यूजे-एमएससी) आशाजनक परिणाम दर्शाता है। वर्तमान अध्ययन में, हमने किरणित माइस (चूहों) में डब्ल्यूजे-एमएससी के रेडियोसुरक्षा प्रभावों की जांच और संभावित चिकित्सीय लाभों का अन्वेषण किया है।

Mitigation of Acute Radiation Syndrome

8

Harnessing the Potential of Wharton's Jelly-derived Stem Cells for Radioprotection & Tissue Regeneration in Acute Radiation Syndrome

Dharmendra Kumar Maurya[1,2]*, **Prashasti Sharma**[1,2] **and Santosh Kumar Sandur**[1,2]*
[1]Radiation Biology & Health Sciences Division, Bhabha Atomic Research Centre, Trombay-400085, INDIA
[2]Homi Bhabha National Institute, Anushakti Nagar, Mumbai-400094, INDIA

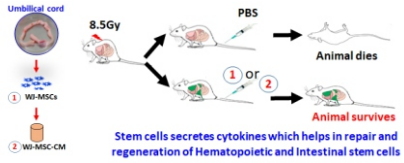

Therapeutic radioprotection by WJ-MSCs (1) and their conditioned medium (2)

ABSTRACT

Unforeseen situations in which individuals are exposed to high doses of ionizing radiation can result in damage to critical radiosensitive tissues within the body, including the hematopoietic system and the gastrointestinal tract. Urgently needed are effective treatments to regenerate these tissues after unexpected radiation exposure incidents. Currently, only four growth factors/cytokines; Neupogen, Neulasta, Leukine, and Nplate are repurposed as radiomitigators, mainly for blood disorders, such as neutropenia, anemia, and thrombocytopenia. FDA-approved drugs for radiotherapy-related damage are limited to Amifostine and Palifermin. Stem cell therapy, particularly Wharton's Jelly Mesenchymal Stem Cells (WJ-MSCs), shows promise in mitigating Acute Radiation Syndrome effects. In the current study, we have investigated the radioprotective effects of WJ-MSCs in irradiated mice, exploring their potential therapeutic benefits.

KEYWORDS: *Ionizing radiation, Radioprotector, Stem cells, Wharton's jelly mesenchymal stem cells*

*Authors for Correspondence: Santosh Kumar Sandur & Dharmendra Kumar Maurya
E-mail: sskumar@barc.gov.in & dkmaurya@barc.gov.in

Introduction

In today's world, the looming threat of radiological and nuclear incidents, whether accidental or deliberate, has propelled a renewed focus on developing effective radiation countermeasures and pharmacotherapeutics. These measures are not only essential for individual safety but also critical for national security. Thus, there is a growing emphasis on the development of treatments to mitigate the effects of radiation exposure. Syndromes associated with radiation exposure can be classified based on the timing of their manifestation: acute, delayed, late, and chronic syndromes. Acute Radiation Syndrome (ARS), distinguished into hematopoietic, gastrointestinal, and neurovascular subsyndromes, based on the absorbed radiation dose and its distribution in tissues [1]. Despite bone marrow transplantation's success in ARS-associated mortality prevention, effective treatments for gastrointestinal injury induced by ionizing radiation remain elusive. Hence, urgent development of novel therapeutics targeting tissues susceptible to acute damage, such as bone marrow and the gastrointestinal system, is imperative. Current research focuses on pharmacotherapeutics including radioprotectors, radiomitigators, and radiation therapeutics, administered pre- or post-exposure to prevent damage or stimulate recovery. Consequently, there's an urgent need to develop novel therapeutics capable of regenerating acutely responding tissues, such as bone marrow, spleen, blood, and the gastrointestinal system, which contain cells with high mitotic potential, emphasizing the high demand for additional FDA-approved agents to address delayed, late, and chronic radiation effects [2].

Stem cells are a distinctive group of cells found throughout life stages, characterized by their capacity for self-renewal and differentiation into various cell types [3]. Adult stem cells like mesenchymal stem cells (MSCs), including those from the umbilical cord, and are favoured due to their versatility and safety. Research has shown promising results regarding Wharton-Jelly mesenchymal stem cells (WJ-MSCs) regenerative capabilities without adverse effects [4]. Previously our lab and others have explored the regenerative potential of WJ-MSCs isolated from the umbilical cord [5-7]. This study aims to investigate the impact of WJ-MSCs infusion on spleen health and morphology of radiosensitive tissues, potentially elucidating therapeutic radioprotective effects. Understanding how WJ-MSCs affect tissue health post-radiation could enhance their clinical application in regenerative medicine and radiation therapy.

Materials and Methods

Ethical approval was secured from the Institutional Ethical Review Board at Bhabha Atomic Research Centre Hospital, Mumbai, India, for umbilical cord collection with written consent. Stem cells were isolated from the cord following established protocols and characterized for stemness. The therapeutic radioprotective potential of these cells was investigated in irradiated mice, assessing spleen colonies and spleen index. Mice were exposed to sub-lethal (6Gy) and lethal (8Gy) radiation doses and infused with WJ-MSCs via tail vein. Histological evaluation of organs like spleen, bone marrow, and jejunum was conducted after 30 days.

Results and Discussion

Radiation-induced septicemia and death are primarily due to damage of the gastrointestinal and hematopoietic system. Due to hematopoietic damage susceptibility to infections increases in parallel to progressive radiation-induced damage of the intestine epithelium lining which allowing for an influx of pathogens into the blood stream. A number of substances have been shown to protect animals from irradiation and include thiol compounds, interleukin 1 (IL-1), tumor necrosis factor-α, granulocyte colony-stimulating factor (G-CSF), and granulocyte/macrophage colony stimulating factor (GM-CSF). Transplantation of normal bone marrow cells into lethally irradiated animals and humans results in long-term survival and provides proof that the hematopoietic system is crucial for defense against the lethal complications induced by radiation. Our study also showed that systemic infusion of WJ-MSCs, 24h after 6Gy radiation exposure increases the formation of endogenous spleen colonies in the 6Gy radiation + WJ-MSCs infused group compared to 6Gy radiation alone (Fig. 1A).

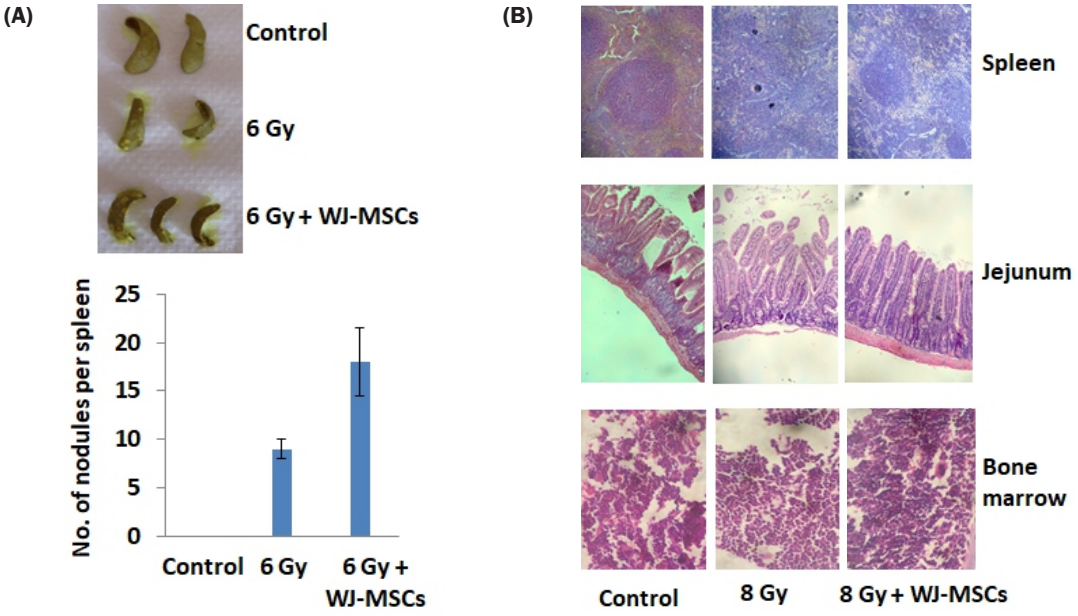

Fig.1: Therapeutic radioprotective effect of WJ-MSCs. (A) Systemic infusion of WJ-MSCs (0.25 million cells/ mice), 24h after 6Gy radiation exposure increases the formation of endogenous spleen colonies in the 6Gy radiation. (B) Systemic infusion of WJ-MSCs (0.25 million cells/mice), 24h after 8Gy radiation exposure restore the tissue morphology in radiosensitive tissues such as Spleen, Jejunum and Bone marrow by day 30.

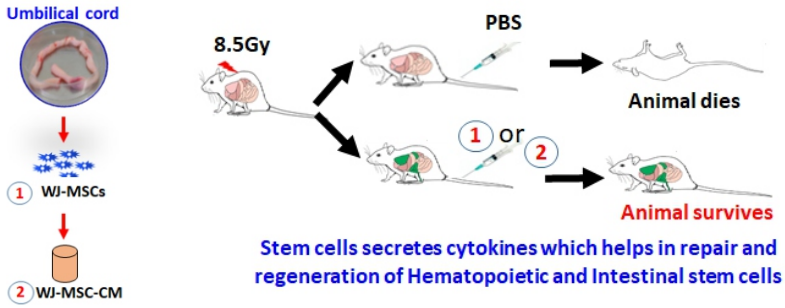

Fig.2: Therapeutic radioprotection by WJ-MSCs (1) and their conditioned medium (2).

The study assessed spleen, jejunum, and bone marrow histology to evaluate the effects of radiation and WJ-MSCs infusion (Fig. 1B). The cellular composition of the spleen's white pulp and red pulp serves as a crucial indicator of spleen function. In the study, histological examination of spleen sections from a control group displayed normal cellular characteristics, while those from a group exposed to 8Gy radiation showed disorganized cellularity in both red and white pulp. However, the group treated with 8Gy radiation and WJ-MSCs exhibited a more organized cellularity, suggesting a better recovery. Physical examination of spleens further supported this, showing less radiation-induced damage and improved morphology in the 8Gy radiation + WJ-MSCs group compared to the radiation-alone group.

The study also observed the effects of radiation on the jejunum and bone marrow. Jejunum morphology in both radiation groups resembled controls after 30 days, with better crypt morphology in the WJ-MSCs infused group. Bone marrow showed morphological recovery in all groups by day 30. These findings suggest that WJ-MSCs infusion aids in mitigating radiation-induced damage, particularly in spleen and jejunum, likely by promoting tissue regeneration. Additionally, bone marrow recovery highlights the importance of replenishing functional hematopoietic stem cells and progenitors for long-term hematopoietic system restoration post-radiation exposure.

Previous studies demonstrate that administering human WJ-MSCs or their conditioned media (WJ-MSC-CM) to mice significantly enhances survival post-lethal radiation exposure [5,6] (Fig. 2). WJ-MSCs migrate to radiosensitive tissues, such as the spleen, bone marrow, and small intestine, promoting tissue repair and modulating the microenvironment by releasing cytokines and growth factors. These cells protect hematopoietic and intestinal stem cells from radiation damage, facilitating regeneration of the hematopoietic system and gastrointestinal tract lining, thus preventing acute radiation syndrome-related fatalities. Xenogeneic WJ-MSCs transplantation stimulates human and mouse cytokine production, with human-derived IL-6 and G-CSF identified as crucial for radioprotection [5]. Additionally, WJ-MSC-CM treatment post-radiation exposure significantly reduces mortality, with anti-G-CSF antibody neutralization abolishing its radioprotective effects. While WJ-MSC-CM provides around 40% protection, indicating potential additional mechanisms, it underscores the significant role of WJ-MSCs and their secretory factors in conferring radioprotection [6].

Conclusion

In conclusion, stem cell-based radioprotection offers promising prospects for enhancing survival post-radiation exposure. WJ-MSCs demonstrate potential in aiding recovery from radiation-induced hematopoietic and gastrointestinal injuries through their secretion of anti-inflammatory and tissue-protective molecules. This presents a viable option for developing radiation countermeasures and as an alternative to bone marrow transplantation.

Acknowledgment

The authors acknowledge the contribution of Dr. Mayuri Bandekar.

References

[1] I.G.M Macià, A. C. Lucas and E.C. López, Radiobiology of the acute radiation syndrome, Rep Pract Oncol Radiother., 2011, 16, 123-130.

[2] V.K. Singh, P.L. Romaine and T.M. Seed, Medical Countermeasures for Radiation Exposure and Related Injuries: Characterization of Medicines, FDA-Approval Status and Inclusion into the Strategic National Stockpile, Health Phys., 2015, 108, 607-630.

[3] S. Poliwoda, N. Noor, E. Downs, A. Schaaf, A. Cantwell, L. Ganti, et al., Stem cells: A comprehensive review of origins and emerging clinical roles in medical practice, Orthop Rev (Pavia), 2022, 14, 37498.

[4] M. L. Weiss, C. Anderson, S. Medicetty, K. B. Seshareddy, R. J. Weiss, I. VanderWerff, et al. Immune properties of human umbilical cord Wharton's jelly-derived cells, Stem Cells, 2008, 26, 2865-2874.

[5] M. Bandekar, D. K. Maurya, D. Sharma, R. Checker, V. Gota, N. Mishra and S. K. Sandur et al., Xenogeneic transplantation of human WJ-MSCs rescues mice from acute radiation syndrome via Nrf-2-dependent regeneration of damaged tissues, American Journal of Transplantation, 2020, 20, 2044-2057.

[6] D.K. Maurya, M. Bandekar and S. K. Sandur, Soluble factors secreted by human Wharton's jelly mesenchymal stromal/stem cells exhibit therapeutic radioprotection: A mechanistic study with integrating network biology, 2022, World Journal of Stem Cells, 2022, 14, 347-361. 10.4252/wjsc.v14.i5.347

[7] C. Zhang, et al., CXCR4-Overexpressing Umbilical Cord Mesenchymal Stem Cells Enhance Protection against Radiation-Induced Lung Injury, Stem Cells International, 2019, 2457082. 10.1155/2019/2457082

न्यूरोएंडोक्राइन ट्यूमर का कृत्रिम मेधा आधारित

न्यूरोएंडोक्राइन ट्यूमर का रक्त-आधारित पता लगाने में सक्षम कृत्रिम मेधा

महेश कुमार पडवाल [1,2], राहुल वी. परघाने [2,3], अविक चक्रवर्ती [2,3], भक्ति बसु [1,2]* और संदीप बसु [2,3]*

[1]आण्विक जीवविज्ञान प्रभाग, भाभा परमाणु अनुसंधान केंद्र, ट्रांबे-400085, भारत
[2]होमी भाभा राष्ट्रीय संस्थान, अणुशक्ति नगर, मुंबई-400094, भारत
[3]विकिरण औषधि केंद्र, भाभा परमाणु अनुसंधान केंद्र, टाटा स्मारक केंद्र उप भवन, परेल, मुंबई-400012, भारत

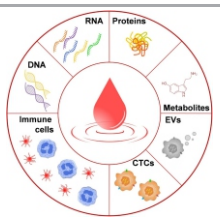

रक्तप्रवाह में ट्यूमर द्वारा जारी/संशोधित विभिन्न प्रकार के छोटे संकेतों का सचित्र चित्रण।

सारांश

मयह शोध पत्र रक्त के नमूने से न्यूरोएंडोक्राइन ट्यूमर (NET) रोग का पता लगाने से संबंधित है। यह तकनीक स्वस्थ नमूनों को न्यूरोएंडोक्राइन ट्यूमर नमूनों से अलग करने के लिए भिन्न-भिन्न अनुकूलित RNA अणुओं और कृत्रिम मेधा-आधारित गणितीय तर्कशास्त्र का उपयोग करती है। कृत्रिम मेधा -आधारित वर्गीकरण गणितीय तर्कशास्त्र ने रोग की उपस्थिति का पूर्वानुमान करने में उच्च सटीकता (> 95%) प्राप्त किया है। यह उपकरण विभिन्न विशेषताओं को एकीकृत कर सकता है, जिसका न्यूरोएंडोक्राइन ट्यूमर रोगियों के व्यक्तिगत प्रबंधन के लिए विविध अनुप्रयोग हो सकता है। उपचार अनुक्रिया की निगरानी और वंशानुगत खतरे का पूर्वानुमान लगाने के लिए उपकरण की क्षमता पर चर्चा की गई है।

AI based Detection of Neuroendocrine Tumors

The Power of AI Enables Blood-based Detection of Neuroendocrine Tumors

Mahesh Kumar Padwal[1,2], Rahul V. Parghane[2,3], Avik Chakraborty[2,3], Bhakti Basu[1,2]* and Sandip Basu[2,3]*

[1]Molecular Biology Division, Bhabha Atomic Research Centre, Trombay-400085, INDIA
[2]Homi Bhabha National Institute, Anushakti Nagar, Mumbai-400094, INDIA
[3]Radiation Medicine Centre, Bhabha Atomic Research Centre, Tata Memorial Centre Annexe, Parel, Mumbai-400012, INDIA

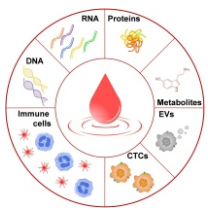

Pictorial depiction of a variety of tiny signals released/ modulated by the tumor in the bloodstream

ABSTRACT

This communication deals with the detection of the Neuroendocrine Tumor (NET) disease from the blood sample. The technique utilizes a set of differentially expressed RNA molecules and an AI-based algorithm to distinguish healthy samples from the NET samples. The AI-based classification algorithm achieved high accuracy (> 95%) in predicting the presence of the disease. The tool can integrate various features that may have diverse applications for the personalized management of NET patients. The potential of the tool for monitoring treatment response and predicting inherited susceptibility is discussed.

KEYWORDS: *Neuroendocrine Tumors, Peripheral blood transcriptome, Machine learning, Blood biomarkers*

**Authors for Correspondence: Bhakti Basu & Sandip Basu*
E-mail: bbasu@barc.gov.in & drsanb@barc.gov.in

Introduction

Why blood biomarkers?

The incidence and prevalence of cancer are increasing by the day and so is the race to detect this dreadful disease early [1-2]. As India transitions to becoming the most populous country in the world, there are high odds of a steep disease burden. Early detection warrants an easy, non-invasive, sensitive (fewer false negatives) and specific (fewer false positives) test that uses a surrogate sample representative of a disease state. Depending on the location of the cancer, several body fluids are potential candidates as the sample source. However, being in touch with the entire body, blood has gained widespread attention and research focus for the detection of disease-specific biomarkers [3]. Moreover, blood analysis also offers insight into the genetic susceptibility to the disease [4]. This emerging tool, called *Liquid biopsy* in comparison to conventional invasive tissue biopsy, is currently the focus of active research the world over [3].

Types of biomarkers

A drop of blood contains millions of cells and billions of biomolecules in equilibrium with the health status of an individual. Blood is a carrier of various biomolecules, vesicles, etc. along with RBCs, WBCs, and platelets. In cancer patients, the cancerous tissue releases tiny signals in the form of circulating tumor DNA (ctDNA), circulating tumor RNA (ctRNA), protein markers, metabolites, extracellular vesicles, and circulating tumor cells (CTCs) into the bloodstream (Fig.1). The evidence suggests that the tumors *educate* certain immune cells and can dysregulate the systemic immune system [5]. If these tiny tumor-specific signals can be detected, quantified, distinguished from the healthy samples, and correlated with the clinical parameters of the patient, it is possible to devise a blood test to diagnose, monitor treatment response, and predict the prognosis of cancer.

Detecting disease-specific biomarkers in blood - A formidable challenge

Routine blood tests to profile levels of sugar, lipids, minerals, vitamins, hormones, parasites, etc. measure monoanalyte markers and associate the marker with the underlying disease condition, e.g., high level of blood sugar (> 120 mg/dL) is associated with diabetes. However, as cancer is a complex disease that involves local and systemic changes, monoanalyte markers often demonstrate low accuracy. The multi-analyte markers are identified in 2 ways. One of the ways is to identify the tumor-specific markers in tumor tissues by comparison with the normal tissues. Such tumor-specific markers represent the local changes in the tumor [6], which can be detected in the blood by qTR-PCR. The second way is to identify the disease-specific markers by directly profiling the blood samples from the cancer patients and comparing them with those of the healthy donors. These markers capture the local as well as the systemic changes induced by the tumor. In the case of DNA or RNA markers, the sequencing method can fish out pathogenic inherited/ sporadic germ-line mutations that impart susceptibility to early disease onset. Here, we present our recent findings on the peripheral blood RNA-sequencing-based multi-analyte tool for the diagnosis of Neuroendocrine Tumors (NETs).

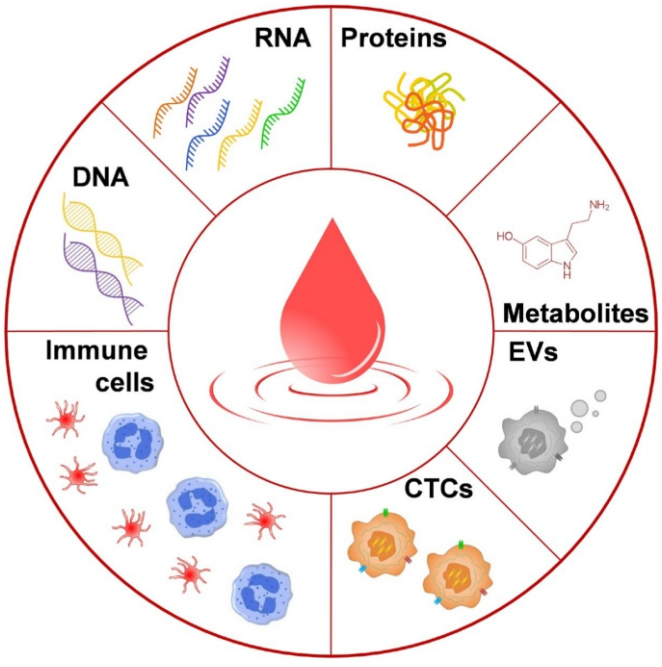

Fig.1: Pictorial depiction of a variety of tiny signals released/ modulated by the tumor in the bloodstream.

Materials and Methods

Study participants

The study participants included healthy donors (n = 51) and NET patients (n = 86) registered for ^{177}Lu-DOTATATE PRRT at Radiation Medicine Centre, India, according to eligibility criteria detailed earlier [7]. Written informed consent was obtained from all the participants and the study was approved by the Institutional Scientific Advisory Committee (SAC) and Institutional Ethics Committee (IEC). All NET samples were collected before the first PRRT cycle. The blood samples were collected in BD Vacutainer® K2 EDTA Tubes and were processed for RBC lysis by hypotonic shock method. The intact blood cells were lysed in TRI reagent (Sigma) and RNA was isolated using RNeasy Mini Kit (QIAGEN). RNA libraries were prepared with Ultra II Directional RNA-Seq Library Prep kit (NEB) and sequenced on Illumina HiSeq X instrument at the CAP-accredited commercial facility of Medgenome Lab Ltd., Bangalore, India.

Processing of RNA-Seq data

Clean RNA-Seq reads obtained using FASTP [8] were mapped to the human reference genome (GRCh38) using a splice-aware STAR aligner [9]. Gene counts were quantified using RSEM [10]. Differential expression analyses were performed on gene counts using the DESeq2 package [11]. The training set and test set samples were normalized separately. Low expression and highly variant genes were removed. The remaining 17220 genes were VST normalized and adjusted for batch effects using SVA.

Feature selection and diagnostic classifier

Relevant and complementary features were selected from VST-normalized and SVs-adjusted counts of 17,220 genes from the training sample set using the mRMRe R package [12]. Random forest algorithm was developed using the CARET package and multi-analyte gene features. Hyper-parameter mtry was optimized and the RF model was cross-validated using a 5-fold cross-validation method repeated 10 times. The performance metrics of the diagnostic classifier were assessed based on sensitivity, specificity, and accuracy.

Results and Discussion

Fig.2 shows an overall study design which includes data from 107 samples in the training set and 30 samples in the test set. The training set samples comprised NETs of the pancreas, gastrointestinal tract, and lung. The NET patients had either

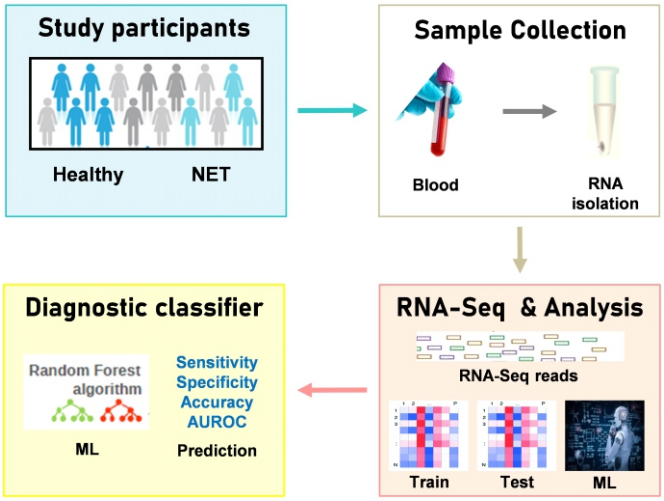

Fig.2: Study design.

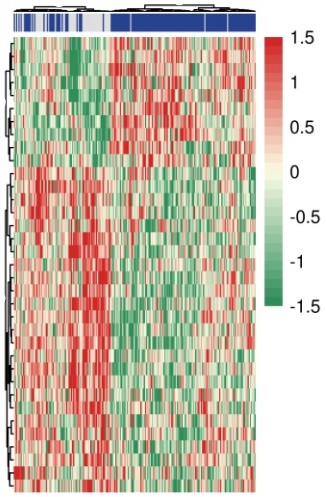

Fig.3: The hierarchical heatmap shows the segregation of samples of NET patients and healthy donors based on the expression of the most relevant gene features. The color bar represents Log2 fold change in the expression levels between the patients' samples (blue bar at the top) and the samples from the healthy donors (grey bar at the top).

localized or metastatic disease. About 40% of the NET patients had hormonal syndrome. More than 94% of RNA-Seq reads aligned to the human genome, and the reads comprised protein-coding genes, long non-coding RNAs (lncRNAs), and other small RNAs. The peripheral blood transcriptome was enriched with the genes encoded by the immune cells as well as the neuroendocrine cells. The differentially expressed genes in the blood of NET patients were used to develop a diagnostic classifier.

In the training set samples, RNA-Seq data revealed 1500 differentially expressed genes. The selection of the NET-specific gene features was guided by the expression levels of each gene and lower variability among the samples. Expression values of the selected gene features grouped the patients' samples and the healthy samples into different clusters, with some overlap (Fig.3).

The expression values of the selected NET-specific gene features were used as input features to train a diagnostic classifier using a random forest algorithm. Random forest is a decision tree algorithm that partitions the sample into either healthy or NET according to the expression levels of the NET-specific gene features (Fig.4 a). Five hundred such decision trees determine the final prediction of the sample.

In the training set, the classifier achieved 100% sensitivity and 100% specificity (Fig.4 b). In the test set, the classifier achieved 94.4% sensitivity and 100% specificity (Fig.4 b). In addition to expression-based prediction, qualitative data on RNA sequencing is useful for the assessment of pathogenic gene mutations potentially associated with the disease.

Conclusion

We have demonstrated an advanced tool for cancer detection from a blood sample. The method can be used to diagnose NET cases with high accuracy and has a potential clinical utility in monitoring the treatment response. Integration of mutation data on genes associated with NET would enable the identification of cases with inherited susceptibility to the disease or predict prognosis when combined with the relevant clinical parameters and imaging modalities. Taken together, the tool offers scope for personalized management of Neuroendocrine Tumor patients. To the best of our knowledge, this is the first report on RNA-Seq-based blood test for cancer in India.

Acknowledgment

The authors gratefully acknowledge the study participants for consenting to donate blood samples for this study. They also acknowledge Mrs. Lalita Gangurde, and Mrs. Anita Shinde, RMC for their technical support in blood collection.

References

[1] R. L. Siegel, K. D. Miller, H. E. Fuchs, and A. Jemal, Cancer Statistics 2022, CA Cancer J Clin., 2022, 72, 7-33.

[2] K. Sathishkumar, M. Chaturvedi, P. Das, S. Stephen, P. Mathur, Cancer incidence estimates for 2022 & projection for 2025:

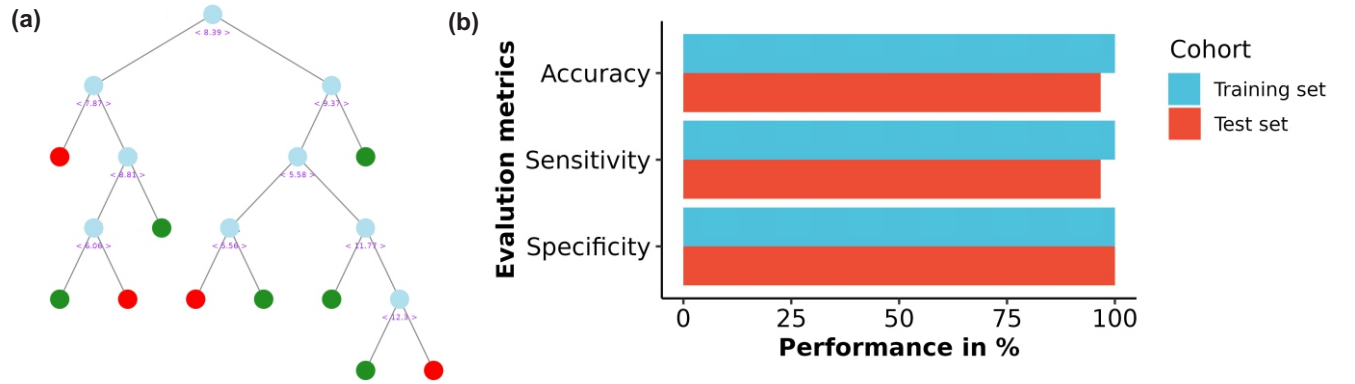

Fig.4: Machine learning to identify NETs from the blood sample. (a) A representative decision tree of the diagnostic classifier. Expression values are indicated (< value >) below each gene feature (light blue circle). Red and green circles represent the prediction of NET and healthy, respectively. (b) Accuracy metrics for detecting NETs in training and the test sets.

Result from National Cancer Registry Programme, India, Indian J Med Res., 2022, 156, 598-607.

[3] J. Marrugo-Ramírez, M. Mir, and J. Samitier, Blood-Based Cancer Biomarkers in Liquid Biopsy: A Promising Non-Invasive Alternative to Tissue Biopsy, Int J Mol Sci., 2018, 19, 2877.

[4] B. Basu and S. Basu, Correlating and combining Proteomic assessment with in vivo Molecular functional Imaging: Will this be the future roadmap for Personalized Cancer management? Cancer Biother. Radiopharm., 2016, 31, 75-84.

[5] K. J. Hiam-Galvez, B. M. Allen, and M. H. Spitzer, Systemic immunity in cancer. Nat Rev Cancer, 2021, 21, 345-359.

[6] M. K. Padwal, S. Basu, and B. Basu, Application of machine learning in predicting hepatic metastasis or primary site in gastroenteropancreatic neuroendocrine tumors. Current Oncology, 2023, 30, 9244-9261.

[7] K. Sitani, R.V. Parghane, S. Talole, and S. Basu, Long-term outcome of indigenous (177)Lu-DOTATATE PRRT in patients with Metastatic Advanced Neuroendocrine Tumours: A single institutional observation in a large tertiary care setting, Br. J. Radiol., 2021, 94, 20201041.

[8] S. Chen, Y. Zhou, Y. Chen, and J. Gu, fastp: An ultra-fast all-in-one FASTQ preprocessor, Bioinformatics, 2018, 34, 884-890.

[9] A. Dobin, C. A. Davis, F. Schlesinger, J. Drenkow, C. Zaleski, S. Jha, P. Batut, M. Chaisson, and T. R. Gingeras, STAR: Ultrafast universal RNA-seq aligner, Bioinformatics, 2013, 29, 15-21.

[10] B. Li, and C. N. Dewey, RSEM: Accurate transcript quantification from RNA-Seq data with or without a reference genome, BMC Bioinformatics, 2011, 12, 323.

[11] M. I. Love, W. Huber, and S. Anders, Moderated estimation of fold change and dispersion for RNA-seq data with DESeq2, Genome Biol., 2014, 15, 550.

[12] N. De Jay, S. Papillon-Cavanagh, C. Olsen, N. El-Hachem, G. Bontempi, and B. Haibe-Kains, mRMRe: An R package for parallelized mRMR ensemble feature selection, Bioinformatics, 2013, 29, 2365-2368.

स्तन कैंसर के लिए पूर्वानुमान कारक चिह्नक

10

स्तन कैंसर रोगियों में पुनरावृत्ति, मेटास्टेसिस और चिकित्सा अनुक्रिया के लिए रोगसूचक और पूर्वानुमानित चिह्नक के रूप में थायोरेडॉक्सिन रिडक्टेस 1

राघवेंद्र एस. पटवर्धन[1], **अर्चिता राय** [1,2], **दीपक शर्मा**[1,2], **संतोष के. संदुर** [1,2]* **और सेजल पटवर्धन** [1,2]*

[1]विकिरण जीवविज्ञान एवं स्वास्थ्य विज्ञान प्रभाग, भाभा परमाणु अनुसंधान केंद्र, ट्रांबे-४०००८५, भारत
[2]होमी भाभा राष्ट्रीय संस्थान, अणुशक्ति नगर, मुंबई-400094, भारत
[3]पटवर्धन लैब, एडवांस्ड सेंटर फॉर ट्रीटमेंट रिसर्च एंड एजुकेशन इन कैंसर, (एक्ट्रेक), टाटा मेमोरियल सेंटर (टीएमसी), खारघर, नवी मुंबई-४१०२१०, भारत

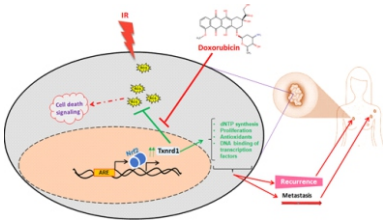

Txnrd1 अति-अभिव्यक्ति स्तन कैंसर में पुनरावृत्ति, मेटास्टेसिस और चिकित्सा प्रतिक्रिया से जुड़ी हुई है।

सारांश

थायोरडॉक्सिन रिडक्टेस 1 (Txnrd1) को स्तन कैंसर रोगियों के एक उपसमूह में रोगनिदान संबंधी महत्व के लिए जाना जाता है। Txnrd1 को कैंसर की प्रगति और मेटास्टेसिस में कई कोशिकीय एवं शारीरिक प्रक्रियाओं को विनियमित करने में एक महत्वपूर्ण भूमिका निभाने के लिए जाना जाता है, हालाँकि, इसका नैदानिक महत्व काफी हद तक पहचाना नहीं गया है। यहाँ, Txnrd1 की रोगनिदान संबंधी और भविष्य निर्धारण की भूमिका का आकलन करने के लिए 43 स्वतंत्र समूहों से 13322 स्तन कैंसर रोगियों का पूर्वव्यापी व्यापक मेटा-विश्लेषण किया गया। यह पाया गया कि Txnrd1 का ट्यूमर ग्रेड और आकार के साथ सकारात्मक संबंध है। इसके अलावा, नकारात्मक-रिसेप्टर और सकारात्मक-HER2 हार्मोन ट्यूमर में Txnrd1 जीन अधिक अनुकूल होती है। उच्च Txnrd1 अनुकूलन वाले रोगी लघु रोग-वैशिष्ट्य और समग्र उत्तरजीविता के लिए महत्वपूर्ण जोखिम प्रदर्शित करते हैं। जबकि, Txnrd1 का ट्यूमर पुनरावृत्ति और मेटास्टेसिस के साथ सकारात्मक सहसंबंध है, तथापि इसकी पुनरावृत्ति और मेटास्टेसिस के समय के साथ नकारात्मक संबंध है। Txnrd1 उच्च रोगियों में Txnrd1 निम्न समूह की तुलना में 2.5 वर्ष पहले पुनरावृत्ति और 1.3 वर्ष पहले मेटास्टेसिस होता है। दिलचस्प बात यह है कि उच्च Txnrd1 जीन अभिव्यक्ति वाले रोगी नियोएडजुवेंट कीमोथेरेपी के लिए एक पैथोलॉजिकल पूर्ण अनुक्रिया (pCR) प्रदर्शित करते हैं, लेकिन रेडियोथेरेपी के बाद, वे जल्दी पुनरावृत्ति का अनुभव करते हैं। Txnrd1 उच्च MDA-MB-231 कोशिकाएं Txnrd1 निम्न MCF7 कोशिकाओं की तुलना में डॉक्सोरूबिसिन उपचार के बाद महत्वपूर्ण ROS उत्पादन और कम व्यवहार्यता प्रदर्शित करती हैं। मेटा-विश्लेषण से प्राप्त निष्कर्षों की पुष्टि करते हुए, Txnrd१ की कमी से जीवित रहने की दर में कमी, विकिरण प्रेरित हत्या के प्रति संवेदनशीलता में वृद्धि, खरोंच-घाव का खराब उपचार और MDA-MB-231 कोशिकाओं में आक्रमण की संभावना कम हो जाती है। इस प्रकार, Txnrd1 स्तन कैंसर रोगियों में पुनरावृत्ति, मेटास्टेसिस और चिकित्सा अनुक्रिया से संबंधित भविष्य की संभावित जानकारी प्रदान करता प्रतीत होता है।

Predictive markers for Breast Cancer

10

Thioredoxin Reductase 1 as a Prognostic & Predictive Marker for Recurrence, Metastasis & Therapy Response in Breast Cancer Patients

Raghavendra S. Patwardhan[1], **Archita Rai**[1,2], **Deepak Sharma**[1,2], **Santosh K. Sandur**[1,2]* **and Sejal Patwardhan**[1,2]*

[1]Radiation Biology & Health Sciences Division, Bhabha Atomic Research Centre, Trombay-400085, INDIA
[2]Homi Bhabha National Institute, Anushakti Nagar, Mumbai-400094, INDIA
[3]Patwardhan Lab, Advanced Centre for Treatment Research & Education in Cancer (ACTREC),
Tata Memorial Centre (TMC), Kharghar, Navi Mumbai-410210, INDIA

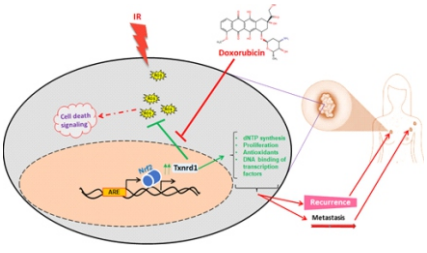

Txnrd1 over-expression is associated with recurrence, metastasis and therapy response in breast cancer

ABSTRACT

Thioredoxin reductase 1 (Txnrd1) is known to have prognostic significance in a subset of breast cancer patients. Txnrd1 is known to play a pivotal role in regulating several cellular and physiological processes in cancer progression and metastasis, however, its clinical significance is largely unrecognized. Here, a retrospective comprehensive meta-analysis of 13322 breast cancer patients from 43 independent cohorts to assess prognostic and predictive roleof Txnrd1 was undertaken. It was observed that Txnrd1 has a positive correlation with tumor grade and size. Further, hormone receptor-negative and HER2-positive tumors exhibit elevated Txnrd1 gene expression. Patients with elevated Txnrd1 expression exhibit significant hazards for shorter disease-specific and overall survival. While Txnrd1 has a positive correlation with tumor recurrence and metastasis, it has a negative correlation with time for recurrence and metastasis. $Txnrd1^{High}$ patients exhibit 2.5 years early recurrence and 1.3 years early metastasis as compared to $Txnrd1^{Low}$ cohort. Interestingly, patients with high Txnrd1 gene expression exhibit a pathologic complete response (pCR) to neoadjuvant chemotherapy, but they experience early recurrence after radiotherapy. $Txnrd1^{High}$ MDA-MB-231 cells exhibit significant ROS generation and reduced viability after doxorubicin treatment compared to $Txnrd1^{Low}$ MCF7 cells. Corroborating with the findings from meta-analysis, Txnrd1 depletion leads to decreased survival, enhanced sensitivity to radiation induced killing, poor scratch-wound healing, and reduced invasion potential in MDA-MB-231 cells. Thus, Txnrd1 appears to be a potential predictor of recurrence, metastasis and therapy response in breast cancer patients.

KEYWORDS: *Thioredoxin reductase, Nrf2, ROS, Ionizing radiation, Therapy response*

*Authors for Correspondence: Raghavendra S. Patwardhan & Santosh K. Sandur
E-mail: spatwardhan@actrec.gov.in & sskumar@barc.gov.in

Introduction

Breast cancer is a complex disease characterized by four major molecular subtypes and 21 distinct histological subtypes, with approximately 81% being invasive and 83% hormone receptor-positive, while around 15% are HER2-positive [1]. The age-standardized incidence and mortality rate for breast cancer are 47.8 and 13.6 per 100,000 cases, respectively [2]. Despite advancements in treatment modalities and early detection, there is an increase in the incidence of local-stage disease, though mortality rates have declined significantly [3]. Treatment modalities like chemo, hormonal, or targeted molecular therapy have shown promising results in locally advanced breast cancers (LABC), triple-negative breast cancer (TNBC), and metastatic disease when combined with surgery [4]. However, there is still a risk of recurrence, reduced disease-free survival (DFS) and poor quality of life (QoL) among survivors [5]. Different factorcontribute to breast cancer recurrence include tumor size, lymph node involvement, close tumor margins, age, lack of hormone and radiotherapy, and inflammatory breast cancer [6]. In addition to traditional prognostic factors, gene expression profiling plays a crucial role in prognosis and treatment planning. Radiotherapy post-breast-conserving surgery aims to eliminate remnant cancer cells [7], yet intrinsic radio-resistance and the acquisition of a resistant phenotype limit its efficacy, necessitating predictive tools for treatment decisions.

Studies from our laboratory have highlighted the role of Nrf2 and oxidative stress response pathways in regulating radio-resistance in cancer cells [8]. Thioredoxin reductase (TrxR), controlled by Nrf2, is a key redox-regulatory protein involved in various cellular processes. Overexpression of Txnrd1, a subtype of TrxR, has been associated with several cancers, including breast cancer, impacting invasion, metastasis, and prognosis [9, 10]. Given its significance, a detailed investigation across global datasets is warranted to understand its predictive value for recurrence, metastasis, and treatment response. A retrospective analysis was conducted, encompassing RNAseq and microarray data from 13,322 breast cancer patients across 43 independent gene expression datasets. The study examined the association of Txnrd1 expression with various clinic-pathological parameters, including tumor grade, size, stage, histology, menopause status, molecular subtypes, overall survival (OS), disease-specific survival (DSS), recurrence, metastasis, and response to chemotherapy and radiotherapy. Experimental validation in breast cancer cell lines further supported Txnrd1 as a valuable predictor for disease recurrence and therapy response in breast cancer patients.

Materials and Methods

Reagents

The human breast cancer cell lines MCF-7, MDA-MB468, and MDA-MB-231 were obtained from the National Centre for Cell Science (NCCS, Pune, India) and cultured in DMEM medium supplemented with 10% fetal bovine serum (FBS), L-glutamine, penicillin, and streptomycin. Reagents used in the study, including the thioredoxin reductase assay kit, RNA isolation kit, cDNA synthesis, RT-PCR kit, doxorubicin, auranofin, formaldehyde, crystal violet, H_2DCF-DA, TrxR1 CRISPR plasmids, and Lipofectamine 3000 transfection reagent, were procured from various suppliers.

Study design and gene expression data

A retrospective meta-analysis was conducted using gene expression data from 43 public datasets, comprising microarray/RNAseq analysis of tumor specimens from 13,322 breast cancer patients. Data sources included the NCBI Gene Expression Omnibus (GEO), Molecular Taxonomy of Breast Cancer International Consortium (METABRIC) database, The Cancer Genome Atlas (TCGA), and other sources. Optimal cut-off points for Txnrd1 gene expression were determined using various methods, and patients were categorized into Txnrd1^{High} and Txnrd1^{Low} subgroups accordingly.

Study endpoints

Study endpoints were divided into three categories: cross-study comparison, survival analysis, and meta-analysis. Cross-study comparison involved analyzing Txnrd1 gene expression across various clinic-pathological parameters. Survival analysis was conducted to determine cumulative mean time to outcome, while meta-analysis combined effect sizes across datasets using multivariate Cox-regression analysis.

In vitro assays

RNA isolation, cDNA synthesis, and qRT-PCR were conducted to analyze gene expression. Transfection of TrxR1 CRISPR/Cas9 KO Plasmid was performed using Lipofectamine 3000 reagent, and clonogenic, wound healing, and invasion assays were conducted to assess cellular functions.

Statistical analysis

Statistical analysis included estimation of differences in gene expression, correlation coefficient calculation, survival curve comparison, hazard ratio and relative risk estimation, and meta-analysis. Statistical significance was determined using t-tests, one-way ANOVA, log-rank tests, and other appropriate methods. Data were presented as mean ± S.E.M.

Results and Discussion

Txnrd1 expression exhibits positive correlation with tumor grade and size

The selection criteria for datasets and the corresponding cohort sizes are outlined in Fig.1(a), providing a visual representation of the dataset selection process. Txnrd1 mRNA levels are altered in ~14% breast cancer patients (Fig.1(b)). In 21 datasets analyzed, a significant variation in Txnrd1 gene expression according to tumor grade was observed, with higher expression correlating with more aggressive tumors (Fig.1(c)). Additionally, tumors with high Txnrd1 expression are larger by 2.59±0.8 mm (95% CI, 0.849-4.331; at $p < 0.007$) compared to those with low expression (Fig.1(d)). Hormone-receptor negative and HER2 positive tumors harbor elevated Txnrd1 expression (Fig.1(e)). Depletion of Txnrd1 in aggressive breast cancer cells reduced clonogenic potential, supporting its role in promoting cell survival and proliferation (Fig.1(f)). This association is particularly relevant for locally advanced breast cancers, where aggressive tumors exhibit elevated Txnrd1 expression, potentially influencing their prognosis. Further, mRNA expression corroborated well with respective breast cancer cell lines (Fig.1(g)).

Txnrd1 over-expressing breast cancer patients exhibit shorter disease-specific and overall survival:

***Abbreviations**: Auranofin, AF; DFS, disease-free survival; DSS, disease-specific survival; DRFS, distant recurrence-free survival; DMFS, distant metastasis-free survival; ER, estrogen receptor; HER2, human epidermal growth factor receptor 2; HR, hazard ratio; LABC, locally advanced breast cancer; MFI, metastasis-free interval; OS, overall survival; pCR, pathologic complete response; PFS, progression-free survival; PR, progesterone receptor; RD, residual disease; RCB, residual cancer burden; RFS, recurrence-free survival; ROS, reactive oxygen species; RR, relative risk; Trx, thioredoxin; TrxR, thioredoxin reductase; Txnrd1, thioredoxin reductase 1; TNBC, triple-negative breast cancer; QoL: quality of life;*

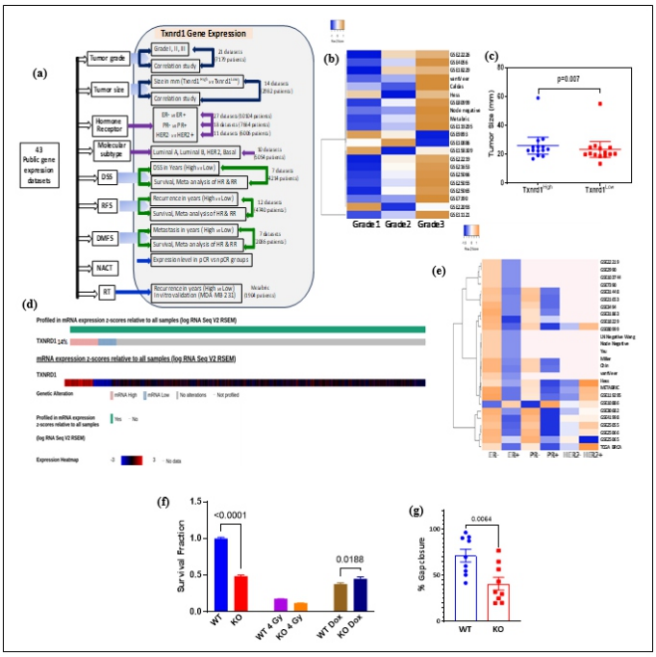

Fig.1: (a) Workflow outlining the strategy employed for analysis of public gene expression data with respect to Txnrd1 gene expression, (b) mRNA expression z-scores relative to all samples from TCGA-Firehose Legacy database with expression heatmap obtained from cBioportal, (c) The expression heatmap of Txnrd1 across tumor grades from different datasets with row z-scores and clustering, (d) The mean tumor size in Txnrd1 High and Low expression subgroups, (e) Expression heatmap of Txnrd1 across ER, PR & HER2 expression status along with row z-scores and clustering. Adapted from Patwardhan et al., Heliyon, 2024. 10(6):e27011

Txnrd1 over-expression is associated with poorer breast cancer-specific survival, as demonstrated in a combined analysis of seven datasets, where Txnrd1^{High} patients exhibited disease-related mortality ~2.03 years earlier than Txnrd1^{Low} patients (Fig.2(a)). Additionally, overall survival analysis across ten datasets revealed significantly shorter (~2 years) survival for patients with Txnrd1 over-expression (Fig.2(b)). Despite some variability across datasets, the overall findings underscore the adverse prognostic impact of Txnrd1 over-expression on breast cancer survival.

Breast cancer patients with over-expression of Txnrd1 are at elevated risk of early recurrence and metastasis

Txnrd1^{High} patients experienced ~2.5 years earlier disease recurrence than Txnrd1^{Low} group (Fig.2(c)). Interestingly, findings from meta-analysis coincided with combined survival analysis illustrating a statistically significant hazard (pooled hazard ratio1.47, p<0.001) of early recurrence in Txnrd1 over-expressing breast cancer patients (Fig.2(d)). The robustness of these findings is supported by very low associated heterogeneity and between-study variance. Moreover, meta-analysis of log-transformed relative risks identified a statistically significant positive risk of early recurrence in Txnrd1^{High} breast cancer patients. Txnrd1^{High} breast cancer patients showed statistically significant hazard for the shorter metastasis-free period and an elevated risk for early metastasis events (Fig.2(e)). Validation experiments revealed that Txnrd1 depletion in Txnrd1^{High} MDA-MB-231 cells abrogated the motility compared to wild type cells (Fig.3(e)). Concomitantly, pharmacologic inhibition of Txnrd1 hampered the invasiveness of MDA-MB-231 cells (Fig. 3(f)), supporting

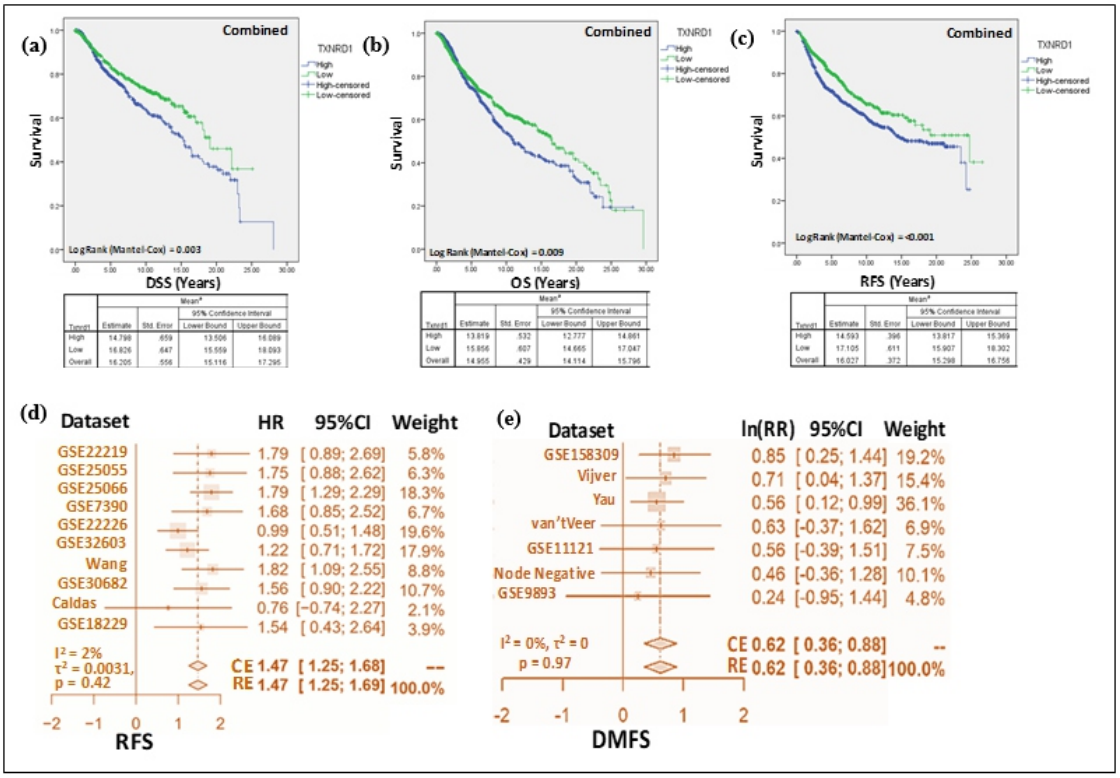

Fig.2: (a) Kaplan-Meier survival curve for disease-specific survival generated by pooling the quantile normalized data from all the datasets along with the Log-Rank (Mantel-Cox) test p-value. The cumulative mean survival time between high (n=722) and low (n=714) expression subgroups is shown below, (b) Kaplan-Meier survival curve for overall survival generated by pooling the quantile normalized data from all the datasets along with Log-Rank (Mantel-Cox) test p-value for Txnrd1High (n=888) and Txnrd1Low (n=886), (c) Kaplan-Meier survival curve for recurrence-free survival generated by pooling the data for all the datasets after quantile normalization along with Log-Rank (Mantel-Cox) test p-value. The cumulative mean survival for Txnrd1High (n=903) and Txnrd1Low (n=807) cohorts is shown below the survival curve, (d) A forest plot shows pooled hazard ratio, 95% CI, weight assignment and heterogeneity obtained by multivariate analysis for datasets included in this study, (e) Meta-analysis for log-transformed relative risk along with associated statistical parameters for metastasis free survival. Adapted from Patwardhan et al., Heliyon, 2024. 10(6):e27011

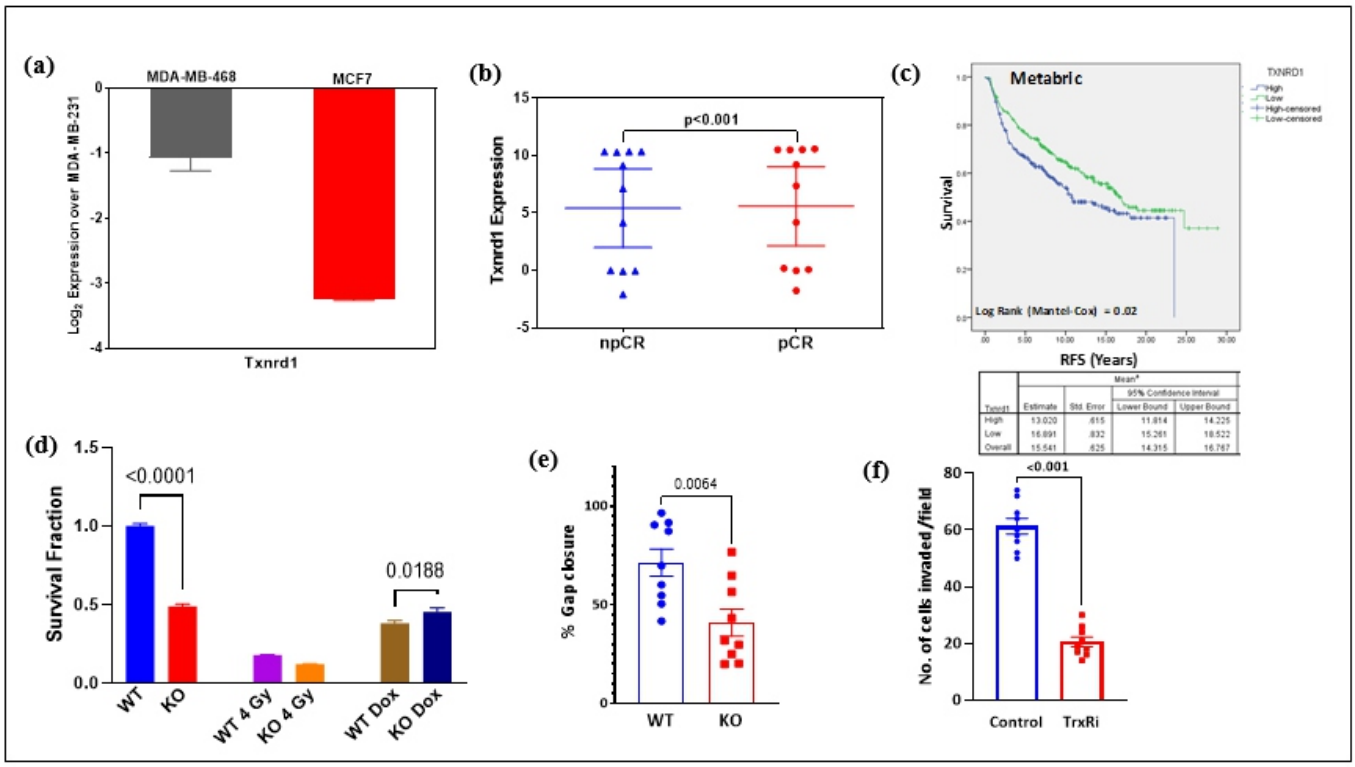

Fig.3: (a) Bar graph shows Log2 expression of Txnrd1 in MCF7 and MDA-MB-468 cells relative to MDA-MB-231, (b) Mean Txnrd1 expression between breast cancer patients with or without pCR, (c) Kaplan-Meier survival curve for recurrence-free survival of breast cancer patients after radiotherapy between Txnrd1 high or low cohorts. Significance is calculated by the Log-Rank(Matel-Cox) test, and the cumulative mean survival of Txnrd1High (n=198) and Txnrd1Low (n=166) cohorts is shown below the survival curve, (d) The bar graph shows survival fraction calculated from clonogenic assay performed with wild type and Txnrd1 depleted MDA-MB-231 cells treated with or without Doxorubicin or radiation 4 Gy, (e) The bar graph shows percent gap closure for wound healing scratch assay at 0 h and 24 h for wild type Txnrd1 depleted cells, (f) The bar graph shows number of cells invaded per field from Transwell Matrigel invasion assay performed with MDA-MB-231 cells treated with or without pharmacologic inhibitor of TrxR. Adapted from Patwardhan et al., Heliyon, 2024. 10(6):e27011

our findings about metastatic behaviour in Txnrd1^{High} cohort. Together these findings reveal that, Txnrd1 over-expressing patients are at elevated risk of local or distant disease recurrence, which enhances the probability of death. However, several other contributing factors will ultimately determine the risk of mortality.

Patients with over-expression of Txnrd1 exhibit better prognosis for chemotherapy but not radiotherapy

Patients achieving pCR after taxane-anthracycline neoadjuvant chemotherapy exhibited significantly elevated Txnrd1 gene expression at $p < 0.05$ compared to the non-pCR group (Fig.3(b)). Higher Txnrd1 expression is consistently associated with pCR across datasets, suggesting its potential as a predictive marker for chemotherapy response. Although radiotherapy exhibits superior tumor control and better QoL with longer event-free survival, not all patients benefit from radiotherapy due to the activation of radioresistance pathways post-radiotherapy. Txnrd1^{High} breast cancer patients undergoing radiotherapy (n=292) exhibited a mean recurrence interval of 13.02±0.61 (95% CI-11.81; 14.22) years as compared to Txnrd1^{Low} cohort (n=244) which showed mean recurrence interval of 16.89±0.23 (95% CI- 15.26; 18.52) years with log-rank (Mantel- Cox) p-value, 0.019 (Fig.3©). Thus, Txnrd1 over-expressing breast cancer patients who have undergone radiotherapy exhibited significantly shorter recurrence intervals as compared to those with low expression of Txnrd1.

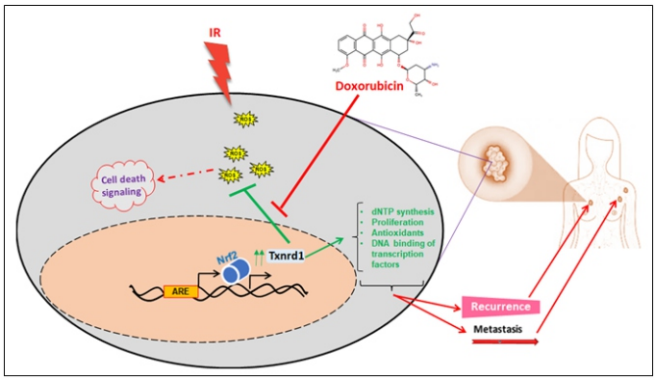

Scheme 1: Txnrd1 over-expression is associated with recurrence, metastasis and therapy response in breast cancer Adapted from Patwardhan et al., Heliyon, 2024. 10(6):e27011

Conclusion

In summary, Txnrd1 over-expression is associated with higher grade, hormone receptor negative, HER2 positive, larger tumors of aggressive subtype and exhibit significant hazard for shorter breast cancer-specific and overall survival. Txnrd1 over-expressing breast cancer patients are at elevated risk of early recurrence and metastasis. Further, Txnrd1^{High}-expression cohort of breast cancer patients exhibit a pathologic complete response to neoadjuvant chemotherapy but are poor responders to radiotherapy (Scheme 1). Hence, in Txnrd1 over-expressing breast cancer patients, radiotherapy can be combined with taxane-anthracycline chemotherapy for better therapeutic outcomes [11].

Acknowledgment

Authors gratefully acknowledge the funding provided by Department of Atomic Energy, Government of India.

References

[1] Cheang, M. C., et al., Defining breast cancer intrinsic subtypes by quantitative receptor expression, The Oncologist, 2015, 20(5), 474-482.

[2] Siegel, R. A.-O., et al., Cancer Statistics, 2022, e1542-4863.

[3] Berry, D. A., et al., Effect of screening and adjuvant therapy on mortality from breast cancer, New England Journal of Medicine, 2005, 353(17), 1784-1792.

[4] Miller, K.D., et al., Cancer treatment and survivorship statistics 2019, CA: A cancer journal for clinicians, 2019, 69(5), 363-385.

[5] Witteveen, A., et al., Survival after locoregional recurrence or second primary breast cancer: Impact of the disease-free interval, PLoS One, 2015, 10(4), 0120832.

[6] Wallgren, A., et al., Risk factors for locoregional recurrence among breast cancer patients: Results from International Breast Cancer Study Group Trials I through VII, Journal of Clinical Oncology, 2003, 21(7), 1205-1213.

[7] Speers, C., and L. J. Pierce, Postoperative radiotherapy after breast-conserving surgery for early-stage breast cancer: A review, JAMA Oncology, 2016, 2(8), 1075-1082.

[8] Singh, B., et al., Oxidative stress associated metabolic adaptations regulate radioresistance in human lung cancer cells, Journal of Photochemistry and Photobiology B: Biology, 2020, 213, 112080.

[9] Cadenas, C., et al., Role of thioredoxin reductase 1 and thioredoxin interacting protein in prognosis of breast cancer, Breast Cancer Research, 2010, 12(3), 1-15.

[10] Bhatia, M., et al., The thioredoxin system in breast cancer cell invasion and migration, Redox Biology, 2016, 8, 68-78.

[11] Patwardhan, R. S., et al., Txnrd1 as a prognosticator for recurrence, metastasis, response to neoadjuvant chemotherapy and radiotherapy in breast cancer patients, Heliyon, 2024, 10(6), e27011.

प्लास्टिक का एंजाइमेटिक अपघटन

11

प्लास्टिक अपघटनकारी एंजाइमों की एंजाइमेटिक गतिविधि की निगरानी के लिए स्पेक्ट्रोफोटोमेट्रिक आमापन का विकास

अंकना साहा [2] और अमित दास [1,2]*

[1]प्रोटीन क्रिस्टलोग्राफी अनुभाग, जैव-विज्ञान समूह, भाभा परमाणु अनुसंधान केंद्र, ट्रांबे-400085, भारत
[2]होमी भाभा राष्ट्रीय संस्थान, अणुशक्ति नगर, मुंबई-400094, भारत

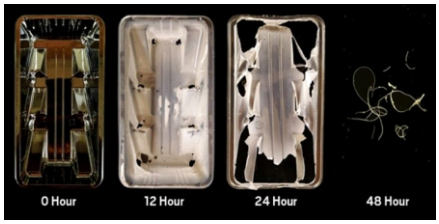

इंजीनियर आई. एस. पी. ई. टी. ए. एस. 48 घंटों में एक प्लास्टिक खाद्य पात्र का क्षरण और घुलनशील करता है।

सारांश

पृथ्वी प्लास्टिक के बोझ से दबी हुई है, जो हमारे पर्यावरण में सदियों तक रह सकती है, और उनके पुनर्चक्रण के लिए आवश्यक नियंत्रण की तत्काल आवश्यकता है। उपभोक्ता के उपयोग के पश्चात प्लास्टिक का एंजाइम-आधारित विकृति प्लास्टिक के बंद-लूप पुनर्चक्रण के लिए एक उभरती हुई दूरगामी हरित कार्यनीति है। एंजाइम, IsPETase पॉलीइथिलीन टेरेफ्थेलेट (PET) को उपयोगी अंतिम उत्पादों में हाइड्रोलाइज करता है जिसका उपयोग वर्जिन PET को संश्लेषित करने के लिए किया जा सकता है। इस प्रकार PETases कम कार्बन फूटप्रिंट के साथ PET के बंद-लूप हरित पुनर्चक्रण में उत्प्रेरक के रूप में कार्य करते हैं। PETases को कुशल PET जैव-अकवर्षक विकसित करने के लिए कृत्रिम बनाया जा रहा है। उनकी उत्प्रेरक क्षमताओं की त्वरित तुलना करने के लिए आमापन विकसित करना आवश्यक है। हमने उत्प्रेरक गतिविधियों और दरों की तेज़ी से निगरानी के लिए पराबैंगनी अवशोषण और प्रतिदीप्ति आधारित सब्सट्रेट का उपयोग करके IsPETase पर स्पेक्ट्रोप्रकाशमिति आमापन विकसित किया गया। इन आमापकों का उपयोग वाइल्ड-टाइप के ISPETase और इसकी उत्परिवर्ती तथा दस गुना अधिक उत्प्रेरक दक्षता प्रदर्शित उत्परिवर्ती की तुलना करने के लिए किया गया।

Enzymatic Degradation of Plastics

11

Development of Spectrophotometric Assays to Monitor Enzymatic Activity of Plastic Degrading Enzymes

Ankana Saha[2] and Amit Das[1,2]*

[1]Protein Crystallography Section, Bio-Science Group, Bhabha Atomic Research Centre, Trombay-400085, INDIA
[2]Homi Bhabha National Institute, Anushakti Nagar, Mumbai-400094, INDIA

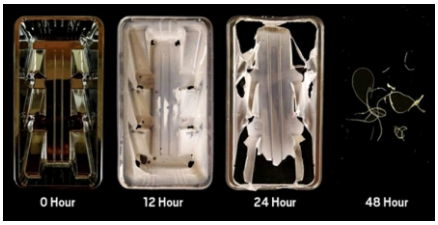

Engineered IsPETase degrading and solubilizing a plastic food container in 48 hours

ABSTRACT

Earth is burdened with plastics, which can stay in our environment for centuries, and necessary controls are required urgently for their recycling. Enzyme-based degradation of post-consumer plastic is an emerging green strategy for sustainable closed-loop recycling of plastics. The enzyme, *Is*PETase hydrolyze polyethylene terephthalate (PET) to useful end products which can be used to synthesize virgin PET. Thus PETases act as catalysts in closed-loop green recycling of PET with a low carbon footprint. PETases are being engineered to develop efficient PET bio-degrader. It is essential to develop assays to quickly compare their catalytic efficiencies. We developed spectrophotometric assays on *Is*PETase using UV absorbance and fluorescence based substrates to quickly monitor the catalytic activities and rates. These assays were used to compare wild-type *Is*PETase and its mutant and mutant exhibiting ten times higher catalytic efficiency.

KEYWORDS: *Plastic degrading enzyme, IsPETase, Michealis-Menten constant, Lineweaver-Burk, Catalytic efficiency*

**Author for Correspondence: Amit Das*
E-mail: amitdas@barc.gov.in

Introduction

The use of plastics in our daily lives is ubiquitous and unavoidable due to convenience and versatility causing a surge in demand for plastics globally. Plastics are resistant to biodegradation, and their natural degradation takes many centuries resulting in accumulation in our environment [1]. Conventional methods of plastic degradation, such as photodegradation and mechano-chemical processes are not environment friendly. Enzymatic bio-degradation of plastics has emerged as a promising green and environment friendly alternative, and closed-loop plastic re-cycling has low carbon footprint [2]. Microorganisms produce plastic degrading enzymes encompassing a diverse array of hydrolases, including lipases, esterases, and cutinases and breaks down bonds present in plastic polymers [3]. Polyethylene terephthalate (PET) is a thermoplastic polymer consisting of the ester-linked monomers of terephthalic acid (TPA) and ethylene glycol (EG). Food packaging industry, water bottles and textile fiber manufacturers use PET. A recently identified bacterium *Ideonella sakaiensis* has two hydrolytic enzymes, PETase (polyethylene terephthalates, *Is*PETase) and MHETase (mono(2-hydroxyethyl) terephthalate hydrolase, *Is*MHETase) capable of depolymerizing PET. *Is*PETase degrades PET into intermediate products, primarily mono (2-hydroxyethyl) terephthalic acid (MHET) and bis (2-hydroxyethyl) terephthalic acid (BHET), TPA and EG as minor products [4] (Fig.1(a)). *Is*MHETase further breaks MHET into TPA and EG (Fig.1(a)) [5]. These enzymes are continuously evolving and are not yet optimized to act on specific plastic substrates. For example, cutinases, known to degrade aliphatic polyester cutin in plants, have evolved to degrade plastics polymers with low substrate specificity. An efficient enzymatic hydrolysis of PET requires a reaction temperature of about 65-70^{0}C. *Is*PETase is active and stable below this temperature. Protein engineering of *Is*PETase using 3D structure-guided and machine learning approaches are being employed to increase the enzymatic activity, thermostability and expand substrate specificity [6-7]. Thus engineered IsPETase can directly recycle post-consumer PET in closed-loop and make virgin PET bottles using TPA and EG produced by enzymatic hydrolysis (Fig.1(b)) [7].

However, comparison of the enzymatic activities of PET hydrolases reported so far are limited to inaccurate weighing methods and cumbersome estimation of complex mixture of end products, BHET, MHET, TPA and EG using HPLC [5]. The development of fast and accurate spectroscopic assays using chromogenic and fluorogenic substrates are necessary to compare these enzymes and their mutants. We report here expression, purification, characterization and assay optimization to develop fast and efficient spectroscopic assays of *Is*PETases using UV absorbance and fluorescence substrates. The catalysis rate, kcat and binding constant, Km were determined for wild-type *Is*PETase and compared with its mutant. Our assays will enable quick comparison of activities of engineered *Is*PETases and other PETases.

Materials and Methods

The plasmids containing genes encoding His6-tagged IsPETase (WT) and its double mutant W159H/S238F (mutant) in pET-21b (+) vector were used to transform *E.coli* BL21(DE3) competent cells using heat shock method. The cells were grown in 600 ml LB media containing ampicillin and induced with 0.1 mM IPTG at 18^{0}C after OD_{600} reached 0.8. Cells were harvested by centrifugation after 18-20 hrs. The cell pellet was lysed in 20 mM Tris-Cl (pH 8), 300 mM NaCl buffer. The his-tagged WT and mutant enzymes were purified by Ni-NTA chromatography and further purified on a size-exclusion column using Akta purifier chromatography system by standard procedures. The purity of protein was checked in 12% SDS-PAGE gel. The UV absorbance substrate, para-nitrophenyl acetate (pNPA) and fluorescence substrate, 4-methylumbelliferyl acetate (4MUA) stocks were prepared in 100% DMSO. The standard calibration curves in triplicates were made using different concentrations of pNP and 4MU. The enzymatic assays were performed in triplicates using 10 mM PBS (pH 7.4) buffer and 1% DMSO in 96-well plates. The reaction progress was optimized by adding enzymes having concentration ranging from 30 nM to 1 nM. The assays were performed by varying the substrate concentrations at an optimized enzyme concentration. The post-cleavage product build-up was measured from the UV absorbance of para-nitrophenol (pNP) at 405 nm and fluorescence emission 4-methylumbelliferone (4MU) at 450 nm after exciting at 320 nm, using Clario Star-multimode plate reader.

Results and Discussion

Purified *Is*PETase and its mutant were obtained using size exclusion chromatography where single peaks of eluted proteins were collected and used in our experiments (Fig.2(a)). Single bands at ~30 kDa were observed on SDS-PAGE indicating that the proteins were very pure (Figure 2b). The UV absorbance substrate, pNPA and fluorescence substrate, 4MUA were used to first optimize the assays at different enzyme concentrations. The enzymes cleave the ester bond present in the substrates and releases the products which gives UV absorbance (pNP) and fluorescence (4MU) signals. Linear Lineweaver-Burk plots were obtained from initial velocities of Michaelis-Menten curves of hydrolysis reactions (Inset Fig.3(a)-3(d)). Michaelis-Menten constants (Km), maximum velocities (Vmax), turnover numbers (kcat) and

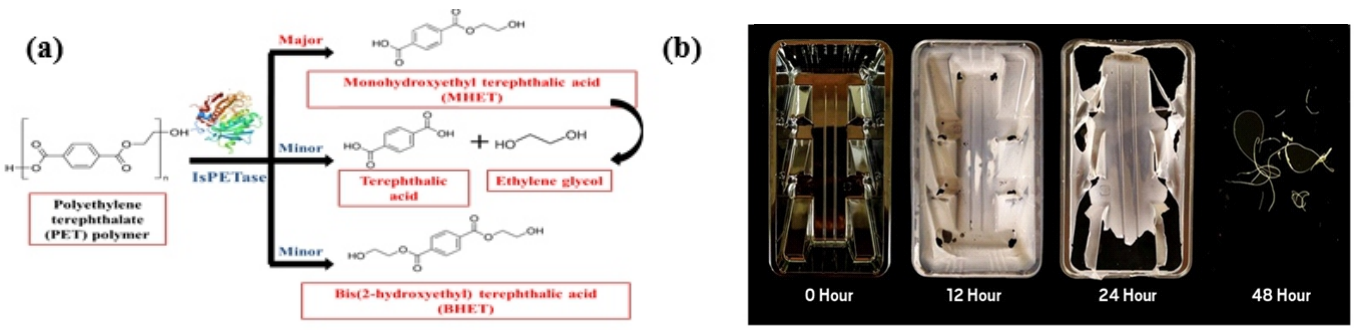

Fig.1: (a) The products released upon PET degradation by IsPETase and IsMHETase. b) Engineered IsPETase degrading and solubilizing a plastic food container in 48 hour [Ref. 7].

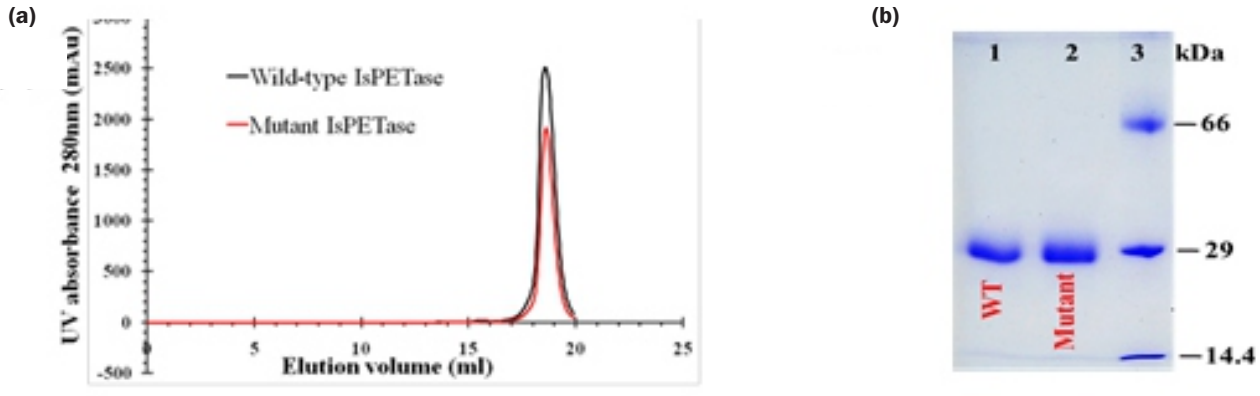

Fig.2: (a) Chromatogram of eluted enzymes from size exclusion column. (b) SDS-PAGE of purified WT IsPETase (lane 1) and its mutant (lane 2). Molecular weight markers are shown in lane 3.

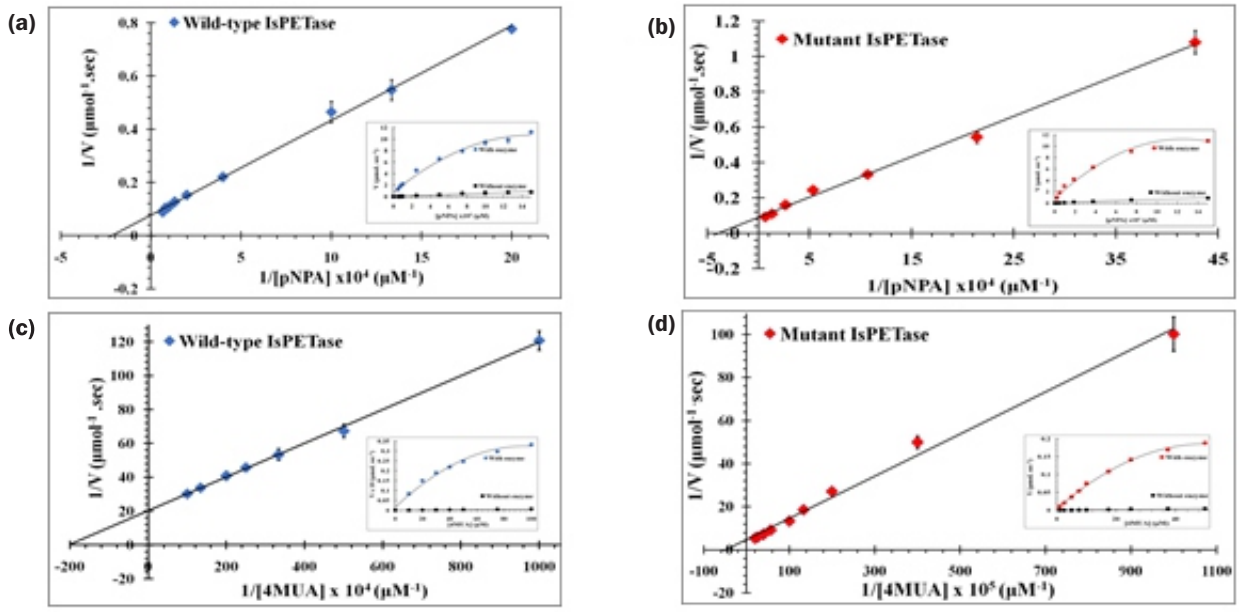

Fig.3: Lineweaver-Burk plot using (a) pNPA substrate with WT IsPETase, (b) pNPA substrate with mutant IsPETase, (c) 4MUA substrate with WT IsPETase, (d) 4MUA substrate with mutant IsPETase. Inset: Michaelis-Menten plots with and without enzyme.

catalytic efficiency (kcat/Km) from the intercepts (Table 1).

The Km value indicate the binding affinity of substrate to the enzyme. Both substrates show lower Km values with mutant enzyme and the values are half than that of WT enzyme, indicating tighter binding of substrates in the mutant active site. The Km values of the fluorescence substrate, 4MUA are about hundred-fold lower than that of pNPA indicating much higher affinity of 4MUA to IsPETase enzymes. The mutant enzyme binds 4MUA more tightly than WT. The kcat values of WT and mutant enzymes are similar for pNPA. The kcat values of mutant enzyme is 4.5 times higher than the WT enzyme for 4MUA indicating faster cleavage of the fluorescence substrate by the mutant. The catalytic efficiency (kcat / Km) of mutant is ten times higher than that of WT enzyme in case of 4MUA cleavage, and in case of pNPA mutant, it is 1.5 times more efficient. Thus, our studies indicate that mutant IsPETase is more efficient than the WT enzyme. Absorbance assays with PETases using pNPA have been used routinely by researchers worldwide. The catalytic efficiencies and Km values of 4MUA are higher than pNPA. The kinetic and binding parameters obtained experimentally indicate 4MUA is better substrate than pNPA and mutant enzyme. Our results indicate that fluorescence assay with 4MUA is more sensitive than

Table 1: Comparison of kinetic parameters of wild-type IsPETase and its mutant.

Substrate / Enzyme	pNPA		4MUA	
	WT	Mutant	WT	Mutant
K_m (µM)	4545 ± 344	2634 ± 235	48.47 ± 2.9	21.51 ± 6.2
V_m (µmol s^{-1})	14.00 ± 0.12	12.00 ± 0.07	0.05 ± 0.0016	0.22 ± 0.004
k_{cat} (s^{-1})	466.67 ± 39	400.00 ± 23	48.94 ± 1.6	217.01 ± 47.5
k_{cat} / K_m ($\mu M^{-1} s^{-1}$)	0.103 ± 0.014	0.152 ± 0.026	1.01 ± 0.034	10.09 ± 0.22

absorbance assay. The assay can be used to compare the relative catalytic efficiencies of engineered PETases and other PET degrading enzymes.

Conclusion

The IsPETase enzyme and its mutant were recombinantly expressed and obtained to high purity in our lab. The enzymatic assays using two different UV absorbance and fluorescence-based substrates were optimized. The kinetic and binding parameters obtained experimentally indicate 4MUA is better substrate than pNPA and mutant enzyme has ten times higher activity than WT enzyme. In future, these assays will be developed further using such substrates to compare engineered PETases and other PET degrading enzymes.

Acknowledgment

The authors are grateful for constant support and encouragement of Group Director, Bio-Science Group and Head, Protein Crystallography Section, Bio-Science Group, BARC.

References

[1] https://plasticseurope.org/knowledge-hub/plastics-the-fast-facts-2023/

[2] I. Taniguchi, S. Yoshida, K. Hiraga, et. al., Biodegradation of PET: Current Status and Application Aspects, ACS Catalysis, 2019, 9, 4089–105.

[3] M. Dimarogona, E. Nikolaivits, M. Kanelli, et. al., Structural and Functional Studies of a Fusarium Oxysporum Cutinase with Polyethylene Terephthalate Modification Potential, Biochimica et Biophysica Acta (BBA) - General Subjects, 2015, 1850, 2308–17.

[4] S. Yoshida, K. Hiraga, T. Takehana, et. al., A Bacterium That Degrades and Assimilates Poly (Ethylene Terephthalate), Science, 2016, 351, 1196–99.

[5] B.C. Knott, E. Erickson, M.D. Allen and J.E. McGeehan, Characterization and Engineering of a Two-Enzyme System for Plastics Depolymerization, PNAS (USA), 2020, 117, 25476–85.

[6] H. F. Son, I. J. Cho, S. Joo, et. al., Rational Protein Engineering of Thermo-Stable PETase from Ideonella Sakaiensis for Highly Efficient PET Degradation, ACS Catalysis, 2019, 9, 3519–26.

[7] H. Lu, D.J. Diaz, N.J. Czarnecki, et. al., Machine learning-aided engineering of hydrolases for PET depolymerization, 2022, Nature, 604, 662–667.

ट्रांसलेशनल रेडियोजीवविज्ञान

12

कैंसर रेडियोथेरेपी में सुधार के लिए प्रासंगिकता के साथ निम्न एवं उच्च एलईटी विकिरण के गैर-लक्षित प्रभाव

पूजा के. मेलवानी [1,2], **वासुमति आर** [1,2], **हंसा डी. यादव** [1], **संजय शिंदे** [1], **मुरली एम. एस. बल्ला**[1,2], **अमित कुमार** [1,2] **और बी. एन. पांडे** [1,2]*

[1]विकिरण एवं कैंसर जीवविज्ञान अनुभाग, विकिरण जीवविज्ञान एवं स्वास्थ्य विज्ञान प्रभाग, भाभा परमाणु अनुसंधान केंद्र, ट्रांबे-४०००८५, भारत

[2]होमी भाभा राष्ट्रीय संस्थान, अणुशक्ति नगर, मुंबई-400094, भारत

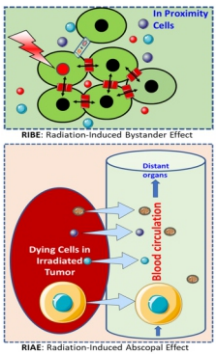

कैंसर रेडियोथेरेपी में गैर-लक्षित विकिरण प्रभाव।

सारांश

गैर-लक्षित विकिरण प्रभाव (NTRE) कोशिकाओं/ऊतकों/अंगों की जैविक अनुक्रिया है, जो किरणित नहीं हुए हैं, लेकिन वे विकिरण स्थल से निकटता/या कुछ दूरी पर हैं। इन घटनाओं को विकिरण प्रेरित बाईस्टैंडर (अति निकटता में) या एब्सकोपल (कुछ दूरी पर) प्रभाव के रूप में जाना जाता है। ट्यूमर/सामान्य ऊतकों की मिश्रित सीमाएँ, आंशिक ट्यूमर विकिरण और मेटास्टैटिक ट्यूमर (विकिरण प्राप्त करने वाले ट्यूमर से दूर) कुछ ऐसी स्थितियाँ हैं, जिनके तहत NTRE कैंसर रेडियोथेरेपी के परिणाम को बेहतर किया जा सकता है, हालाँकि, अभी भी इस पर बहुत अधिक शोध कार्य नहीं किया गया है। कैंसर रेडियोथेरेपी परिदृश्यों का अनुकरण करने वाले हमारे इन-विट्रो और माउस ट्यूमर मॉडल अध्ययनों ने बाईस्टैंडर कैंसर कोशिकाओं/आंशिक रूप से किरणित ट्यूमर और विकिरण स्थल से दूर के ट्यूमर में वृद्धि अवरोधक NTRE दर्शाया है। हमने गामा विकिरण की तुलना में अल्फा कण के संपर्क में आने वाली कोशिकाओं को सीधे किरणित या बाईस्टैंडर कैंसर कोशिकाओं को स्वदेशी रूप से अभिकल्पित और विकसित स्वचालित बेंचटॉप 241 Am अल्फा किरणक (BARC BioAlpha) का उपयोग करके अधिक क्षयित किया। हमारी खोज ने गैप-जंक्शन मध्यस्थता वाले बाईस्टैंडर संचार के माध्यम से फेफड़े के कैंसर कोशिकाओं में साइटोटॉक्सिक प्रभाव के अल्फा कणों के हाई डोज़ पर किन्तु साइटो-प्रोलिफ़ेरेटिव प्रभाव के लो डोज़ को भी प्रमाणित किया। कुल मिलाकर, हमारे परिणाम विकिरण के गैर-लक्षित प्रभावों की नई समझ प्रदान करते हैं, जिसका कैंसर रेडियोथेरेपी के लिए बेहतर प्रोटोकॉल/कार्यनीतियों को अभिकल्पित करने में महत्वपूर्ण उपयोग हो सकता है। इसके अलावा, हमारा शोध बेहतर ट्रांसलेशनल रेडियोजीवविज्ञान अनुसंधान के लिए ट्यूमर माइक्रो-वातावरण परिस्थितियों में NTRE के अन्वेषण के लिए संभावनाओं के नए द्वार खोलता है।

Translational Radiobiology

12

Non-targeted Effects of Low and High LET Radiation with Relevance to Improvement of Cancer Radiotherapy

Pooja K. Melwani[1,2], Vasumathy R[1,2], Hansa D. Yadav[1], Sanjay Shinde[1], Murali M. S. Balla[1,2], Amit Kumar[1,2] and B. N. Pandey[1,2]*

[1]Radiation and Cancer Biology Section, Radiation Biology & Health Sciences Division, Bhabha Atomic Research Centre, Trombay-400085, INDIA

[2]Homi Bhabha National Institute, Anushakti Nagar, Mumbai-400094, INDIA

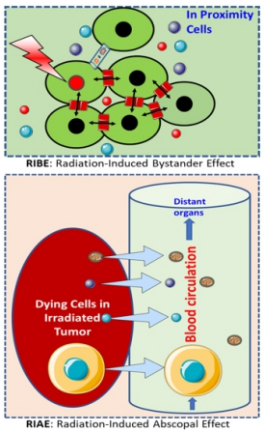

Non-Targeted Radiation Effects in Cancer Radiotherapy

ABSTRACT

Non-targeted radiation effects (NTRE) are the biological response of cells/tissues/organs that didn't receive radiation but are in proximity/ or at a distance from the irradiation site. These phenomena are known as radiation induced bystander (in close proximity) or abscopal (at a distance) effect. The intermixed boundaries of tumor/normal tissues, partial tumor irradiation, and metastatic tumors (distant to the tumor receiving radiation) are a few situations under which NTRE could modulate the outcome of cancer radiotherapy, which however, is still poorly explored. Our in vitro and mouse tumor model studies simulating cancer radiotherapy scenarios showed growth inhibitory NTRE in bystander cancer cells/partially irradiated tumor and the tumors distant from the irradiation site. Using an indigenously designed and developed automated benchtop $_{241}$Am alpha irradiator (BARC BioAlpha), we demonstrated higher killing of cancer cells which are either directly irradiated or bystander to alpha particle exposed cells than gamma radiation. Our finding also established the cyto-proliferative effect of low dose but cytotoxic effect at high dose of alpha particles in lung cancer cells through gap-junction mediated bystander communication. Overall, our results provide novel understanding of non-targeted effects of radiation, which may have significant implication in designing protocols/strategies for improved cancer radiotherapy. Moreover, our research opens new horizons to investigate NTRE in tumor microenvironment conditions for better translational radiobiology research.

KEYWORDS: *Radiation Induced Bystander Effect, Radiation Induced Abscopal Effect, Alpha Particles, Alpha Irradiator, Linear Energy Transfer*

*Author for Correspondence: B. N. Pandey
E-mail: bnp@actrec.gov.in

Introduction

Biological effects of radiation manifest as damage to biomolecules like DNA, proteins, lipids, etc., which subsequently exerted at different tiers ranging from organelle to tissue and organism levels. The deposition of energy (in kilo electron volt; keV) by ionizing radiation along the per unit length (in microns) of the radiation track is referred as linear energy transfer (LET). Gamma and X-rays are considered as low LET radiation, which deposit energy and ionize sparsely in the cells. Consequently, the DNA damage caused mainly consists of single strand breaks, which are easy to repair. Alpha and other charged particles, referred as high LET radiation, deposit their energy very densely resulting in biologically difficult-to-repair complex/clustered DNA damage. While low LET radiation can deeply penetrate and traverse through an organism, the high LET radiation is mainly localized to cells/tissues where such radiation emitting radionuclides reside. This difference also provides the basis for utilization of these radiations for imaging and therapy of cancer. The radiation and radio-isotopes used in diagnosis are low LET X-rays and low energy gamma emitters (such as ^{99m}Tc), while the radiation sources used in teletherapy are high energy gamma emitter like Cobalt-60. Also, high energy beta (^{90}Y, ^{131}I, ^{186}Re, ^{177}Lu) and alpha (^{225}Ac, ^{227}Th, ^{211}At, ^{212}Bi, and ^{213}Bi) emitter radionuclides are used for targeted radionuclide therapy of cancer after conjugating them with various agents and ligands [1]. The pattern of energy loss across the medium for low and high LET radiations is different. When a high LET charged particle passes through matter, its energy decreases, and consequently, the specific ionization increases, resulting in the deposition of energy in a short range as a sharp peak (called Bragg's peak) before the particle stops. This results in minimal energy deposition before or after the peak. This property of high LET radiation is also utilized to kill tumor mass sparing the normal tissue when the peaks of charged particles generated in accelerators are controlled to spread over the tumor region (called spread over Bragg's peak). Since, the radiobiological effects of high LET radiation are almost independent of oxygen presence, they can effectively kill the hypoxic cells in tumors, which otherwise are resistant to gamma and X-rays. Based on these biophysical and radiobiological properties, radiotherapy based on high LET radiation results in higher tumor control with minimal damage to normal tissues and hence emerging as a superior cancer radiotherapy modality compared to the conventional modalities.

Classically, it is believed that damage caused by radiation is limited to the cell that is hit by radiation. Such a notion prevailed due to dominance of DNA-centric dogma without consideration of intercellular communication and tissue microenvironment as contributing factors in the biological effects of radiation. In a landmark paper, Nagasawa and Little observed sister chromatid exchange in ~30 % cells when only <1 % cells in culture were irradiated with low fluence alpha particles. Later on, several studies, including ours, showed that bystander cells which did not receive radiation also showed effects similar to irradiated cells (called Radiation Induced Bystander Effects; RIBE). RIBE is mediated through (a) gap junctions, which connect the cells at the tissue level and mediate the transfer of small molecules (<10 kDa) such as calcium, and (b) secretion of cytokines/chemokines or vesicles such as exosomes from the irradiated cells [2]. More recently, cellular bridges like tunneling nanotubes, which can connect cells even at a few hundred microns away are postulated to play role in RIBE [3]. While RIBE is an intercellular phenomenon between adjacent/neighbouring cells, radiation effects are also observed in the distant tissues/organs, which are kept out of the radiation field. The systemic effect of radiation was first described by R. H. Mole in 1953, who coined the term 'abscopal effects' (*'Ab'* is a prefix with the meaning position away from and 'scopos' Latin meaning a mark or target for shooting). Such effects, known as Radiation Induced Abscopal Effects (RIAE), occur through the release of cytokines and factors in the blood stream from the dying cells which received lethal dose of radiation. In recent years, the scope of these effects has become further complex as it has been established that signals (i) from the irradiated cells/tissues could be damaging as well as protective (or rescue) to the bystander or the distant organs and (ii) the effects can be bidirectional/multi-directional originating from the irradiated cells/tissues as well as vice versa from the bystander/distant tissues. “Non-targeted radiation effects (NTRE)” or “out of the field effects” encompassing RIBE and RIAE have made a paradigm shift in radiation biology, where radiation effects are no more limited only to the irradiated cells/tissues. The emerging evidences supporting NTRE in diverse biological systems and radiation types hold significant implication in radiation risk assessment after environmental, occupational, accidental radiation exposure, and improvement of cancer radiotherapy [2]. The article briefly highlights our research activities to understand radiation biology of NTRE after low and high LET radiation in the framework of cancer radiotherapy.

Non-targeted Radiation Effects in Cancer Radiotherapy

Although RIBE was discovered in the 1970s and RIAE in the 1930s, studies pertaining to cancer radiotherapy are limited in the literature. The NTRE during cancer radiotherapy is highly relevant due to several reasons. (i) In the real scenario, the tumor mass is surrounded by normal tissues and their mixed boundaries provide an excellent platform for bystander interaction when the tumor is targeted to radiation. (ii) In some cases, tumors are located very close to critical organs like lungs and brain, thus to minimize undesired side effects partial tumor irradiation is performed, which provides possibility of bystander interaction between irradiated and non-irradiated regions of the same tumor. (iii) Majority of the cancer patients are diagnosed with metastasis at crucial organs or spread at multiple locations in the body. In such situations, generally radiation oncologists are able to treat only the primary site of tumor, which in turn might affect the growth of distant metastatic/micro-metastatic tumors. Hence, the magnitude, nature (damaging/protective), and direction (unidirectional /bidirectional) of interaction of irradiated and bystander cells/distant tissues and subsequent fate of these cells would govern the clinical outcome of cancer radiotherapy (Fig.1). Our studies employing multiple experimental models/strategies contributed significantly to this research area. In one of the seminal works simulating cancer and normal cell proximity during charged particle therapy, we co-cultured human lung cancer and fibroblast cells together, where nuclei of either cancer or normal cells were selectively irradiated with 500 protons using proton microbeam (3.4 MeV) facility at National Institute of Radiological Sciences, Japan followed by measurement of DNA double strand break in irradiated and bystander cells. The study showed that DNA damaging signal was transmitted from proton irradiated lung cancer to bystander lung cancer cells, however, the magnitude of DNA damage was attenuated in the irradiated lung cancer cells when human normal fibroblasts neighboured these cells. The damaging bystander effect was abrogated when gap-junctions between irradiated and bystander cells were blocked. This study for the first time established the bidirectional and rescuing bystander effect between lung cancer and

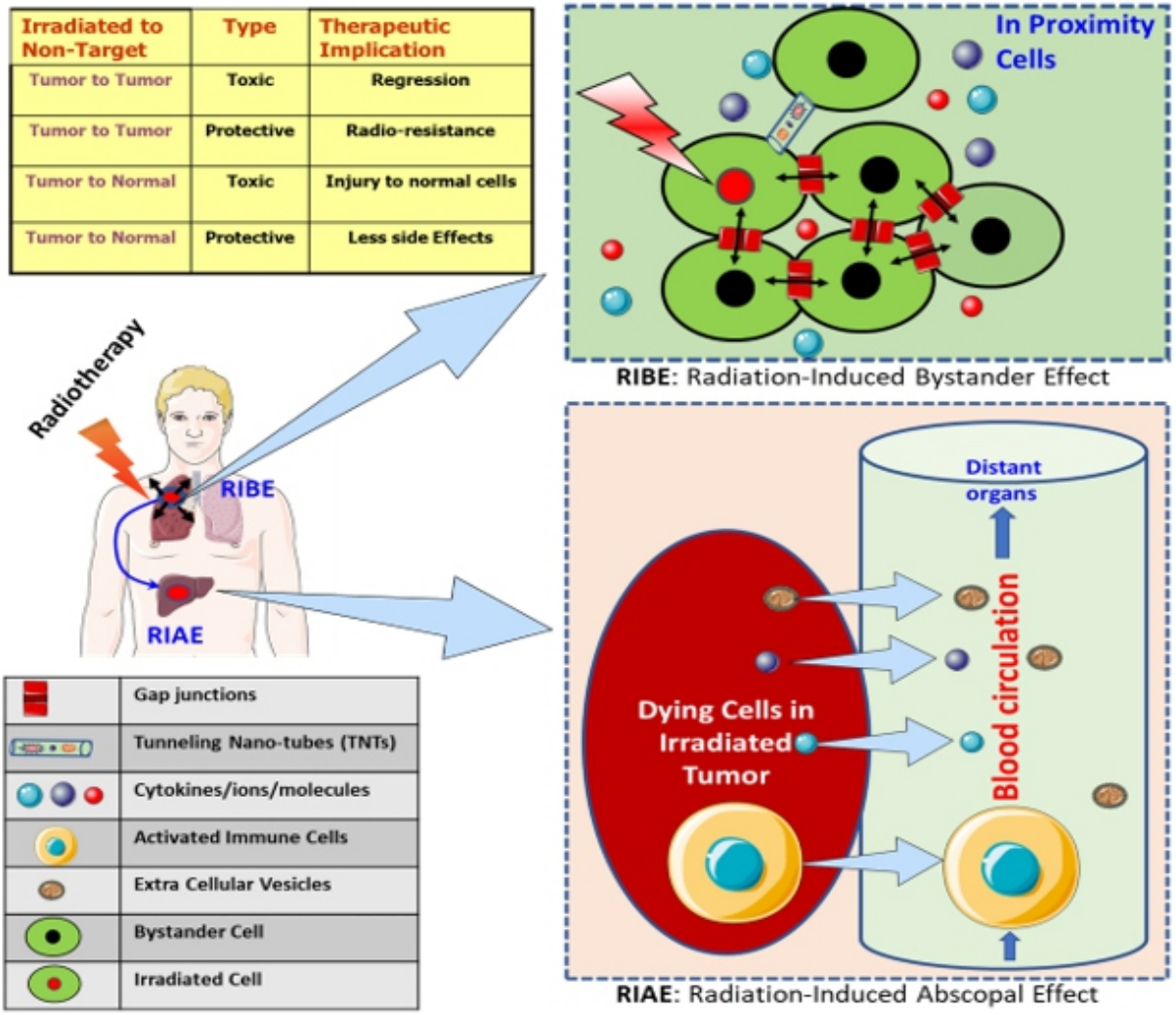

Fig.1: Non-Targeted Radiation Effects in Cancer Radiotherapy. When a tumor mass is irradiated, in addition to directly irradiated cells, the cells in close proximity also show the radiation effects called as Radiation Induced Bystander Effect (RIBE) or effect can be to the distant tissue/organs known as Radiation Induced Abscopal Effect (RIAE). While RIBE is mediated through gap junctions, the RIAE is through release of factors/activated immune cells. Depending on nature and magnitude of NTRE between tumor and normal cells/tissues, the net clinical outcome can affect tumor regression and/or side effects during cancer radiotherapy.

counterpart normal cells after proton microbeam irradiation [4]. The factors/cytokines released from the irradiated cancer cells are also known to contribute to the bystander effect. In this direction, cancer cells of different tissue origins (breast, lung, fibrosarcoma, colon, and brain) showed variation in secretion of cytokine profile when irradiated either with acute (2 Gy) or fractionated (3x2 Gy) doses of gamma radiation. It was interesting to observe that the conditioned medium from the irradiated lung cancer cells showed toxicity to bystander lung cancer cells [5]. Moreover, treatment with macrophage conditioned medium is shown to enhance intercellular communication between breast cancer cells via tunneling nanotube formation and secretion of large extracellular vesicles referred as microplasts [6, 7]. The intercellular communication via tunneling nanotubes modulates chemo-/radio-therapy response and can be important mediator of RIBE. To demonstrate and validate the NTRE results in mouse fibrosarcoma tumor models following strategies were employed.

Co-implantation of lethally irradiated tumor cells with bystander cells

In this approach, only a fraction of tumor cells was irradiated with lethal high doses of gamma radiation (15 Gy), mixed with bystander cells, followed by the implantation of the cell mixture in mice and subsequent measurement of the tumor growth. It was interesting to observe that only a fraction of high dose irradiated tumor cells inhibited the growth of bystander tumor cells, resulting in smaller tumors. The inhibition of tumor growth was found to be associated with secretion of anti-tumor proteins/factors from the irradiated cells, resulting in cell death of bystander cancer cells as well as decrease in angiogenesis during tumor growth [8].

Partial tumor irradiation

Using a cone irradiator designed for Cobalt-60 teletherapy, only a part of mouse tumor was irradiated. Compared to control, significant tumor control was observed when only ~10 % volume of tumor was irradiated. These results showed cytotoxic bystander effect when only a fraction or part of tumor was irradiated.

Non-targeted radiation effects at distant tumors

In this study, we investigated the possibility of controlling the growth of distant tumors when only primary tumor was irradiated. Such studies have gained attention of researchers as well as clinicians as they can be exploited to enhance radio-immunotherapy of metastatic tumors and prevent post-irradiation tumor recurrence. To simulate NTRE at distant tumors, mouse fibrosarcoma tumors were developed in both of hind legs. While one of the tumor was irradiated with gamma radiation, the other tumor and rest animal body parts were

kept shielded. A decrease in tumor growth in radiation shielded tumor was observed when tumor in another leg was irradiated, which was more prominent at higher doses (5 Gy) than at lower doses (2 Gy). The directly irradiated tumors showed expression of immunogenic cell death markers. To enhance the NTRE in distant tumors, radiation in combination with CpG-ODN (cytidine phosphate guanosine-oligonucleotides), an immunomodulatory oligo, was administered in the irradiated tumor. CpG-ODN in conjunction with radiation resulted in better tumor control. These tumor growth inhibitory effects were found to be mediated through an increase in immune-modulatory markers and induction of apoptosis in the shielded tumors. To evaluate whether such combinatorial effects could be exploited to control tumor recurrence, the animals that showed complete tumor regression after CpG-ODN and radiation treatment were implanted with unirradiated tumor cells. It was interesting to observe that in these animals freshly transplanted tumor cells did not produce tumors, suggesting long lasting non-targeted radiation effects.

Cancer stem cells (CSCs) are one of the key factors contributing to recurrence and poor prognosis in cancer radiotherapy [9]. Depending upon the types and stages of tumors, although CSCs constitute only a small fraction (0.5-20%) of the tumor mass, they play a pivotal role in cancer progression, metastasis, recurrence, and resistance to treatment [10, 11]. Our understanding about the magnitude of bystander communication and role of gap junction proteins in the context of CSCs and tumor radio-resistance remains limited [12] and is one of our ongoing research activities.

High LET Radiobiology in Cancer Radiotherapy

Charged particle therapy and targeted alpha therapy are emerging modes of cancer therapy owing to their effectiveness to kill tumor cells while sparing the surrounding normal tissues. However, in addition to technical challenges, such therapies are also limited to a few cancer types and have poor prognosis in some cases. The radiobiology of charged particles is not well studied mainly due to two reasons: (i) the charged particle irradiation facilities are limited all over world owing to high cost and highly sophisticated instrumentation, (ii) the very short range [order of cm in air to few (20-100) µm in water for ~4-10 MeV energy] of alpha particles [13] making it challenging to conduct in vitro radiobiology experiments with accuracy in dose and energy. These limitations have resulted in inadequate optimization of radiobiological parameters and a poor understanding of radiation effects of charged particles, especially in the setting of cancer radiotherapy. Joining the club of few laboratories around the world, for in vitro radiobiological experiments of normal/cancer cells, we have indigenously designed and developed first ^{241}Am alpha particle irradiator, which is a benchtop model automated with several user-friendly features[14]. In human cancer cells, alpha particles were found to induce more damage than gamma radiation measured in terms of DNA double break, chromosomal aberrations, and clonogenic survival. To study the bystander effect, alpha particles irradiated and unirradiated (bystander) cells were cultured in such a way that they share the medium but were physically separated through thin, porous membrane (inserts). In this arrangement, the effect of factors/cytokines released from the irradiated cells on bystander cells could be studied while keeping both cell populations separated. Our results showed that the magnitude of bystander effect from the alpha particle irradiated cells was higher in magnitude than that from the gamma irradiated cells [15,16].

The effect of gamma radiation is known to be governed by several biological factors like DNA repair efficiency, cell cycle, oxygen level. However, these factors are less likely to affect the cellular response to alpha particles. In a typical dose survival curve, the shoulder at lower doses of low LET radiation is known to be associated with capacity of cells to repair the damage. Such shoulder region at the lower doses are absent in a classical dose-survival curve of alpha particles due to poor repair ability of clustered DNA damages. Hence, based on classical understanding in the literature, the cellular response of alpha particles to cancer cells of different origin and dose response at lower doses is not well understood. These questions are very pertinent, especially in the application of charged particle/targeted alpha therapy to different cancer types and how cancer cells would respond if dose delivered to cancer cells is low and sub-lethal. While performing survival curve analysis of lung cancer cells to alpha particles, we unexpectedly encountered a higher proliferation and survival

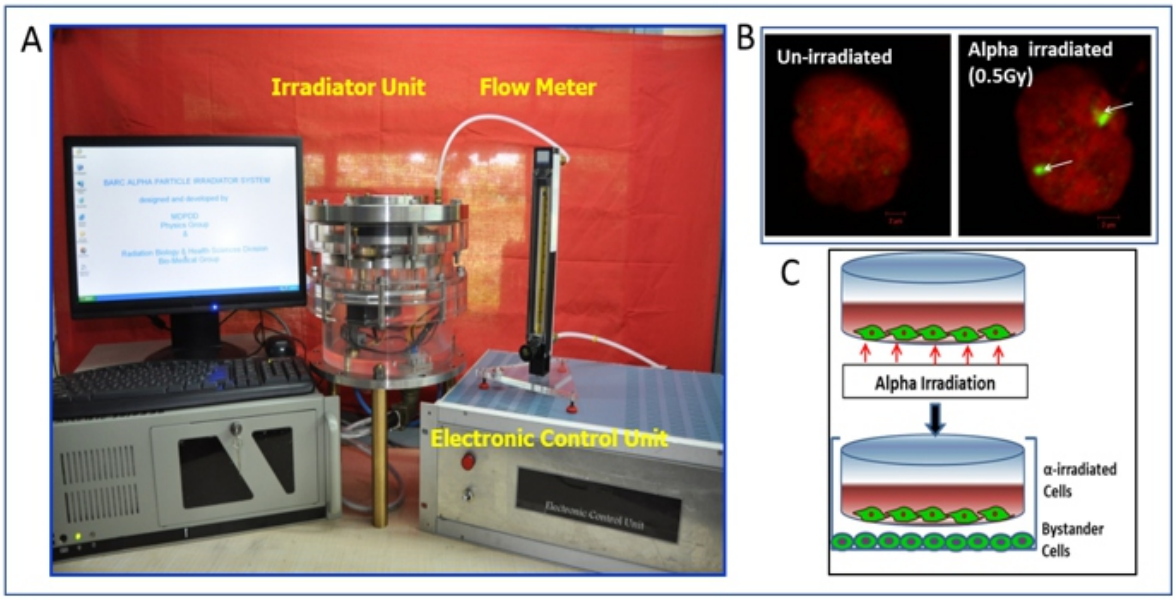

Fig.2: High LET radiobiology studies using automated benchtop alpha irradiator. A. Photograph of indigenously developed $_{241}$Am alpha irradiator and its major components; B. DNA damage in cancer cells after alpha particle irradiation. Green foci (arrows) show the expression of gamma H2AX as marker of DNA double strand break; C. Set up for bystander studies after alpha particle irradiation. Irradiated and bystander cells are cultured on porous membrane so that they share common medium being remained physically separated.

at low doses of radiation (1.36 and 6.8 cGy) contrary to well-known cell killing effect at higher doses (>13 cGy). The cyto-proliferative response of alpha particles to cancer cells was found to be associated with decrease in gap junction communication and Caveolin-1/Survivin signalling pathway. When these low-dose alpha-irradiated cancer cells were transplanted into SCID mice, they showed higher tumor growth [17]. These results suggest that if a lower dose is received to a fraction of tumor cells during charged/targeted alpha therapy, it might make them to survive more and possibly be one of the reasons behind recurrence/poor response in some patients. Hence, there is a need to optimize the dose during charged/targeted alpha therapy for better clinical outcome.

Our further studies determining the radio-sensitivity in cancer cells of different tissue origins also showed differential radio-response, with breast cancer cells showing higher cell killing by alpha particles than glioblastoma cells. This may be governed by cellular factors like status of oxidative stress and gap-junctions. These finding suggest that while selecting the cancer patients for charged particle/targeted alpha therapy, radiation oncologists need to also consider cellular and molecular features promoting non-targeted radiation effects for enhanced tumor radio-sensitivity.

Conclusion

NTRE after low and high LET radiation in the reference of cancer radiotherapy is rather an emerging research area which requires more studies for deeper mechanistic insights. The agents and strategies modulating NTRE for better tumor control would be of great interest to exploit the knowledge in cancer radiotherapy. The knowledge gained from in vitro and pre-clinical models provide further scope to evaluate the findings at the clinical level. The alpha particle radiation biology for cancer radiotherapy is in a nascent stage and requires exploration of the bystander interaction in the real tumor microenvironment conditions like hypoxia.

Acknowledgment

Authors would like to acknowledge the colleagues of Physics Group for design/fabrication and Shri R. V. Kolekar, Health Physics Division for dosimetry of Alpha Irradiator (BARC BioAlpha). Authors would like to acknowledge Dr D.C. Kar, Division of Remote Handling & Robotics and Dr Rajesh Kumar, Radiation Physics and Advisory Division in design/fabrication and dosimetry respectively for the cone irradiator for Bhabhatron teletherapy unit.

References

[1] C. Kumar, N. Shetake, S. Desai, A. Kumar, G. Samuel, B. N. Pandey, Relevance of radiobiological concepts in radionuclide therapy of cancer, International Journal of Radiation Biology, 2016, 92, 173.

[2] M. Buonanno, G. Gonon, B. N. Pandey, E. I. Azzam, The intercellular communications mediating radiation-induced bystander effects and their relevance to environmental, occupational, and therapeutic exposures, International Journal of Radiation Biology, 2023, 99, 964.

[3] P. K. Melwani, B. N. Pandey, Tunneling nanotubes: The intercellular conduits contributing to cancer pathogenesis and its therapy, Biochimica Biophysica Acta Reviews in Cancer, 2023, 1878, 189028.

[4] S. Desai, A. Kobayashi, T. Konishi, M. Oikawa, B. N. Pandey, Damaging and protective bystander cross-talk between human lung cancer and normal cells after proton microbeam irradiation, Mutation Research - Fundamental and Molecular Mechanisms of Mutagenesis, 2014, 39, 763-764.

[5] S. Desai, A. Kumar, S. Laskar, B. N. Pandey, Cytokine profile of conditioned medium from human tumor cell lines after acute and fractionated doses of gamma radiation and its effect on survival of bystander tumor cells,Cytokine, 2013, 61, 54.

[6] Pooja K. Melwani, M.M. Sagar Balla, Aman Bhamani, Shivani R. Nandha, Rahul Checker, and B. N. Pandey, Macrophage-conditioned medium enhances tunneling nanotube formation in breast cancer cells via PKC, Src, NF-κB, and p38 MAPK signaling, Cellular Signalling, 2024, 121, 111274.

[7] P. K. Melwani, R. Checker, M. M. Sagar Balla, and B. N. Pandey, Crosstalk Between Macrophages and Breast Cancer Cells: Networking Within Tumors, Book Titled "Monocytes and Macrophages in Development, Regeneration, and Disease", Chapter 8, Springer Nature. Editors: M. Kloc et al., 213-238.

[8] S. Desai, N. Srambikkal, H. D. Yadav, N. Shetake, M. M. S. Balla, A. Kumar, B. N. Pandey et al., Molecular understanding of growth inhibitory effect from irradiated to bystander tumor cells in mouse fibrosarcoma tumor model, PLoS One11, 2016, 0161662.

[9] Balla M., Kumar A., Pandey B. N., Implications of Cancer Stem Cells in Radiotherapy: Current Understanding and Future Perspectives, Biomedical Research Journal, 2014, 1(2), 137-45.

[10] Balla M. M. S., Yadav H. D., Pandey B.N., Tumorsphere assay provides a better in vitro method for cancer stem-like cells enrichment in A549 lung adenocarcinoma cells, Tissue Cell. 2019, 60, 21-24.

[11] Balla M. M., Ningthoujam R.S., Kumar M., Bandekar J.R., Pandey B.N., Cellular and spectroscopic characterization of cancer stem cell-like cells derived from A549 lung carcinoma, J Cancer Res Ther., 2016, 12(3), 1144-1152.

[12] Hitomi M., Deleyrolle L. P., Mulkearns-Hubert E. E., Jarrar A., Li M., Sinyuk M., Otvos B., Brunet S., Flavahan W. A., Hubert C. G., Goan W., Hale J. S., Alvarado A. G., Zhang A., Rohaus M., Oli M., Vedam-Mai V., Fortin J. M., Futch H. S., Griffith B., Lathia, J. D., Differential connexin function enhances self-renewal in glioblastoma, Cell Rep., 2015, 11(7), 1031–1042.

[13] B. R. Scott and R.A. Guilmette, Radiation Toxicology, Ionizing and Nonionizing, In: Philip Wexler, Editor. Encyclopedia of Toxicology. Second Edition, 2005, 601-615.

[14] M. V. J. Babu., S. G. Shinde, S. S. Kumar, M. Ali, R. Vasumathy, A. Kumar, B. N. Pandey et al., Dosimetry and radiobiological studies of automated alpha-particle irradiator, Journal of Environmental Pathology, Toxicology and Oncology, 2013, 32, 263.

[15] K. Kanagaraj, V. Rajan, B. N. Pandey, K. Thayalan, P. Venkatachalam, Primary and secondary bystander effect and genomic instability in cells exposed to high and low linear energy transfer radiations, International Journal of Radiation Biology, 2019, 95, 1648.

[16] K. Karthik, V. Rajan, B. N. Pandey, K. Sivasubramanian, S. F. D. Paul, P. Venkatachalam, Direct and bystander effects in human blood lymphocytes exposed to 241Am alpha particles and the relative biological effectiveness using chromosomal aberration and micronucleus assay, International Journal of Radiation Biology, 2019, 95, 725.

[17] V. Rajan, B. N. Pandey, Cytoproliferative effect of low dose alpha radiation in human lung cancer cells is associated with connexin 43, caveolin-1, and survivin pathway, International Journal of Radiation Biology, 2021, 97, 356.

पादपरसायन की ट्यूमर-रोधी प्रभावशीलता

13

कैंसर की वृद्धि में माइटोकॉन्ड्रियल रेडॉक्स संतुलन की भूमिका

राहुल चेकर [1,2], **शिवानी आर. नंदा** [1,2], **आर. एस. पटवर्धन** [1,2], **दीपक शर्मा** [1,2] **और संतोष के संदुर**[1,2]*
[1]विकिरण जीवविज्ञान एवं स्वास्थ्य विज्ञान प्रभाग, भाभा परमाणु अनुसंधान केंद्र, ट्रांबे-400085, भारत
[2]होमी भाभा राष्ट्रीय संस्थान, अणुशक्ति नगर, मुंबई-400094, भारत

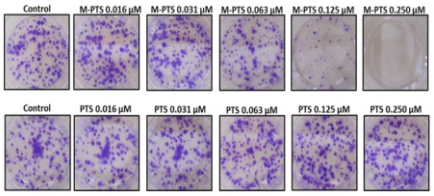

A549 कोशिकाओं की कोशिका व्यवहार्यता पर PTS और M-PTS का प्रभाव।

सारांश

माइटोकॉन्ड्रिया ऑक्सीडेटिव फॉस्फोराइलेशन के माध्यम से ऊर्जा उत्पन्न करके, कोशिकीय उपापचय को नियमन करके और कोशिका उत्तरजीविता और कार्य के लिए महत्वपूर्ण विभिन्न सिग्नलिंग मार्गों में भाग लेकर कोशिका वृद्धि में महत्वपूर्ण भूमिका निभाते हैं। दिलचस्प बात यह है कि कैंसर के विकास और मेटास्टेसिस के सभी लक्षण जैसे कि कोशिका मृत्यु से बचना, जैव और्जिकी में बदलाव और जीनोमिक अस्थिरता भी माइटोकॉन्ड्रिया की शिथिलता से जुड़े हैं। इसके अलावा, माइटोकॉन्ड्रियल रेडॉक्स संतुलन का रखरखाव कैंसर की वृद्धि में महत्वपूर्ण है, क्योंकि यह क्रम प्रसरण और उत्तरजीविता सहित सेलुलर सिग्नलिंग मार्गों को सीधे प्रभावित करता है। कैंसर कोशिकाओं में माइटोकॉन्ड्रिया की यह महत्वपूर्ण भूमिका उन्हें चिकित्सीय हस्तक्षेप के लिए प्रमुख कारक बनाती है। वर्तमान अध्ययन में, हमने ट्राइफेनिलफॉस्फोनियम (टीपीपी+) अंश के साथ संयोजन करके फाइटोकेमिकल्स के नए माइटोकॉन्ड्रिया-लक्षित व्युत्पन्नों की ट्यूमर-रोधी प्रभावकारिता का अध्ययन किया है।

Anti-tumour Efficacy of Phytochemicals

13

Role of Mitochondrial Redox Balance in Cancer Progression

Rahul Checker[1,2], **Shivani R Nandha**[1,2], **R. S. Patwardhan**[1,2], **Deepak Sharma**[1,2] **and Santosh K. Sandur**[1,2]*
[1]Radiation Biology & Health Sciences Division, Bhabha Atomic Research Centre, Trombay-400085, INDIA
[2]Homi Bhabha National Institute, Anushakti Nagar, Mumbai-400094, INDIA

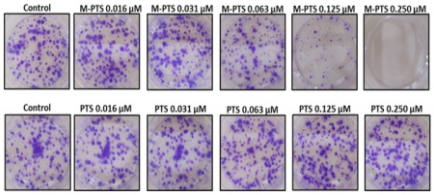

Effect of PTS and M-PTS on the cell viability of A549 cells

ABSTRACT

Mitochondria play a pivotal role in cell growth by generating energy through oxidative phosphorylation, regulating cellular metabolism, and participating in various signaling pathways crucial for cell survival and function. Interestingly, all the hallmarks of cancer growth and metastasis such as cell death evasion, altered bioenergetics, and genomic instability are also linked to mitochondria dysfunction. Further, the maintenance of mitochondrial redox balance is crucial in cancer progression, as it directly affects cellular signaling pathways involved in proliferation and survival. This important role of mitochondria in cancer cells makes them prime candidate for therapeutic intervention. In the present study, we have studied the anti-tumour efficacy of novel mitochondria-targeted derivatives of phytochemicals by conjugating with triphenylphosphonium (TPP+) moiety.

KEYWORDS: *Mitochondrial ROS, Clonogenic potential, Cell death, Triphenylphosphonium, Natural product*

*Author for Correspondence: Santosh K. Sandur
E-mail: sskumar@barc.gov.in

Introduction

Cancer, a multifaceted disease which is characterized by uncontrolled cell proliferation, remains a major challenge in healthcare worldwide. Over the last several decades, researchers have delved into different aspects of cancer biology, including the role of mitochondria (powerhouse of the cell), to understand their role in cancer progression. It is well known that mitochondria play a central role in cellular energy production through oxidative phosphorylation. In addition to their role in fulfilling the metabolic requirements of tumour cells, mitochondria also act as dynamic signaling organelles that control cancer cell survival, motility, stemness and resistance to treatment [1]. Interestingly, mitochondria are also a major source of reactive oxygen species (ROS), which are natural by-products of cellular metabolism. ROS function as signaling molecules at low to moderate levels wherein they regulate cell proliferation, differentiation, and survival. However, excessive ROS production can lead to oxidative stress, causing damage to cellular macromolecules.

Mounting evidence suggests that dysregulation of mitochondrial redox balance plays a pivotal role in cancer initiation, progression, and therapeutic resistance. Furthermore, oncogenic signaling pathways and mutations in key mitochondrial proteins can disrupt mitochondrial function and redox homeostasis in cancer cells. Targeting mitochondrial redox balance represents a promising therapeutic strategy for combating cancer [2]. However, mitochondrial structure and localization are major impediments towards efficient administration of small molecule modulators. Hence, targeting potent anti-cancer compounds to the tumour cell mitochondria by conjugating with delocalized lipophilic cations (DLCs) like triphenylphosphonium (TPP+) may perturb redox balance leading to apoptosis in tumour cells and increase the cytotoxic efficacy of these molecules. The molecule of interest is usually linked via a carbon linker to triphenylphosphonium (TPP+) cation [3]. Several compounds, such as mitochondria-targeted antioxidants and modulators of mitochondrial metabolism, have shown efficacy in preclinical studies and clinical trials. By selectively perturbing mitochondrial redox homeostasis in cancer cells, these agents have the potential to induce oxidative stress-mediated cytotoxicity while sparing normal cells.

In the present study, novel mitochondria-targeted derivatives of Ethyl ferulate (ethyl-3-hydroxy-4-methoxycinnamate; EF) and pterostilbene (3,5-dimethoxy-4-hydroxystilbene; PTS), a methoxylated form of resveratrol (Fig 1) were synthesized. Further, the efficacy of mitochondria targeted derivative of EF (M-EF) and pterostilbene (M-PTS) was compared with with their respective parent molecules in human lung adenocarcinoma cell line (A549) [4, 5].

Materials

Pterostilbene (PTS) was a kind gift from Sami Labs Limited, Bangalore. Ethyl ferulate (ethyl-3-hydroxy-4-methoxycinnamate; EF) was procured from TCI Chemicals. Dulbecco's Modified Eagle Medium (DMEM), fetal bovine serum (FBS), trypsin-EDTA, 3-(4,5-dimethyl-2-thiazole)-2,5-diphenyltetrazolium bromide (MTT reagent), dimethyl sulfoxide (DMSO) and crystal violet were obtained from Sigma Chemical Co. (MO, USA).

Methods

Cell culture

A549 lung cancer cell line was purchased from European Health Protection Agency, cultured in DMEM supplemented with 10% FBS and 1X antibiotic antimycotic solution in a humidified 5% CO2 incubator at 37°C.

Cytotoxicity assay

Anti-proliferative effects of EF and PTS and their mitochondria-targeted counterparts were assessed in A549 cells by performing the MTT cell viability assay. Briefly, A549 cells (3000 cells/well seeded in 96 well plate) were incubated with the indicated concentrations of EF or M-EF or PTS or M-PTS for 72h. 4 hours prior to the completion of 72h, 10µl of MTT tetrazolium dye (5mg/ml) was added to every well. After 4h of MTT incubation, media was replaced with 200µl DMSO in order to dissolve the formazan crystals and the absorbance (570nm) was recorded using a microplate reader (Synergy H1 Hybrid, USA).

Clonogenic assay

A549 cells seeded at a density of 500 cells/2ml in a 6-well plate were allowed to attach overnight followed by incubation with varying concentrations of EF or M-EF or PTS or M-PTS for 14 days. The colonies so formed were rinsed with PBS, methanol-fixed and stained with crystal violet. Colonies with at least 50 cells were counted.

Results and Discussion

Mitochondria-targeted derivative of EF and PTS demonstrated superior anti-tumour effect

Incubation with the parent compounds EF or PTS caused

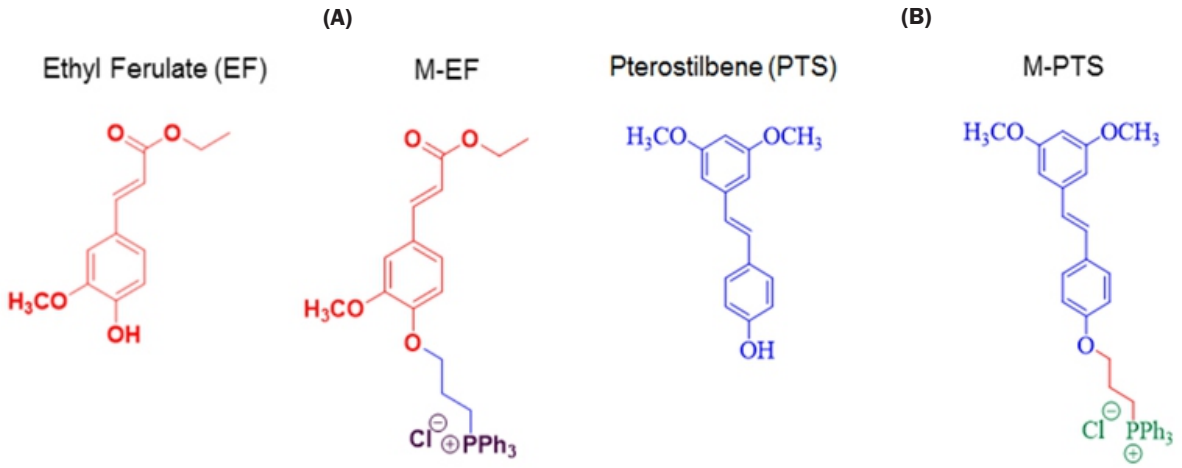

Fig.1: (A) Structure of EF and M-EF and (B) Structure of PTS and M-PTS. Adapted from Patil AS et al., Appl Biochem Biotechnol. 2023 Mar;195(3):2057-2076 and Ibrahim MK et al., Advances in Redox Research 8 (2023) 100071.

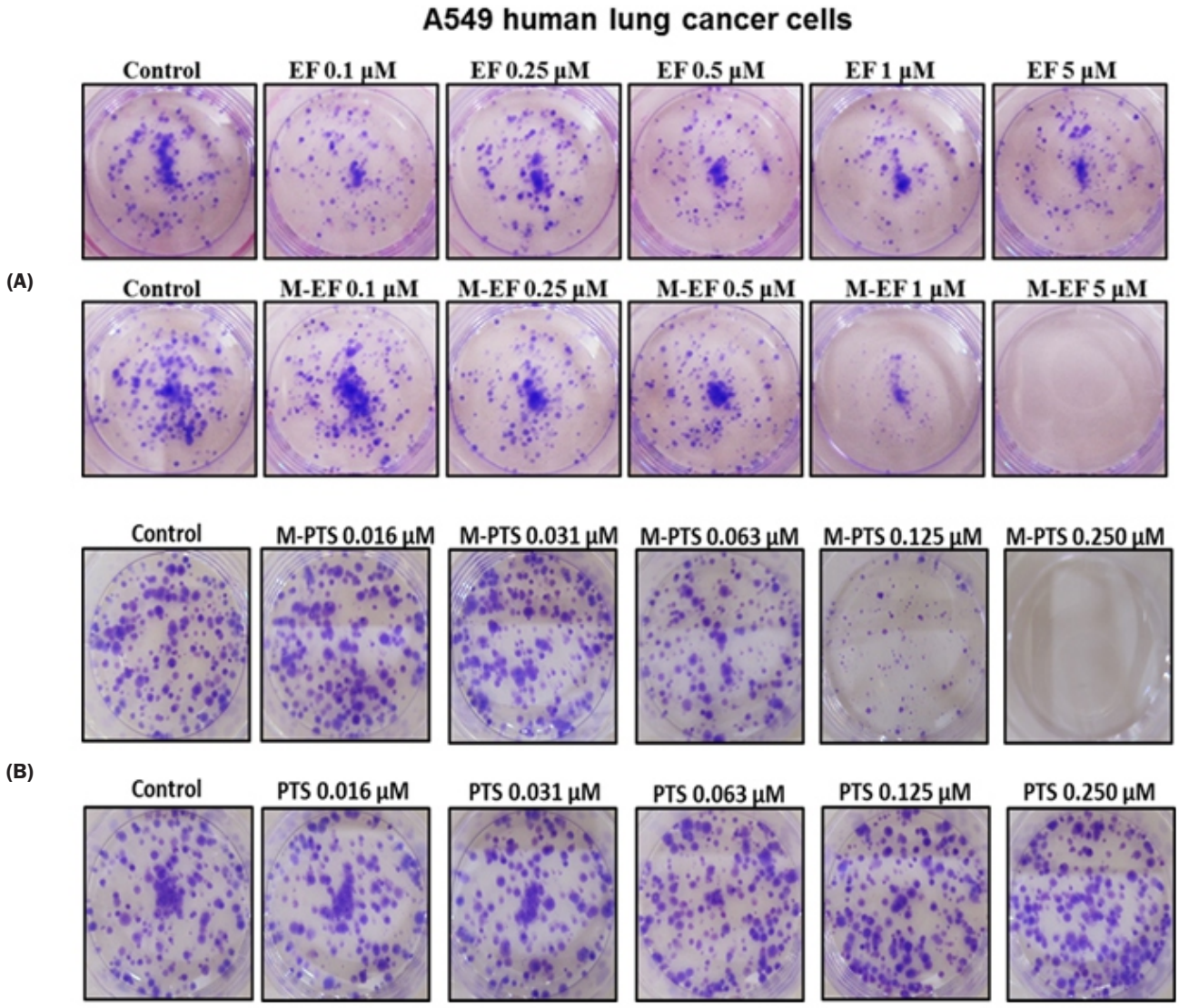

*Fig.4: Effect of (A) EF and M-EF (B) PTS and M-PTS on the mitochondrial ROS levels in A549 cells. **p<0.005; ***p<0.001; ****p<0.0001; as compared to control. Adapted from Patil AS et al., Appl Biochem Biotechnol. 2023 Mar;195(3):2057-2076 and Ibrahim MK et al., Advances in Redox Research 8 (2023) 100071.*

minimal reduction in the cell viability (around 10%) compared to M-EF or M-PTS treatment which resulted in a profound dose-dependent decrease up to 80-90% in the viability of A549 cells (Fig.2(A) & (B)). It was observed that M-EF is around 400-fold more effective than EF and M-PTS is around 200-fold effective than PTS in inducing cell death in A549 cancer cells. Taken together, these results highlight better anti-cancer potency of M-EF and M-PTS over EF and PTS, respectively.

M-EF and M-PTS displayed better efficacy in suppressing the colony-forming potential of lung cancer cells

Addition of EF led to partial reduction in the clonogenic

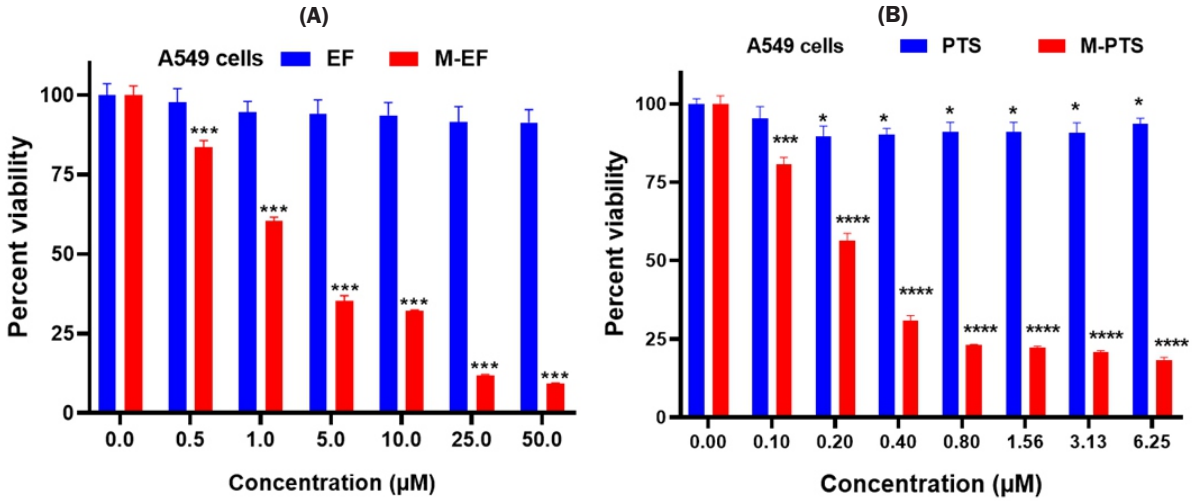

Fig.4: Representative images showing the effect of (A) EF and M-EF and (B) PTS and M-PTS on the clonogenic capacity of A549 cells. Adapted from Patil AS et al., Appl Biochem Biotechnol. 2023 Mar;195(3):2057-2076 and Ibrahim MK et al., Advances in Redox Research 8 (2023) 100071

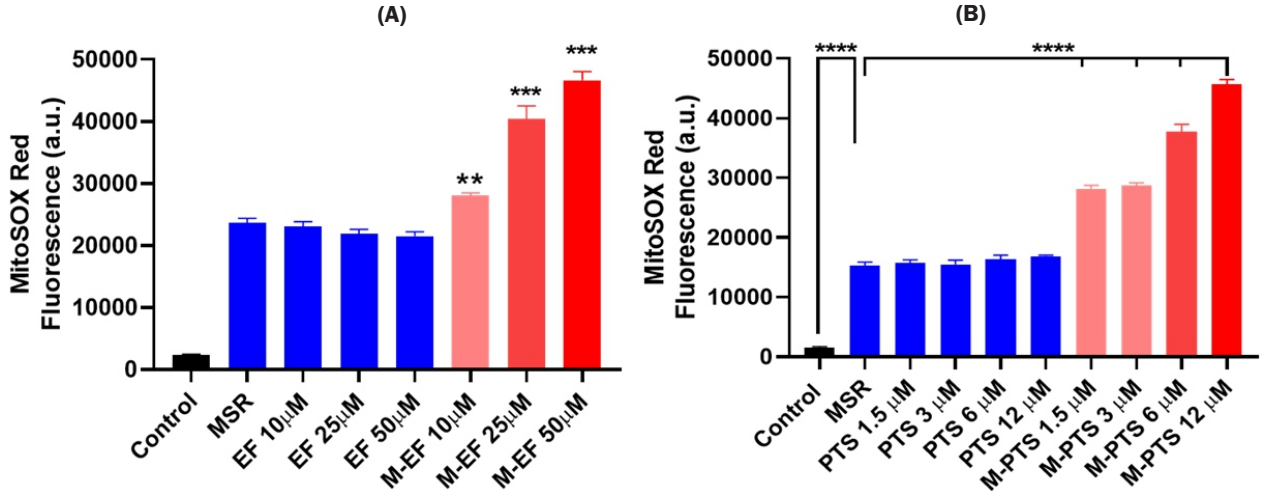

*Fig.4: Effect of (A) EF and M-EF (B) PTS and M-PTS on the mitochondrial ROS levels in A549 cells. **p<0.005; ***p<0.001; ****p<0.0001; as compared to control. Adapted from Patil AS et al., Appl Biochem Biotechnol. 2023 Mar;195(3):2057-2076 and Ibrahim MK et al., Advances in Redox Research 8 (2023) 100071.*

potential of A549 cells while PTS had no significant effect on reducing the colony-forming ability of A549 cells (Fig.3). In contrast, M-EF and M-PTS showed a concentration-dependent decrease in survival fraction of cells with complete loss of clonogenicity observed at 5μM and 0.25μM respectively (Fig.3). These results corroborated M-EF and M-PTS to be more effective than the parent molecules in inhibiting the clonogenic ability of A549 cancer cells.

M-EF and M-PTS increased mitochondrial ROS in cancer cells

Since these derivatives are targeted to the mitochondria, their effect on mitochondrial ROS levels was investigated. It was observed that treatment with both M-EF and M-PTS led to a dose-dependent increase in generation of mitochondrial superoxide in A549 cells (Fig.4(A) & (B)).

Conclusion

In conclusion, mitochondrial redox balance plays a critical role in cancer progression by influencing various cellular processes, including metabolism, signaling, and genomic stability. Combination therapies that integrate mitochondrial-targeted agents with conventional chemotherapeutic agents or targeted therapies may enhance treatment efficacy and overcome drug resistance in cancer patients. However, further research is warranted to elucidate the complex interplay between mitochondrial redox balance and cancer biology and optimize therapeutic interventions.

Acknowledgment

The authors acknowledge that these studies were carried out in collaboration with Institute of Chemical Technology, Matunga, Mumbai.

References

[1] Lopez, J. and S.W. Tait, Mitochondrial apoptosis: Killing cancer using the enemy within, Br J Cancer, 2015, 112(6), 957-62.

[2] Huang, M., et al., Mitochondria as a Novel Target for Cancer Chemoprevention: Emergence of Mitochondrial-targeting Agents, Cancer Prev Res (Phila), 2021, 14(3), 285-306.

[3] Dong, L., et al., Mitocans Revisited: Mitochondrial Targeting as Efficient Anti-Cancer Therapy, Int J Mol Sci., 2020, 21(21).

[4] Patil, A.S., et al., Mitochondriotropic Derivative of Ethyl Ferulate, a Dietary Phenylpropanoid, Exhibits Enhanced Cytotoxicity in Cancer Cells via Mitochondrial Superoxide-Mediated Activation of JNK and AKT Signalling, Appl Biochem Biotechnol., 2023, 195(3), 2057-2076.

[5] Ibrahim, M.K., et al., Mitochondria-targeted derivative of pterostilbene, a dietary phytoestrogen, exhibits superior cancer cell cytotoxicity via mitochondrial superoxide mediated induction of autophagy, Advances in Redox Research, 2023, 8.

यकृत के घातक रोगों का किफायती उपचार

14

भारत में यकृत रोगों के किफायती उपचार के लिए यिट्रिया [^{90}Y] एल्युमिनो सिलिकेट ग्लॉस माइक्रोस्फियर (भाभास्फियर) का विकास, मूल्यांकन और मानव पर क्लीनिकल ट्रांसलेशन

के. वी. विमलनाथ [1], ए. राजेश्वरी [1], अनुपम दीक्षित [2], शरद पी. लोहार [1], रुबेल चक्रवर्ती [1,3], मधुमिता गोस्वामी [2,3] और सुदीप्त चक्रवर्ती [1,3]*

[1]विकिरणभेषज प्रभाग, भाभा परमाणु अनुसंधान केंद्र, ट्रांबे -400085, भारत
[2]ग्लास एवं प्रगत पदार्थ प्रभाग ,भाभा परमाणु अनुसंधान केंद्र ,ट्रांबे -400085,भारत
[3]होमी भाभा राष्ट्रीय संस्थान, प्रशिक्षण विद्यालय परिसर, अणुशक्तिनगर, मुंबई -४०००९४

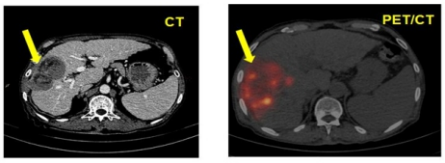

90 एम. सी. आई. [^{90}Y] वाई. ए. एस. ग्लास माइक्रोस्फियर के प्रयोग के 24 घंटे बाद दाहिने लोब हेपेटोसेलुलर कार्सिनोमा के साथ एक 56y पुरुष रोगी की पोस्ट-थेरेपी पी. ई. टी./सी. टी. छवि जो जैव वितरण दिखाती है।

सारांश

[^{90}Y] यिट्रिया एल्युमिनो सिलिकेट ([^{90}Y] YAS) ग्लॉस माइक्रोस्फियर (भाभास्फियर) का बेंच टू बेड क्लीनिकल ट्रांसलेशन, यूएस एफडीए द्वारा अप्रमाणित यकृत कैंसर के निदान के लिए अनुमोदित थेरास्फियर® का एक बायोसिमिलर फॉर्मूलेशन, प्राप्त किया गया है। संरचना $40Y_2O_3$-$20Al_2O_3$-$40SiO_2$ (w/w) एवं 20-36 µm के बीच के व्यास के YAS ग्लास माइक्रोस्फियर को न्यूट्रॉन को 7 डी के लिए ~ 1.4×10^{14} n.cm^{-2}.s^{-1} के थर्मल फ्लक्स पर किरणित किया गया ताकि आंतरिक रूप से विकिरणचिह्नित [^{90}Y] YAS ग्लॉस माइक्रोस्फियर का उत्पादन किया जा सके। मानव नैदानिक उपयोग के लिए संरूपण की उपयुक्तता स्थापित करने के लिए व्यापक रेडियोकेमिकल और जैविक अध्ययन किए गए थे। डीएई-आरपीसी से नियामक अनुमोदन प्राप्त करने के बाद, भाभास्फियर (50-180 एम. सी. आई.) की सोलह अनुकूलित मानव नैदानिक खुराकों को दस बैचों में तैयार किया गया और विकिरणभेषज प्रभाग, भापअ केंद्र से नैदानिक उपयोग के लिए आपूर्ति की गई।

Affordable Treatment of Liver Malignancies

14

Development, Evaluation and Human Clinical Translation of [^{90}Y]Yttria Alumino Silicate Glass Microspheres (BhabhaSphere) for Affordable Treatment of Liver Malignancies in India

K. V. Vimalnath[1], A. Rajeswari[1], Anupam Dixit[2], Sharad P. Lohar[1], Rubel Chakravarty[1,3], Madhumita Goswami[2,3] and Sudipta Chakraborty[1,3]*

[1]Radiopharmaceuticals Division, Bhabha Atomic Research Centre, Trombay-400085, INDIA
[2]Glass & Advanced Material Division, Bhabha Atomic Research Centre, Trombay-400085, INDIA
[3]Homi Bhabha National Institute, Anushakti Nagar, Mumbai-400094, INDIA

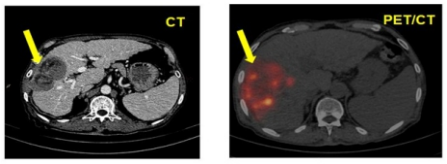

Post-therapy PET/CT image of a 56y male patient with right lobe hepatocellular carcinoma 24 h after administration of 90 mCi [^{90}Y]YAS glass microspheres showing biodistribution

ABSTRACT

Bench to bed clinical translation of [^{90}Y]Yttria Alumino Silicate ([^{90}Y]YAS) glass microsphere (BhabhaSphere), a formulation biosimilar to US FDA approved TheraSphere® for treating unresectable liver cancer, is achieved. YAS glass microspheres of composition $40Y_2O_3$-$20Al_2O_3$-$40SiO_2$ (w/w) and diameter ranging between 20-36 µm was neutron irradiated at a thermal flux of ~1.4×10^{14} n.cm^{-2}.s^{-1} for 7 d to produce intrinsically radiolabeled [^{90}Y]YAS glass microspheres. Extensive radiochemical and biological studies were carried out to establish the suitability of the formulation for human clinical use. Subsequent to obtaining regulatory approval from DAE-RPC, sixteen customised human clinical doses of BhabhaSphere (50-180 mCi) were formulated in ten batches and supplied for clinical use from Radiopharmaceuticals Division, BARC.

KEYWORDS: *SIRT, Yttria Alumino Silicate (YAS) Glass microspheres, ^{90}Y, BhabhaSphere*

**Author for Correspondence: Sudipta Chakraborty*
E-mail: sudipta@barc.gov.in

Introduction

Liver malignancies, either primary or metastatic, are prevalent causes of cancer related deaths worldwide. Hepatocellular carcinoma (HCC), a form of neoplasm of liver cells, is common among the various types of liver malignancies constituting 90% of liver cancer [1-4]. Selective internal radiation therapy (SIRT), which involves intra-hepatic administration of customized doses of β-particle emitting radionuclide in suitable chemical form [Fig.1], is one of the most effective treatment modalities for management of unresectable liver carcinoma [5]. Intrinsically ^{90}Y [$T_{1/2}$ = 64.1h, E_{max} of β-emission = 2.28 MeV] labeled glass microspheres of 20-35 μ particle size range is extensively used radiotherapeutic agent for SIRT [5,6]. The radiotherapeutic agent is approved by US FDA for radioembolization therapy and is commercially available as TheraSphere® with personalized doses as per the therapy requirement. SIRT using TheraSphere® offers a well-tolerated treatment for patients with liver malignancies[7]. In our country, the nuclear medicine hospitals had to rely on import of this product at very high cost (each dose costing around US$ 10000-12000) for treatment of liver cancer patients, severely restricting its wider utility. This gave us the motivation toward indigenous development of ^{90}Y-labeled glass microsphere formulation biosimilar to TheraSphere®, which can be made available at an affordable cost for use in SIRT for treating patients in India suffering from unresectable liver carcinoma.

Yttria alumino silicate (YAS) glass microspheres having particle size in the range of 20-36 μm and chemical composition $40Y_2O_3$-$20Al_2O_3$-$40SiO_2$ (w/w) were synthesized following procedure developed indigenously and characterized to ensure their suitability in SIRT. Intrinsically ^{90}Y-labeled YAS glass microspheres ([^{90}Y]YAS glass microspheres) aka 'BhabhaSphere' were produced by thermal neutron irradiation of cold microspheres in Dhruva research reactor, BARC, such that ^{90}Y becomes an integral constituent of the glass microspheres. BhabhaSphere formulation is delivered to the tumor vasculature through hepatic artery via catheterisation [Fig.1]. The radioactive glass microspheres then penetrate the tumor arteriolar capillaries where they emit lethal beta radiation that is localised to the surrounding tumor tissue. The targeted distribution of microspheres provides high absorbed dose coverage to the tumor while sparing normal tissue.

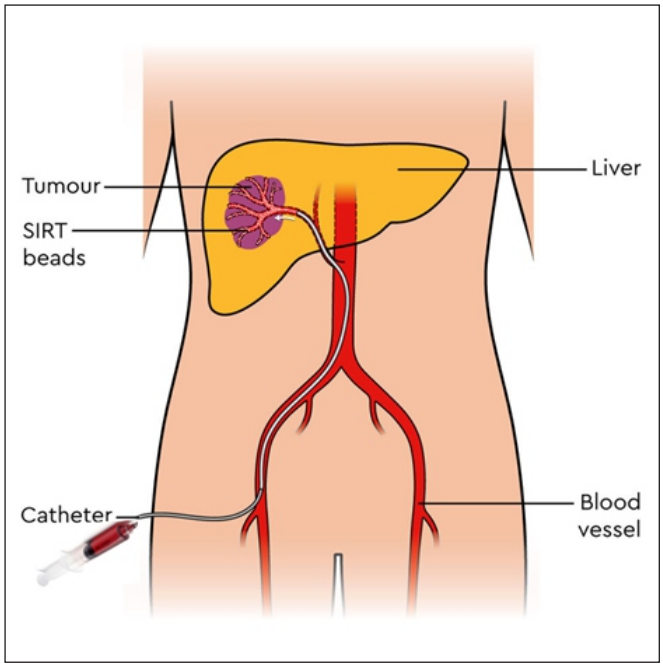

Fig.1: Schematic representation of Selective Internal Radiation Therapy (SIRT) process.

Materials and Methods

Yttria Alumino Silicate (YAS) glass having composition $40Y_2O_3$-$20Al_2O_3$-$40SiO_2$ (wt.%) was prepared by melt-quench process. The glass frits are slowly ground and glass particles of 20-36 mm size range were segregated by sieving. These feed glass particles were converted to glass microspheres by flame spheroidization using H_2-O_2 torch. Subsequently, the microspheres were screened to remove the particles with defects, cleaned with acetone and further heated in a furnace to remove organic impurities. YAS glass microspheres prepared were analyzed under SEM to check for sphericity, size and visible defects. XRD and SAXS are recorded before and after neutron irradiation to observe the glassy nature of the microspheres and evaluate post irradiation surface changes. Analysis of chemical composition of all batches of YAS glass microspheres were carried out by EDXRF and ICP-OES techniques.

Typically, 80-100 mg YAS glass microspheres were taken in a quartz ampoule [5 mm (ϕ) × 12 mm (h)], sealed and irradiated at thermal neutron flux of ~1.4×10^{14} n.cm^{-2}.s^{-1} for 7 days after placing inside a standard Al irradiation container. Post irradiation, quartz ampoule is opened inside a glove box and the irradiated glass microspheres [^{90}Y]YAS transferred into a sterile bottom tapered quartz container. Radioactive glass microspheres were washed twice using sterile water for injection. Finally, 0.6 mL sterile water for injection was added to [^{90}Y]YAS glass microspheres, sealed and autoclaved.

Radioactivity content of ^{90}Y in [^{90}Y]YAS glass microsphere formulation was measured in a pre-calibrated isotope dose calibrator. Radionuclidic purity (RNP) was determined by recording γ-ray spectra of an aliquot withdrawn from [^{90}Y]YAS glass microsphere formulation using an HPGe detector coupled to a 4K MCA system. For determination of radiochemical purity (RCP), the radioactive glass microspheres were allowed to settle and ^{90}Y activity of a measured aliquot from the supernatant was determined. Specific activity was calculated as ^{90}Y activity (mCi) produced per mg YAS irradiated. Sterility of the [^{90}Y]YAS glass microsphere formulation was tested by Direct Inoculation method and pyrogenicity by Gel Clot-BET assay method as per approved Indian Pharmacopeia (IP) procedures.

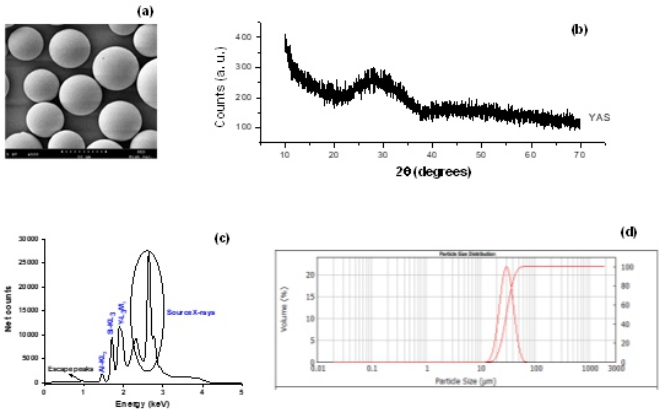

Fig.2: Characterization of YAS microspheres: (a) SEM image (b) XRD pattern (c) EDXRF spectrum (d) particle size distribution.

Biodistribution studies of [^{90}Y]YAS glass microsphere were performed in a group of healthy male Wistar rats each weighing 200-250 g. Appropriately diluted aliquots of [^{90}Y]YAS glass microsphere formulations (0.1 mL, ~135 mCi radioactivity) were injected through portal vein of each animal. Uptake of [^{90}Y]YAS glass microsphere in different organs and tissues are calculated and expressed as percentage injected activity (dose, % ID) per organ. Animal experiments were performed in compliance with national laws for conducting animal experimentations in India with prior approval of Institutional Animal Ethics Committee of Bhabha Atomic Research Centre (BARC).

A proposal comprising comprehensive experimental data for six independent batches was submitted to Radiopharmaceutical Committee of Department of Atomic Energy (DAE-RPC) seeking approval for formulation and deployment of 'BhabhaSphere' for human clinical use. Subsequent to DAE-RPC approval, first clinical investigation of [^{90}Y]YAS glass microsphere formulation was carried out in a male patient (56 y) with right lobe hepatocellular carcinoma. Customized dose of 90 mCi of [^{90}Y]YAS glass microsphere formulation was administered through right hepatic artery. PET/CT images were recorded at 24 h post administration. Subsequently, 15 more customised human clinical doses of BhabhaSphere (50-160 mCi) were formulated in 10 batches and supplied for clinical use.

Results and Discussion

YAS glass microspheres were synthesized using flame spheroidization process with conversion efficiency of almost 100% and sphericity >99%. SEM images (Fig.2(a)) confirmed high degree of sphericity and uniformity. XRD pattern (Fig.2(b)) confirmed its glassy nature. EDXRF spectrum is shown in Fig.2(c) confirmed chemical purity. Particle size distribution (Fig.2(d)) showed >90% of particles were within the range of 20-36 m.

Intrinsically [^{90}Y]Y-labeled glass microspheres were produced with specific activity of 3.9 ± 0.3 μCi ^{90}Y/mg of microspheres that corresponds to ~0.183 μCi (~6800 Bq) ^{90}Y per microsphere. RNP and RCP of formulations were >99.9% and >99.0% respectively, desirable for human clinical applications. Sterility and bacterial endotoxin tests (BET) revealed that all batches of [^{90}Y]YAS glass microsphere formulations were sterile and with <175 EU bacterial endotoxin content.

[^{90}Y]YAS glass microspheres exhibited excellent in vitro stability with regard to release of ^{90}Y activity from the formulation when stored at 37^{0}C in physiological saline and in human serum. Biodistribution pattern of [^{90}Y]YAS glass microspheres revealed excellent retention of administered microparticles in liver (97.62 ± 0.68 %ID at 24 h and 94.23 ± 0.57 %ID at 144 h p.i.). First human clinical investigation was carried out at Tata Memorial Hospital, Parel, where a customized dose of 90 mCi of [^{90}Y]YAS glass microspheres was administered in a 56 year male patient with right lobe hepatocellular carcinoma. Figures. 3a and 3b present the trans-axial CT and PET/CT images of liver of the patient 24 h post administration. Target specific localization and near-complete retention of the formulation in the cancerous site is evident from images. Therapeutic dose of the [^{90}Y]YAS glass microsphere formulation, injected into the patient was well tolerated by the patient, as no adverse side effects of the therapeutic procedure were reported. Total 16 human clinical doses of BhabhaSphere (50-160 mCi) were formulated in 11 batches and supplied for human clinical use from Radiopharmaceuticals Division, BARC. In-house developed BhabhaSphere formulation is envisaged to be made commercially available at cost of ~ Rs. 80,000 (US$ 1000) per patient dose as against US$ 10000-12000 per patient dose of imported TheraSphere®

Conclusion

Preparation of ready to use therapeutic doses of [^{90}Y]YAS glass microsphere aka 'BhabhaSphere' suitable for clinical use in the treatment of unresectable liver cancer in patients in India is achieved. YAS glass microspheres were prepared by flame spheroidization process and [^{90}Y]YAS doses were formulated with radionuclidic and radiochemical purity suitable for clinical use. Human clinical evaluation in patient with hepatocellular carcinoma showed near-quantitative retention of the formulation in the injected lobe by post-therapy ^{90}Y-PET scans. Indigenous development of ^{90}Y-labeled glass microsphere (BhabhaSphere) is a significant achievement that will be utilized in the management of inoperable liver cancer in India at affordable cost.

Acknowledgment

Authors gratefully acknowledge contributions of Reactor Operation Division and Radiation Biology and Health Sciences Division, BARC; and Tata Memorial Hospital, Parel. Authors sincerely express their gratitude to Associate Director, Radiochemistry and Isotope Group; Director, Materials Group; Head, Radiopharmaceuticals Division and Head, Glass and Advanced Materials Division, BARC for their keen interest and support to the program.

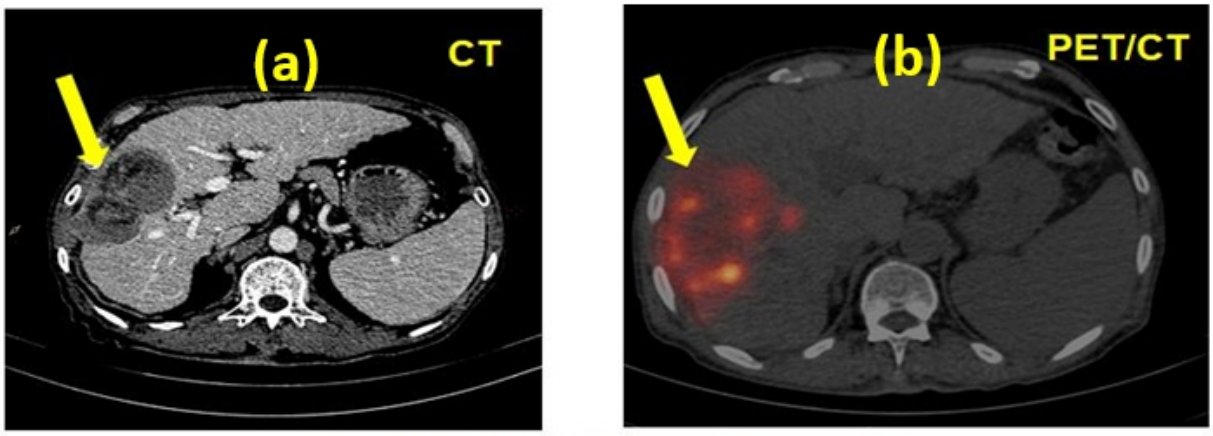

Fig.3: Post-therapy PET/CT image of a 56y male patient with right lobe hepatocellular carcinoma 24 h after administration of 90 mCi [^{90}Y]YAS glass microspheres showing biodistribution (a) trans axial CT of liver and (b) trans axial PET/CT of liver. (Image courtesy: Tata Memorial Hospital, Parel)

References

[1] Llovet J. M., Zucman-Rossi J., Pikarsky E., et al., Hepatocellular carcinoma, Nat. Rev. Dis. Prim., 2016, 2, 16018.

[2] Foerster F., Gairing S. J., Ilyas S. I., Galle P. R., Emerging immunotherapy for HCC: A guide for hepatologists, Hepatology, 2022, 75, 1604.

[3] European Association for the Study of the Liver, European Organisation for Research and Treatment of Cancer, EASL-EORTC clinical practice guidelines: Management of hepatocellular carcinoma, J. Hepatol., 2012, 56, 908.

[4] Shetty V. V., Kellarai A., Comprehensive review of hepatocellular carcinoma in India: Current challenges and future directions, JCO Global Oncol., 2022, 2200118.

[5] Ehrhardt G. J., Day D. E., Therapeutic use of 90Y microspheres, Int J Rad Appl Instrum B., 1987, 14, 233.

[6] Salem R., Fordon A. C., Mouli S., et al., Y-90 Radioembolization significantly prolongs time to progression compared with chemoembolization in patients with hepatocellular carcinoma, Gastroenterology, 2016, 151, 1155.

[7] Goin J. E., Salem R., Carr B. I., et al., Treatment of unresectable hepatocellular carcinoma with intrahepatic yttrium 90 microspheres: Factors associated with liver toxicities, J Vasc Interv Radiol., 2005, 16, 205.

थोरियम के प्रति जैविक प्रतिक्रियाओं में अंतर्दृष्टि

15

मानव स्वास्थ्य एवं पर्यावरण के लिए थोरियम

सौरव के .दास [1,2], **मंजूर अली** [1], **नीना जी .शेताके** [1,2], **बद्री एन .पांडे** [1,2] **और अमित कुमार** [1,2]*
[1]विकिरण जीवविज्ञान एवं स्वास्थ्य विज्ञान प्रभाग ,भाभा परमाणु अनुसंधान केंद्र ,ट्रांबे -400094,भारत
[2]होमी भाभा राष्ट्रीय संस्थान ,अणुशक्ति नगर ,मुंबई -400094,भारत

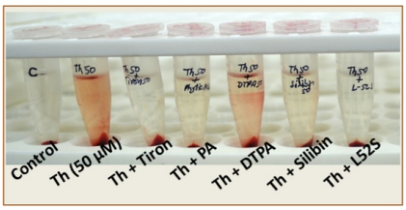

थोरियम सजावट के लिए तर्कसंगत रूप से चयनित एजेंटों की एक्स-विवो स्क्रीनिंगः मानव आरबीसी लाइसिस परख।

सारांश

थोरियम (Th-232) विकसित भारत की ऊर्जा मांग को पूरा करने के लिए एक अति आवश्यक नाभिकीय ईंधन है। नाभिकीय ऊर्जा के अलावा, थोरियम के अन्य समस्थानिक कैंसर के उपचार और अन्य पर्यावरणीय अनुप्रयोगों हेतु सहायक हैं। विभिन्न सामाजिक अनुप्रयोगों के लिए थोरियम की पूरी क्षमता को यथार्थ करने के लिए, हमारा रेडियोजीवविज्ञान अनुसंधान मानव कोशिकाओं (RBCs, यकृत और फेफड़ों की कोशिकाओं) और पशु मॉडल में थोरियम अंतःक्रिया, परिवहन और जैविक प्रतिक्रियाओं के तंत्र के बारे में महत्वपूर्ण अंतर्दृष्टि प्रदान करता है। विषाक्तता तंत्र और थोरियम के जैव-समन्वय से संभावित संकेतों ने थोरियम के लिए लिगैंड के तर्कसंगत अभिकल्पन और विकास का मार्ग प्रशस्त किया है, जिसमें कैंसर के उपचार और नाभिकीय विघटन कार्यनीतियों के विकास के लिए संभावित अनुप्रयोग हैं।

Insight into Biological Responses to Thorium

15

Thorium for Human Health and Environment

Sourav K. Das[1,2], **Manjoor Ali**[1], **Neena G. Shetake**[1,2], **Badri N. Pandey**[1,2]**and Amit Kumar**[1,2]*
[1]Radiation Biology & Health Sciences Division, Bhabha Atomic Research Centre, Trombay-400085, INDIA
[2]Homi Bhabha National Institute, Anushakti Nagar, Mumbai-400094, INDIA

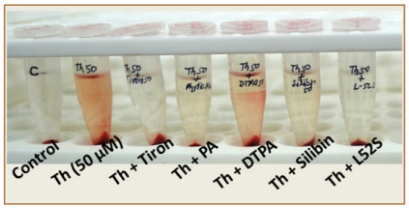

Ex-vivo screening of rationally-selected agents for Thorium decorporation: Human RBC lysis assay

ABSTRACT

Thorium (Th-232) is an indispensable nuclear fuel for meeting the energy demands of *Viksit Bharat* (developed India). In addition to nuclear energy, other Th isotopes hold promise for cancer treatment and other environmental applications. This article presents a comprehensive synthesis of our research findings on Thorium Biology accumulated over the past two decades as part of the Nuclear Radiobiology Research Program. To realize the full potential of Th for various societal applications, our radiobiology research provides significant insight about the mechanism of Th interaction, transport and biological responses in human cells (RBCs, liver and lung cells) and animal models. The potential clues from toxicity mechanism and bio-coordination of Th have paved the way for rational design and development of ligands for Th, having potential applications for cancer treatment and development of nuclear decorporation strategies.

KEYWORDS: *Thorium, Radiobiological Research, Cancer Therapy, Actinide Decorporation*

*Author for Correspondence: Amit Kumar
E-mail: amitk@barc.gov.in

Introduction

The nuclear energy is indispensable with little-to-zero carbon foot print. Importantly, Uranium has been utilized as a nuclear fuel for clean energy generation since last several decades. However due to its limited abundance, alternative nuclear fuels viz. Plutonium and Thorium are gaining significant importance. Plutonium availability is again dependent on natural Uranium. Therefore, Thorium owing to i) its 4-5 times more natural abundance (compared to U), ii) potential of its conversion into fissile fuel, iii) thermo-physical characteristics, iv) lesser long-lived radionuclide generation has been considered as a potential fuel for sustainable energy generation through advanced nuclear technologies, in particular molten salt reactor, high temperature reactor and accelerator driven sub-critical systems (Fig.1).

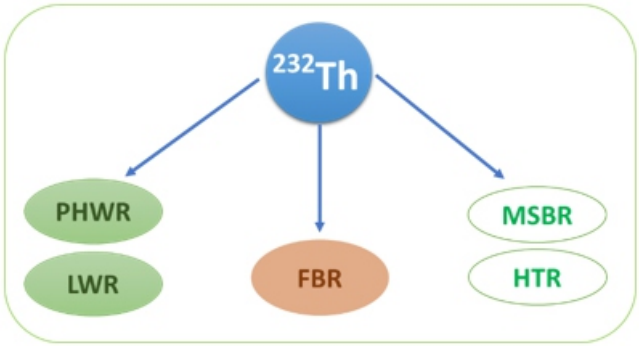

Fig.1: Scheme illustrates the recent development for possible utilization of naturally occurring Thorium (Th-232) in various reactor technologies. PHWR: Pressurised Heavy Water Reactor; LWR: Light Water Reactor; FBR: Fast Breeder Reactor; MSBR: Molten Salt Breeder Reactor; HTR: High Temperature Reactor.

Recently, Thorium-based fuel such as ANNEL (Advanced Nuclear Energy for Enriched Life) has also been developed for existing PHWR or CANDU reactors (Fig. 1). Additionally, the feasibility of Thorium utilization has been explored in Light Water Reactors [1]. Thorium-232 would be used as a blanket in Fast Breeder Reactors (FBR) to convert it into fissile U-233 for third stage reactors of DAE. Notably, the commencement of "Core Loading" at India's first indigenous PFBR (500MWe) at Kalpakkam, Tamil Nadu would pave the way for efficient utilization of India's vast reserve of Thorium. This review provides a comprehensive overview of our research findings on Thorium Biology, gathered over the past two decades through the Nuclear Radiobiology (Bio-Actinide) Research Program.

Thorium and Human Health

In view of Thorium as a future nuclear fuel, the fundamental research aimed towards understanding the radiobiological effects of Thorium in human cells and experimental animals is one of the most relevant areas of Radiation Biology Program of several research areas of nations. Having the largest reserve of Thorium and being equipped with advanced nuclear reactor technologies for Thorium utilization, this research program is even more relevant for India [2]. Following three sub-sections describe potential implications of Thorium biology research in i) targeted alpha cancer therapy, ii) fundamental radiobiology and iii) development of novel decorporation strategies for management of internal nuclear contamination.

Thorium for cancer therapy

One of the isotopes of Thorium is Th-227, which emits five high-energy alpha particles ($t_{1/2}$ =18.7d, average 5.9 MeV) and two beta disintegrations during its decay. These alpha particles are highly favourable for targeted therapy of cancer mainly due to the following reasons: i) short-path length resulting minimal damage to surrounding normal tissue, ii) high linear energy transfer leading to un-repairable and clustered DNA double strand breaks, and iii) cytotoxic effects of alpha radiation independent of oxygen status in tumour. Due to half-lives, large alpha particle energies and rapid decay chains, ^{225}Ac and ^{227}Th have immense potential for targeted alpha therapy of cancer. With regard to yield as compared to ^{225}Ac, ^{227}Th can be obtained from the beta decay of ^{227}Ac, which is a decay product of naturally-occurring ^{235}U. Alternatively, ^{227}Th can be produced by thermal neutron irradiation of ^{226}Ra followed by beta decay of ^{227}Ra. To achieve the full anticancer potential of Th-227 conjugates, a significant scope of research exists for development of constructs with tumor-targeting moiety and a specific bifunctional chelator. Recent reports have shown promising results for antitumor activity of ^{227}Th conjugates in preclinical tumor models and in phase-I clinical trial [3]. In summary, ^{227}Th-based targeted alpha therapy represents a viable cancer treatment modality in future.

Radiobiological research

Under this topic, we summarize the key findings from our learning experience on the basic mechanisms of Thorium interaction with human cells and proteins and its consequences. A more than decade-long research activities revealed crucial answers for i) the mechanism of effects of

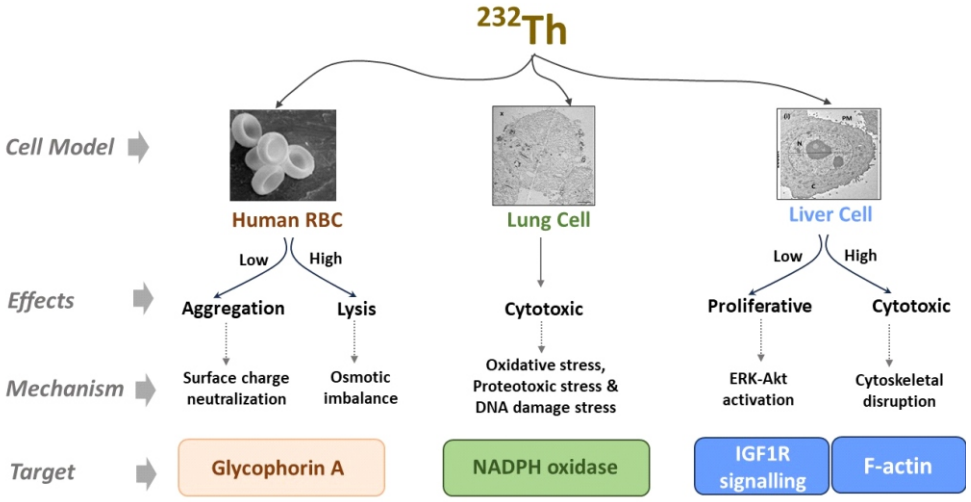

Fig.2: Scheme illustrates the effect of Thorium, possible mechanisms and potential target of toxicity in the indicated human cell models under in vitro conditions. Disclaimer: These effects were observed under experimental conditions and may not occur in real exposure scenario.

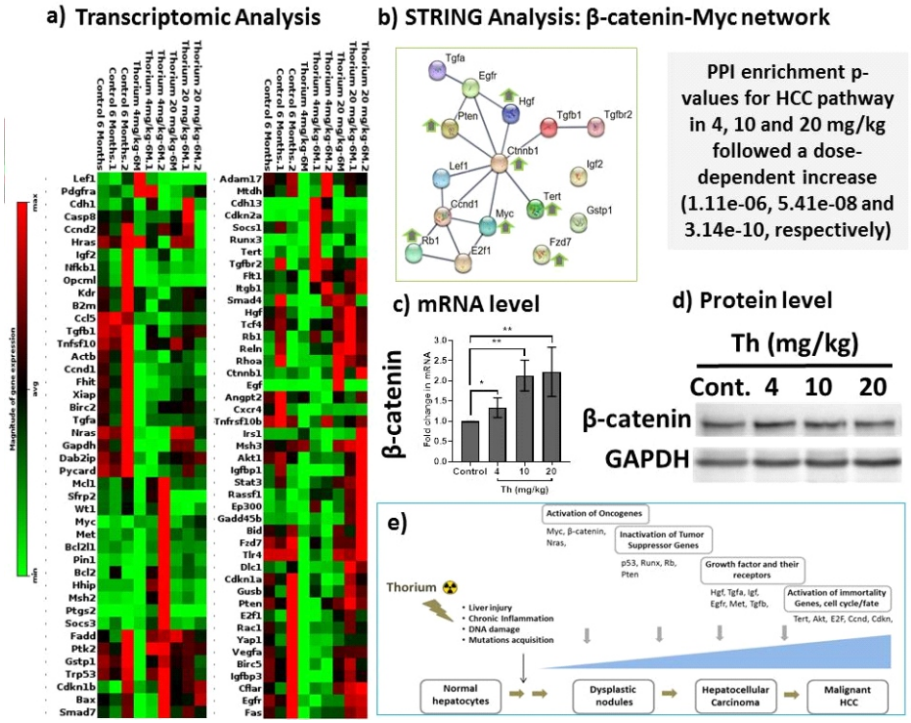

Fig.3: (a) Transcriptomic profile of liver tissues of mice following 6 or 12 months of Th administration (4, 10 and 20 mg/kg). (b) Protein-protein interaction analysis by STRING revealed statistically significant functional interaction among the proteins of hepatocellular carcinoma network, which identified β-catenin as the most significant signalling nodes. (c & d) Validation of role of β-catenin at mRNA and protein level. (e) Scheme illustrates the possible role of Th-induced genes in the sequential process of liver carcinogenesis. Reprinted from "Mechanistic Insights into Thorium-232 induced Liver Carcinogenesis: The Driving Role of Wnt/β-Catenin Signaling Pathway by R. Yadav, S. K. Das, M. Ali, N. G. Shetake, B. N. Pandey and A. Kumar, Science of Total Environment 907 (2024) 168065 with permission from Elsevier.

Thorium in human cells; ii) the mechanism of cellular internalization of Thorium; iii) fundamental aspects of the binding of Thorium to protein and their functional consequences; and iv) major target organs of Thorium and their early and late chronic effects. Understanding these aspects of Thorium toxicology at organ, cell and molecular levels using biophysical, biochemical, microscopic, spectroscopic and computational approaches, we have designed and developed the rational antidotes for removal of Thorium and mitigation of its associated radiological and chemical effects. In conclusion, the Bio-Thorium Research Program at BARC would have significant implications for developing India's capability for efficient utilization of Thorium with adequate human health and environmental protection.

With regard to one of our research objectives, 'the mechanism of effects of Thorium in human cells', we have envisaged to investigate the effect of Th-232 on various human cells viz. red blood cells [4], lung cells [5], liver cells [6-8], and bone [9], which represent the target organ/sites of Thorium accumulation/toxicity in human/animal models (Fig.2). Our experimental data suggest that radiobiological response to Thorium depends on the cell type, chemical forms, concentration and exposure time of Thorium. Briefly, in human lung cells, Th-dioxide (colloidal) was found to be more toxic than the Th-nitrate at equivalent metallic concentration of Thorium. This was found to be due to higher uptake of Th in cells exposed to its dioxide form as compared to the Thorium uptake from its nitrate form of exposure. Moreover, transmission electron microscopy in combination with confocal microscopy further revealed the mechanism of Thorium internalization, which was found to be a clathrin/caveolin-mediated endocytosis following Th-dioxide exposure as compared to membrane perforation in cells exposed to Th-nitrate. Following internalization, Thorium induces oxidative stress, DNA damage response and proteotoxic stress, which play major roles in determining cytotoxicity [5]. Following transmigration through air-blood barrier in lung, Th gets circulated via blood and finally accumulates in liver and skeleton. Our studies on human liver cells have identified the role of cytoplasmic calcium in Thorium uptake, suggesting the possible application of calcium modulators for minimizing Th internalization. Using ultrasensitive analytical techniques, we have identified cytoskeleton as the major intracellular target of Thorium [7]. Interestingly, effect of Thorium on human red blood cells (RBCs) was found to be determined by Th:RBCs ratio. Lower Th-to-RBCs ratio caused aggregation due to neutralization of surface negative charge. However, at higher Th-to-RBCs ratio, RBCs undergoes cell lysis (hemolysis) through colloid-osmotic mechanism [4]. These mechanisms of Th-induced cytotoxicity have significant implications to develop rational approaches for mitigation of Th-toxicity.

During circulation in blood, Thorium ions can also interact (in addition to RBCs) with soluble proteins such as albumin/globulin in blood plasma as well as haemoglobin localized on RBC's membrane. Using biophysical tools, we have determined the binding sites of Thorium ions in human serum albumin [10] and haemoglobin proteins [11]. Interestingly, Th ions were found to perturb the structural and functional integrity of Fe-containing heme of haemoglobin. This was due to the similar charge-to-ionic-radii ratio of Th with Iron. This further explains the binding of Th at Fe-binding sites in iron transport/storage proteins (e.g. transferrin, ferritin, catalase, etc.). Thorium interaction with haemoglobin was also observed in the environmentally-important aquatic midge, *Chironomus*, which may serve as bioindicator of Th contamination in aquatic bodies [11]. Importantly, our spectroscopic data determined the ability of actinide ions including Thorium to unfold the proteins with significant alteration in their functionally important conformations. In this direction, further research in our laboratory using computational modelling and biochemical

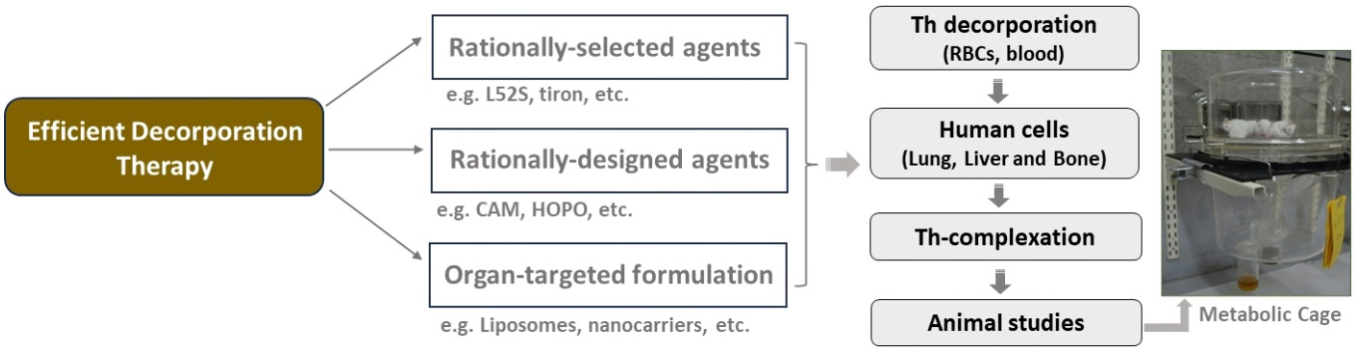

Fig.4:This scheme represents three different approaches for development of efficient decorporation therapy for Thorium and other relevant nuclear contaminants. The lead thorium chelator or its liposomal formulation are assessed for thorium removal efficacy from various human cells and blood. Thorium complexation is studied by a variety of spectroscopic and computational modelling. Finally, animal studies are performed to test thorium decorporation efficacy using in-house fabricated metabolic cages.

approaches, is in progress to characterize the bio-coordination of Thorium and other actinide ions with relevant proteins, which have been identified as a molecular target of toxicity.

We have carried out extensive studies in experimental mice/rat models to identify the major sites of Th accumulation and underlying mechanism of toxicity at cellular and molecular levels. Liver, skeleton and spleen were found to be the major target organs of Thorium following its administration [12-14]. We have determined the biodistribution, histological and functional changes as well as alterations in gene expression in organs/tissues after 6 to 12 months of Thorium exposure. Our recent analysis of gene expression and system biology approaches [15] revealed the identification of β-catenin/Myc driven signalling pathways responsible for Thorium-induced oncogenesis in mice (Fig.3). Currently, mechanism of radiobiological effects of Thorium on lung using specially-designed nose-only inhalation exposure facility is an active area of investigation, which led to the identification of surfactant protein-D as a potential biomarker of Th exposure [16].

Thorium decorporation technologies

Design and development of effective mitigation approaches for internal contamination with Thorium and other radiometals in human and environment is the most important area of research in this field. Presently, there is no FDA-approved antidote for treatment of human subjects in case of Thorium contamination. DTPA (Ca/Zn salt of diethylenetriamminepentacetate) is the only available agent recommended for Plutonium, Americium and Curium contamination. However, our animal data suggest that DTPA is not effective to remove Thorium ions from liver and skeleton. Therefore, further research is required to design Th-specific rational antidote. Our experience on the mechanism of Th interaction at cell and protein levels has provided significant clues about the biological ligands (proteins/DNA, etc.) with which antidote (chelator) need to potentially compete for Th decorporation. In this direction, we adopted multidisciplinary three-pronged approaches viz.: i) rationally-selected existing molecules; ii) rationally-designed new agents and iii) improvement of organ distribution profile of chelators using drug delivery approach (Fig.4).

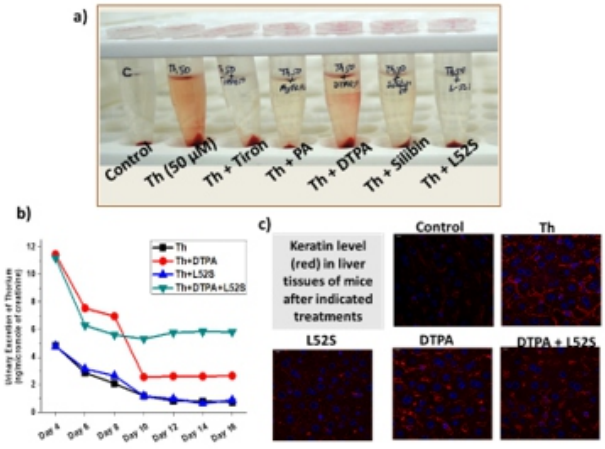

Fig.5: (a) Ex-vivo screening of rationally-selected agents for Thorium decorporation: Human RBC lysis assay; (b) The lead candidate L52S in combination with DTPA enhances Th-232 decorporation in mice and © potentially mitigates liver damage. Reprinted from "Thorium decorporation efficacy of rationally-selected biocompatible compounds with relevance to human application" by M. Ali, B. Sadhu, A. Boda, N. Tiwari, A. Das, S. K. Musharaf Ali, D. Bhattacharya, B. N. Pandey and A. Kumar, Journal of Hazardous Materials 365 (2019) 952-61 (License: 5924850861041) and "Enhanced thorium decorporation and mitigation of toxicity through combined use of Liv52® and diethylenetriamine pentaacetate" by M. Ali, S. K. Das, N. G. Shetake, B. N. Pandey, and A. Kumar, Journal of Hazardous Materials, 477 (2024) 135234 with permission from Elsevier (License 5924851197485).

Our efforts on screening of rationally-selected existing molecules have identified L52S (a hepatoprotective formulation) for its potential of Th decorporation [17]. L52S has been found to be significantly effective to enhance removal of Th from target organs in combination with DTPA (Fig. 5) [18]. Regarding other approaches, we have designed and tested liposomal-DTPA [19] and other ligands [20, 21] for Th decorporation. Further research is in plan to develop more efficient organ-targeted vehicle system to deliver chelating agent for organ-specific actinide decorporation. Recently, collaborative efforts are in progress for development of multidentate chelating agent for actinide decorporation.

Thorium for isotope hydrology

Recent research showed that the monitoring of Th concentrations in water can be used as a chemical signature for rock fracture events, which are integral to the hydrology and geochemistry of watersheds [22]. Moreover, ratiometric determination of Th isotopes (Th-228/230) was found to significantly predict the flood events, suggesting the novel application of Th measurements for environmental and climate change studies [23]. Since Th is sparingly soluble in water, its concentration can be monitored as a signature of water contamination from mining/milling activities also.

Future Research Perspectives

Further research is directed to gain deeper insights about the cellular and molecular mechanisms of radiobiological effects of Thorium and other heavy metal radionuclides in cells and tissues. These biological investigations would lead to the identification of sensitive and

specific biomarkers of Thorium exposure/effects. Our learning suggested the need for development of decorporation therapy according to the route of exposure, which can be applied in real practical scenario for effective management of internal contamination with actinides.

Conclusion

We have delineated the mechanism of cytotoxic effects of Th-232 in relevant human cells (blood cells, liver and lung cells). Cellular effects of Th were found to be dependent upon the cell type and its chemical form. Human RBCs were found to undergo aggregation or lysis upon Th exposure. Th uptake in liver cells was observed to be sensitive to cytoplasmic calcium level and its channels. In lung cells, Th followed either membrane perforation or endocytosis mechanism depending on nitrate or oxide form for internalization. At protein level, Th prefers to bind iron or calcium-binding sites, which is followed by interaction with carbonyl or amide groups. At organ level, omics data revealed the possible mechanism of Th-induced carcinogenesis in mice liver. Extensive efforts are underway to develop rational decorporation therapy for removal of internalized Th from lungs, surface wounds and other vital organs based on the understanding of mechanisms of Th toxicity and interaction.

Acknowledgment

The authors sincerely acknowledge the support of Dr P. A. Hassan, Associate Director, Bioscience Group, BARC.

References

[1] CSTEP, Thorium utilisation pathways for India, CSTEP-RR-2019-12, 2019.

[2] A. Kumar, M. Ali and B. N. Pandey, Understanding the biological effects of thorium and developing efficient strategies for its decorporation and mitigation, BARC Newsletter, 2013, 335, 55.

[3] U. B. Hagemann, K. Wickstroem, S. Hammer, R. M. Bjerke, S. Zitzmann-Kolbe, O. B. Ryan, J. Karlsson, A. Scholz, H. Hennekes, D. Mumberg and A. S. Cuthbertson, Advances in Precision Oncology: Targeted Thorium-227 Conjugates As a New Modality in Targeted Alpha Therapy, Cancer Biother Radiopharm., 2020, 35, 497.

[4] A. Kumar, M. Ali, B. N. Pandey, P. A. Hassan and K. P. Mishra, Role of Membrane Sialic Acid and Glycophorin Protein in Thorium induced Aggregation and Hemolysis of human erythrocytes, Biochimie, 2010, 92, 869.

[5] S. K. Das, M. Ali, N. G. Shetake, R. M. R. Dumpala, B. N. Pandey and A. Kumar, Mechanism of thorium-nitrate and thorium-dioxide induced cytotoxicity in normal human lung epithelial cells (WI26): Role of oxidative stress, HSPs and DNA damage, Environmental Pollution, 2021, 281, 116969.

[6] M. Ali, A. Kumar and B. N. Pandey, Thorium induced cytoproliferative effect in human liver cell HepG2: Role of insulin-like growth factor 1 receptor and downstream signaling, Chemico-Biological Interactions, 2014, 211, 29.

[7] R. Yadav, S. K. Das, M. Ali, B. N. Pandey and A. Kumar, Role of calcium ion channels and cytoskeletal proteins in Thorium-232 induced toxicity in normal human liver cells (WRL 68) and its validation in Swiss mice, Chemosphere, 2022, 288, 132557.

[8] R. Yadav, B. N. Pandey and A. Kumar, Estimation and in-situ detection of thorium in human liver cell culture by arsenazo-III based colorimetric assay, Biometals, 2020, 33, 75.

[9] A. K. Agrawal, R. Yadav, B. Singh, M. Ali, A. Kumar, Y. Kashyap, and B. N. Pandey, Study of thorium-induced micro-structural changes in mice femoral bone using SR-μCT, Toxicology and Environmental Health Sciences, 2023, 15, 399.

[10] M. Ali, A. Kumar and B. N. Pandey, The Interaction of Human Serum Albumin with Lanthanide and Actinide Ions: Binding Affinities, Protein Unfolding and Conformational Changes, Biochimie, 2016, 123, 117.

[11] A. Kumar, M. Ali, R. S. Ningthoujam, P. Gaikwad, M. Kumar, B. B. Nath, B. N. Pandey, The Interaction of Actinide and Lanthanide Ions with Human Hemoglobin and Its relevance to Human and Environmental Toxicology, Journal of Hazardous Materials, 2016, 307, 281.

[12] R. Yadav, A. K. Agrawal, M. Ali, A. Kumar, Thorium-induced anatomical and histopathological changes in liver of Swiss mice, Toxicol. Environ. Health Sci., 2018, 10, 97.

[13] A. Kumar, P. Mishra, P. Sharma, S. Ghosh, M. Ali, B. N. Pandey and K. P. Mishra, Thorium induced oxidative stress mediated toxicity in mice and its abrogation by diethylenetriammine pentaacetate, International Journal of Radiation Biology, 2008, 84, 337.

[14] A. Kumar, M. Ali, P Mishra, P. Sarma, B. N. Pandey and K. P. Mishra, Thorium induced neurobehavioral and neurochemical alterations in Swiss mice, International Journal of Radiation Biology, 2009, 85, 338.

[15] R. Yadav, S. K. Das, M. Ali, N. G. Shetake, B. N. Pandey and A. Kumar, Mechanistic Insights into Thorium-232 induced Liver Carcinogenesis: The Driving Role of Wnt/β-Catenin Signaling Pathway; Science of Total Environment, 2024, 907, 168065.

[16] S. K. Das, M. Ali, N. G. Shetake, B. N. Pandey and A. Kumar, Thorium Alters Lung Surfactant Protein Expression in Alveolar Epithelial Cells: In Vitro and In Vivo Investigation. ACS Environmental Science & Technology, 2024, 58(28), 12330–12342

[17] M. Ali, B. Sadhu, A. Boda, N. Tiwari, A. Das, S. K. Musharaf Ali, D. Bhattacharya, B. N. Pandey and A. Kumar, Thorium decorporation efficacy of rationally-selected biocompatible compounds with relevance to human application, Journal of Hazardous Materials, 2019, 365, 952-61.

[18] M. Ali, S. K. Das, N. G. Shetake, B. N. Pandey, and A. Kumar. Enhanced thorium decorporation and mitigation of toxicity through combined use of Liv52® and diethylenetriamine pentaacetate. Journal of Hazardous Materials, 2024, 477, 135234.

[19] A. Kumar, P. Sharma, M. Ali, B. N. Pandey and K. P. Mishra, Decorporation and Therapeutic Efficacy of Liposomal-DTPA against Thorium Induced Toxicity in Wistar Rat, International Journal of Radiation Biology, 2012, 88, 223.

[20] R. M. R. Dumpala, S. K. Das, M. Ali, A. Boda, A. Kumar, N. Rawat and S. M. Ali, Characterization of Thorium-Pyrazinoic acid complexation and its decorporation efficacy in human cells and blood, Chemosphere, 2021, 271, 129547.

[21] S. Sharma, M. Ali, A. Kumar and N. Rawat, Combined Thermodynamic, Theoretical and Biological Study for Investigating N-(2-acetamido)-iminodiacetic acid as a Potential Thorium Decorporation Agent, Inorganic Chemistry, 2023, 62, 18887.

[22] W.F. Yang, M. Chen, X. X. Zhang, Z. G. Guo, G. X. Li, M. A. Qiang, J. H. Yang, Y. P. Huang, Thorium isotopes (228Th, 230Th, 232Th) and applications in reconstructing the Yangtze and Yellow River floods, International Journal of Sediment Research, 2013, 28, 588.

[23] B. Gilbert, S. Carrero, W. Dong, et al., River thorium concentrations can record bedrock fracture processes including some triggered by distant seismic events, Nature Communication, 2023, 14, 2395.

इम्यूनोथेरेप्यूटिक्स का विकास

16

ट्यूमर के माइक्रोएनवायरनमेंट की जांच के माध्यम से नए इम्यूनोथेरेप्यूटिक्स की पहचान

विपुल के. पांडे [1], **कविता प्रेमकुमार** [1], **प्रयाग जे. अमीन** [1] **and भवानी एस. शंकर** [1,2]*
[1]इम्यूनोलॉजी अनुभाग, विकिरण जीवविज्ञान और स्वास्थ्य विज्ञान प्रभाग, भाभा परमाणु अनुसंधान केंद्र, ट्रांबे-400085, भारत
[2]होमी भाभा राष्ट्रीय संस्थान, अणुशक्ति नगर, मुंबई-400094, भारत

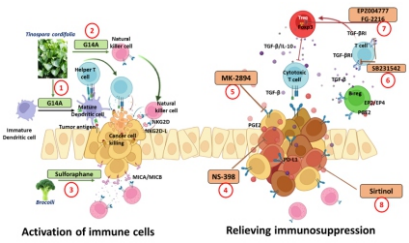

इम्यूनोथेरेपीटिक्स

सारांश

कैंसर प्रतिरक्षा निगरानी में प्रतिरक्षा प्रणाली की भागीदारी लगातार विकसित हो रही है। कैंसर की प्रगति के प्रारंभिक चरणों के दौरान, अन्योन्यक्रिया करने वाली प्रतिरक्षा कोशिकाएं सक्रिय होती हैं, जिसमें विभिन्न प्रकार की कोशिकाएं और साइटोकिन्स ट्यूमर-रोधी गुणधर्म प्रदर्शित होते हैं। हमारे शोध से पता चला है कि G1-4A, टिनोस्पोरा कॉर्डिफोलिया से प्राप्त एक पॉलीसेकेराइड, डेंड्राइटिक कोशिकाओं और प्राकृतिक घातक कोशिकाओं को सक्रिय करके प्रभावी रूप से एंटी-ट्यूमर प्रतिरक्षा को बढ़ाता है। ब्रोकोली से प्राप्त एक अन्य यौगिक, सल्फोराफेन, ट्यूमर कोशिकाओं पर कुछ सतह रिसेप्टर्स को बढ़ाता है जो प्राकृतिक घातक कोशिकाओं को उनका पता लगाने में मदद करता है और ट्यूमर कोशिकाओं को मारने के लिए अधिक अतिसंवेदनशील बनाता है। कैंसर बढ़ने से बचने के चरण के दौरान, कैंसर कोशिकाएं सक्रिय दमन को नियोजित करके प्रतिरक्षा प्रणाली द्वारा पता लगाने से बचती हैं। घुलनशील मध्यस्थ जैसे प्रोस्टाग्लैंडिन और परिवर्तनशील विकास कारक-β(TGF-β), साथ ही नियामक T कोशिकाएं, कैंसर सूक्ष्म वातावरण में प्रतिरक्षा दमन में योगदान देती हैं। हमने पहचान की है कि NS-398, साइक्लोऑक्सीजिनेज-2 का एक अवरोधक, SB-431542, विकास कारक- रिसेप्टर (TGF- R) सिग्नलिंग को बदलने का एक अवरोधक; और EPZ004777 और FG-2216, विनियामक कोशिकाओं के एपिजेनेटिक अवरोधक, ट्यूमर प्रेरित प्रतिरक्षा दमन को रोक सकते हैं और प्रतिरक्षा सक्षम कोशिकाओं को बहाल कर सकते हैं। अपने प्रतिरक्षात्मक गुणों के कारण, G1-4A, NS-398 एवं SB431542 जैसे अणु पूर्व-नैदानिक मॉडल में ट्यूमर के भार को कम करने में सक्षम थे और इनका उपयोग प्रतिरक्षात्मक चिकित्सा के रूप में किया जा सकता है।

Development of Immunotherapeutics

16

Identification of Novel Immunotherapeutics Through Tumor Microenvironment Investigations

Vipul K. Pandey[1], **Kavitha Premkumar**[1], **Prayag J. Amin**[1] **and Bhavani S. Shankar**[1,2]*
[1]Immunology Section, Radiation Biology and Health Sciences Division, Bhabha Atomic Research Centre, Trombay-400085, INDIA
[2]Homi Bhabha National Institute, Anushakti Nagar, Mumbai-400094, INDIA

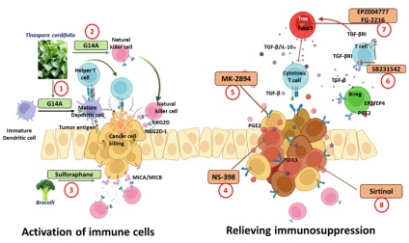

Immunotherapeutics

ABSTRACT

The immune system's involvement in cancer immunosurveillance is constantly evolving. During the early stages of cancer progression, various immune cells interact actively, with diverse cell types and cytokines exhibiting anti-tumor properties. Our research has shown that G1-4A, a polysaccharide derived from *Tinospora cordifolia*, effectively boosts anti-tumor immunity by activating dendritic cells and natural killer cells. Another compound, sulforaphane, derived from broccoli, increases certain surface receptors on tumor cells that help natural killer cells detect them and make tumor cells more susceptible to killing. During the escape stage of cancer progression, the cancer cells elude detection by the immune system by employing active suppression. Soluble mediators such as prostaglandins and transforming growth factor -β (TGF-β), as well as regulatory T cells, contribute to immunosuppression in the cancer microenvironment. Our studies have identified several compounds, including NS-398, an inhibitor of cyclooxygenase-2, SB-431542, an inhibitor of transforming growth factor-β receptor (TGF-βR) signaling; and EPZ004777 and FG-2216, epigenetic inhibitors of T regulatory cells, can prevent tumor induced immunosuppression and restore immunocompetent cells. Due to their immunomodulatory properties, molecules such as G1-4A, NS-398, and Sb431542 have demonstrated the ability to reduce tumor burden in pre-clinical models and may be used as immunotherapeutics.

KEYWORDS: *Tumor microenvironment, Immunotherapeutics, NS-398, G1-4A, SB431542, EPZ004777, FG 2216, Sulforaphane*

*Author for Correspondence: Bhavani S. Shankar
E-mail: bshankar@barc.gov.in

Introduction

The capacity of all somatic cells to divide into two daughter cells is limited. This is known as 'Hayflick's limit' and is due to the shortening of telomeres, which are repetitive DNA sequences present at the ends of linear chromosomes. When cells exceed Hayflick's limit and divide excessively, it can result in uncontrolled cell proliferation or cancer. Although uncontrolled cell proliferation is the initial cause of cancer, as it grows, a number of changes take place, including immune cell infiltration, interaction with nearby fibroblasts, blood vessel development (angiogenesis), resulting in the formation of tumor microenvironment (TME). The way the many components of tumor microenvironment interact impacts how the cancer grows, spreads to other organs, and responds to treatment. The TME of different cancers varies and can be categorized as: (a) 'hot' tumors with numerous lymphocytes and other immune cells infiltrating them (b) 'excluded' or suppressed tumors with immune cells present only at the periphery (c) ignored or 'cold' tumors with no immune recognition at all. The relationship between cancer cells and immune cells is always changing, even in 'hot' tumors. Smaller tumors allow the infiltrating immune cells to be active, identify modified cells and destroy them through activities of cytotoxic T cells or natural killer cells. The immune system gets the upper hand during this phase, which is referred to as the 'elimination' stage, and can destroy the tumor cells with the help of cytotoxic T cells, natural killer cells, and mediators such as tumor necrosis factor (TNF)-α, interferon-γ, interleukins-6 and 12, etc. At this stage, the use of immunomodulators that stimulate the various immune cells that can help with tumor cell detection and destruction will be helpful. As the tumor advances, in addition to secreting various substances that actively suppress the immune system, the tumor actively exploits the growth factors and cytokines produced by immune cells to support its growth. Important mediators in the micro environment that cause immunosuppression include soluble mediators like prostaglandins, transforming growth factor-β (TGF-β) and cells such as T regulatory cells. Therefore, at this point, cancer treatment will benefit from the use of drugs that can prevent the immunosuppressive effects. Abrogation of immunosuppressive T regulatory cells is crucial for the treatment of 'excluded' tumors and enable the immune cells to infiltrate the tumor microenvironment.

Materials and Methods

Dendritic cells, natural killer cells, and cytotoxic T cells were isolated from the mouse spleen for *in vitro* treatments. T regulatory cells and B regulatory cells were generated *in vitro* using appropriate cytokine cocktail treatments. *In vivo* experiments were carried out in syngeneic tumor models. Expression of various markers was analyzed using flow cytometry or Western blot. Cytokines were monitored by ELISA, or ELISpot. Cytotoxicity assays were conducted using fluorometric or flow cytometry-based methods.

Results and Discussion

Immunomodulators that activate immune cells

Dendritic cells are the most effective antigen presenting cells, and are crucial for the development of an adaptive immune response against cancer cells. These cells interact with the cancer cells, process the cancer antigen, and activate the effector T cells, thereby becoming more immunogenic. Microbial products like lipopolysaccharide (LPS) help DC to mature and become more immunogenic. Immunomodulators, particularly those derived from natural resources, are being extensively studied for the treatment of a number of diseases, including cancer. Native to India, *Tinospora cordifolia*, commonly referred to as 'Guduchi', is a climbing shrub that has

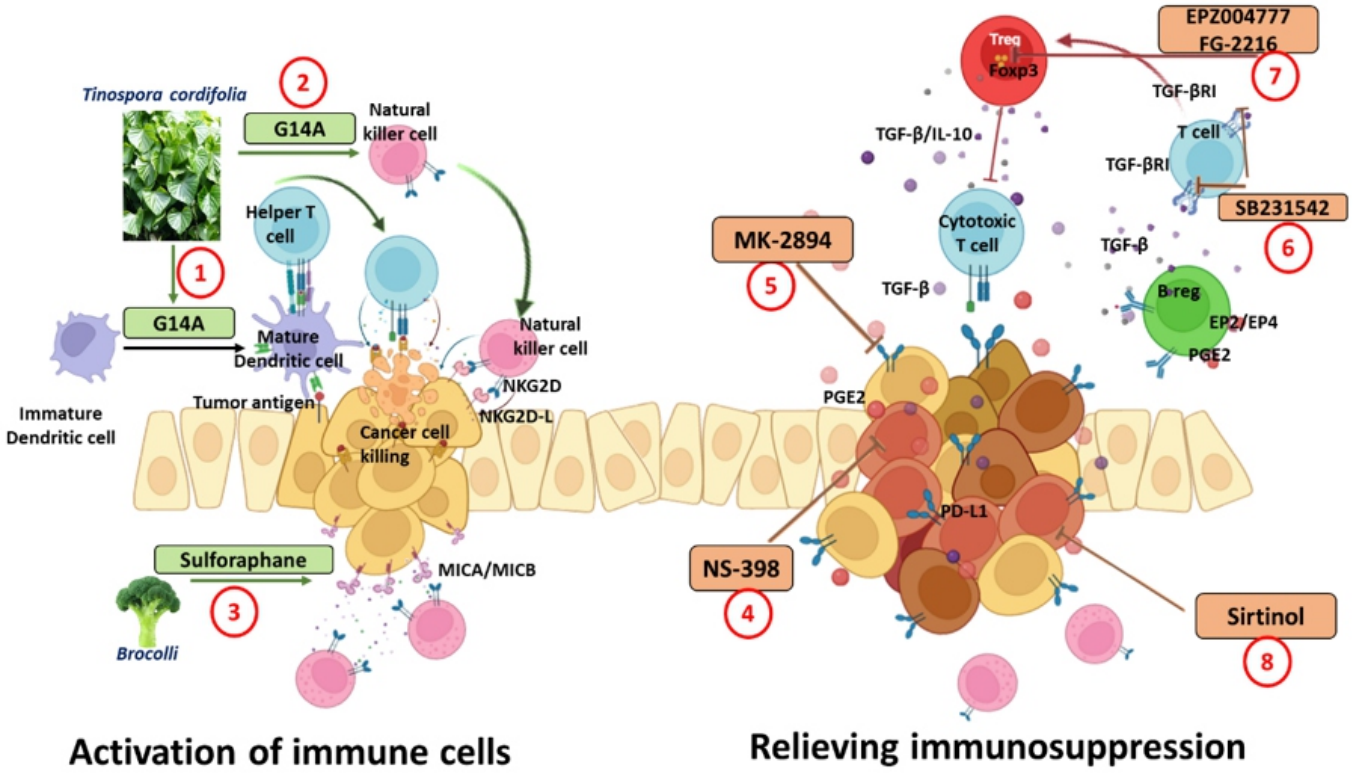

Fig.1: Immunotherapeutics with differing modes of action according to the changing tumor microenvironment: (1) G1-4A, a polysaccharide isolated from Tinospora cordifolia, is efficient in enhancing anti-tumor immunity by activating dendritic cells and (2) natural killer cells. (3) Sulforaphane (derived from broccoli) upregulates tumor cell surface molecules, that aid in detection by natural killer cells and making tumor cells more susceptible to killing. (4) cyclooxygenase-2 inhibitor NS-398; (5) EP4 antagonist MK2894 (6) transforming growth factor -β receptor (TGF-βR) inhibitor SB-431542; and (7) epigenetic inhibitors of T regulatory cells, EPZ004777 and FG-2216 (8) Sirtinol (a class III histone deacetylase inhibitor) prevent tumor induced immunosuppression and restore immunocompetent cells.

long been utilized in Ayurvedic medicine. We examined how the polysaccharide G1-4A, isolated from *Tinospora cordifolia*, affected the functional and phenotypic development of murine bone marrow derived dendritic cells (BMDC) and whether it may be used as an adjuvant in immunotherapy. G1-4A induced the maturation of dendritic cells, making them more immunogenic. These G1-4A treated DC in turn activated cytotoxic T cells that could destroy cancer cells. Administration of the tumor lysate pulsed G1-4A-treated DC reduced tumor burden in both therapeutic and preventative tumor challenge experiments in a mouse lymphoma model [1]. DCs also have cytotoxic ability against tumor cells in addition to their role as antigen presenting cells. We discovered that BMDC matured in the presence of G1-4A, [mBMDC (G1-4A)] killed tumor cells several times more effectively via a mechanism mediated by nitric oxide [2]. According to these results, G1-4A treated mBMDC matures and develops a killer phenotype and therefore may be a good nontoxic maturation agent for use in DC based immunotherapy. In BALB/c mice, immunomodulation with repeated doses of *T. cordifolia* polysaccharide-rich extract (PRE) and the purified polysaccharide G1-4A had comparable effects indicating that PRE can also be used as a viable immunotherapeutic adjuvant in place of G1-4A therapy [3].

Additionally, G1-4A treatment improved NK cell phenotypic and functional activation. NK cells were directly activated by G1-4A in (a) CD11c-depleted splenic cells and (b) purified NKp46^{+} cells. Co-culturing NK cells with bone marrow derived DC matured with G1-4A or splenic DC isolated from G1-4A-treated mice demonstrated DC crosstalk-mediated NK cell activation. In summary, G1-4A treatment has the potential to be employed as an immunotherapeutic drug [4] due to its varied effects on DCs and NK cells. Natural killer group 2, member D (NKG2D) is a receptor that is expressed on the surface of natural killer cells. When this receptor of NK cells interacts with the NKG2D ligand on tumor cells, it can result in tumor cell killing. We found that sulforaphane (SFN), a molecule obtained from broccoli, increased expression of these NKG2D ligands, hence boosting the sensitivity of tumors to NK cell-mediated death, highlighting the immunotherapeutic potential of SFN for application in cancer therapy [5].

Immunomodulators that relieve tumor induced immunosuppression

The relationship between tumor cells and the immune system is a significant factor affecting the cancer progression. Although many of the soluble molecules that mediate immunosuppression in the microenvironment are known, the mechanism by which the tumor affects the distal progenitors is not known. We discovered that the prostanoids produced by the tumor cells alter the development of the distal progenitor cells, by preventing the synthesis of transcription factor Zbtb46, which is specific to classical dendritic cell (cDC) lineage. The COX-2 inhibitor NS-398 reduced tumor induced phenotypic impairment of DC *in vitro*. Tumor-bearing mice treated with NS-398 developed immunocompetent DC and had lowered tumor burden. The conclusion that these effects were due to immunomodulation was reinforced by the lack of such an effect in immunodeficient SCID mice. These findings indicate that COX-2 inhibitors could be useful in cancer immunotherapy and that Zbtb46 expression is a marker of immunocompetent DC [6]. We also elucidated through in silico, *in vitro* and *in vivo* experiments that the PGE2 induced DC dysfunction was mediated through EP4/miR365/IL-6/pSTAT3 signaling. The treatment of mice with NS-398 or EP4 antagonist MK 2894 restored DC function and decreased tumor burden. This effect of EP4 antagonist was abrogated upon *in vivo* depletion of CD11c cells, indicating the crucial role of PGE2 signaling in DCs in tumor progression [7].

Developing immunotherapy methods for soft tissue sarcomas (STS) requires an understanding of the immunological milieu, which is relatively unknown. We demonstrated that the mouse fibrosarcoma evoked the development of B regulatory cells with CD19^{+}CD25^{+}PD-L1^{hi} phenotype that secreted TGF-β. These Bregs suppressed the proliferation of B-depleted T cells in a co-culture system. Treatment with SB431542, a small-molecule inhibitor of TGF-β receptor type I restored T cell responses. This T cell restoratory effect of SB431542 was observed in tumor bearing mice (TBM) along with considerable decrease in tumor burden. Our findings suggest that tumor-induced Breg suppresses immunity via a TGF-β mediated mechanism. Immunotherapy drugs targeting the Breg-Treg axis can thus have potential applications in soft tissue sarcomas [8].

The long-term stability of immunosuppressive regulatory T cells that plays a crucial role in immunological tolerance and homeostasis depends on epigenetic modifications. Identification of small-molecule modulators of Treg differentiation has several applications such as treatment of cancer, autoimmune diseases etc. To identify inhibitors that can potentially affect the generation of TGF-β1 induced T regulatory (iTreg) cells, we screened 160 compounds from an epigenetic chemical library. Two molecules, EPZ004777 and FG-2216 consistently reversed TGF-β1 iTregs without changing TGF-β downstream signaling in terms of (a) the development of naïve T cells into Treg cells, (b) the expression Foxp3 target genes, and (c) the suppressive function of Treg cells. We have thus identified the drugs EPZ004777 and FG-2216 as effective epigenetic modulators that reverse TGF-β1 induced T regulatory cells and could be used to treat a variety of immunological diseases [9]. Additionally, we demonstrated that another epigenetic drug, a class III histone deacetylase inhibitor sirtinol restored the immune microenvironment and inhibited epithelial mesenchymal transition and metastasis of 4T1 breast cancer [10].

Conclusion

The immune landscape of different malignancies might differ and even within a single malignancy, aside from inter-individual differences, it may evolve in tandem with cancer progression in a single individual. Immunotherapeutics, like molecular targeted therapies, must therefore be tailored to the tumor's immune infiltration and activation status. Therefore, immunomodulators which either activate immune cells or those that relieve tumor induced immunosuppression may be useful adjuvants in cancer treatment depending on the immune status of the cancer.

References

[1] V. K. Pandey, B. S. Shankar, K. B. Sainis, G1-4 A, an arabinogalactan polysaccharide isolated from Tinospora cordifolia increases dendritic cell immunogenicity in a murine lymphoma model, International Immunopharmacology, 2012, 14, 641–649.

[2] V. K. Pandey, P. J. Amin and B. S. Shankar, G1-4A, a polysaccharide from Tinospora cordifolia induces peroxynitrite dependent killer dendritic cell (KDC) phenotype, International Immunopharmacology, 2014, 23, 480–488.

[3] K. Premkumar, P. J. Amin, V. K. Pandey, P. Yadav and B. S. Shankar, Repeated dose treatment of Tinospora cordifolia polysaccharide rich extract activates splenic antigen presenting cells with no associated organ toxicity, Phytomed. Plus, 2021, 1, 100065.

[4] P. J. Amin and B. S. Shankar, Arabinogalactan G1-4A isolated from Tinospora cordifolia induces PKC/mTOR mediated direct activation of Natural Killer cells and through Dendritic Cell Cross-talk, BBA General Subjects, 2023, 1867, 130312.

[5] P. J. Amin and B. S. Shankar, Sulforaphane induces ROS mediated induction of NKG2D ligands in human cancer cell lines and enhances susceptibility to NK cell mediated lysis, Life Sciences, 2015, 126, 19–27.

[6] V. K. Pandey, P. J Amin and B. S. Shankar, COX-2 inhibitor prevents tumor induced down regulation of classical DC lineage specific transcription factor Zbtb46 resulting in immunocompetent DC and decreased tumor burden, Immunology Letters, 2017, 184, 23–33.

[7] V. K. Pandey, K. Premkumar, P. Kundu, B. S. Shankar, PGE2 induced miR365/IL-6/STAT3 signaling mediates dendritic cell dysfunction in cancer, Life Sci., 2024, 350, 122751.

[8] K. Premkumar and B. S. Shankar, TGF-βR inhibitor SB431542 restores immune suppression induced by regulatory B–T cell axis and decreases tumour burden in murine fibrosarcoma, Cancer Immunol Immunother., 2021, 70,153-168.

[9] K. Premkumar and B. S. Shankar, Identification of EPZ004777 and FG2216 as inhibitors of TGF-β1 induced Treg cells by screening a library of epigenetic compounds, Life Sciences, 2022, 301, 120643.

[10] S. Satam, N. Palekar, K. Premkumar, B.S. Shankar, Sirtinol, a SIRT1 inhibitor inhibits the EMT and metastasis of 4T1 breast cancer cells and impacts the tumor microenvironment, Immunopharmacology and Immunotoxicology, 2024, 46, 829-842.

पर्यावरण के रक्षा उपाय

17

स्फिंगोबियम प्रजाति आरएसएमएस द्वारा टीबीपी के जैव निम्नन : बृहत अध्ययन

श्याम सुंदर रंगू[1], **सचिन एन. हजारे**[2], **सौरव सरकार**[3], **संदीप भौमिक**[3], **चित्रा एस. मिश्रा**[1], **गार्गी बिंदल**[1,4], **के. के. सिंह**[3,4], **रीता मुखोपाध्याय**[1] **और देवाशिष रथ** [1,4]*

[1]अनुप्रयुक्त जिनोमिक अनुभाग, बायो-विज्ञान वर्ग, भाभा परमाणु अनुसंधान केंद्र, ट्रांबे-४०० ०८५, भारत
[2]खाद्य प्रौद्योगिकी प्रभाग, भाभा परमाणु अनुसंधान केंद्र, ट्रांबे-४०० ०८५, भारत
[3]रसायन इंजीनियरी प्रभाग, भाभा परमाणु अनुसंधान केंद्र, ट्रांबे-४०० ०८५, भारत
[4]होमी भाभा राष्ट्रीय संस्थान, अणुशक्तिनगर, मुंबई-४०० ०९४, भारत

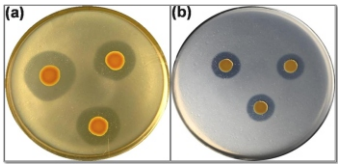

(a) आर. एस. एम. एस. उपभेद द्वारा टी. बी. पी. का क्षरण। जीवाणु संवर्धन (ए) लूरिया बर्टानी अगर माध्यम और (b) एमएमएम अगर प्लेटों पर देखा गया, जो 10 एम. एम. टी. बी. पी. के साथ पूरक थे। निकासी का क्षेत्र ऊष्मायन के 1 सप्ताह के बाद दर्ज किया गया था।

सारांश

कुछ औद्योगिक प्रक्रम बड़ी मात्रा में टीबीपी युक्त अपशिष्ट उत्पन्न करते हैं। टीबीपी के अंतग्रर्हण से समुद्री जीवन और जानवरों में विषाक्तता पैदा होती है। इससे पहले, स्फिंगोबियम प्रजाति आरएसएमएस (आरएसएमएस), भापअकें में आरएसएमएस साइट से विलगित किए गए एक जीवाणु को प्रयोगशाला पैमाने (3 दिनों में 30 mM) पर टीबीपी को प्रभावी रूप से निम्नन करते हुए दिखाया गया। आरएसएमएस स्ट्रेन का उपयोग करके टीबीपी जैवनिम्नन के चरण-वार पैमाने के लिए प्रक्रम विकसित किए गए। 30L पैमाने पर, इष्टतमीकृत परिस्थितियों में, लगभग पूर्ण खनिजीकरण (3 दिनों में 28 mM) प्राप्त किया गया। कम्प्यूटेशनल फ्लूइड डायनामिक्स मॉडलिंग का उपयोग 205L तक के पैमाने के लिए प्रचालन मापदंडों के इष्टतम मानों की पहचान करने के लिए किया गया और 21 mM एमटीबीपी निम्नन 15 दिनों में प्राप्त किया गया जो प्रयोगशाला पैमाने पर देखे गए टीबीपी जैवनिम्नन का लगभग 70% है। ये प्रक्रम टीबीपी जैवनिम्नन के लिए रिपोर्ट किए गए सबसे प्रभावी स्केल अप प्रक्रम हैं।

Safeguarding Environment

17

Biodegradation of TBP by *Sphingobium* sp. RSMS: Scale up Studies

Shyam Sunder Rangu[1], **Sachin N. Hajare**[2], **Sourav Sarkar**[3], **Sandip Bhowmick**[3], **Chitra S. Misra**[1], **Gargi Bindal**[1,4], **K. K. Singh**[3,4], **Rita Mukhopadhyaya**[1] **and Devashish Rath**[1,4]*

[1]Applied Genomic Section, Bio-Science Group, Bhabha Atomic Research Centre, Trombay-400085, INDIA
[2]Food Technology Division, Bhabha Atomic Research Centre, Trombay-400085, INDIA
[3]Chemical Engineering Division, Bhabha Atomic Research Centre, Trombay-400085, INDIA
[4]Homi Bhabha National Institute, Anushakti Nagar, Mumbai-400094, INDIA

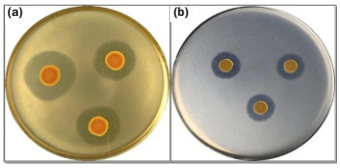

(a) TBP degradation by RSMS strain. Bacterial culture was spotted on (a) Luria Bertani Agar medium and (b) MMM agar plates, supplemented with 10 mM TBP. The zone of clearance was recorded after 1 week of incubation

ABSTRACT

Certain industrial processes generate large volume of TBP-containing wastes. TBP causes toxicity to marine life and to animals upon ingestion. Previously, *Sphingobium* sp. RSMS (RSMS), a bacterium isolated from RSMS site BARC was shown to degrade TBP efficiently at laboratory scale (30 mM in 3 days). Processes for the step-wise scale-up of TBP biodegradation utilizing the RSMS strain were developed. At 30 L scale, under optimised conditions, near complete mineralisation (28 mM in 3 days) was achieved. Computational fluid dynamics modelling was used to identify the optimum values of operating parameters for scale-up to 205 L and 21 mM TBP degradation was achieved over 15 days, which is approximately 70% of the TBP biodegradation observed at laboratory scale. These processes are the most efficient scale up processes reported for TBP biodegradation.

KEYWORDS: *Tributyl phosphate (TBP), Sphingobium sp. RSMS, Biodegradation, Scale up*

*Authors for Correspondence: Devashish Rath
E-mail: devrath@barc.gov.in

Introduction

Tributyl phosphate (TBP), is an organophosphorus compound which finds applications in various industries as a solvent, complexing agent, plasticizer, herbicide, fungicide, defoamer etc. [1]. TBP is also used as an extractant for recovery of radionuclides from nuclear wastes. TBP finds its way into the environment by leakage from production or usage sites, and leaching from TBP containing waste disposed in landfill sites or aquatic environments [2]. Unaffected by natural photolysis and hydrolysis, TBP is known to be very stable in soil and water. Persistence of untreated TBP in natural environment can cause environmental pollution. Even at low concentration of 4.2-18 mg l^{-1}, TBP can present acute toxicity hazard to organisms in freshwater [3]. In humans, penetration of TBP causes irritation of skin and mucous membranes. Animal studies have also shown toxic effects of TBP [4].

Chemical degradation, incineration or immobilisation methods have been considered for treatment and disposal of TBP bearing radioactive wastes [5]. The conventional physico-chemical processes prove uneconomical when TBP concentrations are low and high volumes of waste are encountered [6]. Moreover, these methods either do not completely destroy the compound or merely convert it to other form of contaminant(s) thereby causing secondary pollution. In such scenario microbial degradation of TBP is considered feasible alternative for detoxification. Unlike traditional methods, microbial degradation is relatively simple not requiring harsh or complex conditions.

A TBP degrading bacterial strain was isolated from the TBP storage tanks at RSMS site, BARC and after identification and characterization named as *Sphingobium* sp. RSMS (RSMS Strain) [7]. Here we discuss the TBP degradation efficiency of RSMS strain and development of processes for scale up of TBP degradation from laboratory scale to 30 L and further to 205 L volumes.

Media, Growth Conditions and Measurement of TBP Degradation

Sphingobium sp. RSMS strain (RSMS strain) was grown either in Luria-Bertani medium (LB) or modified mineral medium (MMM) supplemented with 25-100 mM 3-(N-Morpholino)-propanesulfonic acid (MOPS) as a buffer [7]. The cultures were grown with aeration (160 rpm) at 30°C. For TBP degradation experiments, glucose and phosphate source was omitted and TBP was used as the sole source of carbon and phosphorous. The TBP is partially soluble in the aqueous media. The TBP concentrations mentioned in this article are equivalent concentrations when dissolved. The final product of TBP biodegradation, inorganic phosphate (Pi), was monitored by phosphomolybdic acid method for estimating TBP degradation as per published protocol [7,8]. For growth measurement, 20 ml to 40 ml of culture was centrifuged at 5000 rpm (4470 x g) for 10 min, washed twice with equal volume of MMM and the pellet was resuspended in equal volume of MMM. Cell density was measured at 600 nm using a spectrophotometer.

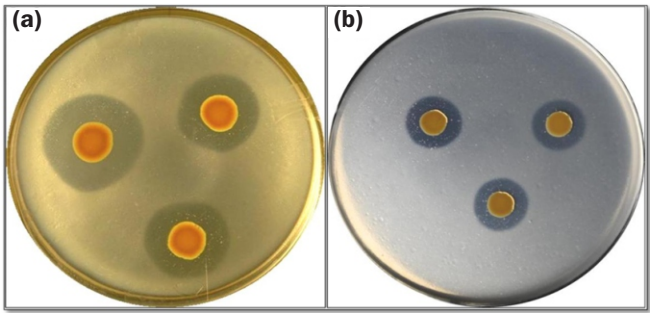

Fig.1: TBP degradation by RSMS strain. Bacterial culture was spotted on (a) Luria Bertani Agar medium and (b) MMM agar plates, supplemented with 10 mM TBP. The zone of clearance was recorded after 1 week of incubation (Source: Rangu SS et al., 2014. Fig.1).

Results and Discussion

Ideally a TBP degrading microorganism should mineralise TBP by using it as the sole source of carbon and phosphorus and degrade high amounts of TBP. As compared to mixed cultures where relative fitness of microbes and growth dynamics make scale up complex, having a pure isolate can simplify the process. The microbes or consortia reported in literature are unlikely to have any practical application as they could degrade only 1-3 mM TBP. [1,9]. In this context *Sphingobium* sp. RSMS a bacterium isolated from storage tanks at RSMS site BARC was evaluated for its TBP degrading potential.

Degradation of TBP by RSMS Strain in Solid and Liquid Medium

RSMS strain was shown to degrade 10 mM TBP on solid medium as evident from the zone of clearance around the grown spot (Fig.1). In liquid medium RSMS strain could degrade 30 mM TBP in 3 days. The strain utilized TBP as sole source of carbon and phosphorous for its own growth. TBP at 10 to 400 µM concentration is known to inhibit cell division in most bacteria. In contrast, the RSMS strain was demonstrated to tolerate ~100 mM TBP when supplemented in solid LB agar media.

TBP Degradation at 30 L Scale

Survey of literature shows very few processes developed for the bio-degradation of TBP. A process reported by Nancharaiah et al., 2015, could degrade 2 mM TBP in 5 h [9]. Two process patents (USA) filed, show 0.6-0.7 mM TBP degradation in 10-30 days using *Acinetobacter* sp. ATCC 55587 while a non-sulphur purple photosynthetic bacterium degraded around 1.6 mM TBP in 3 weeks [10, 11]. As RSMS strain showed excellent TBP degradation at lab-scale, we attempted to develop processes at larger scales using this strain. For scale up of TBP degradation to 30 litres, a fermenter (SU1) made of a stainless-steel vessel with height-to-diameter ratio of 3.2 and with multiple ports on the top was used (Fig. 3). It had an agitator shaft connected to a top driven motor (0.75 hp) and fitted with 3 six-bladed Rushton turbine impellers. Different probes were inserted into the vessel for monitoring pH, DO (dissolved oxygen) and temperature. SU1 fermenter was always maintained in sterile conditions. 400 ml of overnight grown RSMS culture was added to the SU1

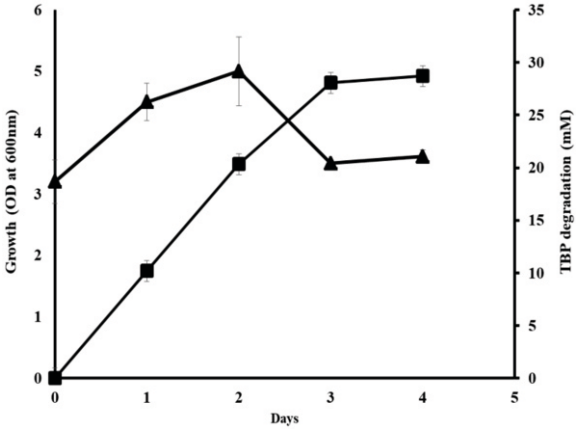

Fig.2: TBP degradation by RSMS strain at 30 litre scale. The growth (▲) in terms of cell density (OD_{600nm}) and degradation of TBP (■) in terms of Pi release is depicted. (Source: Rangu et al., 2022. Fig. 2).

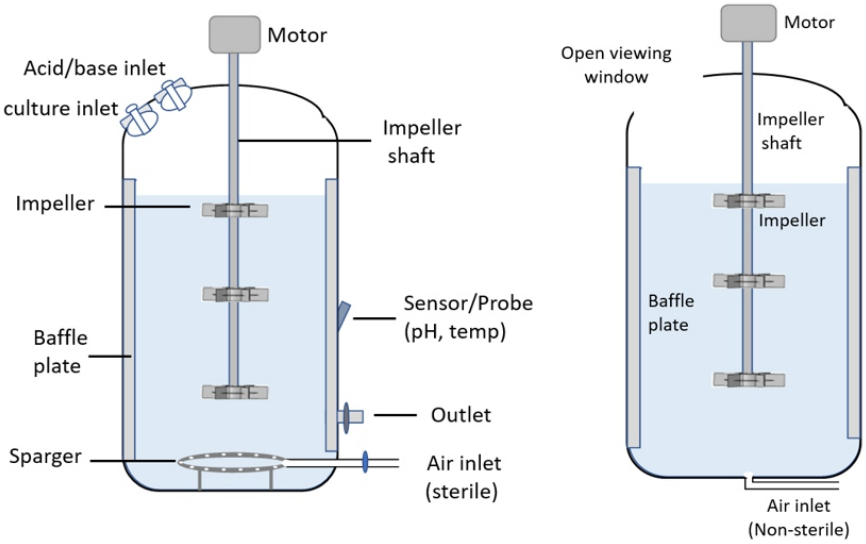

Fig.3: Pictorial depiction of 30 L fermenter (SU1) and 205 L (SU2) fermenter used in the study. (Source: Rangu et al., 2022. Modified Fig. 1).

Table 1: Various parameters of 30 mM TBP degradation at 30 litre scale.

Days	Description	Dissolved oxygen (%)	RPM	Adjusted pH	TBP degradation (mM)	Growth (OD_{600nm})
-1	Inoculation	100	200	7.5 (±) 0.1	NA	0.06 (±) 0.01
0	TBP added	100	150	7.5 (±) 0.1	Nil	3.2 (±) 0.35
1	Day 1 for TBP degradation	100	150	7.5 (±) 0.1	10.2 (±) 0.3	4.5 (±) 0.30
2	Day 2 for TBP degradation	100	150	7.5 (±) 0.1	20.3 (±) 0.8	5.0 (±) 0.56
3	Day 3 for TBP degradation	100	150	7.5 (±) 0.1	28 (±) 0.45	3.5 (±) 0.05
4	Day 4 for TBP degradation	100	150	ND	28.7 (±) 0.2	3.61 (±) 0.11

fermenter containing 30 litres of sterile MMM supplemented with 0.5 % glucose and 2 mM inorganic phosphate using a peristaltic pump. Following conditions were maintained for 20 h of growth period- Agitator speed: 200 rpm; Fermenter temperature: 30^{0}C; Dissolved oxygen: 100 %; Aeration: 10 L min^{-1}. After 20 h of growth, TBP was added to a final concentration of 10, 20 or 30 mM. The growth was continued with a reduced agitator speed of 150 rpm. The pH of the culture was monitored and adjusted to about 7-7.5, if required, by adding NaOH.

The almost complete degradation of 10 mM and 20 mM of TBP was achieved in 30 and 54 hours respectively. In case of 30 mM TBP, a steady rate of TBP degradation was observed over a period of 3 days. After 3 days, ~28 mM of TBP was degraded, which was ~93 % of that seen at laboratory scale. No further degradation of TBP (Fig. 2) was observed. The RSMS strain showed growth as a function of TBP degradation, suggesting utilization of TBP as the source of carbon. Table 1 summarizes the progress of TBP degradation as well as the various parameters used in the standardised experiment. During the growth, a decrease in the pH of the medium to 6.0-6.5 was observed. The pH was adjusted to 7-7.5 by addition of NaOH. The reduction in pH could be attributed to the release of Pi due to TBP degradation.

TBP Degradation at 205 L Scale

After successful scale up at 30 litre, further scale up of the process to 205 litre volume was carried out in a fermenter vessel (SU2) with 1 m height and 0.6 m diameter (Fig. 3). It had three impellers mounted on a single shaft. Agitator shaft was fitted with 3 six-bladed Rushton turbine impellers and connected to a top driven motor. SU2 fermenter had a single open window at the top for the addition of inoculum and reagents. Air was injected from the bottom at the centre of the fermenter. In SU2 probes were not available for monitoring pH, DO, temperate or pressure. To achieve proper mixing, the impeller tip speed was kept the same as in 30 litre reactor. Changes in the fluid dynamics are an important consideration as a process is scaled up. To determine the optimum operating parameters to rule out non-idealities and to visualise the flow patterns, computational fluid dynamics (CFD) modelling of the process was carried out. The cut-section of the computational domain used in CFD simulations, typical spatial variation of velocity magnitude and the velocity vectors in a vertical central plane and the path lines of the liquid in the stirred tank are shown in Fig.4.

Freshly grown overnight culture (900 ml) was added to SU1 fermenter containing 25 litres of sterile MMM supplemented with 5 mM Pi and 1 % glucose. For this initial culture build up, the conditions maintained were identical to the 30-litre experiment. After 20 h of growth, 25 litres of the culture was inoculated into SU2 fermenter containing 180 litres of non-sterile MMM supplemented with 30 mM TBP and glucose. The following conditions were maintained during the experiment (Agitator speed: variable between 44 rpm to 80 rpm; aeration: 26 Nl min^{-1}, non-sterile). The process was

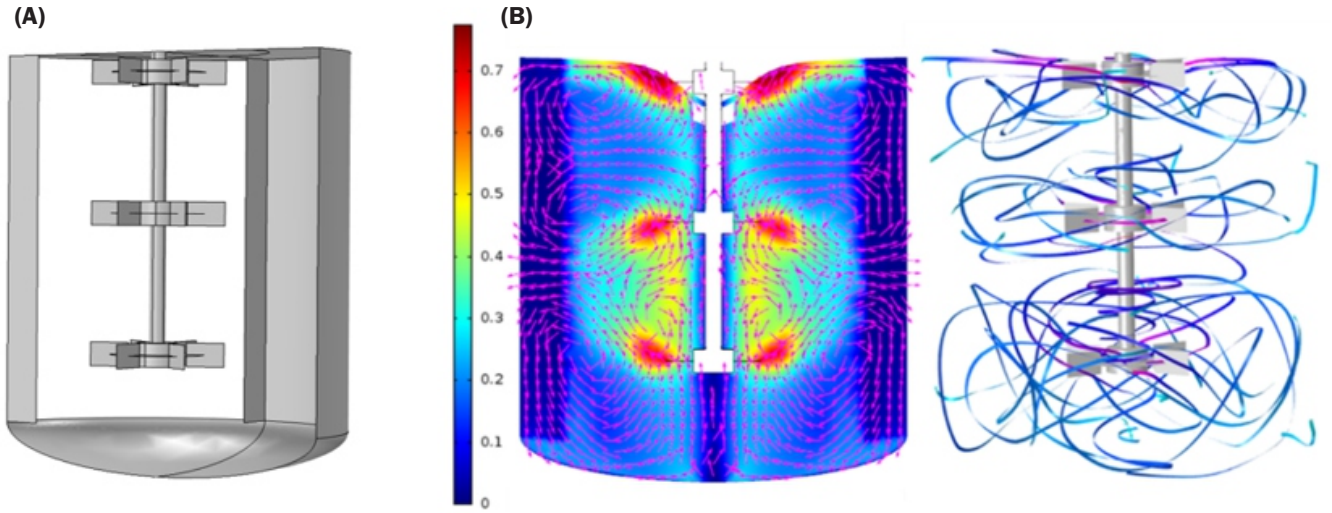

Fig.4: CFD simulation at 205 litre scale. A cut-section of the computational domain representing 205 litre stirred reactor used for CFD simulations (A). Spatial variations of velocity magnitude, velocity vectors in a vertical central plane, path lines of the liquid in 205 litre stirred tank (B). (Source: Rangu et al., 2022. Modified Fig. 2).

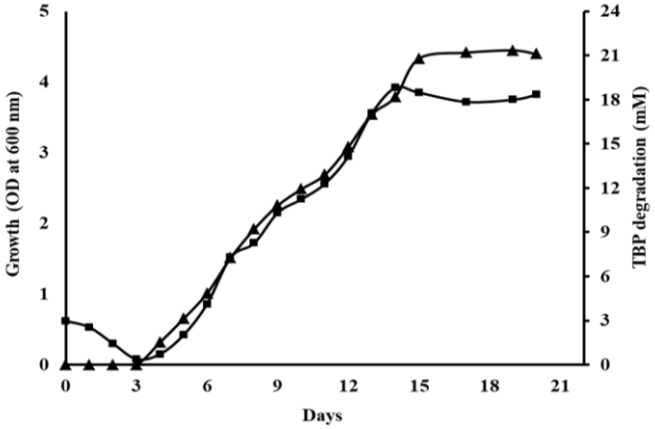

Fig.5: TBP degradation by RSMS strain at 205 litre scale. MMM supplemented with 30 mM TBP was used as medium. TBP degradation (▲) was estimated by measuring Pi by phosphomolybdate method. The culture density (■) was measured spectrophotometrically at 600 nm (OD_{600nm}). (Source: Rangu et al., 2022. Fig. 4).

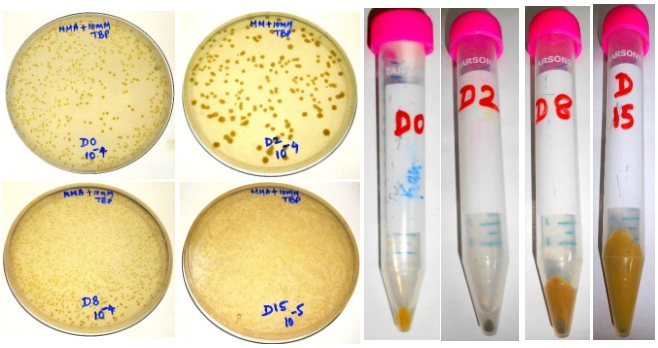

Fig.6: Growth of the Sphingobium sp. RSMS in 205 L tank. Left panel: The colony forming units (cfu count) on Day 0, 2, 8 and 15 respectively. Right panel: A fixed volume of culture was taken from SU2 tank and centrifuged to obtain the cell pellet.

carried out at ambient temperature (24 to 27°C) under non-sterile conditions. TBP degradation (as Pi release), growth of the culture (OD_{600nm}), temperature and pH were monitored over a period of 20 days. The pH of the culture was adjusted to 7-7.5 by adding NaOH as necessary. Earlier attempt to achieve the optimum cell density (OD_{600nm} ~3) by supplementing MMM with glucose led to the contamination of the batch. As glucose is a preferred carbon source for other microbes, non-sterile conditions used would allow their growth. Some of the contaminants were isolated and identified by 16S rDNA gene sequencing (Table 2). Subsequently the process was run without glucose supplementation in SU2.

In SU2 containing medium supplemented with only TBP the degradation could be observed from 4th day onwards at a steady rate up to 15th day. No increase in Pi levels was observed after the 15th day. Between 4th to 15th day, an average TBP degradation of ~1.68 mM/day was measured. Over 15 days, a total of 21 mM TBP degradation was achieved, which was approximately 70 % of the TBP degradation observed at laboratory scale. The period of the active growth of the culture coincided with the degradation of TBP (Fig. 5).

Increase in accumulation of bacterial mass during the course of the experiment is shown in Fig. 5 & 6. A decrease in pH each day from the fourth day onwards was observed and this correlated with the release of Pi (Table 3). The pH of the culture was maintained at 7-7.5 by adding NaOH. Details of the conditions and parameters during the course of the experiment is presented in Table 3.

As the 205-litre batch process was carried out under non-sterile conditions and without regulation of the temperature, it made the process less energy intensive and hence more economical. In future, utilization of environmental waste or industrial waste to generate biomass of RSMS strain, can be explored to further economise the process. Recently, we have assembled the complete genome sequence of this bacterium [12] which will aid in identifying the genetic pathway of TBP bio-degradation and in turn may open up the possibility of

Table 2: Contaminant strains identified in the 205 tank when glucose was added along with TBP.

Strain No.	Strain identified	Percent identity
1	*Paenibacillus* sp. strain	99
2	*Paenibacillus xylanilyticus* strain	93
3	Uncultured bacterium clone 069088	92
4	*Pseudomonas* sp. strain RP4	98
5	Uncultured gamma proteobacterium	83
6	Not identified	No significant identity

Table 3: Various parameters of TBP degradation at 205 litre scale.

Days	Observed pH	Aeration	Observed Temperature	TBP degradation (Pi released mM)	Culture density (OD_{600nm})
		Nl min^{-1}	(^oC)		
0	7.22	26	24	0	0.62
1	6.93	26	24	0	0.53
2	7.2	26	24.5	0	0.3
3	7.3	26	23.5	0	0.08
4	7	26	26.5	1.52	0.15
5	6.89	26	26.5	3.12	0.42
6	6.6	26	26.5	4.85	0.86
7	6.4	26	25	7.25	1.52
8	5.8	26	25	9.21	1.72
9	6.9	26	25.5	10.81	2.15
10	6.9	26	26	11.92	2.34
11	6.9	26	26	12.9	2.56
12	6.9	26	25	14.8	2.95
13	6.6	26	25.5	17	3.56
14	6.68	26	27	18.2	3.92
15	6.63	26	26.5	20.8	3.85
17	6.61	26	26	21.2	3.72
20	6.6	26	26	21.1	3.82

metabolic engineering of the strain to further enhance its TBP biodegradation efficiency.

Conclusion

TBP biodegradation processes reported earlier were inefficient (degradation of 1-3 mM TBP). *Sphingobium* sp. RSMS, a bacterium isolated from RSMS site BARC, showed efficient degradation of TBP at lab scale (30 mM in 3 days). A 30 L scale-up process was developed and optimised to achieve 28 mM TBP degradation in 3 days. Further scale-up to 205 L volume was done and a more economic process was developed. These processes are much more efficient than the patented processes for TBP biodegradation.

Acknowledgment

The authors thank Dr. H. S. Misra, Dr. S. Mukhopadhyay and Mr. K. T. Shenoy for their help and guidance. The authors thank the scientific, technical and non-technical staff of Molecular Biology Division, BARC, Chemical Engineering Division, BARC and Process Development Laboratory, BARC for their help during the experiment. The authors thank Shaikh M. I. for the technical help in conduct of experiments.

References

[1] Ahire, K. C., Kapadnis, B. P., Kulkarni, G. J., Shouche, Y. S., Deopurkar, R. L. "Biodegradation of tributyl phosphate by novel bacteria isolated from enrichment cultures". Biodegradation, 2012, 23, 165-176.

[2] Fries, E., Puttmann, W. "Occurrence of organophosphate esters in surface water and ground water in Germany". J Environ Monit., 2001, 3(6),621-626.

[3] Lin, K. "Joint acute toxicity of tributyl phosphate and triphenyl phosphate to *Daphnia magna*". Environmental Chemistry Letters, 2009, 7, 309-312.

[4] Berdasco, N. A. M., McCready, D. "Risk Assessment and Class-Based Evaluation of Three Phosphate Esters. Human and Ecological Risk Assessment".An International Journal, 2011, 17, 367-380.

[5] Anon. 1992. Treatment and conditioning of radioactive organic liquids. IAEA, Vienna, Austria. http://whqlibdoc.who.int/ehc/WHO_EHC_112_eng.Pdf

[6] Chaudhari, T. D., Melo, J. S., Fulekar, M. H., D'Souza, S. F. "Tributyl phosphate degradation in batch and continuous processes using *Pseudomonas pseudoalcaligenes* MHF ENV". International Biodeterioration & Biodegradation, 2012, 74, 87-92.

[7] Rangu, SS., Muralidharan, B., Tripathi, S. C., Apte, S. "Tributyl phosphate biodegradation to butanol and phosphate and utilization by a novel bacterial isolate, *Sphingobium* sp. strain RSMS". Applied Microbiology and Biotechnology, 2014, 98, 2289-2296.

[8] Ames, B. N. "Assay of inorganic phosphate, total phosphate and phosphatases". in: Elizabeth F. Neufeld, V. G. (Ed.), Methods in Enzymology, Academic Press 1966, 115-118.

[9] Nancharaiah, Y. V., Reddy, G. K. K., Mohan, T. V. K., Venugopalan, V. P. "Biodegradation of tributyl phosphate, an organosphate triester, by aerobic granular biofilms". Journal of hazardous materials, 2015, 283, 705-711.

[10] Stoner, D. L., Tien, A. J. "Method and compositions for the degradation of tributyl phosphate in chemical waste mixtures". United States Patent, 19955, Patent. No. US5453375A.

[11] Garcia, D., Berne, C. "Method of degrading TBP using a photosynthetic bacterial strain". United States Patent, 2015, Patent. No. US9029127 B2.

[12] Rangu, S. S., Beck, A., Sharda, M., Mukhopadhyaya, R., et al. "Whole-Genome Sequencing of *Sphingobium* sp. Strain RSMS, a Highly Efficient Tributyl Phosphate-Degrading Bacterium". Microbiology resource announcements, 2020, 9, e00600-00620.

‘गथुवान’ चावल का प्रतिरक्षात्मक गुणधर्म

18

भारतीय स्वदेशी चावल ‘गथुवान’ के प्रतिरक्षा-संशोधक गुणधर्मों का लक्षण-निर्धारण और उसका कृषि-विज्ञान सुधार

अंजलि चौहान [1,3], **राहुल चेकर** [2,3]*, **दीपक शर्मा** [2,3], **दीपक शर्मा और बी.के. दास** [1,3]*

[1]नाभिकीय कृषि एवं जैव प्रौद्योगिकी प्रभाग ,भाभा परमाणु अनुसंधान केंद्र ,ट्रांबे-400085, भारत
[2]विकिरण जीवविज्ञान और स्वास्थ्य विज्ञान प्रभाग, भाभा परमाणु अनुसंधान केंद्र, ट्रांबे-400085, भारत
[3]होमी भाभा राष्ट्रीय संस्थान, अणुशक्ति नगर, मुंबई-400094, भारत
[4]आनुवंशिकी एवं पादप प्रजनन विभाग, इंदिरा गांधी कृषि विश्वविद्यालय, रायपुर-492012, छत्तीसगढ़, भारत

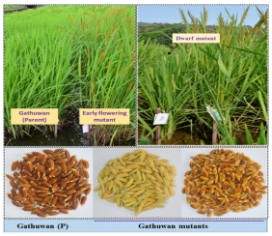

गथुवान की कृषि विशेषता में सुधार के लिए उत्परिवर्तन प्रजनन।

सारांश

स्वास्थ्य और रोगों के प्रबंधन में वर्तमान और संभावित चुनौतियों के वैश्विक परिदृश्य के कारण पौधों के खाद्य भागों में आनुवंशिक विविधता की खोज और उपयोग की आवश्यकता है। चावल की फसल विशिष्ट परिस्थितियों में उनके विकास के परिणामस्वरूप अनाज आकृति विज्ञान और संरचना की एक विशाल विविधता प्रदान करती है। छत्तीसगढ़ का एक देशी चावल, गथुवान, स्थानीय रूप से संधिशोथ के प्रबंधन के लिए उपयोगी रहा है। हालांकि, वैज्ञानिक आधार की कमी और सीमित कृषि विशेषताओं ने इसकी खेती को सीमित कर दिया है और इस पारंपरिक चावल का मूल्य अभी भी अज्ञात है। अध्ययन का उद्देश्य मानव स्वास्थ्य में अपनी कार्यात्मक भूमिकाओं को स्थापित करना और ऐसे आनुवंशिक संसाधनों के मूल्यांकन और संरक्षण की दिशा में एक दृष्टिकोण के रूप में इसके कृषि संबंधी लक्षणों में सुधार करना है।

Immunomodulatory Property of ‘Gathuwan’ Rice

18

Characterization of Immune-modulatory Properties of an Indian Indigenous Rice ‘Gathuwan’ and its Agronomic Improvement

Anjali Chauhan[1,3], **Rahul Checker**[2,3]*, **Deepak Sharma**[2,3], **Deepak Sharma**[4] **and B. K. Das**[1,3]*

[1]Nuclear Agriculture & Biotechnology Division, Bhabha Atomic Research Centre, Trombay-400085, INDIA
[2]Radiation Biology & Health Sciences Division, Bhabha Atomic Research Centre, Trombay-400085, INDIA
[3]Homi Bhabha National Institute, Anushakti Nagar, Mumbai-400094, INDIA
[4]Department of Genetics and Plant Breeding, Indira Gandhi Krishi Vishwavidyalaya, Raipur-492012, Chhattisgarh, INDIA

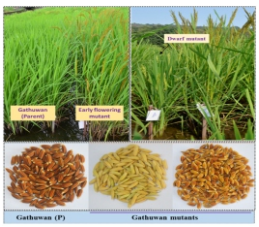

Mutation breeding for agronomic trait improvement of Gathuwan

ABSTRACT

The global scenario of current and potential challenges in the management of health and diseases necessitates exploration and utilization of genetic diversity in edible parts of plants. Rice crop offers a vast diversity of grain morphology and composition resulting from their evolution in specific conditions. Gathuwan, a native rice of Chhattisgarh, has locally been useful for the management of rheumatic arthritis. However, lack of scientific base and limiting agronomic traits have confined its cultivation and the value of this traditional rice remains unrecognized. The study aims to establish its functional roles in human health and improve its agronomic traits, as an approach towards valuation and conservation of such genetic resources.

KEYWORDS: *Immune-suppressive, Traditional rice, Gathuwan, Mutation breeding, Metabolomics*

*Authors for Correspondence: Rahul Checker & B. K. Das
E-mail: rchecker@barc.gov.in & bkdas@barc.gov.in

Introduction

The global challenges posed by increased burden of non-communicable diseases, limitations associated with the treatment of several disorders and sudden emergence of novel health threats have accelerated the adoption of 'food as medicine'. Rice is a major food crop with abundant diversity in plant and grain characters and hence, grown and consumed over wide geographical dimensions. Diversity in rice forms suiting different purposes has also been acknowledged in traditional medicine systems, including Indian *Ayurveda*. These traditional rice landraces/ farmers' varieties have acquired the specialty as a result of evolution over a long period of time in particular agroclimatic conditions. They constitute enriched genetic resources for bio-active compounds, which help in achieving better state of health and genes for resistance to biotic and abiotic stresses, thereby, serving as valuable assets in breeding programmes. However, lack of adequate scientific data supporting their biological effects has been a major limitation in the wider recognition of their values. Also, their non-sustenance in present times, is a result of inferior yield related traits. Scientific validation of their functional roles in human health, along with subtle changes leading to improved agronomic traits, is an effective approach to address both these concerns. Gathuwan, an indigenous rice variety native to Chhattisgarh, is characterized by purple pigmentation in culm, leaf margins and reddish colour husk of bold type grains. This local landrace of rice has been considered to be effective in treating rheumatism (गठिया in Hindi). However, its tall stature, spreading plant type, high tendency to lodge at maturity and long maturity duration, makes it agronomically undesirable. Hence, these limiting traits needed to be improved along with a thorough evaluation of its medicinal property.

Materials and Methods

80% Methanolic Gathuwan brown rice extract (BRE) was used for functional studies and metabolomics.

A. Murine splenic lymphocytes were used for in vitro studies. Lymphocyte activation was studied using fluorescently labelled antibodies, proliferation was studied by CFSE dye dilution method and cytokine levels were estimated using ELISA.

B. For Graft versus host disease (GvHD) induction, immunocompromised Balb/c mice were injected with lymphocytes from C57BL/6 mice. The donor cells were treated with BRE for one group of GvHD mice. A subset of each GvHD group were fed with brown rice on alternate days.

C. Nrf2 nuclear localization was studied using FITC labelled anti-Nrf2 antibody and nuclear staining using Hoechst dye.

D. Metabolomics data was obtained using Ultra-high performance liquid chromatography-tandem mass spectrometry (UHPLC-MS/MS) and analysed using Metaboanalyst 5.0.

E. Gathuwan paddy was mutagenised using 250 Gy gamma rays, with an objective to identify mutants with improved plant stature/maturity duration.

Results and Discussion

Rheumatoid arthritis (RA) is an autoimmune disorder, which renders body susceptible to attack by its own immune system. Self-reactive activated T cells infiltrate into the synovial fluid around the joints and activate macrophages/fibroblasts, turning them into tissue destroying effector cells[1]. The cascade of events includes activation of T cells by self-antigens presented by DCs, clonal expansion and pro-inflammatory cytokine secretion. The current treatment options suffer limitations such as variable responses among patients, drug resistance, side effects of long-term administration and thus, necessitating the use of safer alternatives with more uniform outcomes.

Immune-suppressive effects of BRE on T cell proliferation and functions

Gathuwan BRE decreased mitogen induced proliferation of T -cells (Fig.1) and prevented secretion of IL-2, IL-4, IL-6 and IFN-γ cytokines in a dose-dependent manner, and without imposing any significant cytotoxicity.

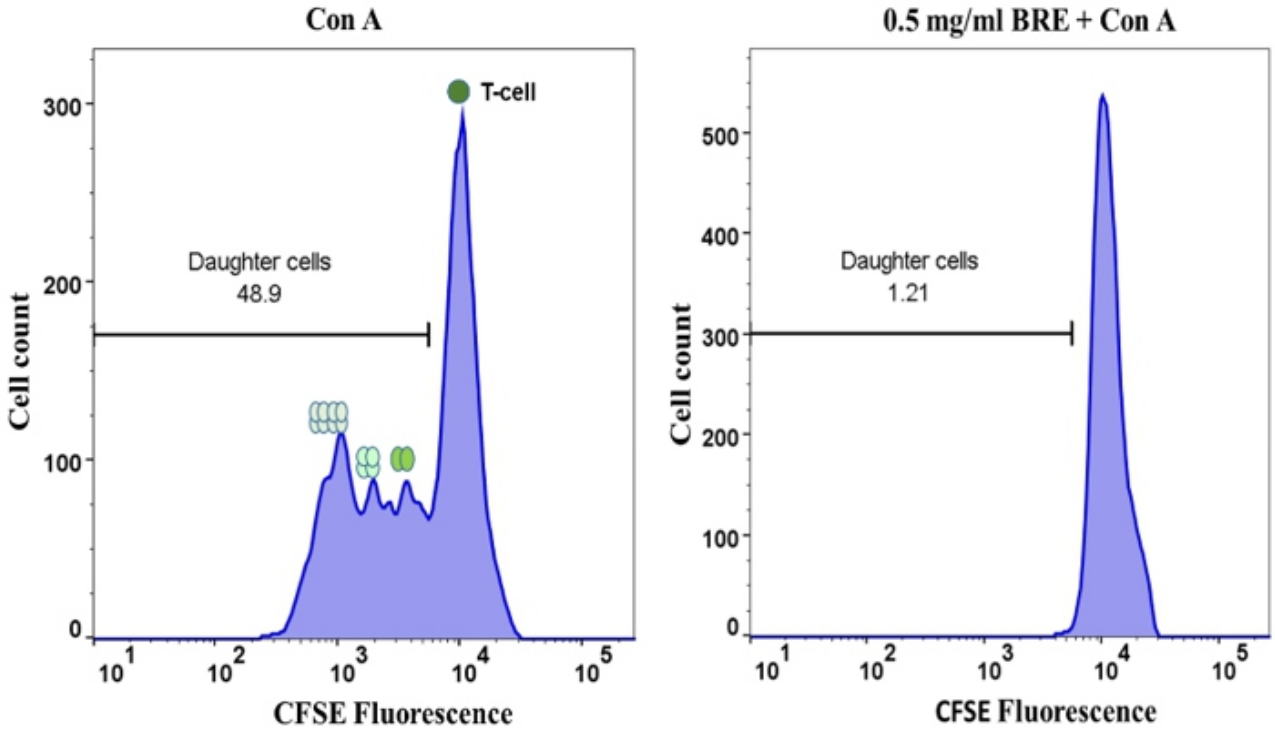

Fig.1: Effects of Gathuwan BRE on lymphocyte proliferation.

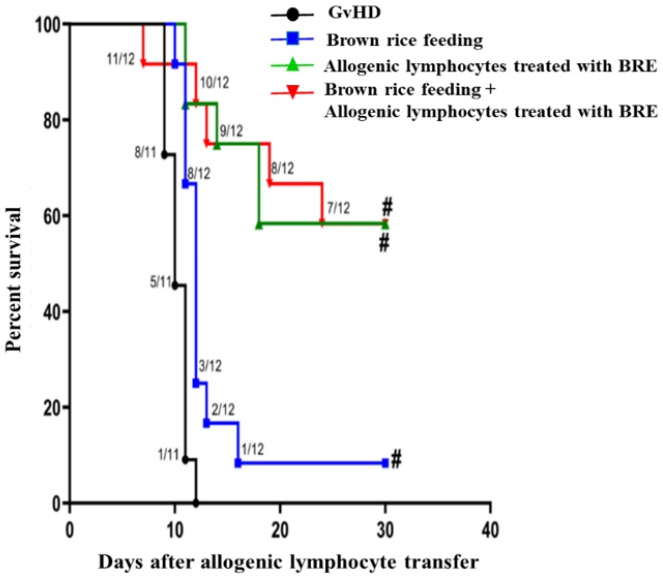

Fig.2: Effects of Gathuwan BRE on mortality in GvHD mice.

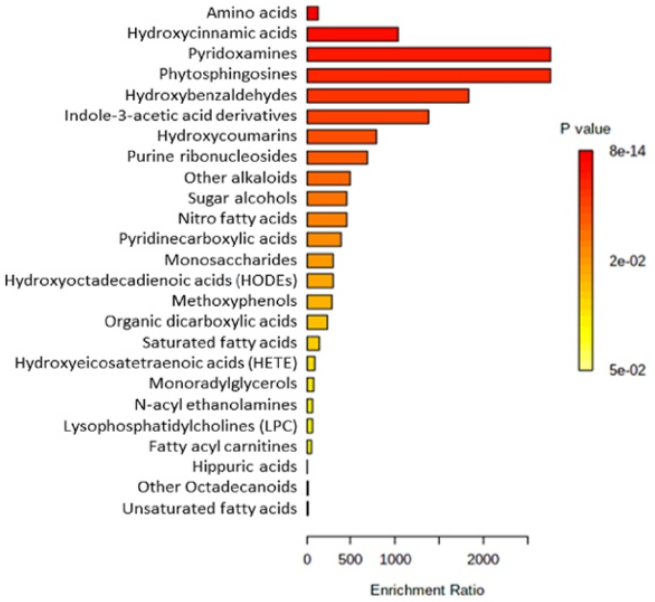

Fig.4: Nrf2 nuclear translocation induced by BRE.

In vivo activity of Gathuwan BRE

GvHDmice model represents a suitable method for in vivo assessment of immune-suppressive potential towards allograft mediated immune attack. Immunocompromised mice, when grafted with donor T-cells treated with Gathuwan BRE, showed reduced mortality compared to mice receiving untreated T cells (Fig.2).

Gathuwan BRE exerts its effects through Nrf2 signalling pathway

Nrf2 signalling pathway is a critical regulator of cellular redox homeostasis and inflammatory responses. [2].Nuclear translocation of Nrf2 and expression of Nrf2 dependent genes was found enhanced in treated lymphocytes (Fig.3). Nrf-2 dependence of the effects were further confirmed in Nrf2 knockout mice.

Metabolomic foundation of Gathuwan brown rice activity

Metabolic features determines the function of grain or other plant parts. Ultra-high performance liquid chromatography-tandem mass spectrometry (UHPLC-MS/MS) data of Gathuwan brown rice featured abundance of pryridoxamines, phytosphingosines, benzofurans, cyclic ketones and hydroxycinnamic acids (Fig.4). Among the many compounds that are reported to exhibit immune-modulatory or redox altering properties, more than half are known to affect Nrf2 signalling pathway[3].

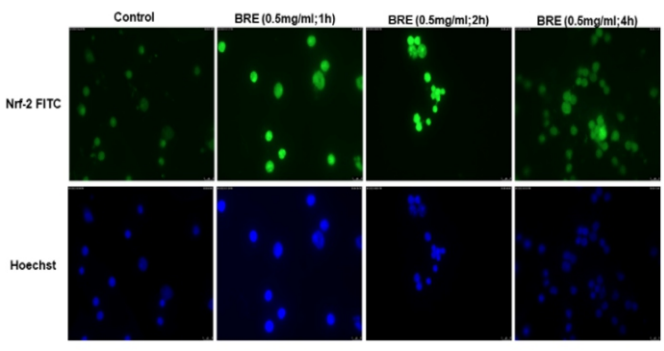

Fig.3: Nrf2 nuclear translocation induced by BRE.

Mutation breeding for improvement of plant stature and/maturity duration

Mutation breeding is a highly sought technique, in present times, to introduce novel mutations or improve few delimiting traits in otherwise highly useful genetic backgrounds. The Gathuwan parent plant attains 140-160 cm height and flowers in 130-140 days. M2 generation of Gathuwan was screened and mutants with either reduced plant height (<110 cm) and/or early maturity (20-25 days earlier than parent) were isolated, followed by homozygosity testing in subsequent generations. Some of the isolated mutants also showed changed grain type and/ husk colour. Mutants have been advanced up to M6 generations. Six mutants have been evaluated for their effects on induced cytokine production by lymphocytes. Two of these mutants have been observed to be promising in terms of bio-activity.

Conclusion

The study highlights the immune-suppressive potential of Gathuwan brown rice along with the mechanistic and biochemical basis and complements traditional knowledge.

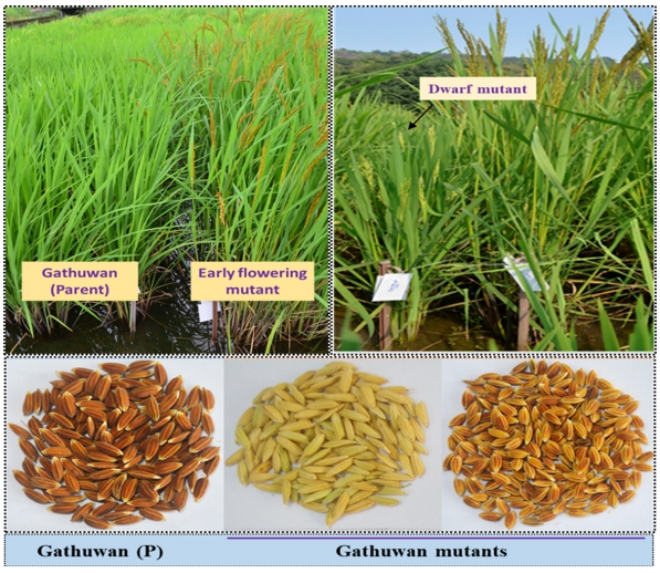

Fig.5: Mutation breeding for agronomic trait improvement of Gathuwan.

Agronomic improvement without compromising the health benefit will not only help its conservation and wider recognition, but will promote more explorations of rice germplasm.

References

[1] C. M. Weyand, J. J. Goronzy, Association of MHC and rheumatoid arthritis, HLA polymorphisms in phenotypic variants of rheumatoid arthritis, Arthritis Res 2, 2000, 212. https://doi.org/10.1186/ar90.

[2] A. Cuadrado, G. Manda, A. Hassan, M. J. Alcaraz, C. Barbas, A. Daiber, P. Ghezzi, R. León, M. G. López, B. Oliva, M. Pajares, A. I. Rojo, N. Robledinos-Antón, A. M. Valverde, E. Guney, H. H. H. W. Schmidt, Transcription Factor NRF2 as a Therapeutic Target for Chronic Diseases: A Systems Medicine Approach, Pharmacol Rev 70, 2018, 348–383. https://doi.org/10.1124/pr.117.014753.

[3] A. Chauhan, R. Checker, S. Nair, P. K. Sahu, D. Sharma, D. Sharma, B. K. Das, Indian traditional rice variety “Gathuwan” suppresses T-cell-mediated immune responses via activation of ERK/Nrf2/HO-1 signalling pathway, Food Funct., 14, 2023, 5232–5250. https://doi.org/10.1039/D3F000125C.

पारंपरिक चावल किस्म में सुधार

19

विकिरण प्रेरित उत्परिवर्तन प्रजनन के माध्यम से पारंपरिक चावल किस्म में सुधार और पुनरुज्जीवन

दीपक शर्मा[1], परमेश्वर के. साहू[2], विकास कुमार[3] and बिक्रम के. दास[3]*

[1]आनुवंशिकी एवं पादप प्रजनन विभाग, इंदिरा गांधी कृषि विश्वविद्यालय, रायपुर-492012 छत्तीसगढ़, भारत
[2]आरएबीएल कॉलेज ऑफ एग्रीकल्चर एंड रिसर्च स्टेशन, इंदिरा गांधी कृषि विश्वविद्यालय, छुईखादान-491885, छत्तीसगढ़, भारत
[3]नाभिकीय कृषि एवं जैव प्रौद्योगिकी प्रभाग, भाभा परमाणु अनुसंधान केंद्र, ट्रांबे-400085, भारत

मूल विष्णुभोग के साथ ट्रॉम्बे छत्तीसगढ़ विष्णुभोग उत्परिवर्ती (टी. सी. वी. एम.) का तुलनात्मक क्षेत्र दृश्य।

सारांश

परंपरागत चावल की प्रजातियों में कई अमूल्य विशेषताएं हैं जिनका उपयोग उपजाऊ, जलवायु के अनुकूल और पोषण से भरपूर व्यावसायिक किस्में विकसित करने के लिए किया जा सकता है। हालांकि, पौधे के लंबे आकार, परिपक्वता की लंबी अवधि, पौधों में झुकाव की संभावना, दाने का बिखड़ना और उपज क्षमता में कमी के कारण ये बहुत कम क्षेत्रफल पर लगाए जाते हैं तथा विलुप्ति के कगार पर हैं। इन भू-अनुकूल प्रजातियों के अद्वितीय गुणधर्म में परिवर्तन किए बिना एक या दो प्रमुख अवांछनीय विशेषताओं को सुधारने के लिए उत्परिवर्तन प्रजनन एक सरल, लागत प्रभावी और कुशल विधि है। भाभा परमाणु अनुसंधान केंद्र, मुंबई और आईजीकेवी, रायपुर ने विकिरण प्रेरित उत्परिवर्तन प्रजनन के माध्यम से इन भू-अनुकूल प्रजातियों के सुधार और पुनरुज्जीवन के लिए सहयोगात्मक अनुसंधान एवं विकास कार्य किया है। १० वर्षों के निरंतर अनुसंधान एवं विकास कार्य में, सुधार के लिए ~१०० चावल की भू-अनुकूल प्रजातियों का अध्ययन किया गया जिसमें से कई उच्च उपज देने वाली एवं आशाजनक उत्परिवर्ती विकसित की गई हैं। अब तक चावल की पाँच उत्परिवर्ती किस्मों (यथाः टीसीडीएम-१, विक्रम-टीसीआर, सीजी जवाफूल ट्रांबे, टीसीवीएम और टीसीएसएम) को जारी किया गया है तथा भारत सरकार द्वारा राजपत्र के माध्यम से वाणिज्यिक कृषि हेतु अधिसूचित किया गया है। अनेक उच्च उपज देने वाली एवं आशाजनक उत्परिवर्ती अन्वेषणाधीन हैं तथा राज्य और राष्ट्रीय स्तर के अनेक परीक्षण स्थलों पर उनका मूल्यांकन किया जा रहा है। व्यापक प्रसार के लिए बड़े पैमाने पर बीज उत्पादन कार्यक्रम शुरू किए गए हैं। सर्वविदित है कि यह भारत में चलाया जा रहा विश्व का सबसे बड़ा व्यापक चावल उत्परिवर्तन प्रजनन कार्यक्रम है। उच्च उपज क्षमता वाली उन्नत उत्परिवर्ती चावल भू-अनुकूल प्रजातियाँ/किस्में सीमांत और पारंपरिक किसानों के बीच व्यापक स्वीकार्यता प्राप्त कर रही हैं जिसके परिणामस्वरूप सामाजिक-आर्थिक परिस्थितियों में सुधार तथा कुपोषण और भूख के स्थायी समाधान के साथ पारंपरिक ज्ञान परंपरा को बचाना संभव होगा।

Improvement of Traditional Rice Landraces

19

Improvement and Revival of Traditional Rice Landraces through Radiation Induced Mutation Breeding

Deepak Sharma[1], Parmeshwar K. Sahu[2], Vikash Kumar[3] and Bikram K. Das[3]*

[1]Department of Genetics and Plant Breeding, Indira Gandhi Krishi Vishwavidyalaya, Raipur-492012 Chhattisgarh, INDIA
[2]RABL College of Agriculture & Research Station, Indira Gandhi Krishi Vishwavidyalaya, Chhuikhadan-491885, Chhattisgarh, INDIA
[3]Nuclear Agriculture and Biotechnology Division, Bhabha Atomic Research Centre, Trombay-400085, INDIA

Comparative field view of Trombay Chhattisgarh Vishnubhog Mutant (TCVM) along with parent Vishnubhog

ABSTRACT

Traditional rice landraces have several invaluable traits which could be utilized to develop high yielding, climate resilient and nutritionally enriched commercial varieties. However, due to tall plant stature, late maturity duration, susceptible to lodging, grain shattering habit, and low yield potential, these have been marginalised and are at the verge of extinction. Mutation breeding offers simple, cost effective and efficient way to improve one or two major undesirable traits without altering the unique characters of these landraces. BARC, Mumbai and IGKV, Raipur, have undertaken collaborative R&D work for improvement and revival of these landraces through radiation induced mutation breeding. Over 10 years of continuous R&D work, ~100 rice landraces have been undertaken for improvement and many promising mutants have been developed. So far 5 rice mutant varieties (*viz*. TCDM-1, Vikram-TCR, CG Jawaphool Trombay, TCVM and TCSM) have been released and gazette notified by Government of India for commercial cultivation. Many high yielding and promising mutants are in pipe line and being evaluated at state and national level multi-location trials. Large scale seed production programme for wide dissemination have been undertaken. Ostensibly, this is one of the world's largest comprehensive rice mutation breeding programme being carried out in India. Improved mutant rice landraces/ varieties with high yielding potential are getting wider acceptability among the marginal and conventional farmers and will result in better socio-economic conditions and bring back the traditional wisdom of combating malnutrition and hunger on sustainable basis.

KEYWORDS: *Rice landraces, Radiation induced mutation breeding, Mutant rice varieties, Farmers' varieties, and Food security*

**Author for Correspondence: B. K. Das*
E-mail: bkdas@barc.gov.in

Introduction

Rice is the most important food crop of the developing world and the staple food of more than half of the world's population. In developing countries alone, more than 3.3 billion people depend on rice for more than 20% of their calories. However, to maintain future global rice supplies many challenges must be addressed, which primarily include high nutrient content, better grain quality, tolerance to different stresses and improved yield. The rice landraces or farmers' varieties are a rich source of several valuable and useful genes viz. resistance to biotic and abiotic stresses (drought, salinity, toxic heavy metals, herbicides), rich in essential micronutrients, premium grain-quality attributes (viz. aroma) and health benefits (medicinal properties). It is a fact that traditional landraces/farmers' varieties (with aroma and unique grain-quality attributes) have great export potential, fetching premium price (Rs. 100-150 per kg). These landraces are being marginalized due to their tall stature, which makes them prone to lodging, late maturity that results in more inputs and time management in field operations, photoperiod sensitivity, grain shattering habit, open plant canopy, non-synchronous maturity in grains of the same panicles, and ultimately poor yield potential. Hence, these are not preferred by the farmers for commercial cultivations (Fig.1). Moreover, due to introduction of high-yielding varieties and hybrids, area of cultivation of these landraces has been significantly reduced. It is a matter of concern that many of these landraces are at the verge of extinction from the farmers' field resulting severe loss of rich rice biodiversity. Such problems need to be addressed carefully in a sustainable manner.

Rectification of undesirable traits by altering few major genes may bring these landraces back into cultivation. This will help to improve the yield potential of these varieties without compromising the premium grain attributes. Conventional plant breeding methods have not been very successful in improving these landraces due to genome-wide recombination and alteration in their premium grain quality traits. However, mutation breeding has been used as a potential tool for rectifying a few defects such as tall stature, late maturity etc. while keeping the original unique quality of the landraces intact/ unaltered and bringing them back into channel of commercial cultivation (Fig.1). High yielding and improved rice landraces will result in wider acceptability among the marginal and conventional farmers, resulting better socio-economic conditions and help to bring back the traditional wisdom of combating malnutrition and hunger on sustainable basis. This will also ascertain national food and nutritional security and gain foreign exchange in the country through worldwide export.

Advantages of Mutation Breeding

Plant mutation breeding accelerates crop improvement through creation of genetic mutations leading to genetic diversity that facilitates selection from a large mutant population. It is a powerful technique to improve one or two major defects in rice landraces by maintaining their original qualities and unique features. It doesn't make huge changes in the genome of plant. It enhances the variability by making minor, random and reversible changes in the genome which allows plant breeders to make efficient selection in the segregating mutant populations. Till date, ~ 3406 mutant varieties in more than 228 crop species have been developed through induced mutagenesis by different countries and registered in the FAO/IAEA Mutant Variety Database (MVD), International Atomic Energy Agency, Vienna, Austria database (FAO/IAEA MVD, 2023, https://nucleus.iaea.org/sites/mvd/SitePages/Search.aspx) which has made significant impact in assuring global food and nutritional security. Moreover, the developed mutant varieties enhance the crop biodiversity and offers useful breeding material for further crop improvement.

BARC-IGKV Collaboration for Improvement & Revival of Traditional Rice Landraces through Radiation Induced Mutation Breeding

Chhattisgarh state of India is endowed with more than 23,250 traditional rice landraces which have several valuable and useful genes for yield and attributing traits, resistance against biotic and abiotic stresses, resistant to herbicides, nutritional properties, medicinal properties, carrying low heavy metal accumulation, micronutrient enrichments, premium quality attributes (viz. aroma) and agronomic suitability etc. These landraces were collected by Dr. R.H. Richharia, a renowned rice breeder in the World during 1970 to 1985 from Chhattisgarh (then Madhya Pradesh) and nearby districts. All these traditional varieties are huge treasures which have unique qualities which are not present in high yielding and hybrid varieties. Mutation breeding is the only option to improve and revive these traditional varieties. Currently, these landraces are being conserved and maintained by Indira Gandhi Krishi Vishwavidyalaya (IGKV), Raipur (C.G.) accounting the largest collection in India and second largest collection in the world after International Rice Research Institute, Manila, Philippines. However, these landraces are not under the

Fig.1: Problems associated with rice landraces and improvement through mutation breeding.

Table 1: Current Status of Rice Landraces Improvement Program under BARC-IGKV joint collaboration.

Sr. No	Mutant Population/ Generation	Number of Mutants/ Entries
1	No. of landraces undertaken for improvement till date	100
2	Rice Mutants Released and Notified by Govt. of India	5
3	Rice mutant identified by UVIC for release	1
4	National AICRIP (MLT) Trials (2023)	5 in the background of 4 landraces
5	National AICRIP (MLT) Trials (2022)	6 in the background of 5 rice landraces
6	State Multi-Location Trials (2023)	8 in the background of 7 landraces
7	State Multi-Location Trials (2022)	8 in the background of 7 rice landraces
8	Station Trials (2023) of Stable Mutants (M8 & above)	33 mutants in the background of 30rice landraces
9	Special type mutants (*Kharif* 2023)	24 in the background of 12 landraces
10	Other agronomic superior mutants (*Kharif* 2023)	49 in the background of 21 landraces
11	Hybridization b/w Mutants & Parents for developing mapping populations & molecular studies	>50 crosses
12	M1 population (*Kharif* 2022)	13 M1 population in the background of 9 landraces
13	M2 Population (*Kharif* 2022)	33 M2 population in the background of 29 rice landraces
14	M3 Population (*Kharif* 2023)	116 lines in the background of 14 landraces
15	M4 population (*Kharif* 2023)	1 mutant line in the background of 1 landrace
16	M5 population (*Kharif* 2023)	108 mutant lines in the background of 24 landraces
17	M6 population (*Kharif* 2023)	56 mutant lines in the background of 3 landraces
18	M7 population (*Kharif* 2023)	63 mutant lines in the background of 13 landraces

cultivation in farmers' field due to their poor yield potential, late maturity duration and tall plant stature. Therefore, these are almost at the verge of extinction from the farmers' field. To utilize these available genetic resources of rice for the societal benefits, IGKV, Raipur and BARC, Mumbai, have undertaken collaborative R&D work for improvement and revival of traditional rice landraces through radiation induced mutation breeding since 2013.

Current Status and Achievements under BARC-IGKV Collaboration

Our collaborative R&D work initially focused on evaluating and characterizing ~300 popular and traditional rice landraces with unique properties, which could be suitable candidates for improvement through radiation-induced mutation breeding. After 10 years of continuous and systematic breeding efforts, ~100 rice landraces have been undertaken for improvement using radiation-induced mutation breeding. These mutants, which may have agronomic or academic significance, are at different developmental stages and are maintained in a huge rice mutant repository (Table 1). More than 80 advanced agronomically superior mutant lines in the background of 50 landraces have already been stabilized and are in final stages of station trials. 24 unique mutant lines such as extremely dwarf, high tillering, male sterile, red kernel, disease resistant mutants have been developed, which can be used as potential donor for future rice breeding programs. In view of quantum of rice mutation breeding work being carried out by BARC and IGKV, this collaborative effort is envisaged as the world's largest comprehensive radiation-induced mutation

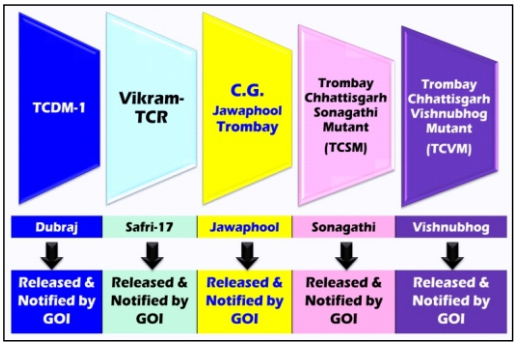

Fig.2(a): Rice mutants released under BARC-IGKV collaboration.

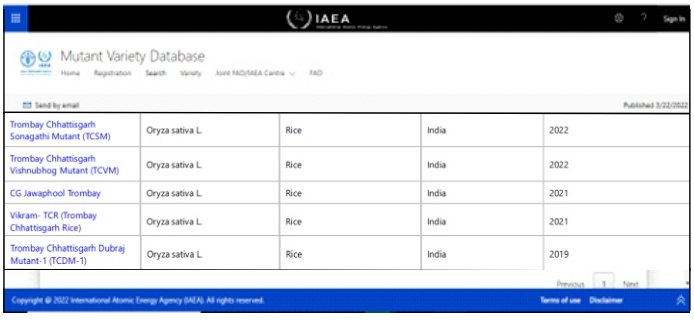

Fig.2(b): Mutant Rice Varieites (released under BARC-IGKV collaboration) at FAO/ IAEA Mutant Variety Database (https://nucleus.iaea.org/sites/mvd/SitePages/Search.aspx)

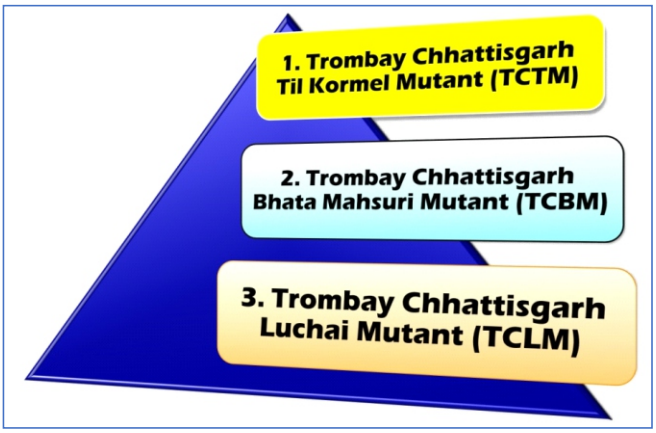

Fig.3: Rice mutants in pipeline of release under BARC-IGKV collaboration.

breeding program for improvement and revival of traditional rice varieties/landraces. It is worth to note that under this joint collaborative effort, five rice mutant varieties viz.(1)Trombay Chhattisgarh Dubraj Mutant-1 (TCDM-1), (2) Vikram-Trombay Chhattisgarh Rice (Vikram-TCR), (3) CG Jawaphool Trombay (CGJT), (4)Trombay Chhattisgarh Vishnubhog Mutant (TCVM) and (5) Trombay Chhattisgarh Sonagathi Mutant (TCSM) All these have been released and notified for commercial cultivation by Government of India (Fig.2(a)). All the 5 rice mutant varieites have been registered under the FAO/ IAEA Mutant Variety Database (https://nucleus.iaea.org/sites/mvd/SitePages/Search.aspx) (Fig.2(b)). In addition, three mutant lines *viz.,* Trombay Chhattisgarh Til Kormel Mutant (TCTM), Bauna Luchai-CTLM (Chhattisgarh Trombay Luchai Mutant) and Trombay Chhattisgarh Bhata Mahsuri Mutant (TCBM) have been developed. These lines are being evaluated in state and national multi-location trials and are in pipeline for identification and release (Fig.3).

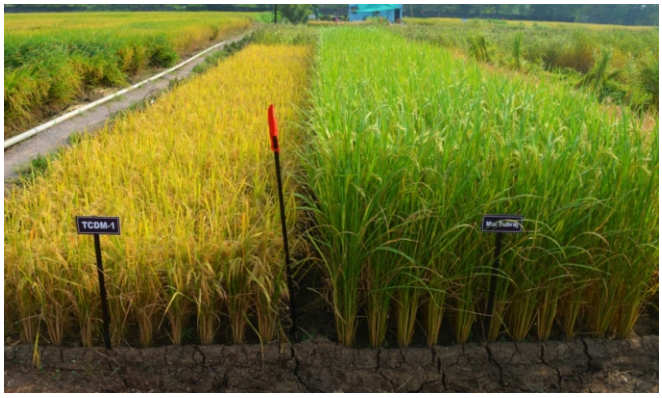

Fig.4: Comparative field view of TCDM-1 along with parent Mai Dubraj.

Brief Description of the Released and Notified Mutant Rice Varieties

TCDM-1

It is the first successful dwarf and high yielding mutant derived from the rice landrace Mai Dubraj parent (Mai Dubraj is very popular rice landraces of Chhattisgarh state and famous as 'Basmati of Chhattisgarh'). It has fine aromatic grains. TCDM-1 has -39.74% reduced plant height and -15.71% reduced maturity duration as compared to Mai Dubraj whereas it has 53.13% higher yield potential over the parent (Table 2; Fig. 4). The average yield of TCDM-1is 45 q/ha whereas its potential yield is about 55 q/ha. Most of the farmers prefer to grow the mutant variety TCDM-1 developed from Mai Dubraj. This variety was notified by Govt. of India [vide S.O. 1498(E), Gazette of India No. 1326, dated 02 April 2019 for commercial cultivation].

Vikram-TCR

It was developed from Safri-17, a traditional rice variety from central Chhattisgarh, India. Safri-17 is very popular for

Table 2: Percentage change in flowering duration, plant height and grain yield of released rice mutant varieties over the original parent landraces.

Sr. No.	Name of Genotypes	Days to 50% Flowering (days)	Percentage reduction in Days to 50% Flowering (%)over corresponding parent	Plant Height (cm)	Percetage reduction in plant height (%) over corresponding parent	Grain Yield (kg/ha)	Percetage increase in Yield over Parent (%)over corresponding parent
1.	Mai Dubraj(Parent)	121		171.11		3236.11	
2.	TCDM-1	102	-15.70	103.11	-39.74	4955.56	53.13
3.	Safri-17(Parent)	110		195.11		3594.44	
4.	Vikram TCR	84	-23.63	109.67	-43.79	5555.56	54.56
5.	Jawaphool (Parent)	123		154.11		3058.33	
6.	C. G. Jawaphool Trombay	114	-7.31	125.89	-18.31	4080.78	33.43
7.	Sonagathi (Parent)	118		121.56		4327.78	
8.	TCSM	107	-9.32	117.22	-3.57	6305.56	45.70
9.	Vishnubhog (Parent)	115		152.56		2783.22	
10.	TCVM	94	-18.26	114.44	-24.98	4312.44	54.94

Fig.5: Comparative field view of Vikram-TCR (R) along with parent Safri-17(L).

Fig.6: Comparative field view of CG Jawaphool Trombay (L) along with parent Jawaphool (R).

long slender grains, drought tolerance ability and good puffed rice making quality. Vikram-TCR has all these traits along with dwarf stature, early maturity habit and high yield potential. It has 54.56% higher yield, -43.79% reduced plant height and -23.64% reduced maturity duration over the corresponding parent, Safri-17 (Table 2; Fig.5). Vikram-TCR name was given in the honor of Professor Vikram Sarabhai (former Chairman, Atomic Energy Commission, Government of India) to commemorate his birth centenary year 2019-2020. This variety was notified for commercial cultivation [vide S.O. 500(E), Gazette of India No. 456, dated on 02-February-2021]. The average yield of Vikram-TCR is 60-65 q/ ha whereas its yield potential is up to75q/ha with drought tolerance and excellent puffed rice (murmura) making quality. This variety has been widely cultivated by the farmers in Chhattisgarh and adjoining states.

CG Jawaphool Trombay (CGJT)

It has aromatic short slender grains with semi-dwarf stature and mid late maturity duration. It has very good grain quality and *Kheer* making quality. It has 33.43% higher yield potential, -18.35% reduced plant height and -7.31% reduced maturity duration over the corresponding parent, Jawaphool (Table 2; Fig.6), a very popular aromatic short grain variety in Chhattisgarh. CG Jawaphool Trombay has yield potential of 40-45 q/ ha; and has been notified for commercial cultivation [vide S.O. 500 (E), Gazette of India No. 456, dated 02-February-2021].

Trombay Chhattisgarh Vishnubhog Mutant (TCVM)

This is the improved mutant variety of a popular traditional rice variety Vishnubhog of Chhattisgarh. It has aromatic short grains (similar to Vishnubhog), semi-dwarf stature (110-115 cm), and medium maturity duration (120-125 days). Plant height and maturity duration of TCVM has been reduced by -24.98% and -18.26%, respectively. Grain yield potential (40-45 q/ha) of TCVM has been increased by ~54.94% as compare to parent (27-30 q/ha) which made this variety more preferable (Table 2; Fig.7). It has high head rice recovery (61%) and intermediate amylose (25%) content which indicated the excellent grain quality of the mutants. Furthermore, it becomes very soft after cooking indicating its good cooking quality. This variety is suitable as steam rice as well as for *Kheer* making purpose. This has been notified for commercial cultivation [vide S.O. 8(E), Gazette of India No. 8, dated 03-January-2022].

Fig.7: Comparative field view of Trombay Chhattisgarh Vishnubhog Mutant (TCVM) along with parent Vishnubhog.

Trombay Chhattisgarh Sonagathi Mutant (TCSM)

This is an improved mutant variety of a popular traditional rice variety Sonagathi of Chhattisgarh. This mutant has very high yield potential (60-65 q/ha) which is comparable to yield potential of a hybrid rice variety. It has semi-dwarf plant stature (110-115 cm) and late maturity duration (135-140 days). Its maturity duration has been reduced by -9.32% (10-15 days) days and grain yield has been increased by 45.70% over the parental Sonagathi (Table 2; Fig. 8). TCSM plant type is similar to most popular rice variety Swarna and has potential to replace it. It is resistant to lodging and shattering and has dark green and erect leaves and good culm strength. Grain type is medium bold having dark straw-colored hull and brown spots on husk. Moreover, it has high head rice recovery (56 %) and intermediate amylose (22 %) content which indicated the excellent grain quality of the mutants. This has been notified for commercial cultivation [vide S.O.8(E), Gazette of India No. 8, dated 03-January-2022].

Large-scale Seed Production & Popularization of Mutant Rice Varieties among the Farmers

In addition to the development of rice mutants, both the institutions are also working for wider dissemination through demonstration of released rice mutant varieties at farmers' field. During *Kharif* season 2022, mini kit seeds of TCDM-1, Vikram-TCR, CG Jawaphool Trombay, Trombay Chhattisgarh Vishnubhog Mutant (TCVM) and Trombay Chhattisgarh

Fig.8: Comparative field view of Trombay Chhattisgarh Sonagathi Mutant (TCSM) along with parent Sonagathi.

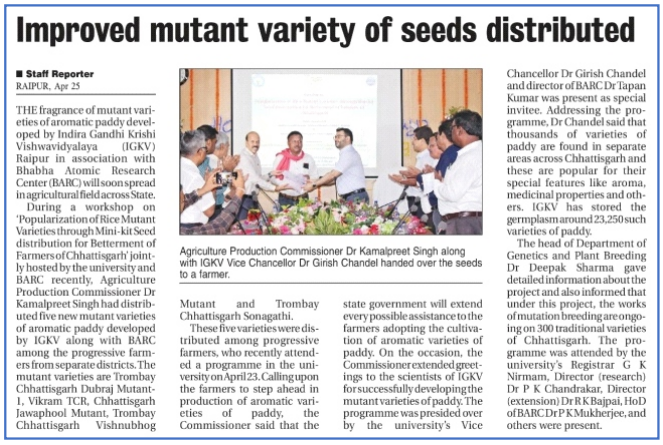

Improved mutant variety of seeds distributed

■ Staff Reporter
RAIPUR, Apr 25

THE fragrance of mutant varieties of aromatic paddy developed by Indira Gandhi Krishi Vishwavidyalaya (IGKV) Raipur in association with Bhabha Atomic Research Center (BARC) will soon spread in agricultural field across State.

During a workshop on 'Popularization of Rice Mutant Varieties through Mini-kit Seed distribution for Betterment of Farmers of Chhattisgarh' jointly hosted by the university and BARC recently, Agriculture Production Commissioner Dr Kamalpreet Singh had distributed five new mutant varieties of aromatic paddy developed by IGKV along with BARC among the progressive farmers from separate districts. The mutant varieties are Trombay Chhattisgarh Dubraj Mutant-1, Vikram TCR, Chhattisgarh Jawaphool Mutant, Trombay Chhattisgarh Vishnubhog Mutant and Trombay Chhattisgarh Sonagathi.

These five varieties were distributed among progressive farmers, who recently attended a programme in the university on April 23. Calling upon the farmers to step ahead in production of aromatic varieties of paddy, the Commissioner said that the state government will extend every possible assistance to the farmers adopting the cultivation of aromatic varieties of paddy. On the occasion, the Commissioner extended greetings to the scientists of IGKV for successfully developing the mutant varieties of paddy. The programme was presided over by the university's Vice Chancellor Dr Girish Chandel and director of BARC Dr Tapan Kumar was present as special invitee. Addressing the programme, Dr Chandel said that thousands of varieties of paddy are found in separate areas across Chhattisgarh and these are popular for their special features like aroma, medicinal properties and others. IGKV has stored the germplasm around 23,250 such varieties of paddy.

The head of Department of Genetics and Plant Breeding Dr Deepak Sharma gave detailed information about the project and also informed that under this project, the works of mutation breeding are ongoing on 300 traditional varieties of Chhattisgarh. The programme was attended by the university's Registrar G K Nirmam, Director (research) Dr P K Chandrakar, Director (extension) Dr R K Bajpai, HoD of BARC Dr P K Mukherjee, and others were present.

Agriculture Production Commissioner Dr Kamalpreet Singh along with IGKV Vice Chancellor Dr Girish Chandel handed over the seeds to a farmer.

Fig.9: Front Line Demonstrations and organization of Field Days & distribution of mini-seed kits for popularization of mutant varieties.

Table 3: Seed production (in q) of Mutant Varieties during Kharif-2022.

Sr. No	Name	Year of Notification	Seed Kit Distribution	Breeder Seed production	Foundation Seed production	Truthful Seed production	Remarks
1	TCDM-1	2019	May-2019 & Apr-2022	27.00	303.11	92.00	This is the 1st mutant variety developed through collaborative R&D work
2	Vikram TCR	2021	May-2019 & Apr-2022	39.00	462.60	15805.00	The variety is spreading fast among the farmers and may cover 14-15 % rice area in coming 2 years
3	CGJT	2021	Apr-2022	6.60	-	132.00	For popularisation, seed kit distribution and Kisan Mela(s) will be taken up in coming years along with Frontline Demonstrations
4	TCVM	2022	Apr-2022	4.60	-	145.00	
5	TCSM	2022	Apr-2022	5.25	-	210.00	

Sonagathi Mutant (TCSM) were distributed to more than 200 farmers of Chhattisgarh and nearby states. During preceding year (*Kharif* season 2021), mini-kit seeds of TCDM-1, Vikram-TCR, TCVM and TCSM were distributed to the farmers of Chhattisgarh, Uttar Pradesh and Maharashtra. Interestingly, all the farmers were happy to grow those mutant varieties and recorded an average yield 46 q/ha for TCDM-1 and 65 q/ha for Vikram-TCR. Workshops-cum-Field demonstrations and Field Days of mutant varieties are being organized every year for popularization of released rice mutant varieties among the farmers and also by distributing them mini kits of seeds (Fig.9). Furthermore, hand ready pamphlets on cultivation practices and unique features of mutants are also published and being distributed among the farmers for their convenience. Moreover, print media are also used for popularization of rice mutants. Many local and national print media covered the miracle of radiation techniques for development of rice varieties. With the help of these activities, huge numbers of farmers are benefitted and mutants are popularized among the farmers in short period of time. All the 5 rice mutant varieties are in National seed Chain(www.seednet.gov.in). The breeder seed indent for *Kharif*-2024 is as follows: Vikram TCR (45. 05 q), TCDM-1(25.00 q), TCVM (21.00 q), CGJT (12.00 q) & TCSM (1.00 q). These new varieties account for ~3.15% of total National seed indent; which is a good indication. Year after year, the Breeders seed indent is increasing and much more quantity of seeds are being produced and disseminated through BARC-IGKV collaboration. Looking at the huge demand from the State Seed Corporations (through Govt. of India national indent) and the farmers, in *Kharif*-2022, large scale

Fig.10: Field view of large scale breeder seed production of Vikram TCR & TCVM.

seed production (Breeders Seed, Foundation Seed, Truthful Seed) of mutant varieties were taken up (Table-2, Fig.10). During the *Kharif*- 2022, Vikram-TCR was cultivated in more than 1000 ha area of Chhattisgarh state. On the basis of breeders' seed dissemination (Breeder Seed-to-Foundation Seed-to-Certified Seed-to-Farmers Field), it is estimated that, 'Vikram TCR' (mutant of Safri-17 rice landrace) may occupy ~14-15% of rice area in Chhattisgarh state within 2 years. Within 4-5 years, this variety (due to its high yield potential, lodging resistance, good grain quality, resistance to major diseases) may replace MTU-1010 (a mega variety occupying ~30% rice area).

Future Road Map & Molecular Mapping/Molecular Insights of Mutant Traits & Validation of Therapeutic Properties of Medicinal Rice Landraces/Varieties

Rice mutation breeding is being practiced all over the world. However, BARC-IGKV collaboration has given a new dimension in improvement of traditional rice landraces/farmer's varieties increasing rice biodiversity using radiation induced mutation breeding. Our efforts have helped to generate large number of mutant reservoirs which will be tested and released for commercial cultivation in future. In addition to this, identification and mapping of causal mutations in the genome through advanced genomic approaches viz. RNA sequencing and MutMap is also being carried out. During *Kharif* season 2021, RNA sequencing of a dwarf and high tillering mutant (Samundchini mutant S-49) of Samundchini landrace along with corresponding parent and TRR-4 & corresponding parent Mai Dubraj were performed to identify the differentially expressed genes and to define the causal mutations. Furthermore, large numbers of crosses (~50) were attempted between mutants and corresponding parents to generate F2& F2:3 mapping population for MutMap studies. These populations will be used for MutMap studies in future to map the mutant loci and to find out the causal mutation. Also, genomic similarity study based on SSR and SNP markers are also being studied to confirm the trueness of mutants. Till now major focus were given for improvement in grain yield potential by reducing their height and maturity duration. Many dimensions are there to go with. Therefore, both the institutions will soon start the mutation breeding for developing disease resistant mutants, biofortified mutants, mutants with medicinal values and climate resilient varieties. Scientific validation of medicinal properties of a few traditional rice varieties has been undertaken. Studies on 'Gathuwan' and 'Layacha' on animal models have been carried out (and published in peer reviewed journals). Further clinical trials in patients will be undertaken.

Conclusion

With this huge quantum of research work carried out under BARC-IGKV collaboration, it is worthwhile to mention that at present, this is ostensibly one of the world's largest active & comprehensive radiation-induced mutation breeding program for the improvement and revival of traditional rice landraces/farmers' varieties. The development of improved rice mutant varieties will not only help for improvement of the socio-economic conditions of the poor and marginal farmers who have been preserving these varieties since generations, but also will bring back the traditional wisdom of combating malnutrition and hunger on sustainable basis.

Acknowledgment

The support from Bhabha Atomic Research Centre (BARC) and Board of Research in Nuclear Sciences (BRNS), Department of Atomic Energy, Government of India, is duly acknowledged. Authors duly acknowledge the support and encouragement from Associate Director, BSG, Head, NA&BTD, BARC and Vice Chancellor and Director of Research, IGKV, Raipur.

References

[1] FAO/IAEA MVD, 2023, https://nucleus.iaea.org/sites/mvd/SitePages/Search.aspx

[2] Oladosu, Y., Rafii, M.Y., Abdullah, N., Hussin, G., Ramli, A., Rahim, H.A., Miah, G.; Usman, M., Principle and application of plant mutagenesis in crop improvement: A review, Biotechnol., Biotechnol. Equip., 2015, 30, 1–16.

[3] Sahu, P. K., Sao, R., Khute, I. K., Baghel, S., Patel, R. R., Thada, A., Parte, D., Devi, Y. L., Nair, S., Kumar, V. Mondal, S., Das, B. K. and Sharma, D., Plant Genetic Resources: Conservation, Evaluation and Utilization in Plant Breeding. Springer Nature Switzerland Pvt. Ltd., 2023, 1-36.

[4] Sahu, P. K., Sao, R., Mondal, S., Vishwakarma, G., Gupta, S. K., Singh, S., Sharma, D. and Das, B. K., Next Generation Sequencing Based Forward Genetic Approaches for Identification and Mapping of Causal Mutations in Crop Plants: A Comprehensive Review. Plants, 2020, 9(1355), 1-47.

[5] Sao, R., Sahu, P. K., Patel, R. S., Das, B. K., Jankuloski, L., & Sharma, D., Genetic Improvement in Plant Architecture, Maturity Duration and Agronomic Traits of Three Traditional Rice Landraces through Gamma Ray-Based Induced Mutagenesis. Plants, 2022, 11(24), 3448. https://doi.org/10.3390/plants11243448.

[6] Sao, R., Sahu, P. K., Sharma, D., Vishwakarma, G., Nair, J. P., Petwal, V. C. and Das, B. K., Comparative study of radio-sensitivity and relative biological effectiveness of gamma rays, X-rays, electron beam and proton beam in short grain aromatic rice, Indian Journal of Genetics and Plant Breeding, 2020, 80(4), 384-394.

[7] Sharma, D., Das, B. K., Sahu, P. K., Tiwari, A. K., Baghel, S., Sao, R., Singh S., and Kumar, V., Improvement of Traditional Farmers' Varieties of Rice through Radiation induced Mutation Breeding, IGKV Pub./2019/Booklet/, 2019, 11, 1-48.

[8] Sharma, D., Sahu, P. K., and Das, B. K., BARC-IGKV MoU: A Unique Model of Mutual Collaboration towards Welfare of Farmers' and Nation. IGKV Pub./ 2020/Book/01, 2020, 1-65.

[9] Thada, A., Sahu, P. K., Sao, R., Chauhan, A., Checker, R., Das, B. K., Sharma, D., Sharma, D., & Ghanty, T. K., Biochemical foundation of the aroma and antioxidant activity of Indian traditional rice landrace Maharaji and the effect of radiation-induced mutagenesis on its metabolome, Food chemistry, 2024, 460(3), 140668.

विकिरण उपचारित भारतीय आम

20

अनुसंधान और विकास नवाचारों से विकिरण उपचारित भारतीय आम की लागत प्रभावी समुद्री-मार्ग से निर्यात

जे. त्रिपाठी[1], **एन. बंदोपाध्याय**[1], **एस. सक्सेना**[1], **एस. कुमार**[1], **वी. मोरे**[1], **ए. के. चौबे**[1], **बी. बी. मिश्रा**[1,2], **एस. एन. हज़ारे**[1,2] **और एस. गौतम**[1,2]*
[1]खाद्य प्रौद्योगिकी प्रभाग, भाभा परमाणु अनुसंधान केंद्र, ट्रांबे-400085, भारत
[2]होमी भाभा राष्ट्रीय संस्थान, अणुशक्तिनगर, मुंबई-400094, भारत

खाद्य संरक्षकों में आमों की डुबकी लगाना

सारांश

आम के विषय में भारत दुनिया का सबसे बड़ा उत्पादक है और भारतीय आम का निर्यात कई देशों में किया जा रहा है। आम के व्यापार विकिरण प्रसंस्करण की संगरोध बाधा को दूर करने के लिए संयुक्त राज्य अमेरिका और मलेशिया, ऑस्ट्रेलिया, दक्षिण अफ्रीका जैसे अन्य आयातक देशों के लिए एक पूर्व-आवश्यकता है और इस फल की अत्यधिक खराब होने वाली प्रकृति के कारण वायु मार्ग, वर्तमान में आम के निर्यात का एकमात्र तरीका है। वर्तमान निर्यात विधियों से जुड़ी उच्च परिवहन लागत और कार्गो क्षमता की सीमाएं भारतीय आम निर्यात के लिए एक बाधा के रूप में कार्य करती है, जिससे देश की बाज़ार हिस्सेदारी पर प्रभाव बढ़ाने और वैश्विक बाजार के भीतर निर्यात राजस्व उत्पन्न करने की क्षमता में बाधा आती है। एफटीडी, भापअ केंद्र में अनुसंधान और विकास प्रयासों के परिणामस्वरूप एक प्रोटोकॉल का विकास हुआ है जिसके परिणामस्वरूप आम की शेल्फ-लाइफ 25-30 दिनों तक बढ़ गया है। यह विस्तारित शेल्फ-लाइफ अंतरराष्ट्रीय बाज़ारों में आम के लागत प्रभावी समुद्री मार्ग परिवहन की सुविधा प्रदान करती है, जिससे बड़ी व्यापार मात्रा की संभाव्यता सक्षम होती है। वर्ष 2022 में समुद्री मार्ग के माध्यम से संयुक्त राज्य अमेरिका में 16 टन आम का एक वाणिज्यिक परीक्षण शिपमेंट किया गया था, जो उत्कृष्ट समग्र उपभोक्ता स्वीकार्यता के साथ संयुक्त राज्य अमेरिका के बाज़ार में सफलतापूर्वक पहुंचा और बेचा गया। यह पूरी तरह से स्वदेशी तकनीक दूर के विदेशी बाज़ार में आम के व्यापार को बढ़ावा देने की क्षमता रखती है।

Radiation Treated Indian Mangoes

20

R&D Innovations Leading to Cost-Effective Sea-Route Shipment of Radiation Treated Indian Mangoes

J. Tripathi[1], **N. Bandyopadhyay**[1], **S. Saxena**[1], **S. Kumar**[1], **V. More**[1], **A. K. Chaubey**[1], **B. B. Mishra**[1,2], **S. N. Hajare**[1,2] **and S. Gautam**[1,2]*
[1]Food Technology Division, Bhabha Atomic Research Centre, Trombay-400085, INDIA
[2]Homi Bhabha National Institute, Anushakti Nagar, Mumbai-400094, INDIA

Dipping of mangoes in food preservatives

ABSTRACT

India is the world's largest producer of mangoes, and Indian mangoes are being exported to many countries. To overcome quarantine barrier of trade radiation processing of mangoes is a pre-requisite for USA and other importing countries like Malaysia, Australia and South Africa. Air route is currently the only way to export the mangoes due to the highly perishable nature of the fruit. The high transportation costs and limitations in cargo capacity associated with current export methods act as a barrier to Indian mango exports the nation's ability to capture market share and generate export revenue within the global market. The R&D efforts at FTD, BARC has resulted in the development of a protocol which results in the shelf life extension of mangoes upto 25-30 days. This extended shelf life facilitates cost-effective sea route transportation of mangoes to international markets, enabling feasibility of larger trade volumes. A commercial trial shipment of 16 ton mangoes to the USA through sea-route was performed in 2022, which successfully reached and were sold in the USA market, with excellent overall consumer acceptability. This completely indigenous technology has the potential of boosting the trade of mango to distant overseas market.

KEYWORDS: *Delayed ripening, Gamma radiation, International trade, Dip-treatment*

*Authors for Correspondence: Satyendra Gautam
E-mail: sgautam@barc.gov.in

Introduction

Mango (*Mangifera indica* L.), belonging to the Anacardiaceae family, constitutes the most economically important fruit crop cultivated in India, which is the world's leading producer of mangoes, contributing approximately 45% of global production, which translates to roughly 18.5 million tons annually (Fig. 1a) [1]. Indian mangoes constitute the most extensive collection of delectable cultivars, distinguished by a remarkable diversity in flavour and aroma; due to which it holds a significant position in the global fruit market. Indian mangoes are currently exported to a wide range of countries, including the United States (the world's leading importer of fresh mangoes), the European Union, Japan, South Korea, New Zealand, Australia, and numerous nations in Asia and the Middle East. Indian mango imports to the United States resumed in 2007, after the gap of 18 years, contingent upon irradiation treatment due to phytosanitary restrictions [2-3]. In 2023, India exported approximately 3000 metric tonnes of irradiated mangoes through air route to the USA.

The break-up of costing (including irradiation and air-freight) involved in trade of mangoes in US market is displayed in Fig. 1b. Current practices in Indian mango export to the USA necessitate air freight following mandatory radiation treatment in accordance with USDA regulations. Since this involves high transportation cost and also limitation in the air cargo capacity, it has resulted in comparatively restricted market share of Indian mangoes and therefore lesser export revenue.

Employing transportation of mango through sea-route presents a compelling alternative, offering significant cost reductions and enabling larger export volumes. This shift in logistics has the potential to facilitate wider market coverage within the USA and other countries. The current findings deal with a successful commercial scale trial for sea-route shipment of Indian mangoes to the USA conducted in 2022. The trial was performed with a protocol developed at Food Technology Division, BARC resulting in delayed ripening of mangoes and therefore extended shelf life.

The hard green 'Kesar' mangoes were harvested from the Agricultural Produce Export Development Authority (APEDA) registered 'Mangonet' orchards [5-6]. Healthy, blemish-free fruits weighing between 220-300 g and total soluble solids ranging between 8 to 10° Brix indicating maturity: 65-70% were selected for the study (Fig.2 a). Desapping was performed for 3 hours and the stalk length of the desapped fruit was between 1-1.5 cm. It was ensured that the fruits are free of pest infestation, sap induced damage, microbial contaminations and any mechanical injury. Fruits with sap oozing out were selectively removed from the lot to avoid sap induced external blackening on the fruit itself and also on the adjoining fruits. Besides, fruits that showed lenticel browning and sap induced blackening were selectively screened out. After desapping, the fruits were subjected to sodium hypochlorite treatment (200 ppm at 52°C for 3 min) in a customized pack house. Following the hypochlorite dip the fruits were subjected to water dip treatment containing Generally Recognized As Safe (GRAS) preservatives at ambient temperature for 3 min. This step, was developed based on R&D done at Food Technology Division, Bhabha Atomic Research Centre, Mumbai, India. After the dip treatment, fruits were air dried prior to packing in foam-nets in a card-board box. Complete removal of moisture was ensured at this stage, without abrasive rubbing of fruits.

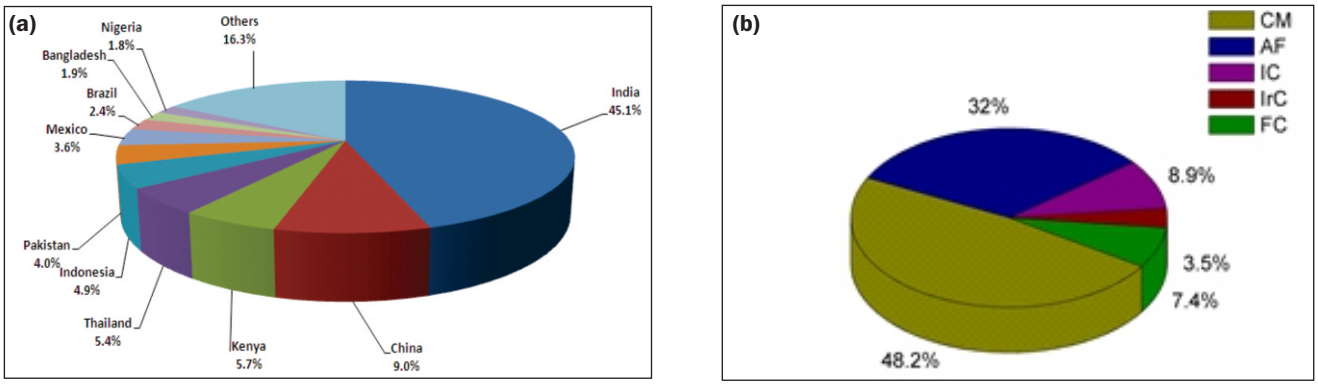

Fig.1: (a) Leading Mango producing countries; (b) Breakup of mango cost (approx.) sold in US markets (Source: Economic Research Survey: USA Federal Agricultural Agency report). [FC: Farm Cost; IrC: Irradiation Cost; IC: Inspection Cost; AF: Air Freight; CM: Cost & margins in the USA market] [4].

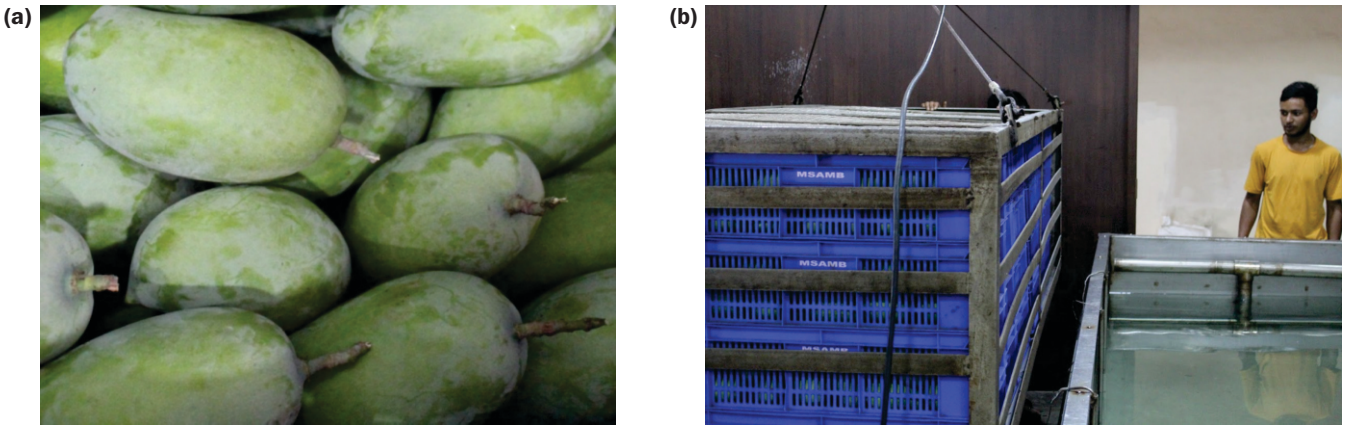

Fig.2: (a) Figure showing hard mature mango fruits which are fit for processing; (b) Dipping of mangoes in GRAS preservatives.

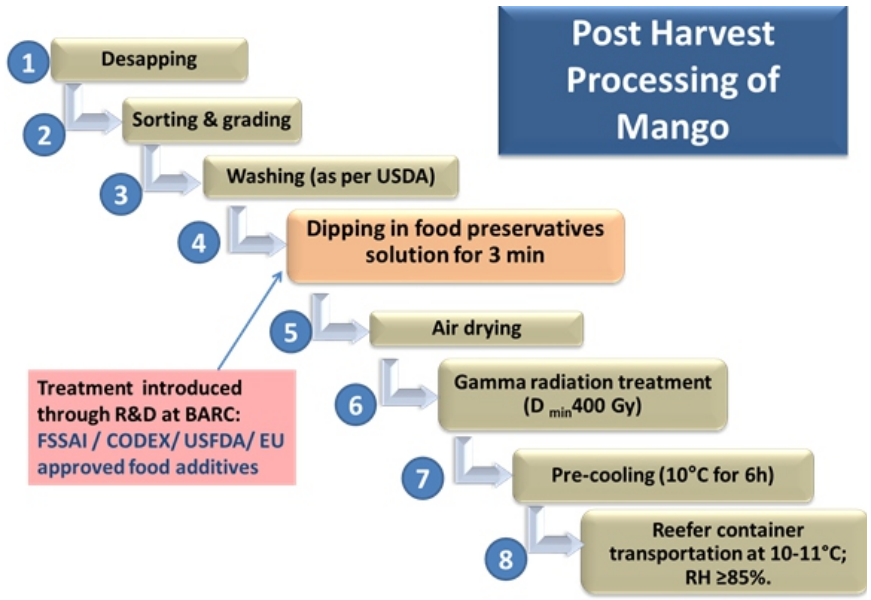

Fig.3: Process flowsheet describing steps for post-harvest processing of mango.

Fig.4: (a) Loading of mango boxes inside the shipping container (b) Reefer controlled atmosphere container (10°C) at NEWARK Port. (c) Sea-route shipped mangoes sold at the US market (d) Box showing mangoes after ripening sold at market.

The mango fruits were placed in boxes and subjected to gamma radiation treatment (minimum absorbed dosage of 400 Gy & maximum 1000 Gy) at a USDA-APHIS certified Cobalt-60 gamma irradiation treatment facility [7]. Dosimetry was performed as per the set guidelines [8-9].

After radiation treatment, the fruit boxes were palletized, followed by pre-cooling at 10°C for 6 hours. This was required before stuffing the fruits in reefer container for transportation at 10 to 11°C and RH ≥85%. The reefer container was provided with ethylene absorber at the return air vent, with air circulation rate of 30 cubic meter/hour. For a controlled atmosphere (CA) container the oxygen and carbon dioxide conc. were 4% and 6%, respectively. A process flow sheet has been described in Fig. 3.

Results and Discussion

The current protocol developed at FTD; BARC has resulted in delayed ripening of hard mature 'Kesar' mango. Now, the shelf life of this delicate and quickly perishable mango variety has been extended upto 25-30 days under regulated cold storage. The extended shelf-life makes it feasible to export sizable quantum of 'Kesar' mango through sea-route shipment to distant shores like the USA, which takes approximately 20-30 days. Thus, 16 tons of 'Kesar' mangoes treated with developed protocol were successfully shipped through sea-route to USA (Fig. 4a, b). Upon arrival at US port, after regulatory approvals by the USDA-APHIS (United States Department of Agriculture-Animal and Plant Health Inspection Service), USFDA (United States Food and Drug Administration) and US-CBP (Custom and Border Protection Force), the shipment was successfully sold in the USA market Fig. 4c, d).

Apart from trade volume, the cost of transport has drastically reduced to 1/8th of the prevalent air fare of the cargo. So, this technology is going to encourage a number of small and medium mango farmers as well as traders for partaking in international trade. Parallelly, Indian mangoes are likely to see a major boost in the global market coverage in near future. Apart from the economical aspect; this treatment also

retains the nutritional values, organoleptic qualities (flavor and taste), firm texture, desirable color and excellent overall consumer acceptability of the mangoes upon ripening. This technology is a typical example of self-reliance as the technology is completely indigenous and has the potential of boosting the trade of mango to distant destinations overseas. Moreover, the GRAS chemicals used in the newly developed protocol have also been approved by the USFDA, USDA-APHIS, FSSAI (Food Safety and Standards Authority of India), CODEX, and EU (European Union) as food additives.

Conclusion

The commercial shipment trial amounting to 16 tons of Indian mangoes through sea-route was successfully accomplished, and the mangoes after ripening retained their overall consumer acceptability as well as the shipment was successfully sold in the USA market. The technology for sea route transportation will result in substantial cost reduction, enable export of larger trade volumes, and capture wider international market.

Acknowledgment

The authors acknowledge the collaborative efforts of APEDA (Agricultural and Processed Food Products Export Development Authority), Mumbai; Maharashtra State Agricultural Marketing Board, MAERSK Shipping Services, and M/s. Sanap Agroanimals Pvt. Ltd.

References

[1] Mango-National Horticulture Board (http://nhb.gov.in/report_files/mango/MANGO.htm).

[2] Importing Indian Mangoes to the United States. (https://www.aphis.usda.gov/publications/plant_health/content/printable_version/faq_imp_indian_mango.pdf).

[3] Importation of Mangoes From India (https://www.federalregister.gov/documents/2007/03/12/E7-4444/importation-of-mangoes-from-india).

[4] U.S. Agricultural Trade (https://www.ers.usda.gov/topics/international-markets-us-trade/us-agricultural-trade/)

[5] Guidelines for export of Indian Mangoes to USA. (http://apeda.gov.in/apedawebsite/Announcements/GUIDELINES_MANGOES_TO_USA.pdf).

[6] Pre-harvest and post-harvest operations for sea shipment of mango. (http://apeda.gov.in/apedawebsite/Announcements/seaprotocolfinalversion170209.pdf).

[7] Standard Operating Procedures-Irradiation Treatment of Indian Mangoes for export to USA (https://www.msamb.com/Documents/266c1794-c171-4694-9279-2c2559ca5ab3.pdf).

[8] Guidelines for Certification of Irradiation Treatment Facilities to meet the Phytosanitary Requirements. (Directorate of Plant Protection, Quarantine & Storage) (https://phytosanitarysolutions.com/wp-content/uploads/2015/06/NSPM-21-Irradiation.pdf).

[9] Guidelines for the use of irradiation as a phytosanitary measure (http://www.fao.org/3/a-y4835e.pdf).

फसल कटाई के बाद के नुकसान का न्यूनीकरण

21

एक एकीकृत दृष्टिकोण के माध्यम से प्याज़ की फसल कटाई के बाद के नुकसान के न्यूनीकरण हेतु वृहद पैमाने पर वाणिज्यिक परीक्षण

एस. सक्सेना[1], एस. कुमार[1], जे. त्रिपाठी[1], एस. एन. हज़ारे[1,2], एन. बंदोपाध्याय[1], वी. मोरे[1], ए. के. चौबे[1], बी. बी. मिश्रा[1,2], बी. सान्याल[1,2], सी. के. सौरभ[1] और एस. गौतम[1,2]*

[1]खाद्य प्रौद्योगिकी प्रभाग, भाभा परमाणु अनुसंधान केंद्र, ट्रांबे-400085, भारत
[2]होमी भाभा राष्ट्रीय संस्थान, प्रशिक्षण विद्यालय परिसर, अणुशक्ति नगर, मुंबई-400094, भारत

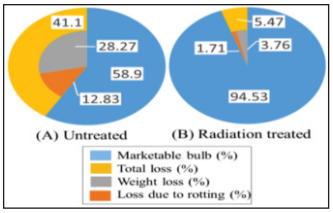

भंडारण के दौरान गैर-विकिरणित और विकिरण उपचारित प्याज में वजन घटाने की रूपरेखा

सारांश

प्याज़ का दीर्घकालिक विस्तारित संरक्षण फसल कटाई के बाद के प्रमुख मुद्दों के कारण सीमित है, जिसमें वजन कम होना, सूक्ष्मजीव खराब होना, सड़ना और अंकुरित होना शामिल है, जिससे 35-40% से लेकर समग्र नुकसान होता है। नियमित और पारंपरिक भंडारण सुविधाओं में रखी जाने वाली प्याज़ इन खराब होने की समस्याओं के प्रति अत्यधिक संवेदनशील होती है। इस संदर्भ में, अत्यधिक चिंता के इस मुद्दे को हल करने के लिए तकनीकी हस्तक्षेप एक पूर्व-आवश्यकता है। खाद्य प्रौद्योगिकी प्रभाग में अनुसंधान और विकास प्रयासों के परिणामस्वरूप, एक ऐसी प्रौद्योगिकी विकसित की गई है जिसमें विकिरण प्रसंस्करण (डोज़ Dmin 60 Gy.) और विशिष्ट भंडारण स्थितियों Dmin 60 Gy) से युक्त एक एकीकृत दृष्टिकोण शामिल है। यह सुनिश्चित करता है कि विकिरण प्रसंस्कृत प्याज़ को व्यावहारिक रूप से 7.5 महीने तक न्यूनतम वज़न घटाने (5 प्रतिशत) और गुणवत्ता विशेषताओं के प्रतिधारण के साथ संग्रहीत किया जा सकता है। इस दृष्टिकोण के साथ, विकसित दृष्टिकोण के महत्व का पता लगाने के लिए हाल ही में 1200 टन के बड़े पैमाने पर सफल वाणिज्यिक परीक्षण भी किए गए। किरणित प्याज़ के मामले में विस्तारित भंडारण के दौरान प्याज़ की गुणवत्ता विशेषताओं को बनाए रखा गया। गैर-किरणित और विकिरण प्रसंस्कृत प्याज़ के प्रतिलेखीय विश्लेषण से पता चला है कि प्रमुख डाउन-रेगुलेटेड जीन में कोशिका विभाजन, कोशिका चक्र, कोशिकीय विकास, विकास, कोशिका दीवार मॉड्यूलेशन, डीएनए प्रतिकृति और गैर-विकिरणित प्याज़ की तुलना में विकिरण उपचारित प्याज़ के बल्बों में मरम्मत शामिल हैं। वर्तमान अन्वेषण प्याज़ संरक्षण के लिए एक प्रौद्योगिकीय समाधान के रूप में कार्य करती है और साथ ही विकिरण मध्यस्थ अंकुरण अवरोध में योगदान करने वाला एक तंत्र प्रदान करती है।

Mitigation of Post-harvest Spoilage

21

Large Scale Commercial Trials for the Mitigation of Post-harvest Spoilage in Onion Through an Integrated Approach

S. Saxena[1], S. Kumar[1], J. Tripathi[1], S. N. Hajare[1,2], N. Bandyopadhyay[1], V. More[1], A. K. Chaubey[1], B. B. Mishra[1,2], B. Sanyal[1,2], C. K. Saurabh[1] and S. Gautam[1,2]*

[1]Food Technology Division, Bhabha Atomic Research Centre, Trombay-400085, INDIA
[2]Homi Bhabha National Institute, Anushakti Nagar, Mumbai-400094, INDIA

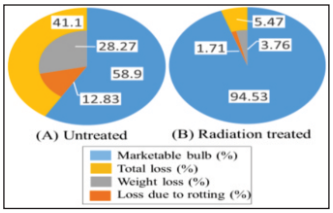

Weight loss profile in non-irradiated and radiation treated onions during storage

ABSTRACT

The long-term extended preservation of onions is limited owing to key post-harvest issues including weight loss, microbial spoilage, rotting and sprouting leading to overall losses ranging from 35-40%. Onions that are kept in routine and traditional storage facilities are highly vulnerable to these spoilage issues. In this context, technological intervention is a pre-requisite to address this issue of immense concern. As an outcome of the R&D efforts at the Food Technology Division, a technology has been developed which involves an integrated approach comprising of radiation processing (Dose: D_{min} 60 Gy) and specific storage conditions (0.2-0.5°C; RH: 65-68%; CO_2: 8000-9000 ppm). This ensures that radiation processed onion can be practically stored for 7.5 months with minimal weight loss (≤ 5%) and retention of quality attributes. With this approach, large scale successful commercial trials to the tune of 1200 Ton were also recently conducted ascertaining the significance of the developed approach. The quality attributes of onion were retained during extended storage in the case of irradiated onions. Transcriptome analysis of non-irradiated and radiation processed onions showed that major down-regulated genes included the ones involved in cell division, cell cycle, cellular growth, development, cell wall modulation, DNA replication, and repair in radiation treated onion bulbs compared to non-irradiated onions. The current investigation serves as a technological solution for onion preservation as well as provides a mechanism contributing to radiation mediated sprouting inhibition.

KEYWORDS: *Onion, Ionizing radiation, Sprouting inhibition, Gene expression, Transcriptome*

**Authors for Correspondence: Satyendra Gautam*
E-mail: sgautam@barc.gov.in

Introduction

Onion (*Allium cepa*) is a highly consumed agri-produce known for its culinary as well as industrial applications [1]. As per the recent data (2020-2021), the annual onion production in India is around 26.91 million MT and Maharashtra is the leading producer followed by Madhya Pradesh and other states (NHB, 2019). Onion crop harvested during the Rabi season accounts for ~65% of the onion production (Tripathy et al., 2014). Its proper storage thus becomes extremely important and relevant to ensure the crop's sustainability as well as fluctuations in onion market price.

However, approx. 35-40% of the onion crop undergoes losses during storage due to weight loss, microbial spoilage, rotting, and sprouting (Laferriere et al., 1988). As per the recent data by the Ministry of Consumer Affairs, Government of India, every year onion crop to the tune of Rs. 11,000 Crore is lost due to improper storage. Therefore, technological interventions specifically in the onion sector are very much essential not only in ensuring a sustained supply of quality produce during the lean period but also in effectively controlling the price stabilization to a greater extent.

To address the issues of sustained availability of quality onions and stabilized market price as well as to establish economic viability, a meticulously designed large-scale study of the most commonly consumed 'Rabi' cultivar was conducted in association with various agencies. Additionally, to unravel the underlying molecular mechanism behind gamma radiation-induced inhibition of sprouting and to provide further molecular insights, transcriptome analysis of onion bulbs was also comprehensively undertaken.

Materials and Methods

Radiation processing and storage

Commercial storage trials were done in multiple batches such as 15 tons (2021), 30 tons (2022), 30 tons (2023), and 1200 tons (2023). Properly cured Rabi onion was procured, packed in mesh bags and radiation processed (D_{min} 60 Gy) at KRUSHAK facility, Maharashtra. Dosimetry was done using a standard Fricke dosimeter. Irradiated onions were transported to multiple cold storage facilities including the newly commissioned cold storage facility at KRUSHAK, Lasalgaon as well as cold storage facility located at Shahapur, Maharashtra (0.2-0.5^{o}C, 65±1% RH) in customized wooden bins with air gaps for proper ventilation.

Quality assessment

Periodically during storage, weight loss, texture (using a Texture Analyzer), and color (using a colorimeter) of onion samples was evaluated. The nutritional profiling of the onion samples was also done as per the standard procedures (BIS, 1984; AOAC, 2001). The onions were also evaluated by the trained panellist for the organoleptic quality attributes on a 9-point hedonic scale.

Transcriptome analysis

To understand the underlying mechanism of gamma radiation induced sprout inhibition in onion bulbs, transcriptome analysis was performed. This involved RNA isolation, library preparation (concentration assessed through qPCR), sequencing (Illumina NovaSeq 6000 was utilized for Paired End Sequencing) and bioinformatics analysis. Alignment of filtered reads was done using Hisat 2 (version - 2.1) genome assembler onto the *Allium sepa* reference genome GCA_000226075.1 Functional annotation clustering was done using DAVID bioinformatics tool (Database for Annotation, Visualization and Integrated Discovery, LHRI). GO enrichment analysis was based on Uniport database and GO terms were placed under molecular function, biological process and cellular compartmentalization.

Results and Discussion

Storage of onion was done in customized cold storage having standardized storage conditions including temperature: 0.2-0.5^{o}C; RH: 65-68%; CO_2: 8000-9000 ppm. Inside the chamber, onion were placed in wooden bins in stacked manner with a provision for proper ventilation (Fig. 1).

Retention of nutrients & sensory attributes during the storage of irradiated onion bulbs

The initial energy content of the irradiated and non-irradiated bulbs varied from 49 to 58 kCal/100 g. In irradiated samples, this did not appear to change significantly throughout

Fig.1: Long term storage of onion in specific cold storage.

the course of storage. Changes in non-irradiated tubers were negligible for the first ninety days; however, because of substantial sprouting, these onion bulbs were unfit for both consumption and nutritional quality evaluation.

The color and texture of radiation treated onion samples remained better as compared to the untreated onion samples. After storage for 7.5 months also, the taste and overall acceptability of radiation treated samples remained unaffected ascertaining the efficacy of radiation processing. Besides, radiation treated bulbs retained their natural internal and external colour over long term cold storage.

Radiation processing mediated sprouting inhibition in onion

Onion has a diploid genome (2n=16), with a genome size of ~16.4 GB. Radiation processing led to sprouting inhibition in onion during storage (Fig. 2). Transcriptome analysis of gamma irradiated and non-irradiated onion bulbs showed total 1194 differentially expressed genes, out of which 862 genes were annotated. Among these, 515 genes showed down-regulation, while 347 genes showed up-regulation of transcript levels in irradiated onion bulbs (depicted as Fig. 3).

The major down-regulated genes were found to be associated with cell division, cell cycle, cellular growth as well as development, cell wall modulation, DNA replication and repair in radiation treated onion bulbs. In the group of cell wall modulation, expansin was maximally down-regulated and pectinesterase was found to have 14 exons down-regulated. Decrease in the expression of these enzymes indicated possible compactness of the cell wall being manifested as unchanged texture parameters in irradiated onions. Auxin responsive family proteins were also found to be down-regulated which included 37 genes with log2 FC of -1.5 to -2.8, while ethylene responsive transcription factors were also found to be down-regulated showing log2 FC of -1.6 to -2.8. Dormancy break in onion bulbs is triggered through modifications in cell wall structure, cellular division and growth which occur through the action of these phytohormones (Puccio et al., 2022). Therefore, down-regulation of their responsive factors will result in dormancy progression, as was observed in the case of irradiated onion bulbs. Interestingly, abscisic acid (ABA) biosynthesis gene, zeaxanthin epoxidases showed up-regulation (log2 FC: 3.4 to 4.7). It has been reported earlier that abscisic acid may serve as a plant growth promoter or inhibitor which depends upon the circumstances. In general, it is known to inhibit growth prior to plant establishment (Chope et al., 2012).

Transcriptome analysis shows that five chalcone synthase exons have been up-regulated in the radiated bulb [Chalcone synthase A: log2 FC 1.8 and Chalcone synthase B: log2 FC 2.0]. Anthocyanin 5-aromatic acyltransferase was found to be up-regulated (log2 FC:1.9) as compared to the non-irradiated onions, indicating the retention of the color pigment in the scales of onion, which was also observed in the color analysis of the irradiated bulb samples. Another very important enzyme lachrymatory factor synthase (LFS) was found to be up-regulated in irradiated bulbs (log2 FC: 6.0). Since LFS is the enzyme responsible for pungency of onions (Imai, 2002; Eady et al., 2008; Silvaroli et al., 2017), as it is known to catalyse the production of lachrymatory factor, propanethial S-oxide, from 1-propenyl sulphenic acid. Up-regulated LFS will provide pungency to onions and their characteristic flavour.

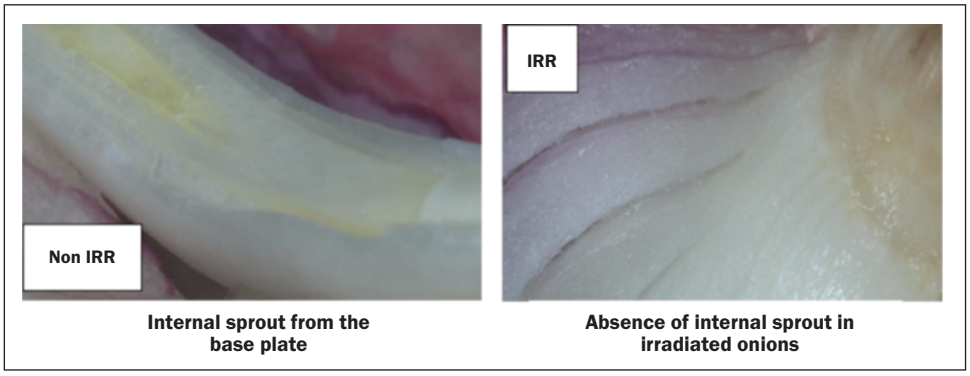

Fig.2: Development of internal sprouting in onion bulb (non-irradiated) and non-occurence in irradiated onion bulbs.

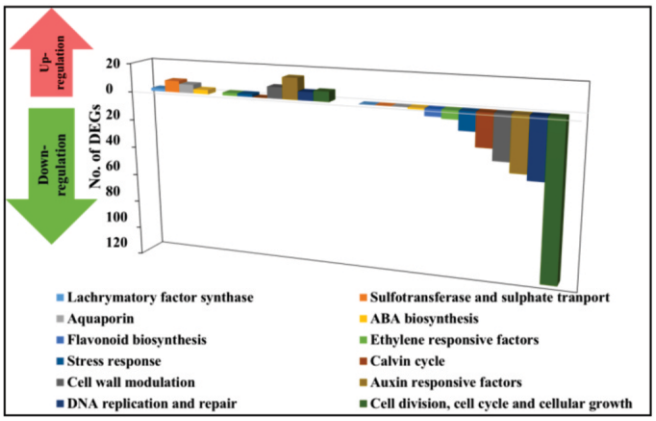

Fig.3: Functional classification of differentially expressed genes in radiation processed onion bulbs as compared to the non-irradiated control bulbs.

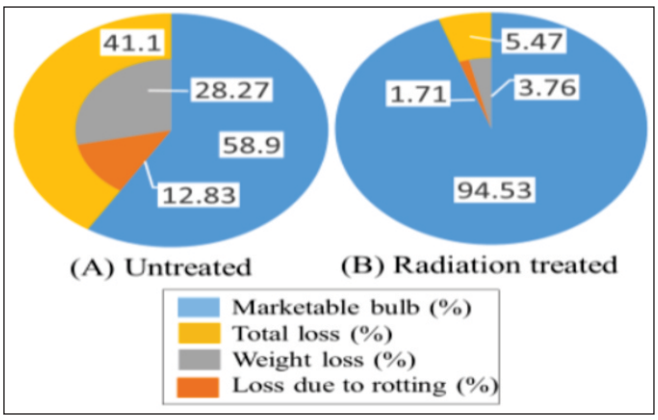

Fig.4: Weight loss profile in non-irradiated and radiation treated onions during storage.

Significant reduction in post-harvest storage loss was noted in radiation treated onion

A substantial 28% loss was noticed in non-irradiated onions, the radiation processed onions suffered a meagre ~4% weight loss. Reduction in bulb weight is a direct consequence of sprouting where, the growing sapling metabolizes the nutrition stored in the scales and thereby resulting in shrinkage. At the end of the storage, 41% of the untreated onion was lost while 95% radiation treated onion was marketable (Fig. 4). These findings ascertain the potential of application of gamma radiation at commercial scale as a sprout suppressant in onion during extended storage.

Loss of firmness of onion bulbs during long term cold storage was improved upon radiation treatment

No significant variation in texture was noted between the untreated control and the radiation treated bulbs immediately after gamma radiation. However, after ninety days of storage, the firmness of non-irradiated control onion decreased noticeably as the control bulbs became 32.9% softer. On the contrary, the loss of firm texture of the radiation treated bulbs over the storage period was not pronounced, as 1.3 and 5.8 % reduction in maximum force were recorded at ninety days and two hundred and twenty-five days respectively with respect to its initial day's value.

Un-irradiated control onion suffered significant moisture loss due to actively transpiring sprouts compared to irradiated bulbs

As discussed above, loss of moisture together with sprouting are the major causes of weight loss and texture deterioration in the stored onion. The loss of moisture became pronounced with progression of storage in both the non-irradiated and irradiated samples. The RH at 65 (± 2) % exerts an inhibitory effect on the mold growth, especially *Aspergillus* growth in the cold storage and, thus higher RH is not conducive for bulk storage at industrial scale. Hence, the difference in moisture content between the control and the radiated samples arises gradually during storage due to indirect effect caused by the differential physiological changes. Suppression of sprouting being the most prominent effect of radiation, it seems that the non-irradiated bulbs underwent dormancy break at an earlier stage and the enhancement in growth could be associated with higher rate of transpiration in the control bulb.

Industrial relevance of integrated approach for long term extended preservation

Overall, it appears that success of long-term storage of onion bulb at large scale depends upon careful regulation of interplay among humidity, temperature and radiation treatment as each of these factors could affect weight loss, dehydration, sprouting, rotting and fungal contamination in a different way. Cold temperature is an essential storage condition for prevention of rotting of bulb and reducing physical water loss by evaporation. Low moisture is a prerequisite for restricting fungal growth while it compromises with evaporation. Additionally, during gradual warming of the cold-stored non-irradiated onion prior to market released resulted in profuse sprouting.

This problem was circumvented by introducing gamma radiation at low dose, which was capable of complete sprout inhibition during long-term low temperature storage as well as during gradual warming of the stored commodity for selling in the market at ambient temperature. Thus, the current large-scale trials indicated that properly cured onions, if treated with gamma radiation at D_{min}: 60 Gy and storage at specific condition (RH 65-68%, temp: 0.2-0.5^{0}C) retain the quality attributes with reasonably low post harvest loss ~ 6 % i.e., 2% rotting & 4% weight loss to thrive over the lean period, leading to price stabilization and its market availability throughout the year.

Conclusion

Post-harvest storage spoilage in onions is quite significant and technological interventions are a pre-requisite to provide sustainable solutions to this challenging concern. The current study provides credible evidence ascertaining the efficacy of gamma radiation processing in ensuring extended preservation of onions based upon various commercial trials with multiple agencies. The outcome of this study provides a substantial basis for the further widespread adoption and implementation of an integrated approach involving radiation technology for the extended preservation of onion with quality retention leading to sustained supply and better commercial gains during the lean period.

Acknowledgment

The authors acknowledge the technical support of M/s. NSSPL and the Department of Consumer Affairs, Ministry of Consumer Affairs, Food and Public Distribution and National Cooperative Consumers' Federation (NCCF) during the course of commercial trials.

References

[1] Suleria, H. A. R., Butt, M. S., Anjum, F. M., Saeed, F., & Khalid, N., Onion: Nature protection against physiological threats. Critical Reviews in Food Science and Nutrition, 2015, 55, 50-66. doi: 10.1080/10408398.2011.646364.

[2] NHB (2019), Indian Horticulture Database, National Horticulture Board, Ministry of Agriculture, Government of India, New Delhi.

[3] Tripathy, P., Sahoo, B.B., Priyadarshini, A., Das, S.K., & Dash, D.K. (2014). Standardization of kharif onion cultivars. International Journal of Bio-resource and Stress Management, 5, 269-274. doi: 10.5958/0976-4038.2014.00566.1.

[4] Gummagolmath, K.C., Lakshmi, S.B.R., Patra, P., Ronitha, A., Price instability of onion in India - An analysis. International Journal of Agricultural Research, 2020, 11, 1-11. doi: 10.15740/has/irjaes/11.1/1-11.

[5] BIS-IS. 11062, 1984, Method for estimation of total dietary fiber in foodstuffs.

[6] AOAC (2001), Fat (Total, Saturated and Unsaturated) in Foods, Hydrolytic Extraction Gas Chromatographic Method," 18th Edition, AOAC Official Method 996.06, AOAC International, Arlington.

[7] Finkers, R., van Kaauwen, M., Ament, K., Burger-Meijer, K., Egging, R., Huits, H., Kodde, L., Kroon, L., Shigyo, M., Sato, S., Vosman, B., Insights from the first genome assembly of Onion *(Allium cepa)*. G3, 2021, 11(9): jkab243. doi: 10.1093/g3journal/jkab243.

[8] Chope, G. A., Cools, K., Hammond, J. P., Thompson, A. J., & Terry, L. A., Physiological, biochemical and transcriptional analysis of onion bulbs during storage, Annals of Botany, 2012, 109(4), 819-831. doi: 10.1093/aob/mcr318.

[9] Wang, X., Wilson, L., & Cosgrove, D.J., Pectin methylesterase selectively softens the onion epidermal wall yet reduces acid-induced creep, Journal of Experimental Botany, 2020, 71, 2629-2640. doi:10.1093/jxb/eraa059.

[10] Coolong, T. W., Randle, W. M., & Wicker, L., Structural and chemical differences in the cell wall regions in relation to scale firmness of three onion *(Allium cepa L.)* selections at harvest and during storage. Journal of the Science of Food and Agriculture, 2008, 88(7), 1277-1286. https://doi.org/10.1002/jsfa.3219.

[11] Cosgrove, D. J., Plant expansins: Diversity and interactions with plant cell walls, Current Opinion in Plant Biology, 2015, 25, 162-172. doi: 10.1016/j.pbi.2015.05.014.

[12] Puccio, G., Crucitti, A., Tiberini, A., Mauceri, A., Taglienti, A., Palumbo Piccionello A., Carimi F., van Kaauwen M., Scholten, O., Sunseri, F., Vosman, B., & Mercati, F., WRKY Gene family drives dormancy release in onion bulbs, Cells, 2022, 11, 1100. doi:10.3390/cells 11071100.

[13] Zhang, C., Li, X., Zhan, Z., Cao, L., Zeng, A., Chang, G., & Liang, Y., Transcriptome sequencing and metabolism analysis reveals the role of cyanidin metabolism in dark-red onion *(Allium cepa L.)* bulbs. Scientific Reports, 2018, 8(1), 14109. https://doi.org/10.1038/s41598-018-32472-5.

[14] Imai, S., Tsuge N., Tomotake M., Nagatome Y., Sawada H., Nagata T., & Kumagai H., An onion enzyme that makes the eyes water, Nature, 2002, 419(6908), 685-685. doi: https://doi.org/10.1038/419685a.

[15] Yasin, H. J., & Bufler, G., Dormancy and sprouting in onion bulbs. II. Changes in sulphur metabolism, The Journal of Horticultural Science and Technology, 2007, 82(1), 97-103. doi: https://doi.org/10.1080/14620316.2007.11512204.

फसलों में नाइट्रोजन-उपयोग दक्षता का अध्ययन

22

टिकाऊ खाद्य सुरक्षा के लिए नाइट्रोजन उपयोग दक्षता में सुधार के लिए बाजरा में अमोनियम ट्रांसपोर्टर जीन की क्षमता को उजागर करनाः एक इनसिलिको विश्लेषण

तनुश्री सरकार और सुमन बक्शी*
नाभिकीय कृषि एवं जैव प्रौद्योगिकी प्रभाग , भाभा परमाणु अनुसंधान केंद्र, ट्रांबे-४०००८५, भारत

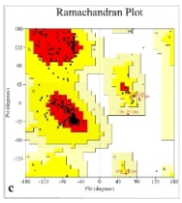

पी. जी. ए. एम. टी. प्रोटीन का रामचंद्रन भूखंड

सारांश

बाजरे (पेनिसेटम ग्लौकम) में अमोनियम ट्रांसपोर्टर (AMT) जीन परिवार के सिलिको विश्लेषण पर केंद्रित है। हम नाइट्रोजन के अवशोषण और उपयोग के आनुवंशिक आधार का पता लगाते हैं, जीन संरचनाओं, कार्यों और विकासवादी संबंधों का पूर्वानुमान लगाने के लिए जैव सूचना विज्ञान का उपयोग करते हैं। बाजरे में AMT जीन के बारे में अध्ययन नाइट्रोजन उपयोग दक्षता (NUE) में सुधार के लिए नई जानकारी के रूप में काम करेगी।

Understanding Nitrogen-use Efficiency in Crops

22

Unlocking the Potential of Ammonium Transporter Genes in Pearl Millet to Improve Nitrogen Use Efficiency for Sustainable Food Security: An *insilico* Analysis

Tanushree Sarkar and Suman Bakshi*
Nuclear Agriculture & Biotechnology Division, Bhabha Atomic Research Centre, Trombay-400085, INDIA

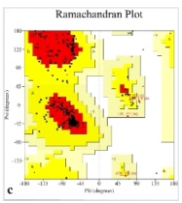

Ramachandran plot of PgAMT protein

ABSTRACT

This study focuses on the *insilico* analysis of the Ammonium Transporter (AMT) gene family in Pearl millet (*Pennisetum glaucum*). We explore the genetic basis of nitrogen uptake and utilization, harnessing bioinformatics to predict gene structures, functions, and evolutionary relationships. Understanding about *AMT* genes in Pearl millet will serve as novel information for improving nitrogen use efficiency (NUE).

KEYWORDS: *In silico analysis, P. glaucum, Ammonium transporter, Nitrogen uptake, NUE*

**Author for Correspondence: Suman Bakshi*
E-mail: sumansud@barc.gov.in

Introduction

Nitrogen (N), a macronutrient for plant growth and development, exists in the form of organic nitrogen, ammonium (NH_4^+), or nitrate (NO_3^-) in soil [1]. Plants have preference for NH_4^+ over NO_3^- due to its direct assimilation into amino acids within plant cells, thus maximizing nutrient uptake efficiency [2]. However, excessive NH_4^+ absorption can be toxic to plants, necessitating precise regulation of NH_4^+ uptake systems to optimize NUE and prevent growth inhibition. Ammonium transporters play a crucial role in NH_4^+ uptake and function as NH_4^+ uniporters, NH_4^+/H^+ symporters, or NH_3/H^+ co-transporters [4]. Pearl millet is a resilient cereal crop and widely grown in arid and semi-arid regions. Understanding and optimizing NUE in this crop is essential for maximizing its productivity and ensuring global food security [6]. Advancements in computational biology have assisted molecular understanding of genes. An *in silico* analysis of the *AMT* gene family was carried out to unravel the genetic basis of ammonium transport in Pearl millet, paving the way for experimental validation and utilization of *AMT* genes for enhancing nitrogen use efficiency.

Materials and Methods

For identification of AMTs, the protein, genomic and coding sequences were downloaded from the IPMGSC (https://cegsb.icrisat.org/ipmgsc/). A Hidden Markov model search was done to obtain ammonium transporter genes. To confirm the candidate gene sequences, belonging to the *AMT* gene family, the NCBI database and HMM-BLAST scores were used. The theoretical molecular weight and isoelectric point of *AMT* proteins were calculated using the ExPASy server [4]. The grand average of hydropathicity (GRAVY) of all the identified proteins was evaluated (www.gravy-calcul-ator.de/). The predictions of the subcellular localization of *AMT* genes were verified using Plant-mPloc online tool [4]. The gene structure of the *AMT*s were determined using the Gene Structure Display Server (https://gsds.gao-lab.org/). Furthermore, the TMHMM server (https://services.healthtech.dtu.dk/services/TMHMM-2.0/) was used for the prediction of transmembrane helices in AMT proteins. Secondary (http://vadar.wishartlab.com/) and tertiary protein (https://swissmodel. expasy.org/) structure was predicted and verified by the PROCHECK test (www.ebi.ac.uk/thorntonsrv/databases/pdbsum/Generate.html), and visualized using Pymol software [4]. The phylogenetic analysis was done by ClustalW and MEGA-XI [4].

Individually, the physical locations of *PgAMT*s were obtained from the database of Pearl millet genome and then, the map of the chromosome location of genes was constructed through the MG2C software (http://mg2c.iask.in/mg2c_v2.1/). Further, *Ks* and *Ka* substitution rates of the paralogs genes were investigated (https://bio.tools/kaks_calculator). Syntenic relationships of the *AMT* genes in *Poaceae* were determined (https://bat.infspire.org/circoletto). To predict cis-regulatory elements on the promoter regions of *PgAMT*s, 2 kb upstream genomic DNA sequences were submitted to the PlantCARE (https://bioinformatics.psb.ugent.be/webtools/plantcare/html/) and visualized using TBtools [4].

Gene	Gene identifier	Strand	Protein (aa)	MW (kDa)	pI	GRAVY	TM	Category
PgAMT2.1	Pgl_GLEAN_10026660	Reverse	492	51.8	7.1	0.555	11	AMT 2
PgAMT3.3	Pgl_GLEAN_10007710	Forward	479	51.85	5.97	0.564	11	AMT 2
PgAMT3.2	Pgl_GLEAN_10030271	Forward	480	51.25	6.29	0.539	11	AMT 2
PgAMT2.3	Pgl_GLEAN_10012021	Forward	445	47.04	7.15	0.513	11	AMT 2
PgAMT2.2	Pgl_GLEAN_10012022	Forward	454	48.56	6.87	0.318	9	AMT 2
PgAMT1.2a	Pgl_GLEAN_10027285	Forward	474	50.24	6.54	0.495	10	AMT 1
PgAMT1.2b	Pgl_GLEAN_10027258	Forward	392	41.34	6.7	0.569	8	AMT 1
PgAMT1.1	Pgl_GLEAN_10009225	Reverse	334	35.55	6.64	0.466	6	AMT 1

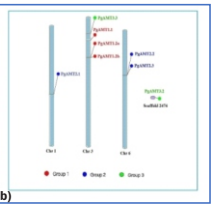

Fig.1: (a) Physicochemical properties of P. glaucum AMT proteins; (b) Chromosomes of P. glaucum showing distribution of PgAMT genes.

Results and Discussion

Among plants, AMT gene was first recognized in Arabidopsis thaliana [2]. In this study, a total of 8 AMT protein sequences were identified and termed as *PgAMT*s. The physiochemical features of AMT proteins include: chromosome location, strand orientation, protein length, molecular weight (MW), isoelectric point (pI), hydrophobicity prediction (GRAVY), subcellular localization, and family categorization were assessed (Fig.1(a)). The length, MW and pI of AMT proteins ranged from 334 (*PgAMT*1.1) to 492 amino acids (*PgAMT*2.1), 35.45 (*PgAMT*1.1) to 51.85kD (*PgAMT*3.3) and 5.97 (*PgAMT*3.3) to 7.15 (*PgAMT*2.3) respectively. Subcellular localization found that of *PgAMT*s were primarily located in the cell membrane. Predictions about the hydrophobic nature of the deduced amino acid sequences indicated that all the AMT proteins exhibit polar characteristics. Chromosomal distribution revealed that *PgAMT*s were located on chromosome 1, 3, 6 and scaffold 2474 (Fig.1(b)). Notably, structural analysis revealed the presence of introns in both the AMT1 and AMT2 subfamilies (Fig.2(a)). The occurrence of introns in the AMT1 subfamily has also been reported in rapeseed [7]. Domain analysis revealed ubiquitous existence of ammonium transporter domain identified in all the queried proteins.

Motif analysis showed that the AMT1 and AMT2 subfamilies had variable motif compositions. Proteins within the same subgroup has identical motif components signifies that differences in the motifs can differentiate subgroups and has evolutionary significance (Fig.2(b)).

Transmembrane domain analysis of *PgAMT*s indicated the presence of 6-11 conserved transmembrane domains (Fig.3(a)). In the secondary structure, *PgAMT*s have shown 56-60% helix, 1-6% beta, 33-40% coil, and 15-17% turn in their structures. The 3D structure of *PgAMT* proteins were predicted based on homology modelling (Fig.3(b)) and found to be analogous to the AMTs analysis in *S. lycopersicum* reported by Filiz and Akbudak (2020). Ramachandran plot was used for validation of the protein 3D structures of *PgAMT* proteins for exploring its biological functions (Fig.3(c)). In the Gene Ontology (GO) study of predicted *PgAMT*s, the AMT1 and AMT2 showed GO terms related to ammonium transportation (Fig.4(a)). The protein-protein interaction study (Fig.4(b-c)) has shown that the proteins associated with *PgAMT* proteins in the network comprise enzymes that participate in nitrogen assimilation and comparable findings were found in the

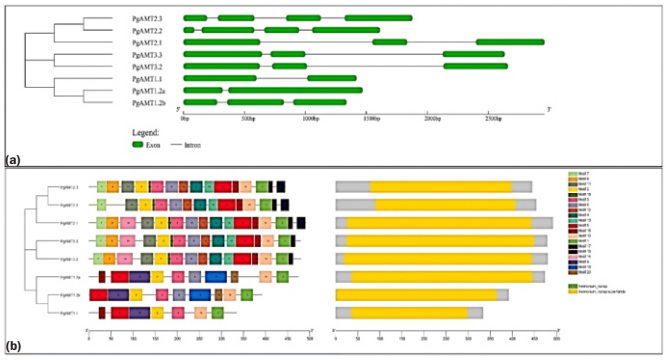

Fig.2: (a) Structure showing exons and introns with the green boxand black lines, respectively; (b) Illustration of conserved protein motifs and conserved domain of PgAMTs.

This paper received the best oral presentation award in the 'International Conference on Millets Cropping in Thar Desert of India and Role of Rural Community in Sustainable Dry Ecology' held at HARSAC, Hisar, Nov. 9-11, 2023.

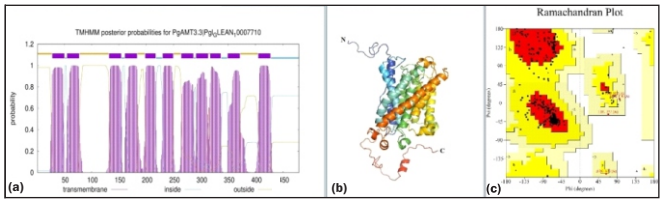

Fig.3: (a) Representative figure of transmembrane structure prediction of AMT proteins; (b) Predicted 3D structure and (c)Ramachandran plot of PgAMT protein.

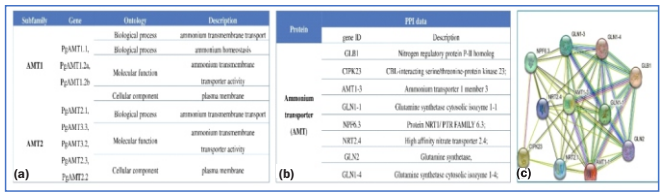

Fig.4: (a) Gene ontology (GO) enrichment analyses of PgAMT genes; (b) List of protein- protein interaction network members of PgAMT proteins; (c)Visualization Protein-Protein Interaction analysis.

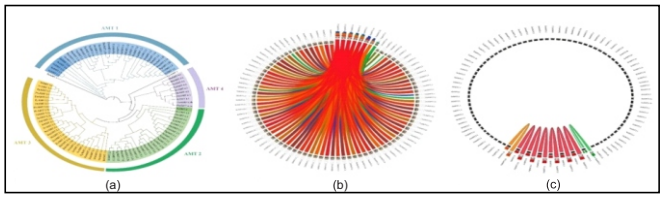

Fig.5: (a) Phylogenetic tree of AMTs of Poaceae; (b) Representation of synteny of PgAMTs; (c)Synteny blocks in best match synteny analysis parameter.

Paralogous Pairs	Chromosomal location	Duplication event	Ka/Ks	Selection
PgAMT1.2b/PgAMT1.2a	Chr 3/Chr 3	Tandem	0.205	Purifying
PgAMT3.2/PgAMT3.3	scaffold 2474/Chr 3	Segmental	0.190	Purifying
PgAMT2.2/PgAMT2.1	Chr 6/Chr 1	Segmental	0.341	Purifying

(a) (b)

Fig.6: (a) Ka/Ks ratios for paralogous PgAMT genes; (b) Chromosomal distribution and inter-chromosomal relationships among AMT genes of P. glaucum.

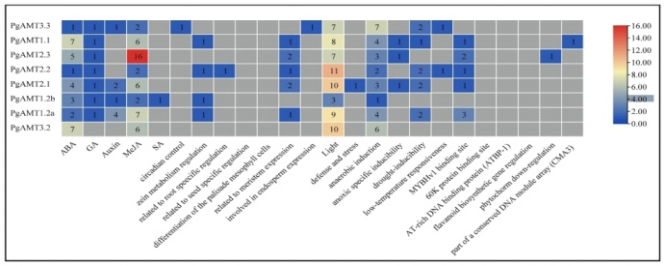

Fig.7: Representation of promoter cis-element analysis of AMT genes in P. glaucum.

analysis of *SlAMT1* of *S. lycopersicum* [5] thus, elucidating an active involvement of AMT proteins in the uptake and assimilation of nitrogen in plants. The phylogenetic analysis categorically separated all plant AMTs to two subfamilies, AMT1 and AMT2 (AMT2/AMT3/AMT4) (Fig.5. a). Phylogenetic grouping showed close association of AMTs in the *Poaceae* family, which includes millets and other cereals. Some similarities exist among AMTs of *Poaceae* with the AMT genes from *A. thaliana*, however, form distinct cladeindicating the divergence of AMTs of monocots from the dicot. The phylogenetic grouping in this study is similar to findings reported in other crops, Apple [1], Soybean [2], Wheat [3] and Tomato [5]. Synteny analysis showed strong conservation among the *PgAMTs* and AMTs of other Poaceae members (Fig.5(b)). The best matched blocks were identified between *PgAMTs* and other members (*S. italica, S. viridis & P. miliaceum*) validating evolutionary similarities (Fig.5(c)).

The cis-elements of *PgAMTs* respond to signals related to plant growth and development (zein metabolism, circadian control), hormones (auxin, gibberellin, and abscisic acid), and environmental stresses (light response, low-temperature, defense, anaerobic conditions, and drought). All the *AMT* gene promoters respond to light, thus, play role in plant growth. Each promoter contains elements for different phytohormones, implying hormone-mediated regulation (Fig.7). In similar studies, Arabidopsis, Tomato and Wheat [3, 4] AMTs display diurnal expression patterns, indicating increased ammonium absorption during daylight hours. Rice AMTs are essential for ammonium uptake under anaerobic conditions. Wheat and rice AMTs are associated with defence response to pathogens [3, 4]. *Lotus japonicus* and *Medicago truncatula* AMTs facilitate ammonium transport in plant-microbe symbiosis [4].

Conclusion

Through in silico analysis, a total of eight *AMT* genes were identified, categorized into AMT1 and AMT2 subfamilies. Investigation of gene sequences, chromosomal locations, and conserved motifs underscores their conservation. These findings elucidate the role of AMTs in efficient ammonium N utilization and stress adaptation paving the way for efficient utilization of AMTs in Pearl millet.

Acknowledgment

Financial support provided to Dr. Tanushree Sarkar (Research Associate) from Bhabha Atomic Research Centre, India is gratefully acknowledged.

References

[1] Huang L., Li J., Zhang B., Hao Y., Ma F., Genome-wide identification and expression analysis of AMT gene family in apple (Malus domestica Borkh.), Horticulturae, 2022, 8, 457.

[2] Yang W., Dong X., Yuan Z., Zhang Y., Li X., Wang Y., Genome-wide identification and expression analysis of the ammonium transporter family genes in soybean. Int J MolSci., 2023, 24.

[3] Sarkar T., Bakshi S., Ammonium transporter gene family in wheat (Triticum aestivum L.): Bioinformatics, physiological, evolutionary and expression analyses under nitrogen stress, In Jasrotia et al (Eds.), 5th International Group Meeting on Climate-Proofing Cereal Agriculture: Strategies for Resilience and Sustainability 2024, 2024, 76.

[4] Sarkar T., Bakshi S., Ammonium transporter genes in millets: Insights into structure, function, evolutionary conservation, divergence, and phylogenetic analysis, Genet Resour Crop Evol., 2024. https://doi.org/10.1007/s10722-024-02092-2

[5] Filiz E., Akbudak M. A., Ammonium transporter 1 (AMT1) gene family in tomato (Solanum Lycopersicum L.): Bioinformatics, physiological and expression analyses under drought and salt stresses, Genomics, 2020, 112, 3773-3782.

[6] Shukla S. S., Panda S. K., Nitrogen Use Efficiency regulates drought stress in Pearl Millet Genotypes: Morpho-Physiological Evaluation, Agriculture, 2023, 13, 680.

[7] Dai J., Han P., Walk T. C., Yang L., Chen L., Li Y., Gu C., Liao X., Qin L., Genome-Wide Identification and Characterization of Ammonium Transporter (AMT) Genes in Rapeseed (Brassica napus L.), Genes, 2023, 14, 658. https://doi.org/10.3390/genes14030658.

Understanding the regulation of human Topoisomerase 1 (TOP1) dynamics and devising TOP1-directed therapeutic strategies

TOP1-DNA covalent complexes (TOP1ccs) are transient DNA-protein adducts arising from TOP1-mediated relaxation of DNA supercoils during replication and transcription. Pathological or drug-induced stabilization of TOP1ccs result in accumulation of lethal (replication and transcription-associated) DNA double strand breaks. Multiple cellular mechanisms (*viz.*, TOP1 phosphorylation, Poly-ADP-ribosylation, SUMOylation, ubiquitination and NEDDylation) efficiently sense TOP1ccs and swiftly degrade or remove the same. Cancer cells are hyper-dependent on TOP1, making it an attractive target of anticancer therapy. Multiple TOP1-targeting drugs (Topotecan, Irinotecan etc.) are in clinical use against ovarian, cervical, lung and pancreatic cancers. TOP1cc removal/degradation factors confer resistance to such drugs. The foregoing work revolves around (a) discovery of CHK1 kinase as a regulator of TOP1 catalysis, and (b) the development of a dual inhibitor of TOP1 and poly-ADP-ribose polymerase (PARP) for efficient targeting of cancer cells.

In order to discover novel TOP1 regulators, we screened 25 small molecule kinase inhibitors (targeting ~42 cellular kinases) for their potential to alter cellular TOP1cc levels. Our results revealed the master checkpoint kinase CHK1 as a positive hit. We validated the finding through biochemical and Fluorescence Recovery After Photobleaching (FRAP) assays. We established the intracellular interaction between CHK1 and TOP1 (through Proximity Ligation and co-immunoprecipitation assays), and demonstrated that CHK1 phosphorylates TOP1 in vitro. Tandem mass spectrometric analysis of catalytically engaged TOP1 from cells revealed that Serine 320, one of the (*in silico*) predicted CHK1 target sites on TOP1 is phosphorylated inside cells. A phospho-resistant mutant of TOP1 (TOP1S320A) revealed that genetic ablation of CHK1-mediated TOP1 phosphorylation results in constitutive stabilization of TOP1S320A on the genome. This was accompanied by copious induction of replication and transcription-associated DNA damage, stabilization of RNA-DNA hybrids (R-loops) and large-scale chromosomal abnormalities. These, and multiple other observations established a previously unreported role of CHK1 in suppression of genomic instability through regulation of TOP1 catalytic activity inside cells. Hence, our study revealed a novel pathway of CHK1-mediated maintenance of genomic stability through regulation of TOP1 (Fig. 1, Left panel).

Owing to the pivotal role of poly-(ADP-Ribose) polymerases (PARPs) in cellular resistance to TOP1 inhibitors, combinatorial inhibition of PARPs and TOP1 inhibitors has been tested in multiple clinical trials. However, pharmacokinetic incompatibilities and dose-limiting toxicities have resulted in mixed outcomes. In order to circumvent such issues, we envisaged the development of a single molecule dual inhibitor of TOP1 and PARP, which would facilitate temporally coupled inhibition of both enzymes. We developed 11 candidate inhibitors involving active pharmacophores derived from Olaparib (an FDA approved PARP inhibitor) and 1,8-naphthalimide (an investigational TOP1 inhibitor). One candidate, DiPT-4, showed significantly higher cytotoxic potential compared to both Olaparib as well as 1,8-naphthalimide. DiPT-4 poisons TOP1 and inhibits PARP activity in vitro. Further, DiPT-4 not only stabilizes TOP1ccs inside cells, but inhibits PARP activation in response to same. Consequently, unlike classical TOP1 poisons, DiPT-4 induces long-lived TOP1ccs without significant degradation of cellular TOP1. Finally, theoretical calculations revealed that DiPT-4 satisfies the majority of criteria for druggability. Our study provided a proof-of-concept for the development of dual inhibitors of TOP1 and PARP1 with significant clinical potential (Fig. 1, Right panel).

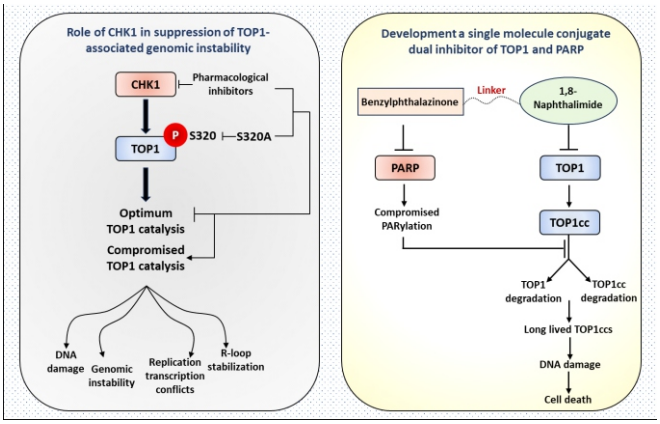

Fig.1: Left panel: A distinct role of CHK1 in prevention of stabilization of TOP1-DNA covalent complex and genomic instability. Right panel: Development of dual inhibitor of Top1 and PARP1 for effective killing of cancer cells.

Taken together, our work reveals novel post-translational regulation of TOP1, and how TOP1 post-translational modifications can be targeted for efficient anticancer therapy.

Highlights of the work being carried out by Ananda Guha Majumdar under the supervision of Dr. Mahesh Subramanian (Guide) and Dr. Birija Sankar Patro (Co-guide) as a part of his doctoral thesis work. This work will be submitted for Ph.D. degree (Life Sciences) to Homi Bhabha National Institute in 2025.

Premature Chromosome Condensation based rapid biodosimetry strategies for high doses and non-uniform exposures

Radiation biodosimetry is an essential part of regulatory investigations, triage and medical management of radiation overexposures. Chromosomal aberration assessed in peripheral blood lymphocytes (PBL) are classical and gold standard biodosimetry markers. To assess the aberrations, PBLs which are usually at resting phase must be stimulated and brought to metaphase for distinct visualization under microscope. Dose estimation takes around 3-5 days for and may require counting up to1000 metaphases. Further, high dose exposures lead to poor metaphase yield due to cell cycle arrest, interphase or mitotic death of heavily aberrated cells. Hence, metaphases may not be available for dose assessment. Challenge further grows when the exposures are localized to a part of the body leading to dilution of cells from un-exposed cells in the blood and resulting in underestimated doses.

Under this thesis, G_0-PCC where mitotic cell fusion to PBLs is used to induced chromosome condensation allowing microscopic visualization at resting phase itself was proposed as alternative, and extensively researched for high dose exposures. With this technique, rapid biodosimetry within 4-6 hours post blood collection can be carried out using quick counting of fragments after Giemsa staining (G_0-PCC-Fragments). It is suitable for high dose and partial body exposure dosimetry as well. In the study, a refined SOP for G_0-PCC was developed, multi-faceted applications were showcased, calibration curve were established to extrapolate dose estimates from an unknown sample. Most importantly, a novel methodology was formulated to distinguish partial exposures from whole body exposures and to derive accurate dose estimations. The technique was refined for the use of cryopreserved mitotic cells to avail them instantly for G_0-PCC upon receipt of accidental exposure case. Further, it was combined with fluorescent in-situ hybridization to analyze aberrations more accurately. G_0-PCC-FISH with locus or chromosome specific probes enabled identification of dicentrics (centromere-FISH), chromosome specific breaks/interchanges (whole chromosome painting and multiplex FISH) and within chromosome arrangements like inversions and interstitial deletions (mBAND-FISH) at resting phase stage of the PBLs. Broad range calibration curves (0-15Gy Co-60 Gamma ray) were established for overall fragments and for breaks combined with interchanges using G0-PCC-FISH for chromosome 1, 2 & 4. For the fragments a linear radiation response was found with a slope of 1.09 ± 0.031 fragments/cell Gy^{-1}(R^2=0.999) with

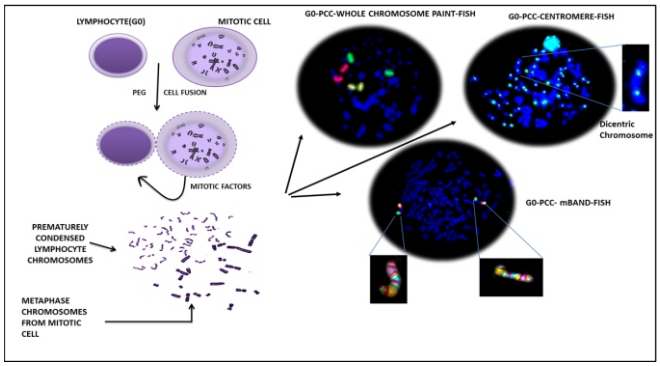

Fig.1: A pictorial diagram of G0-PCC technique and its extensions with FISH (Yadav et.al. Scientific Reports, (2021) 11:13498).

intercept/background of 0.19 ± 0.10 while for G_0-PCC-FISH response followed a linear quadratic curve with $Y=\alpha D+\beta D^2+c$ *where* α= 0.28±0.037 Gy^{-1}, β= 0.039±0.004 Gy^{-2} and c= 0.0568 respectively (R^2= 0.985). The curves were validated with 5 dose blinded samples. Further, no significant difference in the response was observed with respect to age and sex which was evaluated for at 0, 2 & 4 Gy. Further, partial body exposures were simulated ex-vivo with the dilution of exposed blood samples with un-exposed ones. Dilution factors as well as doses were varied among the simulations (8Gy 1:0, 1:1, 1:3 & 1:5 and 4Gy 1:1, 12Gy 1:1). Statistical distribution and dispersion analysis were carried out with three individual donors for all the simulations and compared with that of whole-body exposures. Finally, multiple key features were identified which can distinguish partial exposures from whole body exposures and derive accurate dose estimations. The sensitivity and accuracy of the dose estimates were compared with that of conventional dicentric assay and G_0-PCC-Fragment in all the donors and simulations. It was observed that sensitivity and accuracy of Dicentric assay reduced with increasing dilution and dose but not in PCC methods. G_0-PCC-FISH was found to be most accurate among all.

Highlights of the work carried out by Usha Yadav under the supervision of Dr Nagesh N Bhat as a part of her doctoral thesis work. She was awarded PhD degree from Homi Bhabha National Institute in Life Sciences in 2022.

Studies on Tumor Microenvironment Induced Changes in T Cell Differentiation

Cancer is the unregulated proliferation of transformed cells that can invade nearby tissues. In addition to transformed cells, the tumor microenvironment (TME) includes innate immune cells, adaptive immune cells, fibroblasts, stromal cells, and the extracellular matrix. Cytokines in the TME have an important role in the communication between different cell types, which influences tumor growth and evasion. Transforming growth factor-β (TGF-β) and T regulatory cells (Treg) play a significant role in tumor-induced immunosuppression. Despite the fact that B cells are abundant in tumors, their role in tumor regulation is little understood. Though the involvement of regulatory B cells (Breg) in inflammatory and autoimmune disorders is known, its role in cancer has not been fully investigated.

This thesis investigates Breg's role in Treg differentiation and immunosuppression in cancer as well as the molecular mechanisms of TGF-β-induced Treg generation. We identified that the fibrosarcoma secreted prostaglandin E2 (PGE2), a signaling molecule produced by the breakdown of membrane arachidonic acid by the action of the cyclooxygenase (COX) enzyme, which conferred a Breg like immunosuppressive function in B cells. This tumor-evoked regulatory B cell (tBreg) subtype was found with a unique combination of surface markers along with a TGF-β and IL-10 secretory phenotype not previously reported. Blocking PGE2 synthesis by NS-398, a pharmacological inhibitor of COX2 or PGE2 signaling in B cells with PGE2 receptor antagonists, inhibited the generation of tBregs. The administration of NS-398 to tumor bearing mice markedly reduced tumor burden, lowered Breg and Treg production and rescued T cell responses. These tBregs converted $CD4^+$ T cells to Treg cells, suppressing T cell responses via TGF-β release. SB431542, a small-molecule inhibitor of TGF-β receptor, inhibited TGF-β signaling in T cells, prevented the formation of tBregs, and rescued T cell responses in vitro. The administration of SB431542 to tumor-bearing mice significantly reduced tumor burden and increased T cell responses. To identify inhibitors of Tregs, we screened 160 compounds from an epigenetic inhibitor compound library, as epigenetic pathways are involved in the differentiation of naïve T cells to Tregs. Using an IFN-γ production-based functional screening strategy, we identified two compounds, EPZ004777 and FG-2216, that lowered the expression of Foxp3, the master regulator of Tregs, and its downstream target genes and impaired Treg's suppressive capacity.

Epigenetic modifications are heritable alterations in gene expression that are not attributable to changes in DNA sequences. The precise epigenetic changes involved in TGF-β-induced Treg cells are not fully understood. Using chromatin immunoprecipitation (ChiP) assays, we performed epigenetic profiling of the *Foxp3* locus in Tregs. TGF-β-induced Tregs showed higher levels of H3K4me3, H3K27ac, and lower levels of H3K27me3 and DNA methylation. In Treg generated by physiologically relevant tBregs and PGE2Bregs, higher H3K4me3 and lower H3K27me3 were observed. However, either DNA methylation

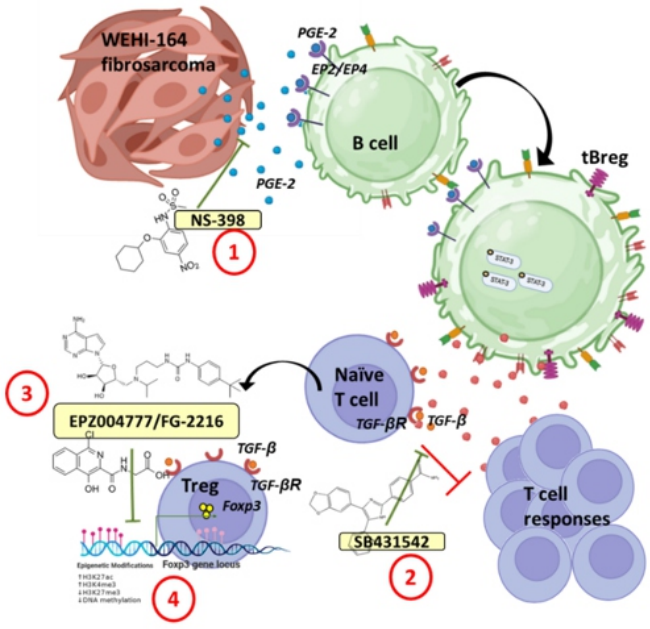

Fig.1: Immunosuppression in the tumor microenvironment: (1) NS-398, a pharmacological inhibitor of COX2; (2) SB431542, a small-molecule inhibitor of TGF-β receptor; (3) EPZ004777 and FG-2216, epigenetic inhibitors of T regulatory cells; (4) Epigenetic landscaping of the Foxp3 locus in T regulatory cells.

was significantly reduced with no change in H3K27ac or H3K27ac was hyperacetylated with no alteration in DNA methylation. Epigenetic profiling of the *Foxp3* locus therefore indicate that increasing H3K4me3 or decreasing H3K27me3 as well as increasing H3K27ac or decreasing DNA methylation are the minimal epigenetic requirements for Foxp3 expression and Treg phenotype.

Many researchers have elucidated the roles of several players in the TME, including dendritic cells, macrophages, NK cells, etc., but the role of B cells and tumor-evoked Bregs has received less attention. The work described in this thesis addresses this critical aspect of the TME and answers several key problems. This is the first-time epigenetic landscaping of TGF-β-induced Tregs has been done to determine the minimum needed modifications. This thesis has also identified two promising epigenetic modifiers as well as COX-2 and TGF-βR inhibitors as potential immunotherapeutics.

Highlights of the work carried out by Kavitha Premkumar under the supervision of Dr. Bhavani S. Shankar (Guide) as a part of her doctoral thesis work. She was awarded a Ph.D. degree from Homi Bhabha National Institute in Life Sciences in 2022.

Studies on Macrophage Conditioned Medium Induced Tunneling Nanotubes and Microplasts Formation in Human Breast Cancer Cells

Tumor-associated macrophages (TAMs) are major infiltrating innate immune cells in the tumor microenvironment (TME) and are associated with poor prognosis in breast cancer patients. The complex milieu of inflammatory cytokines, chemokines, and growth factors secreted by infiltrating macrophages in the TME acts on cancer cells in a paracrine manner and regulates several stages of cancer progression. However, the effect of pro-inflammatory cytokines secreted by macrophages on novel modes of communication via tunneling nanotubes (TNTs) and microplasts in cancer remains elusive. This thesis explores the impact of macrophage-conditioned medium (MΦCM) on breast cancer cells, revealing that MΦCM mimics the inflammatory TME, induces an epithelial-to-mesenchymal transition (EMT) phenotype, and enhances cell migration in MCF-7 cells. Additionally, MΦCM induces TNT formation and stimulates the release of cytoplasmic fragments, referred to as microplasts.

MΦCM-treated MCF-7 cells were found to be viable and migratory, suggesting that microplasts derived from these cells are not apoptotic bodies. Time-lapse microscopy reveals that microplasts exhibit independent migration and also show the dynamic process of microplast release from parent cancer cells through TNT-like structures. In addition, the data also show novel modes of TNT formation facilitated by migratory microplasts, leading to the formation of a complex network of cells. The presence of metalloproteinases in microplasts suggests their role in invasion and metastasis. Furthermore, transcriptomic and proteomic analyses of isolated microplasts reveal their similarity to parent cells in terms of mRNA and protein cargo, potentially serving as carriers of intercellular signalling.

Despite the known roles of TNTs and macrophages in cancer, the impact of macrophage-induced TNTs on therapy resistance remains unclear. Additionally, the mechanisms underlying macrophage-driven TNT and microplast formation are not well understood. In this study, it was shown that TNT formation in MΦCM-treated MCF-7 cells contributed to increased resistance to doxorubicin. Transcriptomic analysis of these treated cells revealed activation of the NF-κB and focal adhesion pathways, along with upregulation of genes involved in epithelial-mesenchymal transition (EMT), extracellular remodeling, and actin cytoskeleton reorganization. By using pharmacological inhibitors targeting key proteins within these pathways, it was demonstrated that TNT and microplast formation in MΦCM-treated MCF-7 cells was mediated by the PKC/Src/NF-κB and p38 signaling pathways. These findings provide valuable insights into the complex mechanisms of intercellular communication in breast cancer, driven by TAMs, and highlight potential therapeutic targets for cancer treatment.

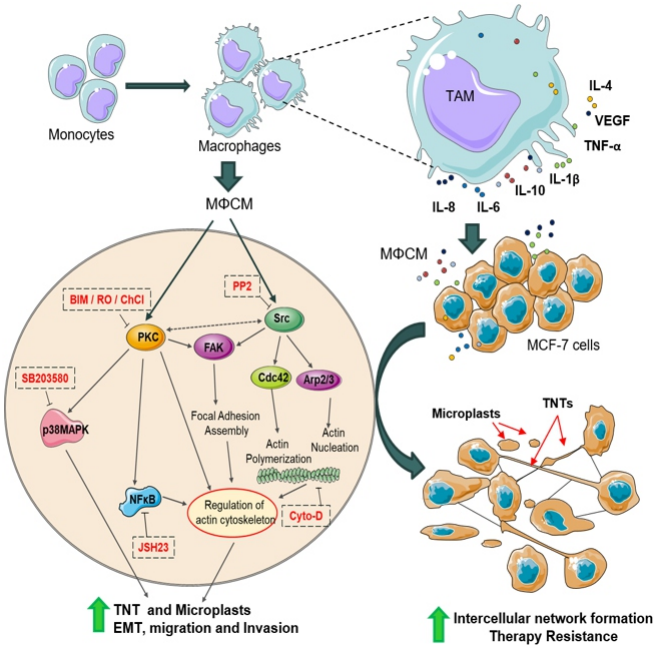

Fig.1: Macrophage conditioned medium (MΦCM) increased epithelial-to-mesenchymal transition (EMT), migration, tunneling nanotube (TNT), and microplast formation in MCF-7 cells via PKC, Src, NF B, and p38 signaling (Melwani et. al, BBA Reviews on Cancer, 2023 and Melwani et. al, Cellular Signaling, 2024).

Highlights of the work carried out by Dr. Pooja Kamal Melwani under the supervision of guide Prof. B. N. Pandey as a part of her doctoral thesis work. She was awarded PhD degree from Homi Bhabha National Institute in Life Sciences in 2023.

Development of Peptides Targeting HER2-Receptor Overexpression in Breast Cancer

Breast cancer has the highest global incidence amongst all the cancer types. Early detection is the key for timely intervention and proper treatment planning. Human epidermal growth factor receptors (HER2) are over-expressed in breast cancers and are associated with poor prognosis and aggressively metastatic disease. The present work focused on development of HER2-targeting ligands for breast cancer detection and therapy. Towards this, peptides exhibiting attractive advantages of high target affinity, specificity, favorable pharmacokinetics, and ease of synthesis were chosen as suitable ligands. A HER2-targeting A9 peptide was subjected to several modifications (pegylation, cyclization, D-amino acid incorporation, retro variant) to overcome the challenges of *in vivo* enzymatic degradation.

The peptides were synthesized by solid phase synthesis methodology manually (Fig. 1), purified and characterized. Peptides were then radiolabeled with theranostic radionuclide, $^{177}LuCl_3$. ^{177}Lu-labeled original A9 peptide exhibited rapid blood clearance resulting in low tumor uptake. It also underwent high metabolic degradation. The pegylated variant, [^{177}Lu]Lu-DOTA-PEG$_4$-A9 demonstrated improved metabolic stability, tumor uptake and retention.

Further the peptide was cyclized on-resin by copper (I)-catalyzed azide-alkyne cycloaddition (CuAAC) 'click reaction'. The cyclic variant [^{177}Lu]Lu-DOTA-c[Tz]-A9 exhibited increased binding affinity towards HER2-positive cells, high metabolic stability and tumor uptake. To introduce changes in the backbone all the L-amino acids were replaced by D-amino acids and thus inverso- and retro-inverso A9 peptides were synthesized. These peptides had enormously enhanced metabolic stability, tumor uptake/retention was observed to be higher for the retro-inverso variant. Another analogue studied was the retro-variant where the C- and N-terminal were swapped and the L-amino acids were arranged in reverse manner. The retro variant showed most promising results with highest tumor uptake amongst the six investigated A9 analogs (Fig. 2). SPECT/CT imaging studies further demonstrated higher *in vivo* tumor retention of the retro analogue (Fig. 3).

In conclusion arrangement of amino acid sequence in reverse manner either D-amino acids (retro-inverso peptide) or L-amino acids (retro peptide) conferred improved features to the A9 peptide. Swapping of C- and N-terminal (retro) introduces significant changes in the backbone of the peptide. In the case of presently studied HER2-targeting A9 peptide, swapping imparted positive features suggesting higher participation of backbone towards receptor interaction.

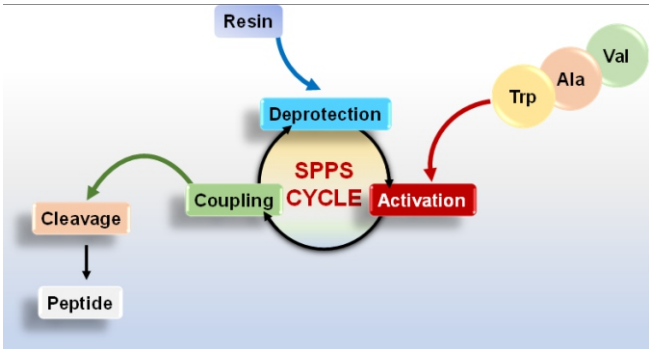

Fig.1:Solid phase peptide synthesis methodology scheme

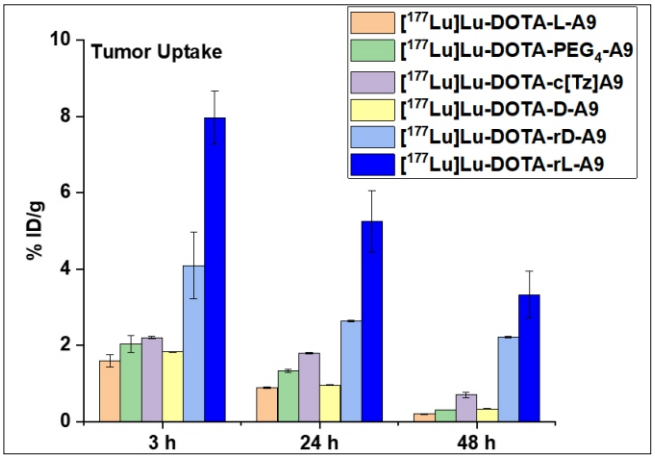

Fig.2: Tumor uptake of A9 peptide analogues.

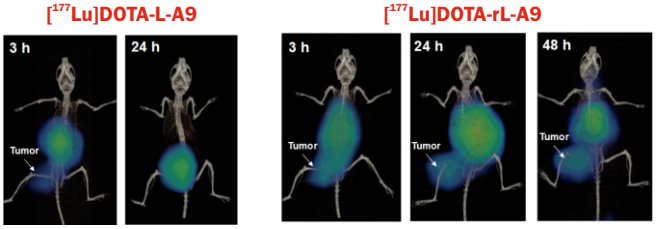

Fig.3: SPECT/CT images of female SCID mice bearing SKBR3 tumor xenografts.

Highlights of the work carried out by Amit Kumar Sharma under the supervision of Dr. Drishty Satpati (Guide) and Dr. Tapas Das (Co-guide) as a part of his doctoral thesis work. He was awarded PhD degree from Homi Bhabha National Institute in Chemical Sciences in 2024.

Mechanistic Studies on Ubiquicidin-Membrane Interaction & Development of Infection Imaging Probes

The work presented in this thesis encompasses research aimed at comprehending the interaction mechanism between the antimicrobial peptide Ubiquicidin (UBI) and bacterial membranes. Subsequently, infection imaging probes were developed for detecting bacterial infections like osteomyelitis and fever of unknown origin, which pose challenges for conventional detection techniques.

Significantly, this thesis marks the first report providing a mechanistic understanding of the antimicrobial action of ribosomal protein S30/Ubiquicidin (UBI). Using phospholipid membrane models, various biophysical studies i.e., Dynamic Light Scattering (DLS), Circular Dichroism (CD), Infrared Spectroscopy (IR), and Quasielastic Neutron Scattering (QENS) were conducted to unravel the intricacies of UBI-membrane interactions. Additionally, microbiological investigations were carried out to grasp the impact of UBI on bacterial growth and survival. Overall, these findings revealed that UBI selectively binds to bacterial membranes, inducing a conformational change in this peptide. This interaction exerts a catastrophic effect on the bacterial membrane by altering its fluidity, causing permeabilization, and inducing depolarization, ultimately leading to the loss of bacterial viability. Furthermore, it was demonstrated that UBI fragments, i.e., UBI (29-41) and UBI(31-38), also retained their binding and selectivity towards bacteria. Importantly, UBI and its derivatives were shown to be non-toxic to human cells, through haemolysis and cell toxicity studies.

Leveraging the mechanistic insights gained through biophysical and microbiological methods, efforts were made to develop UBI-derived peptide fragments into infection imaging radiotracers for SPECT (Single Photon Emission Computed Tomography) and PET (Positron Emission Tomography) imaging to detect S. *aureus*-driven focal infections. UBI fragments, namely UBI (29-41) and UBI (31-38), were labeled with ^{99m}Tc and ^{68}Ga for this purpose, and the resulting radiotracers underwent *in vitro* and *in vivo* studies. UBI-derived radiotracers were confirmed to be selective towards bacteria through *in vitro* uptake in bacterial cells and *in situ* detection of S. *aureus* in animal models of infection and sterile inflammation. Furthermore, efforts were also made to enhance the detection sensitivity and salt tolerance of UBI-based radiotracers by modifying UBI (29-41). The introduction of the Lysyl-phosphatidyl-glycerol (Lys-PG) specific group, 2-APBA, at the C-terminal of UBI (29-41) resulted in an improved infection imaging probe, which interacted synergistically via electrostatic and covalent modification of Lysyl-PG via iminoboronate with the bacterial membrane. Through this work, the conjugation of 2-APBA is demonstrated as an effective strategy for improving the therapeutic potential of existing antimicrobial peptides (AMPs). Remarkably, this work also resulted in the successful clinical translation of ^{68}Ga-labeled UBI fragments as a PET-based radiotracer for the early identification of bacterial focal infections. The formulated radiotracers were evaluated at KMCH, Coimbatore, PGI, Chandigarh, and MPMMRC, Varanasi, and could detect lung infection, soft tissue infection, bone prosthesis, and spinal TB (tuberculosis) infections with high sensitivity (Fig. 1).

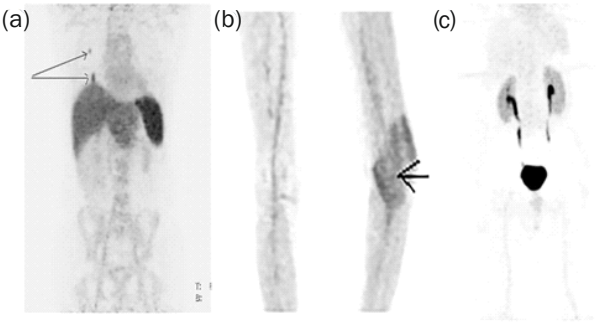

Fig.1: PET/CT images of patients injected with ^{68}Ga-UBI (31–38) at 1 h p.i. (a) lung infection (true positive scan). (b) soft tissue infection in left knee (true positive scan) joint. (c)Image of a suspected left hip prosthesis infection (true negative scan).

Highlights of the work carried out by Jyotsna Bhatt under the supervision of Dr. Archana Mukherjee (Guide) and Dr. Mukesh Kumar (Co-guide) as a part of her doctoral thesis work. She was awarded Ph.D degree from Homi Bhabha National Institute in Life Sciences in 2023.

Interplay Between DNA Damage Repair, Replication Stress and Autophagy Under the Functional Deficiency of PARP in Cancers

Small molecule inhibitors of Poly (ADP-ribose) polymerases (PARPi) are approved for clinical usage in patients with hereditary breast and ovarian cancers with compromised homologous recombination (HR) mediated DNA repair, a strategy referred to as synthetic lethality (Fig. 1A). However, therapeutic resistance remains a challenge, with only about ~50% of the target cohort of patients (*viz*. 5-15% of the total breast and ovarian cancer patients that harbour BRCA1/2 mutations, or are HR deficient) responding well to this therapy (Fig. 1B).

Recent findings indicate that HR-proficient cancers can also be targeted with the combination of PARP inhibitors and chemosensitizing agents. This necessitates research into avenues targeting cancers with PARP inhibitors along with targeting alternative pathways in HR-proficient cancers. Moreover, why certain HR-proficient cancers are *de novo* PARPi resistant, while certain others are comparatively sensitive was envisaged in this thesis. Understanding these mechanisms enable extension of PARPi therapy to a wider set of patients with BRCA1/2-wild-type (WT) or HR-proficient cancers.

Autophagy, a cellular process aiding in the removal of dysfunctional and superfluous biomolecules and organelles, is implicated in acquired chemoresistance and is recognized for its interplay with DNA damage repair pathways. However, molecular underpinnings of this interplay, and how and if this could be exploited for cancer therapy, is unclear. In this work, we successfully demonstrated that autophagy confers *de novo* resistance to PARP inhibitors in HR-proficient breast cancers. Using chloroquine, an anti-malarial drug now repurposed as an autophagy inhibitor, we show that combined PARP and autophagy inhibition leads to better therapeutic outcome in breast cancer cells and in SCID mice xenograft models. Mechanistically, DNA repair switched from faithful HR pathway to deleterious 53BP1-mediated NHEJ which further led to genomic instability and mitotic catastrophe under this autophagy- and PARP inhibited condition (Fig. 1B,C). Additionally, we showed synergistic induction of cancer cell death both *in vitro* and *in vivo*, when resveratrol, natural molecule, was combined with PARPi, talazoparib. This synergistic action of the combination was attributed to the inhibition of late-stage autophagy and suppression pro-survival pathways such as PI3K leading to p38 mediated apoptosis and mitotic catastrophe (Fig. 1B,C).

DNA replication is a vulnerability in many cancers and replication stress induction presents as an attractive therapeutic strategy that can be harnessed for efficient cancer therapy. PARP inhibitors induce replication stress mainly by trapping PARPs on DNA forming PARP-DNA-PARPi ternary complexes, and dysregulating replication fork speed. Resveratrol analogues are also reported to enhance replication stress. In this regards, we have shown the combinatorial therapies involving talazoparib with resveratrol analogue, 4,4'-dihydroxystilbene (DHS), post screening a library of resveratrol analogues for DNA damage induction and HR downregulation. Talazoparib (PARPi) *plus* DHS was found to induce extensive DNA damage double strand breaks, and downregulate RAD51, a key modulator of both DNA repair and replication, to induce extensive replication stress and S-phase catastrophe (Fig. 1D). This suggests a novel replication-dysfunction-mediated approach for enhancing PARPi sensitivity in cancers.

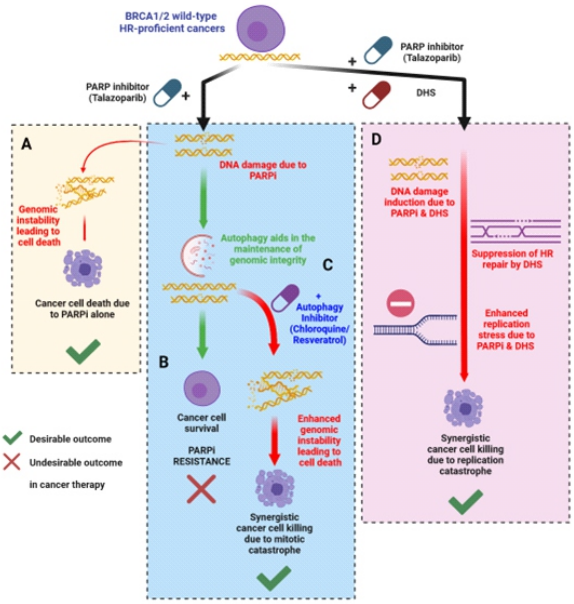

Fig.1: Schematic of the PARP inhibitor combinatorial strategies used to sensitize BRCA1/2 wild-type HR proficient cancers. (A, B, C and D represent different outcomes of PARPi therapy as depicted).

In conclusion, we have identified that the combination therapies involving PARP inhibition with agents that suppress/modulate autophagy such as chloroquine and resveratrol, or those inducing replication stress such as DHS show promise in sensitizing HR-proficient cancers to PARPi induced cell death (Fig. 1A-D). This study unravels the potential for the broadening of the limited scope of PARP inhibitors to a larger population of patients with HR-proficient breast cancers and for tumours resistant to PARP inhibitors.

Highlights of the work carried out by Ganesh Pai B under the supervision of Dr. Birija Sankar Patro (Guide) as a part of his doctoral thesis work. This PhD thesis was submitted recently (May, 2024) to Homi Bhabha National Institute for the PhD Award in Life Sciences.

Advancing Retrospective, Cumulative and Rapid Biodosimetry- Innovative Molecular Cytogenetics Approach

As scientific advancements continue, the utilization of radiation is becoming more prevalent in our daily lives, thus increasing the likelihood of inadvertent exposures. Biodosimetry serves as a crucial tool, providing accurate dose measurements in the absence of physical dosimetry methods or corroborating results obtained through physical dosimetry, particularly in cases of exposures exceeding 100 mGy. This study investigates various biodosimetry methods to address dosimetry challenges across a wide range of radiation exposure scenarios.

Radiation-induced phosphorylation of γH2AX and 53BP1 stands out as reliable, reproducible, and highly sensitive markers for biodosimetry. This study has meticulously characterized the decay kinetics and dose-response curves essential for rapid biodosimetry, offering a valuable resource for dose estimation within 96 hours of exposure during radiological emergencies. Investigation into γH2AX and 53BP1 foci induction, progression, saturation, and decay was conducted using both microscopy and flow cytometry techniques. Notably, a rapid exponential rise in foci induction was followed by an exponential decay over 96 hours for both methods. Data analysis revealed that the initial kinetics followed the function $Y=A - Be^{(-kt)}$ for both techniques. Subsequent to saturation, microscopic foci detection exhibited a bi-exponential decay pattern described by the function $Y= A + Be^{(-k1t)} + Ce^{(-k2t)}$, while flow cytometry followed a single exponential decay pattern represented by $Y= A + Be^{(-kt)}$. It is worth to note here is that the foci formation rate (k) and decay rates (k1 and k2) showed no dependency on the initial doses delivered. The established calibration curves were rigorously validated using three blinded samples with dicentric and Reciprocal-Translocation (RT), with results indicating that the γH2AX assay via microscopy provided the closest estimate at the lowest dose (0.5 Gy, 8% variation), while at higher doses (1 & 2 Gy), all techniques performed almost equally well (maximum 14% variation).

Translocations, considered as stable aberrations, are particularly suitable for dosimetry of cumulative past exposures spanning months to decades. This study focused on analyzing the yield and distribution of translocations (both reciprocal and non-reciprocal), involving painted chromosome pairs 1 and 2, subsequent to *ex vivo* irradiation ranging from 0 to 4 Gy, using blood samples from three volunteers. Approximately 21,000 metaphases were meticulously analyzed, averaging around 7,000 metaphases per individual. All datasets exhibited agreement with the Poisson distribution, facilitating the utilization of Poisson weighted curve fitting. The data were fitted utilizing a linear quadratic model of the form $Y = C + \alpha D + \beta D^2$. The resulting fit yielded a linear coefficient $\alpha = 0.90 \times 10^{-2}$ translocations per cell per Gy and a quadratic coefficient $\beta = 3.58 \times 10^{-2}$ translocations per cell per Gy^2. Given their stability, the Reciprocal-Translocation Dose Response Curve is suitable for cumulative biodosimetry of both recent and past exposures. Conversely, the Non-Reciprocal-Translocation Dose Response Curve, pertaining to unstable aberrations, is applicable solely for biodosimetry of recent exposures.

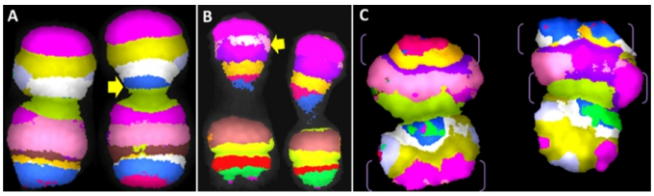

Fig.1: Illustration depicting interstitial deletion of (A) blue and (B) light pink bands from one homolog of the chromosome pair. (C) Represents a complex intrachromosomal rearrangement.

Distinct chromosomal aberrations induced by low and high Linear Energy Transfer (LET) radiations exhibit structural differences. Low LET radiation predominantly induces inter-chromosomal changes, whereas high LET radiation predominantly induces intra-chromosomal rearrangements, which can be visualized and quantified using advanced mBAND-FISH techniques (Fig. 1). Human blood samples were subjected to doses ranging from 0 to 200 mGy of 14 MeV neutrons at the DT neutron facility, Purnima, BARC. Dose Response Curves (DRCs) were generated for interstitial deletions, intra-chromosomal rearrangements, and complex rearrangements, revealing a linear nature with slopes of 2.33, 1.49, and 0.799 aberrations per cell per Gy for interstitial deletions, intra-chromosomal rearrangements, and complex rearrangements, respectively. Interstitial deletions were found to be predominant across all dose points examined. Comparative analysis with low LET radiation (^{60}Co-γ-rays) exposures revealed significantly lower frequencies of intra-chromosomal changes, even at higher doses (0/310 for 2 Gy and 2/352 for 4 Gy).

Utilizing established cytogenetic and immunofluorescence techniques (specifically γH2AX & 53BP1), this study investigated critical clinical cases to assess radiation sensitivity and genetic instability. Genetic instabilities and chromosomal aberrations induced by radiation were analyzed in the lymphocytes of a pediatric Wiscott Aldrich Syndrome (WAS) patient, with a comparison to a healthy volunteer (control). The irradiated WAS sample exhibited a significant excess yield of dicentrics (51%), reciprocal translocations (59.1%), and non-reciprocal translocations (80%) compared to the control sample, indicating a notable increase (ranging from 51% to 80%) in misrepair events. Moreover, analysis of γH2AX foci decay kinetics revealed a sustained elevation in foci numbers up to 48 hours post-irradiation. These results suggest that high radio-sensitivity and genetic instability may predispose WAS patients to cell transformation and genetic complications.

Highlights of the work carried out by Rajesh Kumar Chaurasia under the supervision of Dr. N. N. Bhat (Guide) as a part of his doctoral thesis work. He was awarded a Ph.D. degree from Homi Bhabha National Institute in Life Sciences in 2022.

Detection and Mitigation of Intracellular Labile Iron pool

Iron overload in the human body, whether extracellular (labile plasma iron, LPI) or intracellular (labile iron pool, LIP), generates oxidative stress leading to cell death either via lipid peroxidation and/or DNA damage and is associated with many diseases viz. Heart failure, liver diseases, skin diseases, diabetes, Alzheimer's disease, etc. Hence detection and mitigation of intracellular labile Iron (primarily in Fe^{2+} form due to reductive cellular environment) is important, not only for exploring various iron dependent physiological processes but also for diagnosis and treatment of Iron overload.

Operationally simple, inexpensive, and highly sensitive turn-on fluorescence probes to detect iron overload in living cells are rarely reported. The present studies provided a unique, triplet-stable, Fluorinated Boron-Dipyrromethene (BODIPY) based pro-fluorescent nitroxide (PFN) probe with highly Fe^{2+} selective, high-fold turn-on fluorescence response towards Fe^{2+}. Moreover, the dye detected different amount of intracellular iron in a variety of iron-overloaded cells, which showcased its advantage over other similar probes.

Chelation therapy has emerged as a treatment of choice to mitigate iron overload, and FDA approved chelators e.g. Desferioxamine (DFO) have been the chelator of choice in clinics. However, the drawbacks of DFO towards being cell impermeable and low bio-availability along with short systemic circulation time, have made the use of DFO difficult. In this research, a nanoformulation of DFO was designed, synthesized, characterized, and evaluated in a pre-clinical iron-overload mice model, which demonstrated better iron mitigation along with increased systemic circulation time. These studies will open up the field of nanochelators that can be used as more effective drug candidates for iron overload diseases.

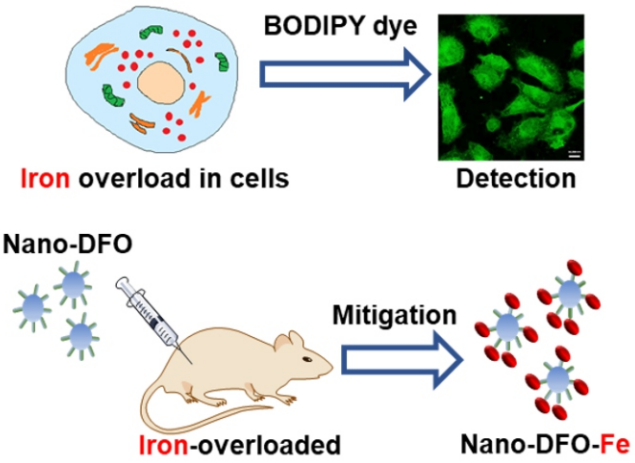

Fig.1: Strategies for detection and mitigation of iron overload.

Highlights of the work carried out by Ms. Pradnya K. Pachpatil under the supervision of Dr. Dibakar Goswami (Guide) as a part of her doctoral thesis work. She will be submitting her thesis in 2025 for a Ph.D. degree from Homi Bhabha National Institute in Life Sciences.

Understanding DNA Repair Pathways to Sensitize Werner (WRN) RECQL Helicase Deficient Cancers

Mutations in WRN protein (DNA helicase) leads to a condition called Werner Syndrome (WS) where patients are predisposed to cancer and premature aging. Cancer patients harbouring tumors with epigenetic inactivation of WRN showed better response to DNA damaging drugs like camptothecin and its derivatives. The present work has explored the novel role of WRN in various compensatory DNA repair pathways and the potential inhibition of these pathways to enhance the efficacy of widely used cancer therapeutic such as radiation and chemotherapy.

We have established that WRN deficient cells are dependent on a critical but compromised CHK1-mediated HR (homologous recombination) pathway for repair of radiation induced DSBs. As, WRN deficient cells (WRN-KD) were found to be hyper sensitive to ionizing radiation in combination with CHK1 inhibitor. Similar to CHK1 inhibitor, WRN-KD cells are also hyper sensitive to radiation in presence of p38 inhibitor. As p38-MAPK activation is regulated negatively by WRN in a CHK1-dependent manner for the repair of IR induced damage. We also showed that CHK1-p38-MAPK axis plays important role in RAD51 mediated HR repair in WRN-deficient cells. Hence, it has been established that inhibiting HR repair pathway either by CHK1 or p38 inhibitor, WRN deficient cells become hyper-sensitive radiation, which can enhance the therapeutic response of radiation treatment of cancer (Fig. 1, left panel).

Our whole genome transcriptome analysis showed a robust activation of NF-KB related gene expression in response to low dose of camptothecin (CPT). CPT, topotecan and irinotecan are used as chemotherapeutics to target Topoisomerase 1 (TOP1) to generate TOP1-covalent complex (TOP1cc) to kill cancer cells. Upon unravelling the detailed molecular mechanism of TOP1-CPT-DNA (TOP1cc) complex formation and removal, we found that WRN is responsible for TOP1cc complex degradation, which leads to activation of NF-KB pathway. Mechanistically, WRN induced TOP1cc complex leads to generation of ssDNA, which phosphorylates CHK1 and later on activate NF-B pathway by increasing nuclear localization of p65. This activation follows the canonical pathway of NF-$_{\kappa}$B activation via ATM and NEMO. Interestingly, neither helicase nor exonuclease activity of WRN was involved in ssDNA generation and NF-KB activation, establishing the non-enzymatic role of WRN in NF-KB activation Fig. 1, middle panel). In preclinical studies, WRN proficient melanoma tumors were highly resistant while WRN-deficient tumors were sensitive to pharmacological treatment of CPT.

Success of cisplatin treatment is limited by its acquired drug resistance and autophagy is one of mechanism responsible for it. In the present study, we revealed that WRN deficient cells are sensitive to cisplatin treatment and increased ROS production, which causes the mitochondrial dysfunction and induce mitophagy. Imperatively, mitophagic clearance and lysosomal fusion with autophagosome were severely impaired in WRN deficient cells. The key adaptor protein p62 was accumulated more while lipidation of LC3 were defective in these cells, suggesting that autophagosome formation is impaired due to lack of LC3 lipidation. ATG7, a key regulator of LC3 lipidation, was significantly downregulated in WRN deficient cells, which further substantiate the defective mitophagy process in these cells. Mechanistically, our in-depth analysis showed that WRN regulates ATG7 expression via resolving several DNA G4-quadruplex structures in the ATG7 gene and assisting maturation of ATG7 mRNA. Together, our study revealed hitherto an unknown function of WRN in mitophagy and its regulation through ATG7 expression (Fig. 1, right panel).

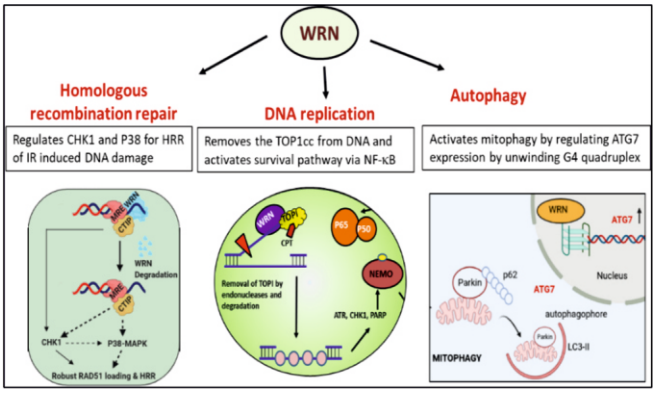

Fig.1: Schematic of the role of WRN in HR repair, DNA replication and NF-kB pathway activation and autophagy by ATG7 gene regulation.

In summary, this investigation highlights important role of WRN in regulating multiple genes like CHK1, p38, p65 localisation and ATG7, which contributes in cell survival pathways such as homologous recombination, NF-B pathway and mitophagy (as shown in Fig. 1). Inhibiting WRN in combination with cancer therapy can lead to better outcome in terms of cancer treatment.

Highlights of the above work was carried out by Pooja Gupta under the supervision of Dr. Birija Sankar Patro (Guide) as a part of her doctoral thesis work. She was awarded Ph. D degree from Homi Bhabha National Institute in Life Sciences in 2022.

Studies on Development of Radioimmunotherapy Agents and Understanding their Mechanism of Action

Breast, ovarian, and gastric cancers often exhibit overexpression of Human epidermal growth factor receptor 2 (HER2), leading to aggressive forms with poor prognoses. Immunotherapy using monoclonal antibodies against HER2, Trastuzumab and Pertuzumab has revolutionized treatment of HER2 positive cancer. However, the emergence of resistance poses a significant challenge, emphasizing the urgency to explore alternative therapeutic approaches. Radioimmunotherapy (RIT) utilizing radiolabeled antibodies has gained significant attention in cancer management, however an ideal radioimmunotherapeutic agent for solid cancers is still not available.

The work documented in the thesis encompasses the development of ^{177}Lu labeled Pertuzumab as RIT agent for targeting HER2 overexpressing cancers. Procedure optimization for conjugating chelators to antibodies,radiolabeling with therapeutic radioisotope Lu-177, characterization by chromatography studies followed by comprehensive biological evaluation in tumor cell lines and animal tumor model was performed. Multiple batches of patient dose of ^{177}Lu labeled Pertuzumab were prepared to verify the reproducibility of results. SPECT imaging studies indicated enhanced tumor uptake and significant retention of the radioimmunoformulation when studied up to 120 h *p.i* confirming its potential as a promising radioimmunotherapy (RIT) agent. Additionally, the radioformulation exhibited a robust tumor-inhibiting response in HER2 tumor-bearing SCID mice. In addition, studies with ^{177}Lu labeled F(ab')$_2$-fragments were performed to compare the difference in the pharmacokinetics of the radioformulations.

Understanding the molecular mechanisms responsible for the clinical synergy observed during combination therapy involving Trastuzumab and Pertuzumab is crucial for effectively managing breast and other similar cancers. While computational models have proposed mechanisms for the synergistic effects of Trastuzumab and Pertuzumab, experimental evidence supporting these hypotheses was lacking. To address this gap, experimental analyses were conducted to assess the interactions of radiolabeled antibodies (Pertuzumab/Trastuzumab) in the presence and absence of a second unlabeled antibody. Furthermore, F(ab')$_2$-fragments of both the antibodies were produced and radiolabeled to investigate the role of the Fc region of the monoclonal antibody in these binding interactions. The study revealed that the radioimmunoconjugates preserve the existing binding synergism between Pertuzumab and Trastuzumab to HER2 receptors and significant binding enhancement of radiolabeled Pertuzumab and its fragments was observed in the presence of Trastuzumab in both *in-vitro* and *in-vivo* testing conditions.

The existence and potential impact of radiation-induced biologic bystander effects (RIBBEs) in radionuclide therapy is inadequately understood. The studies on investigating the RIBBEs mediated by Trastuzumab antibody radiolabeled with three therapeutic radioisotopes , ^{90}Y (a pure β^- emitter), ^{177}Lu (a β/γ emitter), and ^{125}I (an auger electron emitter) were performed. Treatment of cells with radiolabeled formulations not only resulted in inhibitory bystander effects in recipient (bystander) cells but also notable toxicity in irradiated cells (both directly irradiated and donor cell groups) was observed. Moreover, elevated levels of reactive oxygen species were observed at higher doses in bystander cells, suggesting their significant contribution in RIBBE. The thesis work led to the development of radiolabeled formulations suitable for clinical translation. Furthermore, these formulations were utilized to investigate mechanisms aimed at enhancing their efficacy for cancer management.

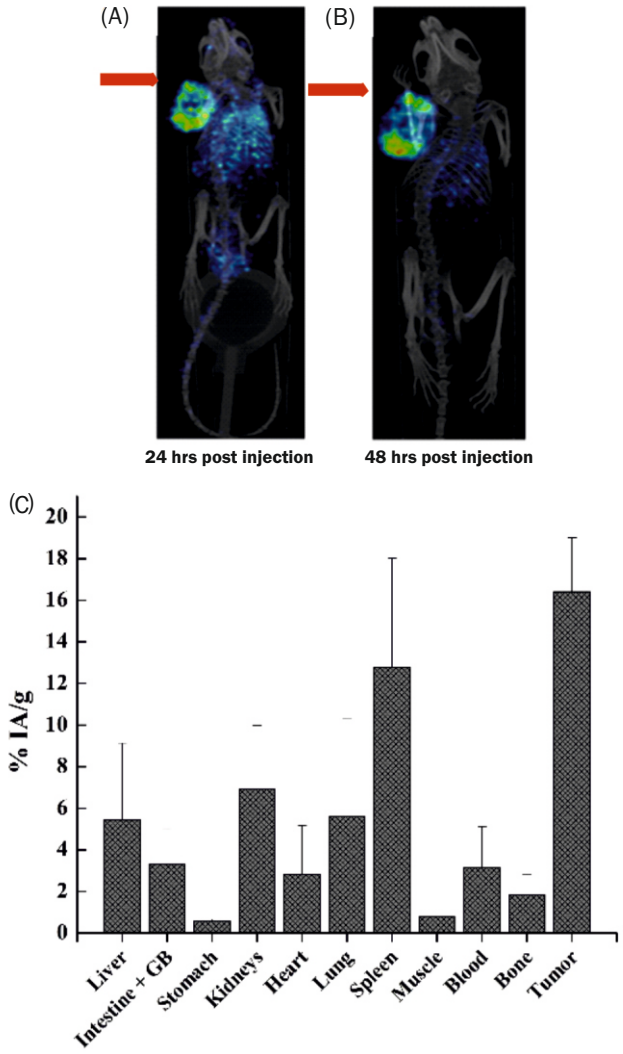

Fig.1: [^{177}Lu]Lu-CHX-A′-DTPA–Pertuzumab injected in SK-OV-3 tumor bearing SCID mice. SPECT/CT imaging studies (A) at 24 h post injection ,(B) 48 h post injection.(C) Biodistribution data showing % Injected activity / gram of tissues at 120h p.i .

Highlights of the work carried out by Dr. Rohit Sharma under the supervision of Dr. Archana Mukherjee (Guide) as a part of his doctoral thesis work. He was awarded Ph.D degree (Life Sciences) from Homi Bhabha National Institute in July 2024.

Development of Targetable Radiolabeled Self-assembly Structures for Combination Cancer Therapychanism of Action

Combination radionuclide therapy (CRT) for cancer treatment involves the use of radionuclide therapy in combination with multiple therapeutic modalities, to target cancer cells through different mechanisms. This approach aims to maximize treatment efficacy while minimizing the development of resistance and reducing the risk of tumor recurrence.

Liposomal formulations have emerged as a powerful tool in cancer management, offering unique advantages in drug delivery and enhancing therapeutic efficacy. These lipid-based nanoformulations can encapsulate a wide range of therapeutic agents, including chemotherapeutic drugs, nucleic acids, and imaging agents, within their aqueous core or lipid bilayer. This encapsulation provides several benefits, such as protecting the payload from degradation, prolonging circulation time, and enabling controlled release at the tumor site. Additionally, surface modifications of liposomes with targeting ligands, such as antibodies or peptides, facilitate active targeting of cancer cells, further enhancing specificity and therapeutic efficacy (Fig. 1)

To leverage these unique strengths of liposomal nanoformulations, work on development of targetable self-assembly structures was undertaken.Liposomes of size < 100 nm were prepared by ethanol injection method. Doxorubicin (Dox), an FDA-approved drug was encapsulated into liposomes using the pH gradient method. These liposomes encapsulating doxorubicin (Lip-Dox) were actively targeted to the HER2 receptor overexpressed in breast cancer using the monoclonal antibody trastuzumab. The conjugation of trastuzumab to Lip-Dox was validated and Ab-Lip-Dox was radiolabeled with ^{99m}Tc and ^{177}Lu using bifunctional chelator conjugated lipid moieties and were characterized using chromatography techniques. The affinity of the Ab-Lip-Dox for HER2 receptor was ascertained by confocal microscopy and cell binding & inhibition studies. The ^{99m}Tc labeled Ab-Lip-Dox showed targeting to HER2 overexpressing SKBR3 xenograft tumor and improved clearance from blood compared to ^{99m}Tc labeled Lip-Dox as observed by SPECT imaging studies (Fig. 2).

Further, ^{177}Lu-labeled Lip-Dox was formulated and evaluated for combinatorial cytotoxicity of Dox and ^{177}Lu at different doses for treatment of breast cancer. The synergistic therapeutic effect was observed at lower doses of Dox (5-50 nM) and ^{177}Lu (1-25 µCi) when used concurrently via radiolabeled Lip-Dox in breast cancer cells. The synergistic effect of Dox and ^{177}Lu was also observed in vivo in SKBR3 tumor bearing animals by tumor growth delay studies. The synergism at lower doses of Dox and ^{177}Lu with non-sphering toxicity will reduce the side effects of the formulations resulting in enhanced therapeutic index.

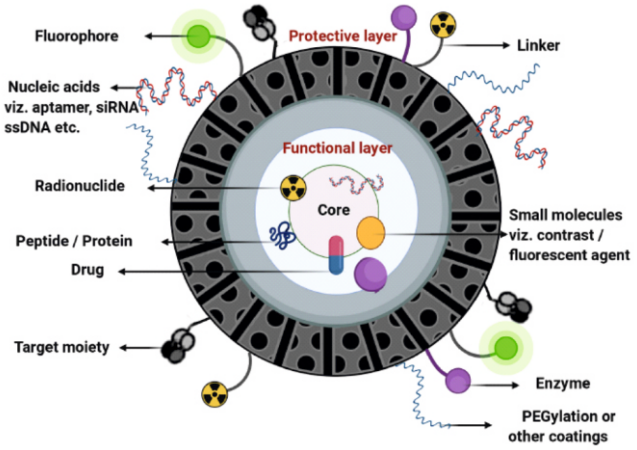

Fig.1: A graphical representation of nanoliposomal formulation that can encapsulate a combination of different anti-cancer therapeutic strategies.

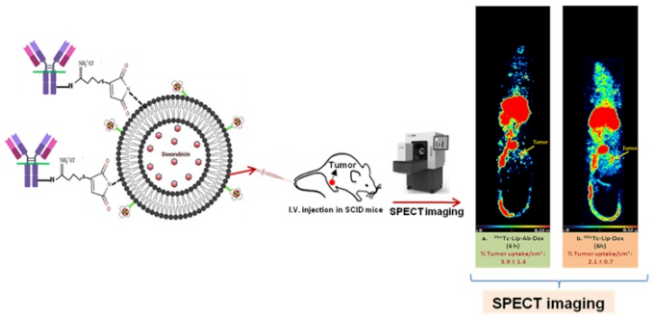

Fig.2: SPECT images after injecting radiolabeled nano formulations in SCID mice bearing SKBR3 tumors.

In this thesis work, radiolabeled nano liposomal formulations loaded with a drug were successfully formulated and were actively targeted to tumors using antibodies for imaging and therapy applications. These formulations hold great promise for personalized cancer treatment through combination radionuclide therapy.

Highlights of the work being carried out by Shishu Kant Suman under the supervision of Dr. Archana Mukherjee (Guide) as a part of his doctoral thesis work. This work will be submitted for Ph.D. degree (Life Sciences) to Homi Bhabha National Institute in 2025.

Exploring the Potential of Novel Radiolabeled Biomolecules and Biomolecule-Drug Conjugates for Imaging and Therapy of Cancers

Nuclear medicine, a specialized field of modern-day medical sciences, uses radiolabeled drugs/biomolecules, known as 'Radiopharmaceuticals', for diagnosis and treatment of various types human ailments. Radiopharmaceuticals play a pivotal role in the management of many diseases, predominantly cancer. As a result, there is a great interest in the development of novel target-specific radiolabeled agents for diagnostic and therapeutic applications. A radiopharmaceutical usually contains a radionuclide and a carrier moiety, which determines the target-specificity of such agents. Therefore, developing radiopharmaceutical requires careful selection of the carrier ligand.

Different carrier moieties, such as, peptides, antibodies, drugs, nano-carriers exhibit preferential uptake in tumorous/cancerous lesions. Porphyrins also exhibit similar tendency to preferentially accumulate in the neoplastic tissues. However, undesired non-target accumulation is one of prime reasons which limit their intended clinical applications. Conjugation of the targeting vectors with suitable secondary targeting moieties may help in circumventing this problem. The work reported in this thesis is related to the development of radiolabeled agents involving porphyrin conjugates and antibody-drug conjugates having unique properties and potential for specifically targeting the tumorous lesions.

Present work involves syntheses of variety porphyrin derivatives and their thorough characterization by standard spectroscopic techniques, such as, UV-Vis, FT-IR, ^{1}H- and ^{13}C-NMR spectroscopy as well as by mass or MALDI-TOF spectrometry. One such porphyrin derivative [5-carboxymethyleneoxyphenyl-10,15,20-tris(4-methoxyphenyl) porphyrin, UTRiMA] was synthesized and radiolabeled with ^{nat}Cu as well as ^{64}Cu with an aim to explore the utility of such complexes in PDT (Photodynamic Therapy) and PET (Positron Emission Tomography), respectively. Detailed biological investigations carried out in healthy as well as cancer cell lines demonstrated significant reduction in photo-cytotoxic potential of porphyrin derivative upon complexation with Cu. However, [^{64}Cu]Cu-UTRiMA exhibited potential as an agent for targeted radionuclide therapy.

In another work, an in-house synthesized porphyrin derivative namely, 5,10,15,20-tetrakis-(4-carboxymethyleneoxyphenyl)porphyrin was conjugated with PAMAM [poly(amidoamine)] dendrimers and subsequently radiolabeled with ^{177}Lu, a well-established therapeutic radionuclide. Biological studies performed with [^{177}Lu]Lu-labeled porphyrin-PAMAM conjugate in tumor bearing small animal models revealed significant accumulation of the radiolabeled particles in the tumor, which was further corroborated through scintigraphic imaging. However, lower retention of the radiolabeled agent in the tumorous lesions at the longer time points may pose a limitation toward its envisaged application as a radio-therapeutic agent.

With an aim to augment the tumor uptake and improve the pharmacokinetic behavior of porphyrin, its conjugation with a cell penetrating peptide (Transactivator of Transcription, TAT) was attempted. Porphyrin-TAT conjugate was synthesized using solid phase synthesis. MTT assay revealed preferential light dependent toxicity for porphyrin derivative which was further enhanced upon peptide conjugation. Fluorescence and flow cytometry studies revealed relatively higher cellular internalization of porphyrin-TAT conjugate in comparison to the porphyrin derivative. Porphyrin-TAT conjugate was further radiolabeled with ^{68}Ga, a generator produced radionuclide used for PET imaging. Ex-vivo evaluation of [^{68}Ga]Ga-porphyrin-TAT complex in fibrosarcoma bearing Swiss mice model revealed higher tumor uptake for [^{68}Ga]Ga-porphyrin-TAT conjugate as compared to [^{68}Ga]Ga-porphyrin. However, observation of higher non-target retention of both the radiolabeled agents during ex-vivo studies might pose limitation towards their possible application in PET imaging.

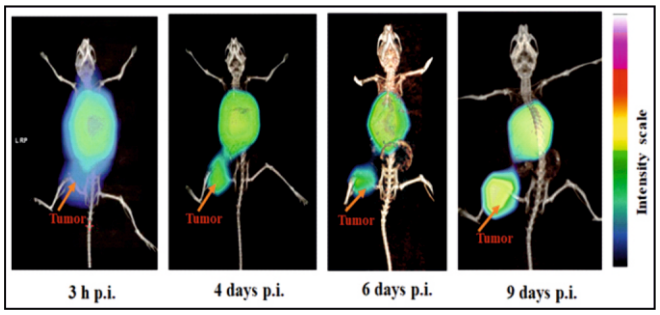

Fig.1: Whole-body SPECT-CT images of the tumor (femur region) bearing Swiss mice acquired after administration of [^{177}Lu] Lu-porphyrin-NLS conjugate at different time-points.

To strike a balance between the hydrophilicity and lipophilicity for obtaining an optimum pharmacokinetic behavior, a porphyrin derivative (UTriMA) was conjugated with NLS sequence [PKKKRKV] (synthesized via solid phase peptide synthesis method). Fluorescence cell imaging studies carried out in HT1080 cancer cells revealed intra-cellular accumulation for the NLS conjugated porphyrin, whereas unconjugated porphyrin failed to reach inside the cells. Porphyrin-NLS conjugate was radiolabeled with ^{177}Lu. Biological distribution studies in fibrosarcoma bearing Swiss mice model revealed significantly higher accumulation and prolonged retention of [^{177}Lu]Lu-porphyrin-NLS conjugate in the tumorous lesion, which was further corroborated by recording serial SPECT-CT images (Fig. 1).

In continuation with the aim of improving the uptake and pharmacokinetic behavior of radiolabeled agents for cancer management, radiolabeled antibody and antibody-drug conjugate were also synthesized during the course of the present work. Conjugation reaction between Rituximab (antibody) and Chlorambucil (drug) was optimized and the resultant antibody-drug conjugate was radiolabeled ^{177}Lu with high radiochemical purity. Ex-vivo studies for the radiolabeled antibody and antibody-drug conjugate, performed in cancer cells and SCID mice bearing Non-Hodgkin's lymphoma xenografts showed significant improvement in the non-target uptake of antibody post-conjugation with the drug (chlorambucil) without compromising the tumor avidity.

Results obtained during above-mentioned studies revealed a definite effect in the targeting ability of molecular cargo upon conjugation with secondary targeting moieties. The studies indicate that this strategy may be helpful in the preparation of radiolabeled biomolecule-drug conjugates to obtain potent radiopharmaceuticals having high tumor uptake and optimum pharmacokinetic behavior for applications in cancer management.

Highlights of the work carried out by Shri Naveen Kumar under the supervision of Prof. Tapas Das (Guide) as a part of his doctoral thesis work. Shri Naveen has submitted his doctoral thesis (in Chemical Sciences discipline) to Homi Bhabha National Institute in April, 2024.

CRISPR Systems and Gene Modulation in Anabaena

Archaea and bacteria possess the 'CRISPR-Cas' systems to combat the invasion of external nucleic acids. CRISPR stands for Clustered Regularly Interspaced Short Palindromic Repeats and refers to the specific genetic sequences found in these organisms. The proteins involved in this defense mechanism are known as CRISPR-associated proteins (Cas proteins). The regions, known as CRISPR loci, present on bacterial genomes, contain repeats as well as short sequences derived from phages or plasmids. Together, Cas proteins and CRISPR loci provide a form of adaptive immunity, defending against external nucleic acid invasions. Cyanobacteria also encode CRISPR systems in their genome. Bioinformatic analysis using various tools and web servers has revealed that *Anabaena* PCC 7120 genome harbors three distinct CRISPR systems: two class 1 systems (type I-D and type III-D) and one class 2 system (type V-K) and a total of eleven CRISPR loci.

In-depth *in silico* analysis of all the proteins related to type I-D locus showed, this system to be the most complete CRISPR system present in *Anabaena* PCC 7120. Genes related to expression, interference module and adaptation components, were identified and found to constitute a complete CRISPR system. 3-D models of all proteins related to the type I-D system were generated using homology modelling/ab initio/threading. Specifically focusing on the type I-D system, we found that the Alr1562 protein played a crucial role, acting as a backbone of the type I-D (CRISPR Associated Complex for Antiviral Defense) CASCADE interference complex. When purified from *E. coli*, Alr1562 exhibited the ability to exist in either a dimeric or higher oligomeric form. Interestingly, Alr1562 showed a stronger binding affinity towards repeat-spacer-repeat (RSR) RNA as compared to a non-specific RNA. The residues essential for RNA binding were identified and subsequently mutated using site-directed mutagenesis. These mutated proteins, mostly existing in dimeric forms, exhibited significantly reduced binding to RNA, demonstrating that dimer formation is independent of RNA binding (Fig. 1A). This marks the first documentation of a Cas7 protein characterization in a photosynthetic organism.

Cyanobacteria, have developed intricate mechanisms to safeguard themselves against oxidative stress caused by increased production of reactive oxygen species (ROS). 2-Cysteine-Peroxiredoxins (2-Cys-Prx), present in all organisms, utilize the two catalytic cysteine residues at their active site to detoxify peroxides. The exogenous CRISPR-dCas9 system from S. pyogenes was employed to generate a knockdown (CRISPR interference, CRISPRi) strain for the Alr4641

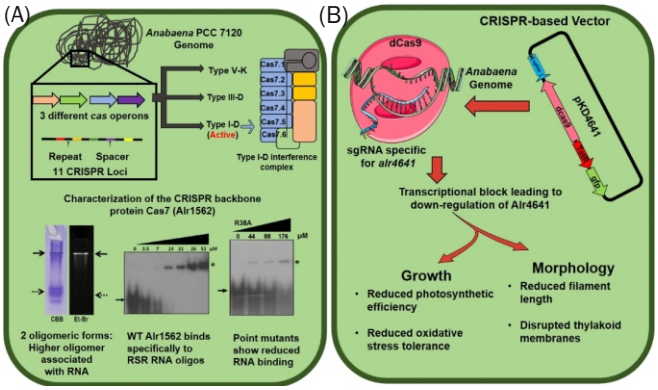

Fig.1: (A) Exploration of endogenous CRISPR system and (B) Use of exogenous CRISPR system to knockdown alr4641 in Anabaena PCC 7120.

protein (Fig. 1B), which is a typical 2-Cys-Prx in *Anabaena* PCC 7120. The growth of An-KD4641 (knockdown strain) was slower with smaller filament size and reduced photosynthetic efficiency as compared to the An-dCas9 (control strain). Ultrastructural analysis (TEM) revealed the knockdown strain to have disrupted and discontinuous thylakoid membranes, whereas the An-dCas9 strain had well-structured, multilayered thylakoid membranes. Interestingly, the total ROS content was higher in An-KD4641 under unstressed conditions. Notably, the knockdown strain was more vulnerable to the oxidative effects of H_2O_2. Furthermore, the knockdown strain exhibited a significantly greater vulnerability to oxidative stress induced by H_2O_2 compared to the control strain.

In conclusion, the work described here has (a) identified the different CRISPR-systems present in Anabaena PCC 7120 (b) thoroughly characterized the Alr1562 protein, identifying the residues responsible for binding to crRNA (c) successfully demonstrated the use of CRISPRi technology in repressing genes in Anabaena, and (d) revealed the vital role of the Alr4641 protein in defending this ecologically significant cyanobacterium against oxidative stress.

Highlights of the work carried out by Prakash Kalwani under the guidance of Dr. Anand Ballal (Guide) and Dr. Devashish Rath (Co-guide) as a part of his doctoral thesis work. He was awarded a Ph.D. degree from Homi Bhabha National Institute in Life Science in 2022.

Understanding the Defence Response to Stem Rust Disease of Wheat

Wheat is one of the important cereals contributing to nutritional security of millions of people worldwide. Wheat production is threatened by stem rust (black rust) disease caused by fungal pathogen *Puccinia graminis* f. sp. *tritici (Pgt)*, which can cause 50–100% loss in yield. In recent years, new pathogenic races of *Pgt* (e.g. Ug99, Digalu race) have emerged overcoming resistance conferred by important *Sr* genes. In the current study resistance response conferred by *Sr24* (major race specific *Sr* gene) was investigated in two wheat Near Isogenic Lines (NILs) using phenotypic, microscopic and transcriptomic analysis. In addition, these responses were also examined in another *Sr* gene (*Sr26*) harbouring genotype. Results showed that, in presence of *Sr24* the resistant NIL showed low infection type (IT) in seedling stage as well as reduced disease coverage at adult plant stage. Time-course study of the disease development showed induction of hypersensitive response (HR)-based resistance within 2–3 days post inoculation (dpi) leading to minute uredia pustule size in the *Sr24* carrier (Fig. 1A). The histological studies showed post haustorial resistance to Pgt with restricted fungal structures at early and late stages (Fig. 1B). Transcriptomics-based analysis showed elevated levels of genes involved in pathogen recognition, multiple signalling pathways involved in activation of transcription factors (TFs) which activate the expression of multiple defence pathways (Fig. 1C). The antifungal responses activated by R gene included elevated ROS levels, synthesis of antifungal secondary metabolites, activation of ion and solute transporters, PR protein induction, cell wall fortification, and modulation of multiple metabolic pathways. Certain antifungal response genes remained upregulated at late stages, showing their sustained involvement in restricting the *Pgt* growth. The DEGs identified in resistant NIL were mapped to the donor genome (*Thinopyrum elongatum*) in vicinity of linked marker to *Sr24* (Fig. 1D). The phenotypic, microscopic and gene-expression study upon Pgt infection in an additional NLR type *Sr* gene (*Sr26*) also showed similar trend, suggesting overlapping resistance mechanism to *Pgt* with some variations (Fig. 1E).

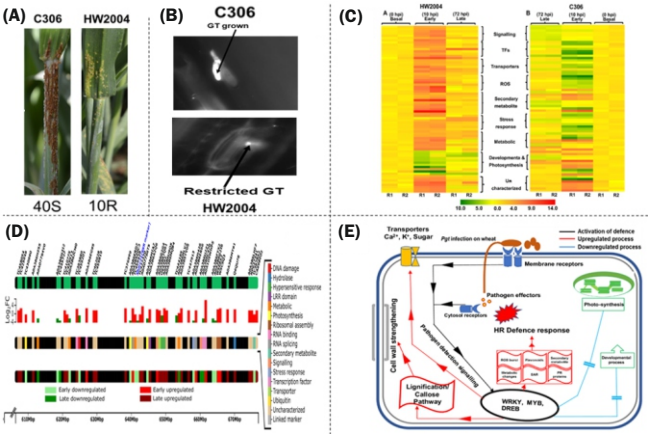

Fig.1: A) Susceptible and resistant response of wheat NILs to Pgt. B) Restriction of Germ Tube (GT) in resistant NIL. C) Expression profile of key genes in NILs upon Pgt infection. D) DEGs mapped on Sr24 donor species genome, in vicinity of linked marker. E) Overall mechanism of resistance to Pgt in wheat.

This research work was carried out by Dr. Gautam Vishwakarma under the supervision of Dr. B. K. Das (Guide) and Dr. Ajay Saini (Co-guide) as a part of his doctoral thesis work. He was awarded a Ph.D. degree from Homi Bhabha National Institute in Life Science in August, 2024.

Forward Genetics of a Chickpea (Cicer Arietinum L.) Mutant Identifies a Novel Locus (CaEl) Contributing to Increased Seed Size, Organ Elongation and Early Vigor

Chickpea is one of the top three grain legumes (pulses) grown worldwide. It is a good source of protein, carbohydrates and dietary fibers. India is the largest producer and consumer of chickpeas and contributes more than 70% (13.54 Mt) of the total world production (18.09 Mt). Chickpea production is challenged by various abiotic and biotic stresses, causing significant yield losses. Trait-based breeding approaches have been useful to counter these challenges. One such trait is 'early vigor', characterized by fast seed germination, seedling growth and early plant establishment with dense canopy. Such a phenotype confers advantages such as reduction of competition from weeds, reduction of direct evaporation, improving plant growth under prevalent stresses etc. Combined with early maturity, plants with high vigor are also suitable for terminal drought prone environments. In the present study, through induced mutagenesis using gamma rays, a novel chickpea mutant was isolated. The mutant showed a distinct phenotype of elongation in vegetative and reproductive organs, than the wild type (WT) (Fig. 1a) and was named "*elongated mutant*" (*elm*). The *elm* also showed early emergence and early vigor that contributed to more shoot biomass at the early vegetative stage. This also resulted in a better performance of elm as compared to the WT in terms of germination and growth under salinity stress. In addition, *elm* accumulated less Na^+ in leaves and a higher proline content indicating a better stress response as compared to WT under salinity stress. The cellular morphology was altered in *elm*. The size of the pavement cells was larger with lesser number of cells per unit area than the WT, indicating that both cell division and cell expansion are affected in *elm* (Fig. 1b). The inheritance study showed monogenic regulation of organ elongation trait with incomplete dominance of WT allele over mutant allele (Fig. 1c). Further, using a 'Bulked segregant analysis' approach, molecular markers linked to this mutation were identified. Genetic mapping study, mapped all markers to single linkage group on chromosome 1 of chickpea genome with one marker (CaGM04793) co-segregated with the mutant locus (*el*) (Fig. 1c). *In-silico* analysis positioned this marker (CaGM04793) in the gene Ca_13541 (LOC101503252 in NCBI database) (Fig. 1d). Polymerase chain reaction to amplify the full-length gene showed a complete deletion of this gene in the mutant (Fig. 1d), with loss of expression in mutant as well as in recombinant inbred lines having mutant phenotype (Fig. 1e). The gene 101503252 showed homology to Arabidopsis AT1G79060, which is annotated as Tetrapeptide Repeat Homeobox Like (TPRXL), with no known function to date. Recently, AT1G79060 was shown to correspond to STIGMA AND STYLE STYLIST 1 in *A. thaliana* regulating

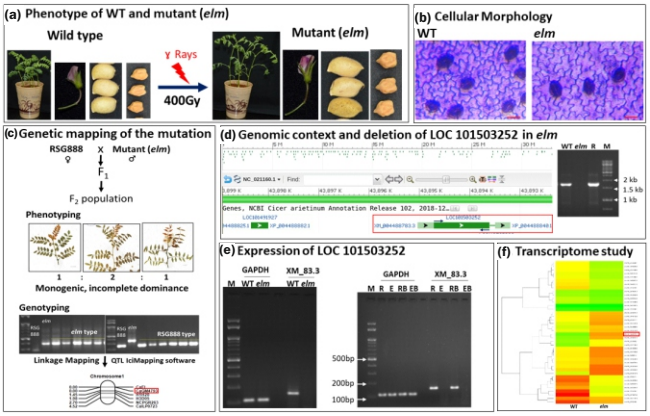

Fig.1: (a) Phenotype of WT and elm (b) Cellular morphology of pavement cells in WT and elm (c) Genetics and mapping of elongation trait (d) Snapshot showing genomic context of gene 101503252 (red box) at NCBI database and PCR amplification showing deletion of gene 101503252 in elm (e). RT-PCR showing loss of CaEl expression in elm (left) and in elm type inbred lines (right), GAPDH used as reference gene in RT-PCRs (f) Clustering of top 20 differentially regulated transcripts between WT and elm.

structural patterning and functional specification in apical gynoecium. Our *in-silico* analysis suggested that this gene is present as a single copy in chickpea and related legumes and has possibly acquired a broader function in regulating cell division and/or proliferation in multiple tissue types. Transcriptomics of *elm* and WT, highlighted possible role of gene 101503252 in cell division, mitotic cell cycle, cell wall metabolism, carbohydrate metabolism, cell wall organization, xyloglucan metabolic process and hemicellulose metabolic processes (Fig. 1f).

The present work identified a previously uncharacterized gene contributing to organ elongation and early vigor in chickpea that can be further explored to gain mechanistic insights into regulation of these traits and its exploitation in the breeding programs for increasing seed size and plant vigor.

Highlights of the work carried out by Golu Misra under the supervision of Dr. Archana Joshi-Saha (guide) as a part of his doctoral thesis work. This PhD thesis was submitted recently (Nov, 2024) to Homi Bhabha National Institute for the PhD Award in Life Sciences.

Genomic Basis of an Electron Beam Induced Mutant of Groundnut

Seed size plays an important role in groundnut (*Arachis hypogaea* L.) as it directly influences seed yield and market value. Being a quantitative trait, understanding the genetic basis of seed size is complex. However, usage of an induced mutant simplifies the approach of identifying the key genes governing seed size variation in groundnut. Towards this, we utilized an electron beam-induced large seed mutant, TG 89, to locate the genomic regions contributing to the seed size. This mutant has hundred kernel weight (HKW) of 75-82 g as compared to 40-48 g in its parent, TG 26. The histological analysis using Environmental Scanning Electron Microscopy (ESEM) revealed that the seed development in the mutant was primarily attributed to an increase in cotyledonary cell area rather than cell number. To map the genomic loci associated with the large seed size, a mapping population was developed by hybridization of TG 89 with normal seeded, genetically distant parent ICGV 15007 (Fig. 1A). A comprehensive genetic analysis of F_2 mapping population was carried out by utilizing simple sequence repeats (SSRs), miniature inverted-repeat transposable elements (MITEs), allele-specific and single nucleotide polymorphism (SNPs) markers. Initially, genotyping of the F_2 mapping population with 85 MITEs and SSRs revealed a significant QTL for seed size in the A05 linkage group, indicating potential regions for fine mapping. Towards fine mapping, 781 SNP markers were developed from genomic DNA sequencing using ddRAD-seq, of which 297 were utilized to construct a genetic linkage map spanning 20 linkage groups. QTL analysis identified two major QTLs on chromosomes A05 and A02, explaining notable phenotypic variance and two minor QTLs on B01 and B10 chromosomes (Fig. 1B). Interestingly, markers associated with the two major QTLs exhibited additive effects from either of the parental alleles, with the major positive additive effect contributed by the mutant allele in the '*mutant_qHKW_1*' (Fig. 1C). This primary QTL is originated from mutant and was mapped at 229 cM, spanning the genomic region 99.2–103.7 Mbp on the A05 chromosome (Fig. 1D). Markers flanking this mutant allele were developed and utilized to validate the QTL in other high yielding breeding lines. The analysis of candidate genes within this QTL region revealed various genes potentially involved in the regulation of seed size, including those coding for pentatricopeptide repeat (PPR) proteins, receptor kinase proteins, and notably, a gene, *arahy.5M7JWE*. Gene expression analysis with real-time PCR revealed a significant down-regulation of this gene *arahy.5M7JWE* in the mutant compared to the parent, suggesting that a recessive mutation in *arahy.5M7JWE* may be the cause of the observed phenotype in the mutant (Fig. 1E). This gene encodes the protein *Arahy.5M7JWE*, which belongs to the *Ah*TIFY family that is an ortholog of *BIG SEEDS1 (BS1)*, a plant-specific transcriptional repressor (Fig. 1F). This TIFY protein is known to play a crucial role in jasmonate signalling, a pathway well-known for its involvement in plant stress responses and seed and leaf developmental processes. The observed down regulation of *arahy.5M7JWE* in the mutant suggests the suppression of transcriptional repression by TIFY family proteins, thereby influencing seed size. These findings provide valuable insights into the genetic architecture of large seed trait in groundnut and offer potential target for future breeding efforts aimed at improving yield and quality characteristics.

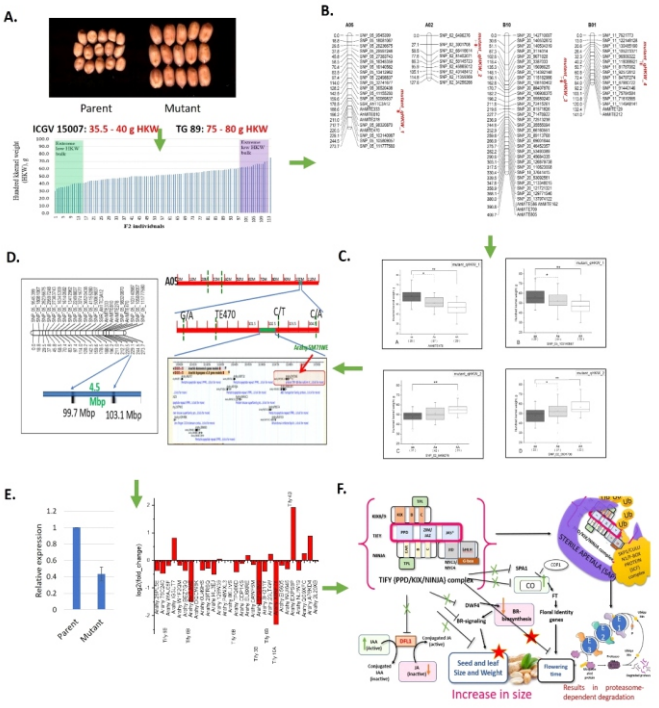

Fig.1: A). The variation in seed size of mutant TG 89, its parent TG 26, and F2 mapping population derived from the cross of ICGV 15007 and TG 89. B). QTLs detected for hundred kernel weight on the genetic linkage map. C). Allelic classification for hundred kernel weight for markers flanking two major QTLs. Solid line connecting box plots indicated additive effect while dotted line indicated dominance effect of allele D). Physical map corresponding to Mapped distance of mutant_HKW1. E). Relative expression of arahy.5M7JWE and other TIFY genes in mutant and parent. F). Schematic overview of the putative role of Tify protein in seed size control. The downregulation of the Tify protein, a transcriptional repressor, brings about the proteasome mediated degradation of the repressor complex, leading to alleviating the suppression of downstream pathways.

Highlights of the work carried out by Ms. Poonam Gajanan Bhad under the supervision of Dr. Anand M. Badigannavar, Professor, HBNI (Guide) and Dr. Suvendu Mondal (Technical Supervisor) as a part of her doctoral thesis work.

Molecular Mapping of Resistance Gene to Bacterial Leaf Pustule in Soybean

Soybean is the most important grain legume in the world in terms of production and international trade. It is an economically important leguminous crop for oil, feed, and soy food products. In India, soybean has become the number one oilseed crop and occupies the largest crop area in the rainfed *kharif* season. However, its continuous cultivation with a simultaneous increase in the area has led to increased incidences of several diseases, insects, and weeds. Among the various bacterial diseases, Bacterial Leaf Pustule (BLP), caused by *Xanthomonas axonopodis* pv. *glycines* (*Xag*), is a serious disease of soybean, particularly in northern and central India. The disease causes premature defoliation and consequent reduction in seed yield. The use of resistant cultivars is a cost effective and ecofriendly approach to minimize the losses due to disease. Progress in the development and use of BLP resistant soybean genotypes is hampered due to scarcity of high yielding BLP resistant soybean genotypes and further, unavailability of molecular markers linked to BLP resistance genes in Indian soybean genotypes. Keeping these points in view, the present study was taken up with major objectives including standardization of excised leaf technique and identification of resistance sources against BLP, molecular mapping of BLP resistance genes and their validation, biochemical changes in response to BLP and development of high yielding BLP resistance lies.

An excised leaf technique was standardized and 310 soybean lines were screened for BLP. The BLP resistant genotype (TS-3) identified in the study was used in hybridization with the BLP susceptible genotype (PK 472) and a segregating population was developed. Inheritance studies indicated that two recessive genes governed BLP resistance in soybean genotype TS-3.

Parental polymorphism followed by bulked segregant analysis identified 12 SSR markers, of which five SSR markers are located on chromosome 2 and seven SSR markers are located on chromosome 6, putatively linked to BLP resistance genes. Linkage analysis mapped the BLP resistance locus (*r1*) and five SSR markers (BARCSOYSSR_02_1585, BARCSOYSSR_02_1589, BARCSOYSSR_02_1590, BARCSOYSSR_02_1613 and Sat_183) on chromosome 2 with in a map distance of 5.5 cM (centiMorgon). Two SSR markers namely Sat_183 and BARCSOYSSR_02_1613 flank the r1 locus at a distance of 0.9 cM and 2.1 cM respectively. Similarly, second BLP resistance locus (*r2*) and seven SSR markers (BARCSOYSSR_06_0013, BARCSOYSSR_06_0024, BARCSOYSSR_06_0029, BARCSOYSSR_06_0040, Satt681, AW734043 and TSSR_06_01) were mapped on chromosome 6 (Fig.1). Two SSR markers BARCSOYSSR_06_0024 and BARCSOYSSR_06_0013 flank the *r2* locus at a distance of 1.5 cM and 2.1 cM respectively. All the flanking SSR markers identified in the study were validated on the 24 soybean genotypes, which included eight BLP resistant and fourteen BLP susceptible soybean genotypes along with the mapping parents. The SSR markers linked to resistance locus *r1* (Sat_183 and BARCSOYSSR_02_1613) and *r2* (BARCSOYSSR_06_0024 and BARCSOYSSR_06_0013) got amplified with the clear polymorphism that distinguishes the BLP resistant soybean genotypes from BLP susceptible genotypes. Biochemical studies indicated that the total phenolic and total flavonoid contents were higher in resistant genotype compared to the susceptible genotype. The total chlorophyll content was found to decrease rapidly in PK472 (susceptible genotype) compared to TS-3 (resistant genotype). Ten advanced selections, showing high yield potential and BLP resistance reaction, were identified. Among these, five resistant selections TSR-8, TSR-3, TSR-19, TSR-1 and TSR-7 gave significantly higher yield over the best check JS-335. The SSR markers tightly linked to BLP resistance loci identified in this study will help soybean breeders in marker assisted selection of BLP resistant sources.

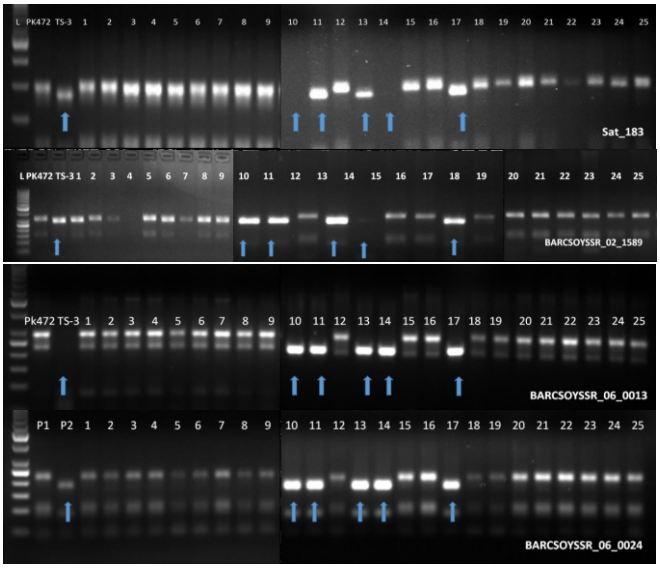

Fig.1: Genotyping of mapping population using SSR markers
Legend P1: PK472 (susceptible parent); P2: TS-3 (resistant parent); 1-25 F2 individuals; ⬆ Indicate resistant individuals.

Highlights of the work carried out by Sumit Prakashrao Totade under the supervision of Prof. J. G. Manjaya (Guide) and Dr. S. K. Gupta as a part of his doctoral thesis work. He was awarded PhD degree from Homi Bhabha National Institute in Life Sciences in 2023.

Radiation Induced Value Addition of Microalgae as Feed and Fuel

Microalgae are sunlight-driven factories that can turn fertilizer-rich water under sunlight into a vibrant green lawn within a day or two. They have received the most attention for their oil which can range from 50 to 60 % of their biomass. In the same area, the theoretical yield of oil from microalgae can be 10 times more than oil crop plants. Besides being bestowed with high photosynthetic rates, rapid growth, and ability to grow on wastelands, sewage water, and synthesize biomass rich in protein, carbohydrates, and oils, they can be further tuned to produce more oil by exposing to stress conditions (nutrient-limitation and high-salt condition) making them the 'Green gold' of the future. Microalgae-based bioproducts exploitation is limited to the production of fine chemicals such as carotenoids or as an aquaculture feed. The major bottleneck for utilizing microalgal oil in the fuel sector is the cost factor. The downstream applications such as harvesting and extraction contribute to increased expenses, while the use of PUFA from microalgae for food purposes is hindered by its low content. Nevertheless, starting with an oil-rich microalga can mitigate the above-listed drawbacks. Varying efforts have been made by researchers to produce oil-laden microalgae. In this view, we undertook the study to enhance oil production in microalgae using two different radiations (UV- and γ-rays).

The optimum dose for rapid oil accumulation along with minimum cell damage was finalized for both UV- (1 J/cm^2) and γ-radiation (1 kGy). Within 48 h, more than 1.5-fold increase in oil content was observed. Triacylglycerols were identified as one of the major constituents of accumulated oil. Radiation causes ionization of the molecules, and water constituting about 80 % of cytoplasm becomes the major target resulting in the formation of Reactive Oxygen Species (ROS). Apart from being highly reactive, ROS also serves as a secondary messenger for counteracting the cascade of damage. ROS was immediately measured after radiation and a more than 1.5-fold increase in ROS fluorescence was observed. To justify the role of ROS as a messenger towards enhancement in oil content, ROS formation was monitored under ascorbic acid (a physiological ROS scavenger) supplementation. UV- and γ-radiation-induced lipid accumulation was significantly reduced by 2.95-fold and 1.43-fold, respectively compared with their respective controls, indicating ROS as one of the major drivers of lipid accumulation. The molecular changes responsible for radiation-induced oil accumulation were also studied at different organizational levels using a systems biology-based approach. In brief, whole genome RNA-sequencing and SWATH-MS-based proteomics were used to identify the global reprogramming in genes and proteins, respectively. The integration of gene- and protein-level data as well as protein suggested the increase in abundance of starch-degrading enzymes, which implied the rerouting of carbon from starch towards oil accumulation. GC-MS-based fatty acid profiling revealed that UV-radiation favored the accumulation of saturated over unsaturated lipids; while γ-radiation treated lipids had a higher accumulation of an essential omega-3 fatty acid. Taken together, this study highlighted UV- and γ-radiation for inducing rapid lipid accumulation, which can impart value addition to microalgae-based "food-fuel" applications.

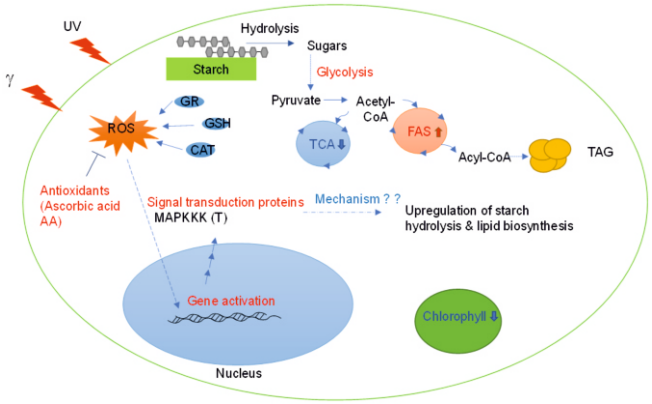

Fig.1: Radiation triggers "starch-to-oil" carbon-switching.
The pathways upregulated are indicated in red font while the downregulated in blue. Abbreviations: MAPKKK, mitogen-activated protein kinase kinase kinase; T, Transcript; TCA, tricarboxylic acid cycle; FAs, fatty acid biosynthesis; TAG, Triacylglycerol; GR, glutathione reductase; CAT, catalase; GSH, glutathione.

Highlights of the work caried out by Reema Devi Singh under the supervision of Dr. Ashish Kumar Srivastava (Guide) as a part of her doctoral thesis work. She was awarded a PhD. degree from Homi Bhabha National Institute in Life Sciences in 2023.

Salt Tolerance in Sugarcane: Lessons Learnt from a Radiation-induced Mutant

Sugarcane is a major food and biofuel crop of immense socio-economic relevance, on both national and global scale. Progressively increasing soil salinization in sugarcane-cultivating regions causes 25-30% reduction in cane yield and poor sugar recovery. This necessitates the development of robust and sustainable approaches for improving salt tolerance in sugarcane. However, due to its long life cycle and genome complexity, salt-adaptive mechanisms in sugarcane remain poorly understood. To address these lacunae, we characterized M4209, a promising salt-tolerant sugarcane mutant, derived from popular but salt-sensitive variety Co 86032, through radiation induced *in vitro* mutagenesis (RiMu).

Compared with Co 86032, M4209 exhibited 30% higher yield under saline field conditions, without significant yield penalties under control field conditions. This 'inducible salt tolerance' trait was investigated using a combination of transcriptomics and physio-biochemical studies. M4209 exhibited improved growth and survival under both moderate and severe salt stress, by maintaining ionic equilibrium, redox homeostasis, and photosynthetic efficiency. The activation of a chloroplast-centric transcriptional network in salt-stressed M4209 plants was suggestive of active nucleus-chloroplast communication. Thus, M4209's inducible salt tolerance was attributed to the salt-responsive transcriptional reprogramming of ion transport and antioxidant defense-related pathways, coupled with enhanced photosystem efficiency. Among the core genes associated with salt tolerance in M4209, a novel transcription factor, *SoSATA* (SALT-ACTIVATED TRANSCRIPTION ACTIVATOR), was selected for further characterization, due to its robust salt-responsive expression and putative regulatory function. The overexpression of *SoSATA* in Arabidopsis and soybean significantly improved plant growth under salt stress, suggesting its putative role as a positive regulator of salt tolerance.

At present, major sugarcane-cultivating states are facing the co-occurrence of increasing soil salinity with rising temperatures. However, the effect of combined heat and salt stress (HS-stress) and corresponding adaptive responses have not been investigated in sugarcane till date. Thus, a comparative evaluation of M4209 was performed under HS-stress scenario, wherein it exhibited significantly improved growth than Co 86032. In addition, M4209 exhibited lipid reprogramming towards higher plastidic:non-plastidic lipid ratio and lower root-to-shoot Na^+ translocation. Interestingly, M4209 exhibited a novel 'OSD' (Open Small Dense) stomatal phenotype, which was linked to an inherent transcriptional shift within the EPF9 (EPIDERMAL PATTERNING FACTOR 9)-EPF2 regulatory module. The OSD phenotype facilitated transpirational cooling and gas-exchange under HS-stress. This, coupled with enhanced photosynthetic assimilation, served as the major determinants of M4209's improved performance under HS-stress scenario. Our study demonstrates the enormous potential of the RiMu approach for development of agronomically important mutants in sugarcane, with the dual benefit of advancing fundamental understanding and accelerating crop-improvement programs.

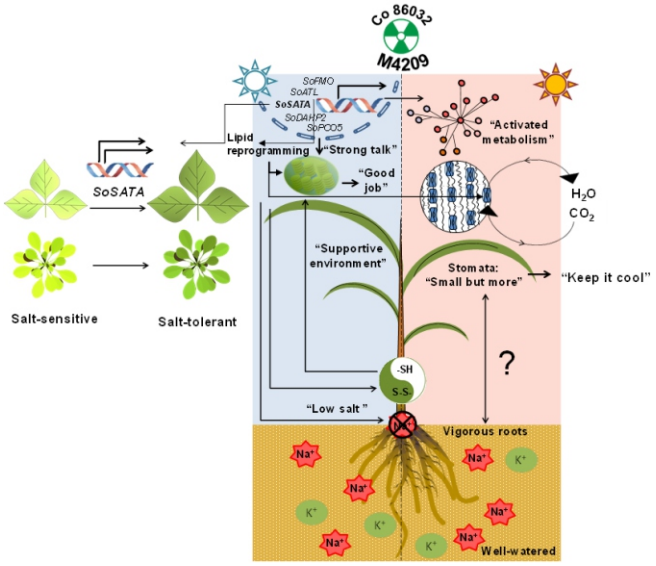

Fig.1: Proposed model for physio-molecular adaptions mediating improved tolerance to salt and HS stress in sugarcane mutant line M4209.

Highlights of the work carried out by Pooja Negi under the supervision of Dr. Ashish K. Srivastava (guide) as a part of her doctoral thesis work. She was awarded Ph.D. in Life Sciences from Homi Bhabha National Institute in 2024. [Best thesis award in SFRR-2024].

Functional Characterization of Site Specific Recombination System in *Deinococcus radiodurans*

During cell proliferation, the processes of DNA replication, genome segregation and cell division must be synchronized for stable inheritance of the genetic material. This is achieved by multiple checkpoint regulations in eukaryotes. But in prokaryotic cells, no such temporal or spatial regulatory mechanisms exist which would help in co-ordinating the various cellular processes together. Due to this reason, the eukaryotes are well suited to harbour multiple chromosomes whereas most bacterial cells harbour only a single chromosome in order to avoid any further complexity. But, the discovery of bacteria containing multiple chromosomes has raised attention-grabbing questions regarding the mechanisms involved in maintaining various genomic elements. One such bacterium is *Deinococcus radiodurans* which is an extremophile. It is one of the most radioresistant bacteria with a D_{10} value of 10 kGy i.e. about 3000 times the radiation tolerance of humans. It is a polyploid multipartite genome containing bacteria with two chromosomes and two plasmids which are tightly packed as compact doughnut shaped toroidal structure. The extreme phenotype of *D. radiodurans* can be attributed to its robust genomic structure, strong anti-oxidative stress response and an efficient DNA damage repair mechanism. But, how this unique genome architecture is maintained and segregated properly is still unknown. Bacteria in general contain circular chromosomes and chromosome dimers are formed after Bacteria in general contain circular chromosomes and chromosome dimers are formed after DNA replication. In *D. radiodurans*, the polyploidy increases the chances of formation of chromosome dimers. So, how these dimers are resolved and whether that has any significance to radiation resistance in this bacterium are the most intriguing questions.

The present study focuses on finding whether any chromosome dimer resolution system exists in *D. radiodurans* or not. The chromosome dimer resolution involves the function of site-specific recombination (SSR) system by tyrosine recombinases that could function independently or by the activation from the FtsK protein. Bioinformatics analysis has revealed that *D. radiodurans* encodes FtsK and six putative tyrosine recombinases. In-vivo functional role of FtsK in genome segregation and cell division is reported. For this, *ftsK-rfp* knock-in mutant cells expressing fluorescently tagged FtsK protein (FtsK-RFP) were generated. Time lapse imaging of live cells showed the dynamic movement of FtsK-RFP foci on the membrane and the nucleoid under normal conditions as well as post gamma irradiation (Fig. 1). Different domains of FtsK were also deleted from the genome which resulted in drastic changes in the nucleoid arrangement, cell membrane structure and cell morphology. Deletion of FtsK also resulted in delayed growth under normal (Unirr) and irradiated (Irr) conditions (Fig. 2A, B). All these results indicate towards an important role of FtsK in synchronizing the process of nucleoid separation with early cell division in *D. radiodurans*.

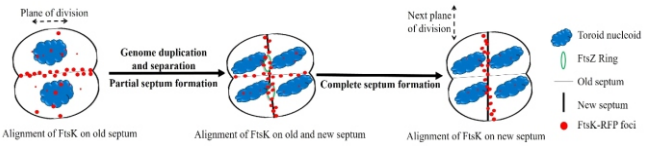

Fig.1: Schematic model of localization dynamics of FtsK during cell division in *Deinococcus radiodurans.*

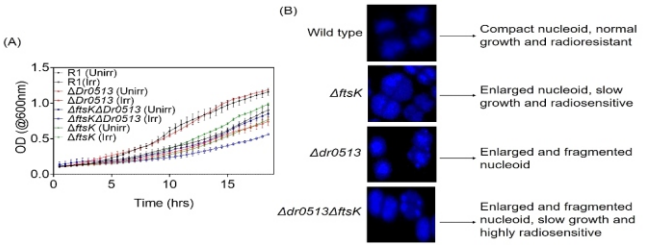

Fig.2: Deletion of FtsK and Dr0513 affects (A) the cell growth, the radioresistance and (B) the nucleoid structure in *Deinococcus radiodurans.*

The functional characterisation of one of the tyrosine recombinases of *D. radiodurans* (Dr0513) was also done. Deletion of coding sequence of Dr0513 leads to significant changes in the cells. In the absence of Dr0513, *D. radiodurans* cells failed to maintain the compact genome architecture. When both FtsK and Dr0513 were deleted from the cells, the growth was drastically reduced and various abnormal nucleoid arrangement was seen (Fig. 2A, B). Recombination assay showed that Dr0513 could perform SSR and FtsK could activate SSR.

All these results propose the functional significance of the site specific recombination system consisting of Dr0513 and DrFtsK in maintaining the unique nucleoid compactness of *D. radiodurans* R1. Lack of these proteins causes alterations in the nucleoid structure which ultimately effects the growth and gamma radiation response of the cells.

Highlights of the work carried out by Shruti Mishra under the supervision of Dr. Swathi Kota (Guide) as a part of her doctoral thesis work. This PhD thesis was submitted recently (Nov, 2024) to Homi Bhabha National Institute for the PhD Award in Life Sciences.

Selective Detection of Thorium (IV) in Aqueous Systems Using Advanced AIE Materials

Water-Soluble AIE Sensor for Thorium Detection

Madhusudan Ghosh[1], Sachin S. Kadlag[1,2], Kallola K. Swain[1,2], Prabhat K. Singh[2,3]*

[1]*Analytical Chemistry Division, Bhabha Atomic Research Centre, Trombay-400085, INDIA*
[2]*Homi Bhabha National Institute, Anushakti Nagar, Mumbai-400094, INDIA*
[3]*Radiation & Photochemistry Division, Bhabha Atomic Research Centre, Trombay-400085, INDIA*

*****E-mail for Correspondence: prabhatk@barc.gov.in*

Thorium (Th), a naturally occurring radioactive element critical to India's strategic nuclear energy programs, also poses significant health risks due to its radiological and chemical toxicity. Accurate detection of Thorium in water is essential not only for environmental monitoring and health safety but also for ensuring its safe and sustainable utilization within the Department of Atomic Energy's initiatives. Traditional detection methods like ICP-MS require complex setups, while optical sensors offer cost-effective, simple, and selective solutions. However, achieving effective aggregation-induced emission (AIE)-based turn-on sensing for Th(IV) in 100% aqueous media has been a challenge due to the need for water-soluble, low-background fluorescence fluorophores.

A novel fluorophore, tetra(4-sulfophenyl) ethylene (SuTPE), was developed, exhibiting significant emission enhancement upon aggregation induced by Th(IV) in pure water. This fluorophore demonstrated remarkable sensitivity with a limit of detection to 56 ppb and high selectivity, even in complex matrices such as tap and seawater. The underlying sensing mechanism was thoroughly validated using several techniques, including steady-state and time-resolved fluorescence, FTIR, SEM, AFM, and DLS. The aggregation of Th(IV) effectively restricts the intramolecular rotation in SuTPE, thereby blocking nonradiative decay pathways and significantly enhancing its fluorescence intensity.

This method establishes a significant precedent for environmentally friendly, aqueous-phase detection of Th(IV), effectively addressing the limitations of traditional organic solvent-based sensors. The study also investigated dual-metal interference and demonstrated very less impact from U(VI), a common co-contaminant with Th(IV), thereby ensuring precise and reliable detection. Advanced computational analysis further validated the superior interaction of SuTPE with Th(IV) compared to other metal ions, underscoring its high selectivity. This work not only offers potential for monitoring natural radioactive elements in environmental water bodies to enhance health safety standards but also paves the way for developing more robust AIE-based sensors for detecting other toxic elements.

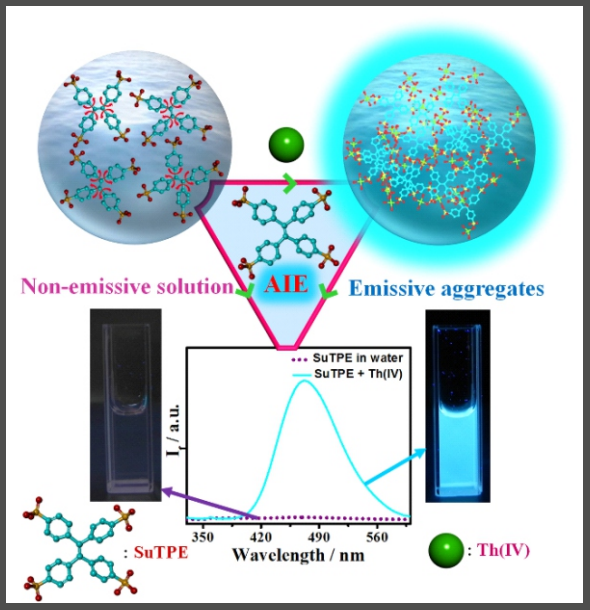

Fig.: Schematic representation of Th (IV) induced aggregation of SuTPE and the molecular structure of SuTPE (ACS Applied Materials & Interfaces 16 (2024), 57004-57016)

Reference:

Advanced AIE Materials for Environmental Monitoring: Selective Sensing of Thorium(IV) in Aquatic Systems, M. Ghosh, S. Kadlag, S.V. Bhosale, S. V. Bhosale, K. K. Swain, A. Ghosh, P. K. Singh*, ACS Applied Materials & Interfaces 16 (2024), 57004-57016.

Evolution of International Occupational Health and Safety Management Systems

Vyom Saxena
Health, Safety & Environment Group
Bhabha Atomic Research Centre (BARC), Trombay-400085, INDIA
E-mail for Correspondence: vsaxena@barc.gov.in

Introduction

A management system is a set of policies, processes, and procedures that an organization utilizes to manage tasks such as safe operation, product quality, legislative and regulatory conformance, etc. to achieve its objectives. An Occupational Health and Safety Management System (OHSMS) promotes a healthy working environment by providing a framework to identify, control, and manage Occupational Health and Safety (OHS) risks and opportunities [Boyle, 2019]. Gallagher describes Occupational Health and Safety Management Systems (OHSMS) as "an integrated framework comprising planning and review processes, organizational and management structures, consultative mechanisms, and specific program components, all working cohesively to enhance health and safety performance" [Gallagher, 2003]. Implementation of an effective OHSMS aims at bringing down workplace injuries and minimizing the accompanying costs. Many studies have shown that safety management has a positive influence not only on safety performance but also on parameters like competitiveness and economic-financial functioning [Fernández-Muñiz, 2009]. Occupational health and safety management systems (OHSMS) have evolved significantly over time, reflecting advances in industrial practices, societal awareness, technological innovation, and the identification of human factors as an important aspect in relation to OHS [Cohelo, 2005]. This evolution has transitioned from basic reactive measures to sophisticated, proactive, and integrated systems aimed at preventing workplace incidents, illnesses, and fatalities.

Occupational Health and Safety (OHS) practices were rudimentary in the pre-industrial era. Workplaces, primarily agricultural or artisanal, often relied on traditional methods without formal systems for managing risks. Hazards such as accidents or diseases were addressed reactively and informally. The Industrial Revolution (18th-19th Century) marked the beginning of large-scale factory systems, introducing machinery and mass production. These advancements also brought significant hazards such as exposure to harmful substances (e.g., coal dust, lead), dangerous machinery without safeguards, Poor ventilation and lighting, etc. Governments responded with some early legislations, e.g., the UK's Factory Acts (1833, 1844) introduced basic safety regulations, limiting working hours and mandating safeguards for machinery. The U.S. implemented state-level laws addressing workplace safety by the late 19th century [Manuele 2019].

The early 20th Century saw the emergence of Regulations saw development of formal OHS standards (20th century) with the establishment of formal health and safety standards. Workers' compensation laws were first introduced in Germany in the late 19th century and adopted globally in the early 20th century, these laws incentivized employers to reduce workplace hazards. Occupational diseases were recognized with Silicosis and asbestosis cases that highlighted the need for exposure limits and preventive measures. Institutionalization of OHS regulation began to take shape in the Mid-20th Century after World War II and subsequent industrial expansion emphasized workplace safety. The U.S. Occupational Safety and Health Act (1970) created OSHA, setting enforceable standards for workplace hazards, and organizations like the International Labour Organization (ILO) and the World Health Organization (WHO) promoted global OHS standards [ILO 2005].

Systematization of OHSMS started in the late 20th Century with rapid industrialization that gave rise to the

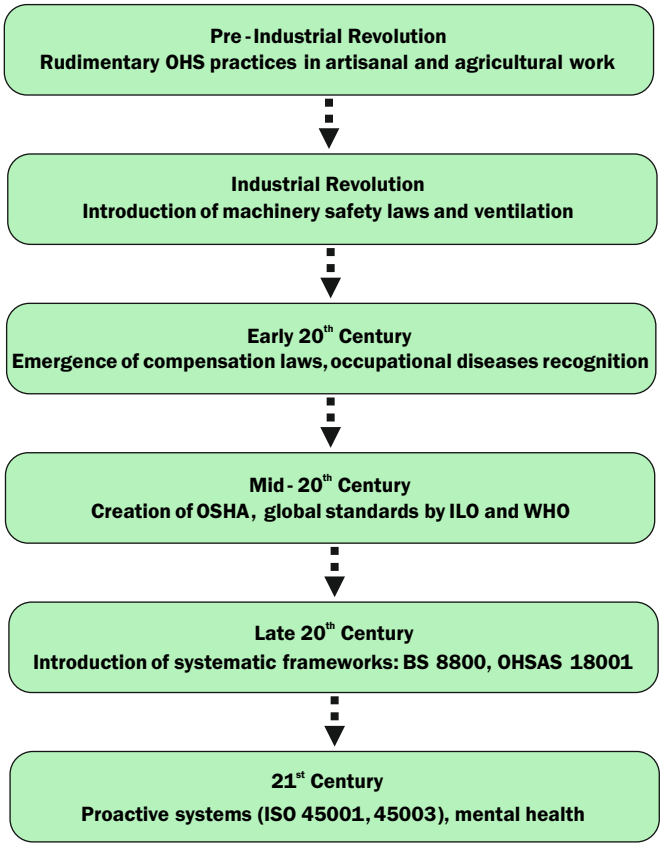

Fig.1: Evolution of systematization in Occupational Health and Safety.

Table 1: A comparison of various OHS management systems.

Aspect	ISO 45001	OHSAS 18001	ILO-OSH 2001	ANSI/ASSP Z10	BS 8800
Origin	International Organization for Standardization (ISO)	British Standards Institution (BSI)	International Labour Organization (ILO)	American Society of Safety Professionals(ASSP)	British Standards Institution (BSI)
Adoption	2018	1999 (withdrawn 2021)	2001	2005 (latest revision 2019)	1996 (superseded by OHSAS 18001)
Focus	Risk-based approach; worker participation	Hazard identification, risk assessment	Continuous improvement in OSH performance	Management systems for improving OSH	Guidance framework for OHSMS
Applicability	Global	Global	International	Primarily US	UK (guidance-level, non-certifiable)
Certifiability	Yes	Yes (until 2021)	No	No	No
Key Principle	PDCA Cycle, leadership commitment, and worker involvement	PDCA Cycle	Tripartite approach (employers, workers, and government)	Risk-based and performance-oriented	Framework and guidance
Structure	Annex SL (10 Clauses)	PDCA Cycle (non-Annex SL)	Flexible	High-level framework	Guidance document
Risk Management	Emphasis on proactive risk management	Reactive focus on hazard control	Proactive and preventive focus	Risk-based thinking and reduction	Hazard and risk guidance
Worker Participation	Strongly emphasized	Limited emphasis	Strongly emphasized	Encouraged	Encouraged
Integration with Other Standards	Easily integrates with ISO 9001, ISO 14001	Limited integration	Not explicitly designed for integration	Can be integrated with other systems	Limited integration
Legislation Alignment	Can be tailored to national regulations	Broadly aligned with existing laws	Focused on ILO standards	Focuses on US regulations and ANSI standards	Aligned with UK regulations
Context	Organization -specific context considered	Limited focus on organizational context	Not explicitly considered	Organizational factors considered	Limited contextual consideration
Migration	Replaces OHSAS 18001	Superseded by ISO 45001	Standalone	Standalone	Precursor to OHSAS 18001
Certification Benefits	Globally recognized; enhances credibility	Previously widely recognized	Not certifiable	Improves safety culture	Non-certifiable
Major Limitation	Requires significant implementation effort	Limited flexibility	Non-certifiable; guideline-based	US-centric	Superseded and outdated

concept of Management System Frameworks [Parvu, 2024]. The rise of total quality management (TQM) influenced OHSMS development. Frameworks emphasized a systematic approach, integrating health and safety into business processes. The earnest efforts towards OHS management systems were first attempted with the release of a guide to OHS in 1996 based on Health and safety at Work Act 1996 of the International Labour Organization. The British Standard BS 8800 (1996) and later the Occupational Health and Safety Assessment Series (OHSAS 18001) in 1999 provided a structured approach to implementing OHSMS globally [McKinnon 2019].

The 21st Century is the era of Modern OHSMS which emphasizes proactive risk management, employee engagement, and integration with other business systems. Modern systems focus on hazard identification, risk assessment, and prevention rather than incident response [Lynda, 2007]. The first international standard for occupational health and safety management systems came into being in 2007 as Occupational Health and Safety Assessment Series 18001 (OHSAS 18001). Over the past three decades, there have been constant efforts to improve the OHSMS and to make it more wide-ranging, realistic and comprehensive [Karanikas, 2019]. Fig. 1 depicts the evolutionary time chart on the systematization and standardization in OHS.

Published in 2018, this international standard replaced OHSAS 18001. It provides a risk-based approach aligned with ISO management system standards (e.g., ISO 9001 for quality management). ISO 45001, designed to drastically improve the levels of workplace safety and productivity is the new standard for management systems of OHS. It was first proposed in 2013 and the final document was published after many deliberations and revisions in March 2018. ISO45001 has now completely replaced the earlier international standard, OHSAS 18001. The OHSAS 18001-certified organizations had time till September 2021 to migrate to ISO 45001. With an emphasis on management commitment, worker involvement, and risk control, ISO 45001 intends to prevent work-related injuries, illnesses, and fatalities by specifying requirements for an OHSMS [Lindholm 2023]. This new standard follows the approach of other management systems such as ISO 14001 and ISO 90001. Although ISO 45001 draws on certain aspects of OHSAS 18001, it is a new and distinct standard, not a revision or update.

ISO 45001 significantly differs from its predecessor OHSAS 18001 which focused more on controlling hazards and provided a framework for the effective management of occupational health and safety including risk management and legal compliance. OHSAS 18001 had a reactive approach that focussed solely on risks and not solutions, whereas ISO 45001 has a proactive and preventive approach requiring hazard risks to be evaluated and remedied before they cause accidents and injuries. ISO 45001 is process-based and dynamic in all clauses whereas OHSAS 18001 is procedure-based and static. Similarly, ISO 45001 considers both risk and opportunities but OHSAS 18001 deals only with risk. Another major difference is that unlike OHSAS 18001, ISO 45001 considers the views of interested parties too. Table 1 Highlights the significant differences between Various international OHS guidelines and management systems.

In the course of continual evolution, ISO 45003, the most recent addition to OHSMS and the first global standard giving in-depth practical guidance on managing psychological health in the workplace was introduced in June 2021. An add-on extension of ISO 45001, it provides guidance on the management of psychosocial risks as part of the occupational

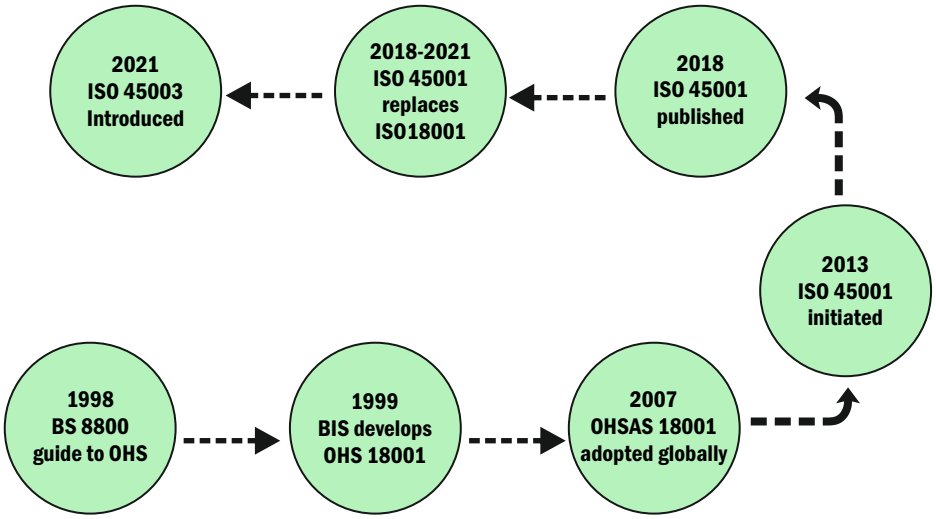

Fig.2: Timeline of the evolution of systematic International OHS guidelines and management systems.

health and safety management system [Leka, 2010]. ISO 45003 is not an accreditation in itself but a proactive attempt to encourage ISO 45001-certified organizations to consider mental health as an integral part of their working lives. Fig. 2 gives the timeline of the integrated standards in OHS culminating into OHS Management Systems (OHSMS).

Factors Influencing the present state of OHSMS Evolution and the Challenges

Technological Advancements of the present times have transformed the industry and workplaces like never before. The rapid strides made in fields like information technology, Automation, Digitalization, Robotics, and drone technology have not only revolutionized the occupational space but also the OHS facet. Real-Time monitoring is possible with IoT devices and sensors that allow continuous monitoring of workplace hazards, such as noise, air quality, and ergonomics. Predictive Analytics and Data-driven approaches can predict potential hazards with great precision and guide preventive actions. Digital Training Tools such as virtual reality (VR) and augmented reality (AR) offer immersive training experiences. However, the most unique feature of the latest OHSMS is its Employee-Centric Approaches. odern OHS management systems emphasize employee well-being and considers stress, burnout, and mental health as workplace concerns [Gallagher, 2001]. It acknowledges diversity and inclusion as important considerations to address unique risks faced by vulnerable groups, including women and older workers.

Government regulations have been a primary driver of OHSMS advancements, mandating compliance and setting minimum standards. Major industrial accidents like the Bhopal gas tragedy (1984) and the Chernobyl disaster (1986) underscored the importance of robust safety systems, leading to stricter regulations and better practices [Hale, 1998]. Globalization and the resultant global integration of supply chains has prompted multinational organizations to adopt consistent OHSMS frameworks across borders. Companies increasingly view OHS as a part of their ethical responsibilities, improving reputation and stakeholder trust. These influencing factors and the concomitant challenges are presented in Fig. 3.

The integration of advanced technologies such as AI, robotics, drones, and automation into workplaces brings numerous occupational hazards that require careful management. AI systems, while enhancing efficiency, can perpetuate biases, create privacy concerns through extensive data collection, and lead to overdependence, which may result in operational failures or errors. Workers interacting with robotics face risks of mechanical injuries, programming errors, and electrical or hydraulic failures. Additionally, drones introduce hazards like physical accidents, airspace interference, noise pollution, and cybersecurity breaches, while automation can lead to skill degradation, job insecurity, system failures, and ergonomic issues from repetitive monitoring tasks. These challenges are not only physical but also psychological, as workers may experience stress over adapting to these technologies or facing potential displacement [Nuhu 2024].

To address these hazards, organizations must adopt proactive safety measures. Training and awareness programs can equip workers with the skills needed to manage and mitigate risks associated with new technologies. Ergonomic design and user-friendly systems can minimize physical strain and errors. Conducting comprehensive risk assessments ensures that potential hazards are identified and mitigated early [Reese 2018]. Cybersecurity measures are crucial for protecting sensitive data, especially in AI-driven and drone-enabled environments. Furthermore, psychological support systems can help workers cope with the stress and anxiety arising from job insecurity and workplace changes. By implementing these strategies, industries can cultivate a safer and more inclusive environment, ensuring the benefits of advanced technologies are harnessed without compromising worker well-being.

Small and medium enterprises (SMEs) often face significant challenges in implementing comprehensive occupational health and safety management systems (OHSMS) due to limited resources [Robson 2007]. Financial constraints make it difficult for SMEs to invest in advanced safety technologies, hire dedicated safety professionals, or conduct regular risk assessments. Additionally, a lack of technical expertise can hinder the development and maintenance of systematic frameworks aligned with standards like ISO 45001. SMEs also struggle with time constraints, as small teams often prioritize operational demands over safety initiatives. Compliance with complex regulations can be overwhelming, especially in industries with stringent safety requirements, leading to a reliance on reactive measures rather than proactive systems. These constraints highlight the need for tailored support, such as simplified guidelines, affordable training programs, and government subsidies to help SMEs enhance workplace safety effectively.

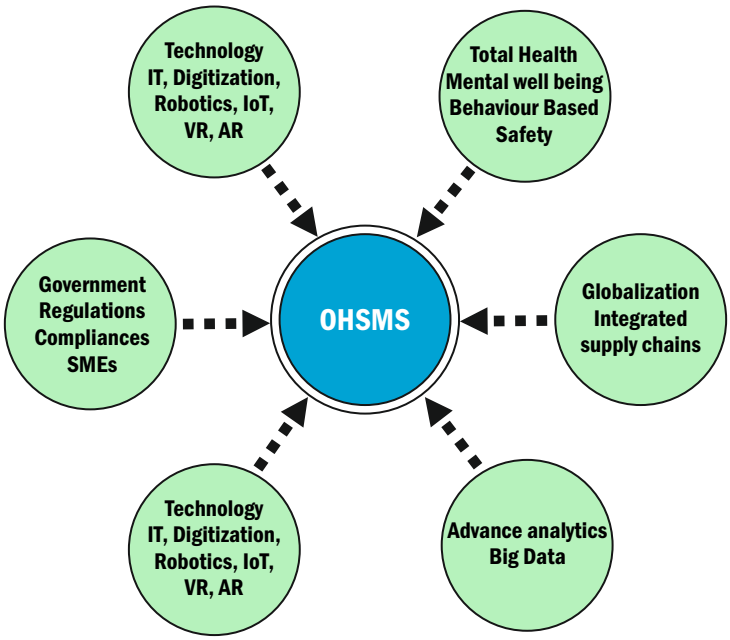

Fig.3: The current Influencing Factors and the associated challenges for OHSMS.

Future Trajectory of OHSMS

Aligning Occupational Health and Safety Management Systems (OHSMS) with Environmental, Social, and Governance (ESG) goals represents a holistic approach to workplace safety and sustainability. By integrating OHSMS with ESG frameworks, organizations can address worker safety while promoting environmental stewardship and social responsibility. This alignment ensures that safety practices consider environmental impacts, such as reducing waste or emissions, and prioritize inclusivity and well-being for all employees [Wang 2020]. Governance principles enhance accountability, encouraging transparent reporting of health and safety metrics alongside ESG performance. Such integration not only boosts compliance and stakeholder trust but also drives sustainable growth by embedding safety and ethical considerations into core business strategies.

Leveraging big data and AI for predictive risk management enables organizations to proactively identify and mitigate potential workplace hazards. By analyzing vast datasets from sensors, equipment logs, and employee feedback, AI algorithms can detect patterns and predict risks before incidents occur. For example, machine learning models can forecast equipment failures or highlight high-risk areas based on historical trends. This data-driven approach enhances decision-making, allowing for timely interventions and resource optimization. Additionally, predictive tools improve compliance with safety regulations by providing actionable insights in real time. Integrating big data and AI into risk management systems not only enhances workplace safety but also fosters a culture of continuous improvement and innovation [Parvu 2024].

Occupational Health and Safety Management Systems (OHSMS) can ensure psychological safety by creating an inclusive, supportive, and mentally healthy work environment. Key strategies include promoting open communication, where employees feel safe to express concerns or ideas without fear of retaliation or judgment. Incorporating mental health initiatives, such as stress management programs, access to counseling, and training managers to recognize and address psychological stressors, helps mitigate burnout and anxiety. OHSMS can also establish policies against workplace bullying, harassment, and discrimination, ensuring fairness and respect for all employees. Regular assessments of workplace culture, combined with feedback mechanisms, allow organizations to identify and address psychosocial risks proactively [Lindholm 2023]. By embedding psychological safety into OHSMS, businesses not only enhance employee well-being but also improve engagement, productivity, and overall organizational resilience.

National Regulatory Frameworks

United States

Occupational Safety and Health Administration (OSHA) primarily governs the United States' regulatory framework. OSHA sets permissible exposure limits (PELs) for various workplace hazards, including airborne contaminants, noise, and exposures from various chemicals. organizations like the American Conference of Governmental Industrial Hygienists (ACGIH) Complement OSHA, and provide Threshold Limit Values (TLVs) that often influence international standards. Additionally, the National Institute for Occupational Safety and Health (NIOSH) conducts research and issues recommendations that guide OSHA's regulations [ILO 2024].

European Union

Occupational Health and safety standards in the European Union (EU) are codified under the European Framework Directive 89/391/EEC. This directive mandates that employers assess and mitigate risks while advancing a culture of preventive safety. The EU's regulatory approach often emphasizes worker participation in safety programs. Additionally, the REACH (Registration, Evaluation, Authorisation, and Restriction of Chemicals) regulation directly impacts industrial hygiene by enforcing stringent controls over chemical use and exposure [ILO 2024].

Japan

Japan's industrial hygiene framework is regulated by the Industrial Safety and Health Act (ISHA) which mandates comprehensive risk assessments, regular health check-ups for workers, and strict adherence to exposure limits for hazardous substances. Japan's emphasis on proactive measures, including education and training, aligns closely with international best practices [ILO 2024].

Australia

Australia's Model Work Health and Safety (WHS) Act and related codes of practice ensure robust industrial hygiene measures. The Safe Work Australia agency supports compliance through guidelines and exposure standards. Australia's system is distinguished by its clear guidelines for industries like mining, agriculture, and construction [Gallagher, 2001].

The Indian Regulatory Picture

India's industrial hygiene regulations are governed by multiple frameworks, including the Factories Act, 1948, and the recently introduced Code on Occupational Safety, Health, and Working Conditions (OSH Code), 2020. These regulations mandate provisions for workplace ventilation, dust control, chemical safety, and occupational health services. However, significant challenges persist, including limited enforcement, fragmented regulatory oversight, and lack of worker awareness. The recent legislative framework, the OSH Code 2020 consolidates and simplifies existing labor laws, offering an opportunity for streamlined implementation. Industries like mining, chemicals, and construction are under stricter scrutiny for compliance. However, Insufficient staffing and resources for inspectorates hinder effective implementation [OSH 2020].

Conclusion

Occupational Health and Safety Management Systems (OHSMS) have progressed from reactive, informal measures to structured, proactive frameworks that prevent workplace hazards. Early efforts, influenced by industrial milestones like the Industrial Revolution, included legislation such as the UK's Factory Acts and U.S. safety laws. The 20th century formalized OHS with global standards, such as BS 8800 and OHSAS 18001, emphasizing systematic integration into business operations. Modern OHSMS, like ISO 45001, focus on proactive risk management, employee engagement, and addressing psychological health (ISO 45003). Technological advancements, including IoT, AI, and predictive analytics, enable real-time monitoring and hazard prediction, while SMEs face challenges due to limited resources. Future trends include aligning OHSMS with Environmental, Social, and Governance (ESG) goals, leveraging big data for predictive safety, and fostering psychological well-being. Global regulations, tailored to regional needs, continue to drive advancements. This evolution highlights a growing commitment to safer, more inclusive, and conducive workplaces.

References

[1] Boyle, T. (2019). Health and Safety: Risk Management (5th ed.). Routledge. United Kingdom. https://doi.org/10.4324/9780429436376

[2] Coelho, D., & Matias, J. C. O. (2005). The Benefits of Occupational Health and Safety Standards. In W. Karwowski (Ed.), Handbook of Standards and Guidelines in Ergonomics and Human Factors (pp. 30-58). CRC Press. United States. https://doi.org/10.1201/9781482289671-30

[3] Fernández-Muñiz, B., Montes-Peón, J. M., & Vázquez-Ordás, C. J. (2009). Relation between occupational safety management and firm performance. Safety Science, 47(7), 980-991. DOI: 10.1016/j.ssci.2008.10.022.

[4] Lynda S. Robson, Judith A. Clarke, Kimberley Cullen, Amber Bielecky, Colette Severin, Philip L. Bigelow, Emma Irvin, Anthony Culyer, Quenby Mahood, (2007), The effectiveness of occupational health and safety management system interventions: A systematic review, Safety Science, Volume 45, Issue 3, pp. 329-353, ISSN 0925-7535.

[5] Parvu Adriana, Lucian-Ionel Cioca (2024) The evolution of work and safety and health at work in Industry 4.0 / Industry 5.0, MATEC Web of Conferences 389, DOI: 10.1051/matecconf/202438900074.

[6] Gallagher Clare, Elsa Underhill, Malcolm Rimmer (2003) Occupational safety and health management systems in Australia: Barriers to success; Policy and Practice in Health and Safety 1(2):67-81, DOI: 10.1080/14774003.2003.11667637.

[7] Hale, A. R., & Hovden, J. (1998). Management and culture: The third age of safety. A review of approaches to organizational aspects of safety, health, and environment. Occupational Injury: Risk, Prevention and Intervention, 129-165.

[8] International Labour Organization (ILO). (2015). Occupational Safety and Health in Mining: Anthology on the Situation in 16 Mining Countries. ILO Publications. Switzerland.

[9] Karanikas, N., & Pryor, P. (2019). OHS Management Systems. In "The OHS Body of Knowledge" (Chapter 12.2). Australian Institute of Health and Safety. Australia. https://www.ohsbok.org.au/bok-chapters/

[10] Leka, S., & Jain, A. (2010). Health Impact of Psychosocial Hazards at Work: An Overview. World Health Organization, Switzerland. ISBN: 9789241500272

[11] Manuele, F. A. (2019). Occupational Safety and Health Management. In R. L. Harris & P. A. Heaney (Eds.), Handbook of Occupational Safety and Health (3rd ed., pp. 653-670). Wiley. United States. https://doi.org/10.1002/9781119581482.ch21

[12] McKinnon, R. (2019). The Design, Implementation, and Audit of Occupational Health and Safety Management Systems. CRC Press. United States. https://doi.org/10.1201/9780429280740

[13] Lindholm M. et al. (2023). The evolution of new and emerging occupational health and safety risks. Work, 79(2), 15-27. DOI: 10.3233/WOR-230005.

[14] Nuhu, O. Y. (2024). Occupational Safety and Health Management: A Bibliometric Analysis from 1979 to 2024. Scientific African.

[15] Reese, C. D. (2018). Occupational Health and Safety Management: A Practical Approach (3rd ed.). CRC Press, United States.

[16] Robson, L. S., Clarke, J. A., Cullen, K., Bielecky, A., Severin, C., Bigelow, P. L., & Mahood, Q. (2007). The effectiveness of occupational health and safety management system interventions: A systematic review. Safety Science, 45(3), 329-353. DOI: 10.1016/j.ssci.2006.07.003.

[17] Wang, Y., Chen, H., Liu, B., Yang, M., & Long, Q. (2020). A Systematic Review on the Research Progress and Evolving Trends of Occupational Health and Safety Management: A Bibliometric Analysis of Mapping Knowledge Domains. Frontiers in Public Health, 8, Article 81. Switzerland. https://doi.org/10.3389/fpubh.2020.00081

[18] ILO(2024), Global database on occupational safety and health legislation, https://www.ilo.org/resource/global-database-occupational-safety-and-health-legislation

[19] OSH (2020) The Occupational Safety, Health and Working Conditions Code, 2020 No. 37 of 2020 https://labour.gov.in/whatsnew/occupational-safety-health-and-working-conditions-code-2020-no-37-2020

Homi Bhabha Science & Technology Maanpatra – HBSTM

Recognizing Excellence in Science, Engineering and Technology

The Department of Atomic Energy (DAE) introduced a one-time internal recognition, with no cash component, in place of DAE Science and Technology Awards, named the HBST - Maanpatra (HBSTM), to acknowledge exceptional achievements and outstanding contributions in science, engineering and technology. The age of the nominee shall not exceed 45 years on 01st January of the year for which he/she is being considered for HBSTM.

Scientists and engineers from various DAE units i.e., AERB, AMDER, BARC, BHAVINI, BRIT, DCSEM, DPS, ECIL, GCNEP, GSO, HWB, IGCAR, IREL, NFC, NPCIL, RRCAT, UCIL and VECC are eligible for this honour.

The complete process, from nomination to declaration of winners, was paperless and handled through an online portal. The Maanpatra(s) are presented annually on Founder's Day.

The Director, BARC invited nominations from all Units on August 5, 2024 for the HBST-Maanpatra. A total of 107 nominations were received through the portal from various DAE units, which included 56 nominations in engineering category, 32 in science category and 19 in technology category. These nominations were meticulously evaluated at two levels and the most deserving candidates were shortlisted for their remarkable contributions. The fourteen selected officers which included five awardees in science category, five awardees in engineering category and four awardees in technology category. List of awardees is presented here.

The Maanpatra, were presented on October 30, 2024 at the Central Complex Auditorium, BARC. The Chairman, AEC & Secretary, DAE conferred the winners with handcrafted Maanpatra and its scroll-box, recognising their dedication and achievements in advancing science, engineering and technology.

The HBST-Maanpatra stands as a testament to DAE's commitment to fostering excellence and innovation within its scientific and engineering communities, encouraging scientists and engineers to continue contributing to the nation's progress in field of nuclear science and technology.

Awardees of maiden HBSTM

Science Category

Dr. A. K. Srivastava
BSG, BARC

Dr. Amit Kunwar
CG, BARC

Dr. Mohit Tyagi
PG, BARC

Dr. P. C. Rout
PG, BARC

Dr. Tapan Kumar Rana
Physics, VECC

Engineering Category

Dr. V. P. Sinha
NFG, BARC

Shri Alok Prakash
RPG, BARC

Shri Suneel Gattu
NRB, BARC

Dr. M. V. S. R. Ravi Kanth
Zinc & Special Material, NFC

Shri Shrikant D. Mishra
Civil, NPCIL

Technology Category

Shri S. K. Vadali
NFG, BARC

Dr. Nafees V. Ahmed
ChTG, BARC

Dr. Khageswar Sahu
MSATG, RRCAT

Dr. Diptimayee Samantaray
MMG, IGCAR

HBST Maanpatra 2024 Awardees, Director of BARC, and Chairman of AEC pose for a group photograph in Central Complex Auditorium, BARC Trombay.

BARC Scientists Honoured

Dr. Kinshuk Dasgupta (on the left hand-side) receiving the IIM-Hindustan Zinc Gold Medal 2024.

Dr. Kinshuk Dasgupta, Scientific Officer and Head, Advanced Carbon Materials Section, Glass & Advanced Material Division, Materials Group, Bhabha Atomic Research Centre and Professor, Homi Bhabha National Institute, has been awarded the IIM-Hindustan Zinc Gold Medal 2024 in recognition of his significant contributions to Non-Ferrous Metallurgical Industries. Dr. Dasgupta was also conferred with the Indian Institute of Chemical Engineers' Herdillia Award 2024 for Excellence in Basic Research in Chemical Engineering, especially for his pioneering research in the field of carbon materials.

Dr. Dasgupta joined BARC as a Scientific Officer after completing his Bachelors in Engineering (Metallurgy and Materials Science) from Jadavpur University, Kolkata. He completed his PhD in Chemical Engineering from the Institute of Chemical Technology, Mumbai. He visited University of Cincinnati, USA as a Fulbright visiting scholar during 2018-19. Dr. Dasgupta's research interest includes carbon materials, composites and coatings. He has published more than 140 research papers in international journals, 90 conference papers, 3 book chapters and 3 patents. He has transferred several technologies to the industries. Dr. Dasgupta has delivered many invited lectures.

Dr. Kinshuk Dasgupta has received many awards, including the most coveted Shanti Swarup Bhatnagar Prize in Engineering Sciences in 2020. The Ministry of Steel, Govt. of India, bestowed upon him 'Young Metallurgist of the Year' in 2007. Further he received 'Young Engineer Award' in 2012 and 'Scientific and Technical Excellence Award' in 2017 from Department of Atomic Energy, "N. J. Suchak Innovation Award 2019", "Distinguished Alumnus Award 2022" from the Institute of Chemical Technology, and "VASVIK Industrial Research Award" in 2020.

Shri Amit Kaushal (centre) receiving honors from the office bearers of the Indian Institute of Chemical Engineers (IIChE).

Shri Amit Kaushal, Scientific Officer, Advanced Carbon Materials Section, G&AMD, Materials Group, BARC has been awarded the Amar Dye-Chem Award 2024 for Excellence in Basic Research and Development in Chemical Engineering, instituted by the Indian Institute of Chemical Engineers (IIChE). The award recognises Shri Kaushal for developing high-performance carbon nanotube fibres by floating catalyst chemical vapour deposition method.

Shri Kaushal began his career in BARC after earning a Bachelor's degree in Chemical Engineering from BIT Sindri, Dhanbad, Jharkhand. Further, he pursued Masters in Chemical Engineering from the Homi Bhabha National Institute, Mumbai and is currently pursuing his PhD from the same institute. His research focuses on chemical process development and intensification with a strong emphasis on carbon nanomaterials. Among his significant achievements, Shri Kaushal has successfully transferred two key technologies to industry-Flexible and Freestanding CNT Sheets, and Bulk Production of CNT Powder. He has over 18 research papers published in reputed international journals. Additionally, he has received multiple best presentation awards at prominent conferences.

Industry

BARC's Nuclear

On November 22, 2024, the Technology Transfer and Collaboration Division (TT&CD) of Bhabha Atomic Research Centre (BARC) and Atal Incubation Centre (AIC-BARC) conducted a significant technology transfer ceremony in Mumbai. The AKRUTI programme for propagation of BARC-DAE technologies among the rural environs too witnessed significant new developments. The ceremony underscored BARC's commitment to technological innovation and entrepreneurial support across multiple domains. A brief update on these developments is presented here.

Technology Transfers Agreements

The event featured 16 technology transfer agreements with notable companies. The technologies transferred to the industry encompass Pharmaceutical and Biotechnology Innovations, Environmental and Sustainability Technologies, Advanced Material and Manufacturing Technologies, and Specialized Detection and Monitoring Technologies.

In Pharmaceutical and Biotechnology Innovations landscape, Asian Aerosol OAN Pvt. Ltd., Mumbai secured the technology on Bio-available curcumin formulations with significant applications in pharmaceutical and nutraceutical sectors. The technology for synthesizing o-Tolylbenzonitrile (OTBN) which functions as an advanced intermediate for anti-hypertensive drugs was secured by Prashant Industries, Ahmedabad. Enerchii Minchem Pvt. Ltd., Bhubaneswar secured the technology of Superabsorbent BARC-Hydrogel (MRIDAMṚT) with potential impact across advanced material sciences. The technology of atmospheric pressure portable catalytic air plasma system for fast synthesis of aqueous Nitrate & Nitrite fertilizers was also transferred to industry partners, including to a Pune-based firm M/s. United Bio Energy Pvt. Ltd.

Signing of the technology transfer agreement with Pune based M/s. United Bio Energy Pvt. Ltd., in presence of Shri Martin Mascarenhas, Director of the Beam Technology Development Group, BARC and Dr. S Adhikari, Director of the Knowledge Management Group and Dr. Padma Nilaya, Head of the Laser & Plasma Division in BARC.

Signing of the technology transfer agreement with M/s Okosu Industries LLP, Surat (Gujarat) in presence of Dr. Raghvendra Tewari, Director of the Materials Group, BARC and Dr. S. Adhikari, Director of the Knowledge Management Group, BARC and Shri Daniel Babu P., Head, TT&CD, BARC and other high-ranking officials.

In Environmental and Sustainability Technologies landscape, H_2O Dynamics India Limited, South Goa secured the technology of Hybrid Granular SBR for Wastewater Treatment as well as the Process system for cleaning contaminated wastewater. The technology of Rapid Composting for organic waste decomposition with

beckons

Spin-off technologies

AKRUTI Kendra-Tarapur Agreement with Palghar-based firm M/s. K.K. Enterprises for transfer of 'Banana Health Drink' technologies.

applications in Municipal and temple waste management has been transferred to Arihant Bioscience and Adrem Solutions. Additionally, Radiation Assisted Adsorbent Technology for Textile Effluent Decolouration, and Compact Helical Biodegradable Waste Converter – SHESHA, was also transferred to the industry partners.

In Advanced Material and Manufacturing Technologies landscape, OKOSU Industries LLP, Surat secured the technology of Titanium diboride (TiB2) powder production & Zirconium diboride (ZrB2) powder fabrication with significance in advanced materials engineering industries.

In Specialized Detection and Monitoring Technologies landscape, Electronics Corporation of India Limited, Hyderabad (a unit of DAE) secured the technology of Portable Radio Isotope Detection with significant applications in radiation monitoring & safety.

Start-up Incubation

In startup incubation and entrepreneurship landscape, Team Cassion is incubating on developing an efficient technology for extracting kokum butter which has the characteristics of good taste, texture and flavor and can become a potential alternative to vegetarian fat used in cooking and confectionery.

The in-house technology incubation landscape, an agreement was inked with Hyurja Fuel Systems and Vasantdada Sugar Institute for incubation on Plasma pyrolysis plant for low-carbon hydrogen production and Gamma-irradiated chitosan crop production formulation, respectively. For the technology of Bioavailable Cold Water Dissolvable Formulation of Astaxanthin and Pomegranate Peel Extract, an agreement was inked under Collaborative Technology Incubation category with Pluviago Pvt. Ltd. Ace-Ex Industries has successfully graduated from the incubation program on the technology of Handheld Gamma Spectrometer based on Cesium Iodide (CsI) Single Crystal.

AKRUTI Programme Expansion

The Advance Knowledge and Rural Technology Implementation initiative (AKRUTI) continued its mission of encouraging entrepreneurship. Key developments in AKRUTI landscape are as follows.

Four new AKRUTI Kendras established with academic institutes viz., **UBKV** (Uttar Banga Krishi Vishwavidyalaya) at Cooch Behar in West Bengal, **DYPACSC** (Dr. D. Y. Patil Arts, Commerce and Science College) at Pimpri, Pune in Maharashtra, **MGU** (Mahatma Gandhi University) at Kottayam in Kerala, **PAHSU** (Punnyashlok Ahilyabai Holkar Solapur University) at Solapur in Maharashtra.

Two new technology transfer agreements were inked with a Pune-based firm M/s. Organic India, LLP for 'Micropropagation of Banana' and a Palghar-based firm M/s. K.K. Enterprises for 'Banana Health Drink' technologies through AKRUTI Kendra-Tarapur, established in 2021 through NPCIL CSR funding arrangement and is managed by Shree Vitthal Education and Research Institute - SVERI, Pandharpur. The AKRUTI Kendra-Tarapur generated a revenue of Rs.250,000 (70% of accrued through license fee) in the last trimester of 2024.

The agreement for establishing an AKRUTI Kendra at Mahatma Gandhi University in Kottayam, Kerala MGU was inked in presence of Prof. Dr. Bismi Gopalakrishnan, Registrar of MGU, Dr. S. Adhikari, Director of the KMG and Shri Daniel Babu P., Head, TT&CD, BARC and other high-ranking officials.

Reports from conferences, theme meetings, symposia, and outreach

The inaugural function of NDE-2024.

ISNT Conference and Exhibition on Non-Destructive Evaluation & Enabling Technologies

The 34th Annual Conference and Exhibition on Non-Destructive Evaluation & Enabling Technologies (NDE-2024) was organized by the Indian Society for Non-Destructive Testing (ISNT) during 12-14 December, 2024 at Chennai, Tamil Nadu and the conference was inaugurated on 12th December, 2024 by Anil V. Parab, Sr. Executive Vice President, L&T (Heavy Engg. & L&T Valves). More than 1000 delegates from national and international research & development laboratories, academia and industries, participated in the proceedings of the three-days conference. Dr. V. H. Patankar, Head, UIEFS, Electronics Division, BARC chaired a technical session on 'Applications of NDE in Energy Sector' and he delivered an invited talk on 'Ultrasonic Instrumentation for NDE of Components & Structures and Way Forward', in the technical session on 'Advances in Ultrasonics: Instrumentation & Acquisition'. Other officers from BARC who participated in the conference and presented research papers include Manojit Shaw, QAD; Roshan R. Sahu, CnID; Kum. Samadrita Chakraborty, CDM; Dr. Lakshminarayana Yenumula, ITIS; Sayan Banerjee, ED; Ashutosh Srivastava, CDM; Anant Mitra, ITIS, and Rajesh V. Acharya, ITIS. NDE 2024 conference was aimed to address the specific needs and challenges of a myriad of industries, including aerospace, automobile manufacturing, power generation, infrastructure, and others.

1 Komal Kapoor, Chairman, NDE 2024 & Chief Executive, Nuclear Fuel Complex, Hyderabad speaking at the event.

2 Dr. V.H. Patankar, Head, UIEFS, Electronics Division, BARC speaking in the technical session on 'Advances in Ultrasonics: Instrumentation & Acquisition'.

Reports from conferences, theme meetings, symposia, and outreach

Group photograph of delegates to DAE-BRNS symposium SAACM-2024.

Symposium on Advances in Atomistic and Continuum Modeling

The DAE-BRNS Symposium on Advances in Atomistic and Continuum Modeling (DAE-SAACM-2024) was organized at the DAE Convention Center in BARC Campus, Mumbai during 23-26 November 2024. The three-days symposium was organized jointly by Chemical Engineering Group (ChEG), BARC in association with the Board of Research in Nuclear Sciences, DAE and the Society for Atomistic and Continuum Modeling (SACM). During the inaugural day of the symposium, the welcome address was made by Dr. S. Mukhopadhyay, Head, ChED followed by introductory remarks by Dr. R. Tewari, Director of the Materials Group, BARC. In his speech, Shri K.T. Shenoy, Director, ChEG and Chairman of the SAACM-2024 emphasized the need to work out a common platform that will function as a bridge between atomistic and continuum modeling research. Professor R.B. Grover, Member, Atomic Energy Commission had been invited as the chief guest to the symposium. In his inaugural speech, Prof. Grover discussed the needs of the atomistic modeling based multi-scale approach in advanced scientific research. The proceedings of the workshop, presented in the form of a souvenir, was released by him. The special issue of SACM was released by Prof. E.D. Jemmis of IISc, Bangalore, who was the guest of honor to the symposium. The vote of thanks was delivered by Dr. Sk. Musharaf Ali, Head, AMCAS, ChED and Convener of the SAACM-2024. The symposium saw participation of 300 delegates from both DAE units and non-DAE institutes. A total of 185 abstracts were submitted by the invited speakers and research scholars for the symposium. A plenary lecture, invited lectures and short lectures were delivered on varied topics, including on electronic structure calculations such as density functional theory, equilibrium and non-equilibrium statistical mechanics, molecular dynamics and Monte Carlo simulations and computational fluid dynamics. Machine learning-driven atomistic modeling was also discussed. The subject experts from several Pan-India institutes such as IISc, TIFR, IACS (Kolkata), JNCASR, IITs (Mumbai, Chennai, Patna, Hyderabad, Jodhpur), ICT (Bhubaneswar), IISER (Pune), CEBS (Mumbai), IGCAR (Kalpakkam) and from BARC made their presentation on various aspects of atomistic modeling. SAACM handed over the certificates of participation to all participants. The Atomistic Modeler of Year-2024 plaque was awarded to Dr. Arya Das of Nuclear Recycle Board, BARC, Mumbai at the symposium.

PARMANU JYOTI

Empowering Future Innovators in Nuclear Scitech through Outreach

The Parmanu Jyoti Program, launched by the Department of Atomic Energy (DAE), is designed to foster awareness of atomic energy research and development among school students throughout India. The program aims to educate students about the peaceful applications of nuclear technology, inspiring interest in scientific careers, and enhancing scientific literacy.

Initiated in 2022, the program has already reached nearly 100,000 students across various Jawahar Navodaya Vidyalayas (JNVs) by engaging over 100 young and experienced scientists, referred to as 'Parmanu Mitras,' predominantly from BARC, and other DAE units.

This initiative particularly targets JNVs, which are established in every district of the country to provide quality education to gifted children from rural backgrounds.

In November 2024, during its fourth campaign, the Parmanu Jyoti Program expanded its outreach beyond JNVs to include schools under the Atomic Energy Education Society, particularly those in remote regions of central and eastern India Chhattisgarh and Jharkhand.

This broadening of scope underscores DAE's commitment to cultivating a scientifically informed society that recognizes the potential of nuclear technology for sustainable development. The program highlights the significance of outreach as part of DAE's dedication to Scientific Social Responsibility (SSR) and community involvement.

By engaging with students directly, the initiative not only disseminates knowledge but also builds a bridge between young minds and the scientific community, fostering a culture of curiosity and innovation.

JNV DAMOH, MADHYA PRADESH

JNV SAHUKHANTA, ODISHA

JNV BHOPAL, MADHYA PRADESH

JNV JHABUA, MADHYA PRADESH

Transforming Nuclear Building

During November-December 2024, the Human Resource Development Division of BARC inaugurated a new digital studio equipped with state-of-the-art facilities, designed to enhance training capabilities for scientific officers and technical manpower across BARC and other DAE constituent units. This initiative aligns with BARC's ongoing commitment to providing advanced training and knowledge transfer in nuclear sciences.

Education & Scientific Future

The inauguration function of renovated BARC Training School Hostel and Guest House in Anushakti Nagar during December 2024 was presided over by Dr. Ajit Kumar Mohanty (Chairman AEC & Secretary DAE), Shri Vivek Bhasin (Director BARC), and other senior officers from HRDD, HBNI, and DCSEM. The infrastructure upgrade was aimed to modernize the existing facilities to better support the growing academic and training requirements of the Homi Bhabha National Institute and BARC Training School.

New Crop Varieties Developed by BARC released for Commercial Cultivation

Nuclear Agriculture & Biotechnology Division, BARC and SIRD Newsletter Editorial Team

Over the past several decades, Bhabha Atomic Research Centre (BARC), Trombay has played a pivotal role in developing new crop varieties by employing radiation-based mutation breeding techniques. This method, which involves exposing seeds to radiation (such as gamma rays or electron beam) for inducing beneficial genetic changes, has enabled BARC to develop climate resilient, non-GMO, high-yielding crops that are suited to India's diverse agricultural conditions. Recently, BARC, in collaboration with different state universities, has released eight new crop varieties – five cereals and three oilseeds- for commercial cultivation across various states. BARC has now dedicated a total of 70 crop varieties to the farmers and people of India with more in the offing.

Radiation for Rice Gains

Chhattisgarh Trombay Luchai Mutant (CTLM)

	Parent	Mutant
Plant Height (cm)	161	105
Maturity duration (days)	145	111
Grain yield (q/ha)	33.4	47.5

- 40% high yield
- Soft cooking quality

Traditional Rice Heals - Sanjeevani Rice

Rice for Saline Frontiers

Trombay Konkan Khara

- 15% higher yield
- Tolerance: 6-7 dS/m EC

Heat Resilient Wheat

Trombay Jodhpur Wheat - 153

Tolerance	TJW-153
Iron & Zinc	Multiple diseases
Grain yield (q/ha)	~ 40 ppm
	50

Wheat Thriving in Stress

Trombay Raj Vijay Wheat - 155

	TRVW-155
Tolerance	Wheat Blast & Rust
Iron & Zinc	40 ppm
Grain yield (q/ha)	58

An all-weather Groundnut

Chhattisgarh Trombay Mungfali

➢ 18% high yield

	CGTM (TG-88)
Season	Rainy & Summer
Maturity duration (days)	105

High Yielding Sesame

Trombay Latur Til - 10

- 15% high yield
- Bold Seed

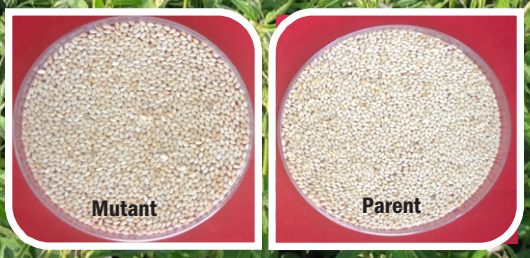

Mustard for Oil Prosperity

Trombay Jodhpur Mustard - 2

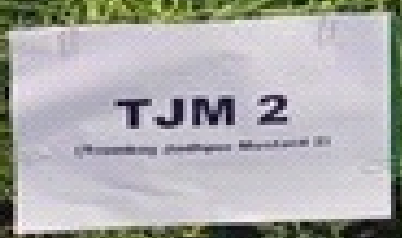

- 14% high yield

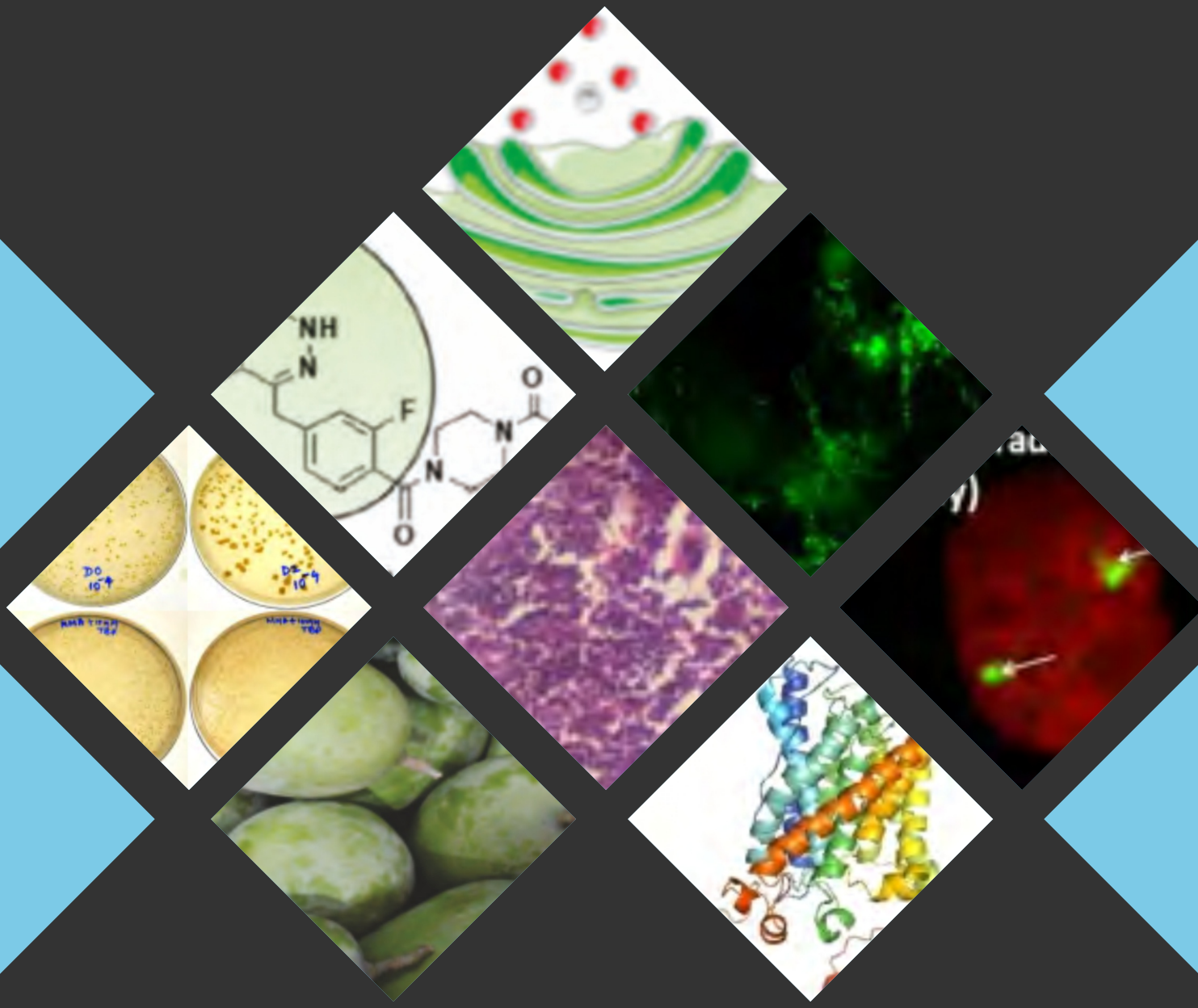

Edited & Published by
Scientific Information Resource Division
Bhabha Atomic Research Centre, Trombay, Mumbai-400 085, India
BARC Newsletter is also available at URL:https://www.barc.gov.in